Application and Evaluation of Sediment Fingerprinting Techniques in the Manawatu River Catchment, New Zealand

A thesis presented in partial fulfilment of the requirements for the degree of

Doctor of Philosophy in Geography

at Massey University, Palmerston North, New Zealand

Simon Vale

2016

Abstract

Suspended sediment is an important component of the fluvial environment, contributing not only to the physical form, but also the chemical and ecological character of river channels and adjacent floodplains. Fluvial sediment flux reflects erosion of the contributing catchment, which when enhanced can lead to a reduction in agricultural productivity, effect morphological changes in the riparian environment and alter aquatic ecosystems by elevating turbidity levels and degrading water quality. It is therefore important to identify catchment-scale erosion processes and understand rates of sediment delivery, transport and deposition into the fluvial system to be able to mitigate such adverse effects. Sediment fingerprinting is a well-used tool for evaluating sediment sources, capable of directly quantifying sediment supply through differentiating sediment sources based on their inherent geochemical signatures and statistical modelling.

Confluence-based sediment fingerprinting has achieved broad scale geochemical discrimination within the 5870 km^2 Manawatu catchment, which drains terrain comprising soft-rock Tertiary and Quaternary sandstones, mudstones, limestones and more indurated greywacke. Multiple sediment samples were taken upstream and downstream of major river confluences, sieved to < 63 µm and analysed through step-wise discrimination, principle component analysis and a range of geochemical indicators to investigate and identify the sub-catchment geochemical signatures. Discrimination between the main sub-catchments was attained despite each sub-catchment containing similar rock types, albeit with varying proportions of specific lithologies. This meant that source groups were categorized as a mixture of both lithological and geomorphological sources in order to best capture the unique sediment origins. Comprehensive sampling quantified 8 geomorphological sediment sources using two mixing models; the traditional mixing model after Collins *et al.* (1997) and the Hughes *et al.* (2009) mixing model which were each optimized using a 'Generalized Reduced Gradient (GRG) Nonlinear' and an 'Evolutionary' technique providing four mixing model scenarios. These models showed good agreement attributing mudstone derived sediment (≈ 38 – 46 %) as the dominant source of suspended sediment to the Manawatu River. Sediment contributions were also estimated from the Mountain Range, ≈ 15 – 18 %; Hill Surface, ≈ 12 – 16 %; Hill subsurface, ≈ 9 – 11 %; Loess, ≈ 9 – 15 %; Gravel Terrace, ≈ 0 – 4 %; Channel Bank, ≈ 0 – 5 %; and Limestone, ≈ 0 %. Intra-storm analysis of sediment sources was investigated through hourly suspended sediment samples taken in the lower Manawatu River during a 53 hour storm event to detect changes in sediment sources. The suspended sediment samples

displayed high hourly variability which was attributed to model uncertainty and sediment pulses occurring between sampling. Mudstone proportions fluctuated ≈ 20 – 60 % throughout the storm duration from a range of erosion processes, while Mountain Range sediment fluctuated from ≈ 24 – 46 % and Hill Subsurface and Hill Surface both were near 0 %, but approached upper values of ≈ 23 % and ≈ 24 % respectively. Significant shifts in sediment source proportions were observed between 2:00 – 8:00 am 29th November 2013 in relation to flow dynamics of the Pohangina River and shifting flow dominance from the Pohangina River to the Upper Manawatu. The geochemical suite was reanalysed to determine the variability of source groups and individual geochemical elements, in order to evaluate the suitability and impact of changing the geochemical suite used in estimated relative sediment source proportions. Mountain Range sediment displayed the highest average S.D. % of 39.4, followed by Gravel Terrace (S.D. % = 34.6) and Loess (28.1), while the lowest was found in Limestone (S.D. % = 18.1) and Channel Bank (S.D. % = 18.3). The highest variability of individual elements was found in the transition elements such as Cu, Ni, Cr, and Mn, as well as Ca, and Tm. Revised mixing models were run based on two geochemical tracer suites which removed elements with S.D. percentage of > 40 and > 35 respectively. The revised mixing model estimated Mudstone terrain to contribute 59.3 % and 61.8 %, with significant contributions estimated from Mountain Range (12.0 % and 11.4 %) and Hill Surface (11.5 % and 11.3 %) respectively, indicating that Tm, Ni, Cu, Ca, P, Mn and Cr have an influence on these sediment source estimations.

Acknowledgements

I would like to express my very great appreciation to my supervisors, Associate Professor Ian Fuller (Massey University), Dr Jonathan Procter (Massey University), Dr Les Basher (Landcare Research) and Dr John Dymond (Landcare Research) for their support and guidance during this doctoral research. I am also particularly grateful for the resource and assistance given by Associate Professor Ian Smith (Auckland University)

I wish to thank Landcare Research for the financial support through the administration of the Murray Jessen Scholarship as well as financial support provided from the George Mason Charitable Trust, L.A. Alexander Agricultural College Trust Board Inc. and New Zealand Geographical Society.

I would also like to thank Dr Chris Phillips (Landcare Research) for providing me exposure to the Clean Water Productive Land Portfolio, Ms Mandy James (Landcare Research) for overseeing my placement within Landcare Research, and Dr Anja Moebis (Massey University) and John Dando (Landcare Research) for their laboratory assistance.

My special thanks are also extended to the staff based at Landcare Research Palmerston North as well as the staff and postgraduates of Physical Geography Group for providing an enjoyable and suitable working environment.

Last but not least, my deepest thanks to my family, friends, and the global community of Congress-WBN for their support, guidance and inspiration.

Thesis Structure and Authorship

This thesis consists of four manuscripts written for publication (two accepted and two in submission) with 4 supporting chapters.

Simon Vale carried out all the fieldwork in the Manawatu between April 2012 and December 2014 and was assisted at different times by Dr Ian Fuller and Dr Jonathan Procter. Simon Vale also undertook all the laboratory work included in this thesis with some assistance by Dr Anja Moebis (Massey University), XRF technicians (Auckland University), LA-ICP-MS technicians (Australian National University), as well as Ian Smith (Auckland University) who also assisted in data preparation following XRF and LA-ICP-MS analysis.

Simon Vale wrote all the text in this thesis as the principal author in the preparation of manuscripts included in this thesis (referenced in Appendix B) with all supervisors providing general advice and editing to manuscripts.

Signed by Principal Supervisor

Dr. Ian Fuller

Contents

List of Figures

List of Tables

Chapter 1

Introduction

1.1 General Introduction

Suspended sediment is the portion of sediment within the fluvial transport system which remains in suspension throughout downstream movement and is regarded as a critical component to the character of each fluvial environment and wider catchment (Collins and Owens, 2006, Bracken, 2010). Erosion, transportation and deposition processes are all associated to fine sediment production and are able to cause physical, chemical and ecological effects directly to the river channel as well as the surrounding catchment environment (Collins and Owens, 2006, Kemp *et al.*, 2011, Walling, 2006b, Owens *et al.*, 2005). In agricultural catchments, erosion of sediment from the surrounding environment results in the loss of nutrient rich soil, reducing agricultural productivity and potentially contributing to land instability (Collins and Owens, 2006). Upon entering the active channel, fine sediment can influence channel morphology, navigability and result in the infilling of reservoirs, while also altering the aquatic habitat due to changes in turbidity and light attenuation, pH, sedimentation and food availability, all of which can have adverse effects for the aquatic environment (Walling and Fang, 2003, Bilotta and Brazier, 2008, Wood and Armitage, 1997, Owens *et al.*, 2005, Kemp *et al.*, 2011, Collins *et al.*, 2011).

Although sediment movement is a natural process and inherent to the structure and character of the fluvial environment, anthropogenic influences have had dramatic consequences on the rates of sediment production and delivery to the fluvial system. Surface erosion, bank erosion, gully erosion, earthflows and landslides are all key process which deliver sediment into the channel system and can be drastically modified through human activity and land management practices. In fact, the influence of anthropogenic actions on the rates of soils erosion have been considered to outweigh the natural soil production rates in many parts of the Earth (Montgomery, 2007). This is especially true for New Zealand, where the most critical issues affecting land are erosion caused by human activity, and subsequent reduction in land productivity and degradation of water quality (Environment Aotearoa, 2015).

In order to engage with these issues, it is important to understand the spatial origin and the processes which deliver fine sediment into the active channel. A variety of tools exists, such as aerial photography, erosion pins, erosion plots and gauging stations which can provide information on erosion rates and total sediment being transported downstream. However, these techniques do not necessarily identify the origin and nature of the sediment actually being transported through the system.

Sediment fingerprinting is a technique capable of identifying and differentiating unique sediment sources throughout a catchment and quantifying relative source proportions. This is achieved through geochemical and non-geochemical analysis of the sediment sources in order to select variables or tracers which can adequately characterise the unique sediment sources followed by implementation of statistical mixing models to derive source estimates. The technique gained momentum in the 1970s and has been successfully used in specific environments but with few applications within a New Zealand environment and where the catchment is large and dominated by variable sedimentary terrain patterns.

Global sediment discharge is estimated to be around 15–20 billion tonnes per year (Walling, 2006a) and represents a significant, globally important process. In New Zealand, estimates of sediment contribution to the ocean have ranged between 190 -209 million tonnes of soil, equating to 1.5 percent of global sediment loss, despite making up only 0.2 percent of the global land area (Syvitski *et al.*, 2005, Walling, 2008, Ministry for the Environment & Statistics New Zealand, 2015, Hicks *et al.*, 2003). This implies that sound knowledge of New Zealand's fine sediment behaviour is essential to environmental health and agricultural stability, which creates that imperative for additional tools and techniques to aid in increasing this knowledge.

The sediment fingerprinting methods employed in this research are specific for each case study but generally reflect the traditional sediment fingerprinting approach after Collins *et al.* (1998). This approach first selects appropriate tracers which can characterize unique sediment sources, then uses discriminant function analysis to derive the best set of tracers to characterize the sediment sources. The selected tracers can then be utilized to quantify relative sediment source proportions through a multivariate mixing model comparing the geochemical character in the source groups to the suspended sediment sampled downstream. In this research, tracers have been limited to concentrations of bulk geochemistry including major, minor and rare earth elements. There are a large range of other geochemical tracers which could be utilized but given the size of the catchment and number of samples required, bulk geochemistry was the most straightforward and affordable to attain. Sediment sources

also were characterised most readily by geomorphological and geological parameters rather than other source categorization formats such as land-use, allowing the large geochemical suite to adequately characterize sediment sources.

This research is novel in that it seeks to identify eight unique sediment sources in a large sedimentary-rock dominated catchment and represents the largest sediment fingerprinting project carried out in New Zealand to date.

1.2 Study Site

The Manawatu River catchment provides an appropriate location to test the effectiveness of the sediment fingerprinting technique in a large, dynamic catchment subject to significant anthropogenic influences.

The Manawatu Catchment flows east to west, distinctively crossing the North Island's dividing axial range draining a total area of 5,870 km^2 of the lower North Island, New Zealand (Fig. 1). The headwaters of the Upper Manawatu begin on the eastern flanks of the Ruahine Range and the river flows 235 km to the Tasman Sea on the west coast. However, due to the unique catchment, tributaries rise on both sides of the Ruahine and Tararua Range. Population is centred in Palmerston North (≈ 85,000) the largest city in the catchment, followed by the Feilding (≈ 15,000) and Dannevirke (≈ 6,000).

Like most of New Zealand, European settlement from the mid-19^{th} century has drastically changed the landscape of the Manawatu Catchment and continues to be a major influence on the environmental condition of the entire catchment. Anthropogenic influences have generally been regarded as detrimental to environmental health with water quality indicators, such as Dissolved Reactive Phosphorus (DRP), nitrates (NO_3) and turbidity, having displayed alarming trends of increasing concentrations at a number of Manawatu sites (Gibbard, 2006) while the Macroinvertebrate Community Index (MCI) has also shown negative trends since 1999 in the Oroua and Manawatu River (Stark, 2008). Large storms have exacerbated anthropogenic influences with a 2004 storm causing widespread erosion in the hill country, changing stream courses and causing over $300 M of damage (Dymond *et al.*, 2006a). These negative indicators have raised the profile of the catchment and accordingly drawn significant attention towards addressing issues relating to sediment erosion and transport, farm runoff, and environmental health. Sediment fingerprinting is an important tool in addressing these problems, but the application of sediment fingerprinting in a New Zealand environment has, to date, received

limited attention. The most significant fingerprinting research carried out in New Zealand to date has been by Roddy (2010) and Gibbs (2008) while no research has been undertaken in the Manawatu.

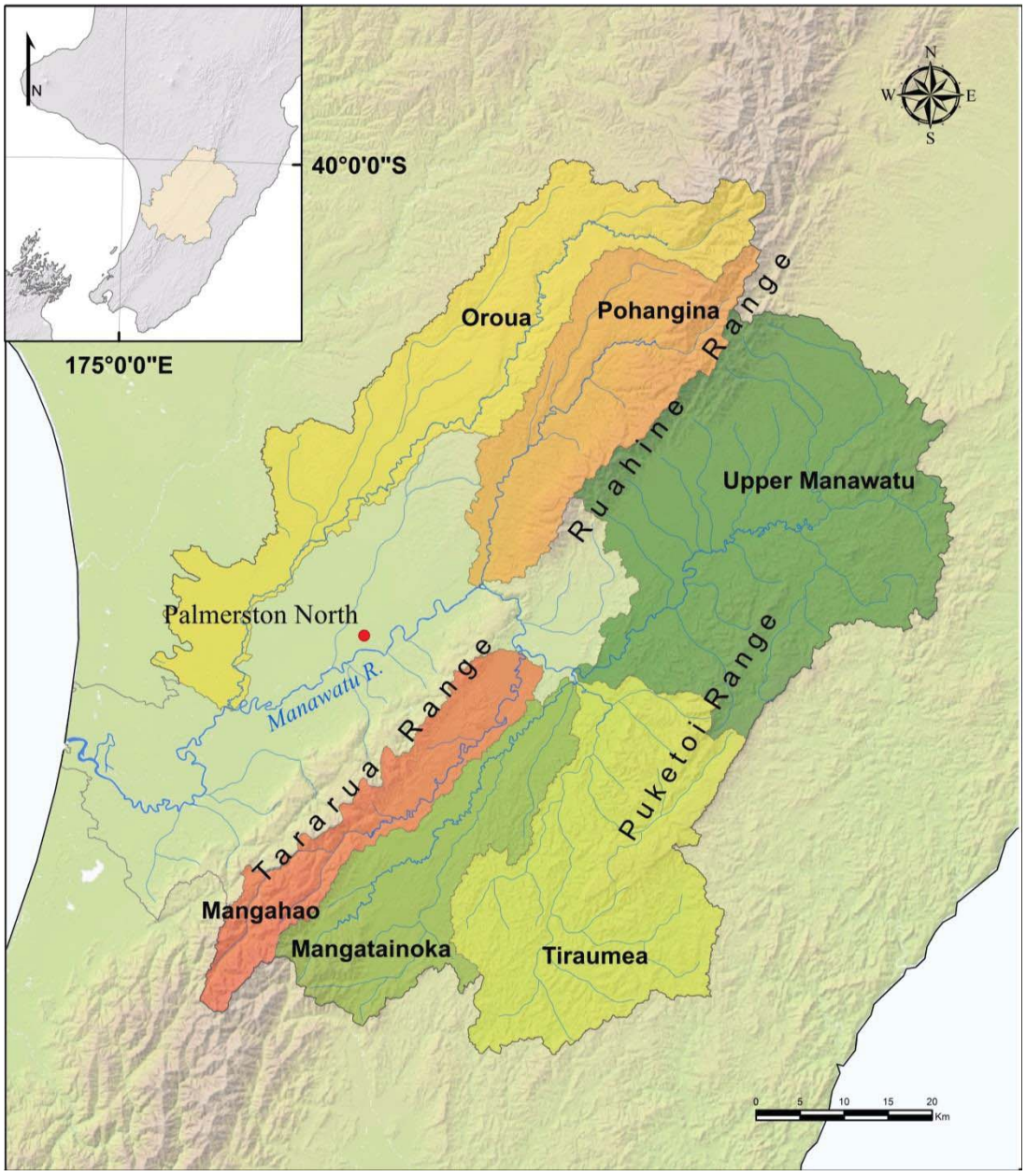

Fig. 1: *Study Location Mangahao, Mangatainoka, Tiraumea, Pohangina and Oroua River*

1.3 Catchment Character

The main sub-catchments of the Manawatu Catchment are the; Upper Manawatu (1301 Km^2), Tiraumea (876 Km^2), Mangatainoka (481 Km^2), Mangahao (339 Km^2), Pohangina (551 Km^2) and Oroua sub-catchment (903 Km^2) with each sub-catchment containing a unique composition of

geology, albeit all sedimentary in nature. The mean discharge of the Manawatu taken at Palmerston North is c.110 m^3 s^{-1} with contributions from the main sub-catchments: Upper Manawatu (c. 27 m^3 s^{-1}) , Tiraumea (c. 16 m^3 s^{-1}), Mangatainoka (c. 18 m^3 s^{-1}), Mangahao (c. 15 m^3 s^{-1}), Pohangina (c. 17 m^3 s^{-1}), and Oroua (c. 13 m^3 s^{-1}) (Henderson & Diettrich 2007). Channel morphology ranges from semi-braided to pseudo-meandering over gravel and sand-bedded alluvium in the mainstem of the Manawatu River. Headwaters are largely confined single channels with bedrock step-pool sequences, or narrow slot channels where cut into mudstone. Late Quaternary river terraces confine river channels in the upland fringes of the catchment (i.e. adjacent to the greywacke ranges). Many of the lower reaches have undergone straightening and narrowing of the channel, transitioning from multi-thread braided channels to a laterally-confined single thread channel as evidenced in the Pohangina River (e.g. Fuller 2009). Riparian planting and the construction of rip-rap are also prevalent throughout the catchment in order to reduce bank erosion. Middle reaches are often semi-confined through contact with bedrock cliffs or alluvial terraces and where the river crosses the greywacke axial range it flows through a 10 km long, 200 m deep bedrock gorge.

Catchment geology comprises almost exclusively sedimentary material, predominantly mudstone, greywacke and sandstone interspersed heterogeneously throughout the catchment with limestone and alluvial gravels (Fig. 2). There is some volcanic material found in the greywacke, particularly in the Manawatu Gorge but it is not substantial enough relative to the catchment size to contribute a distinctive sediment source. Eastern catchments are dominated by soft hillslope terrains underlain primarily by mudstone e.g. Tiraumea sub-catchment, which is also common throughout some western catchments (Table 1). Upper Manawatu, Pohangina and Oroua hillslopes consist of mixed geology i.e. commonly sandstone in varying proportions with poorly or well bedded siltstone and mudstone with additional shellbeds and conglomerates.

The Tararua and Ruahine Ranges are predominantly greywacke (with some minor volcanic) while the Puketoi Range also includes a significant amount of limestone. Lowland areas consist of alluvial floodplains of gravels and sands and nearer to the west coast the introduction of coastal wind-blown sands begins to dominate the geology. The New Zealand Soil Classification (NZSC) after Hewitt (1998) states the soils in region consist predominantly of orthic/firm brown soils, consisting of mica/illite, across the catchment with limited distributions of allophanic brown soils associated with the flanks of the greywacke range. Argillic pallic soils are found in eastern catchments, particularly Puketoi Range, with immature pallic soils common in both the eastern catchments as well as Pohangina. Perched-Gley pallic

soils are also found on the western flanks of the Tararua Range, and in the lowland areas surrounding the Oroua and north of Palmerston North. Recent alluvial soils are found on extensive floodplains following the channel outlines. Limited melanic soils are found in the limestone regions.

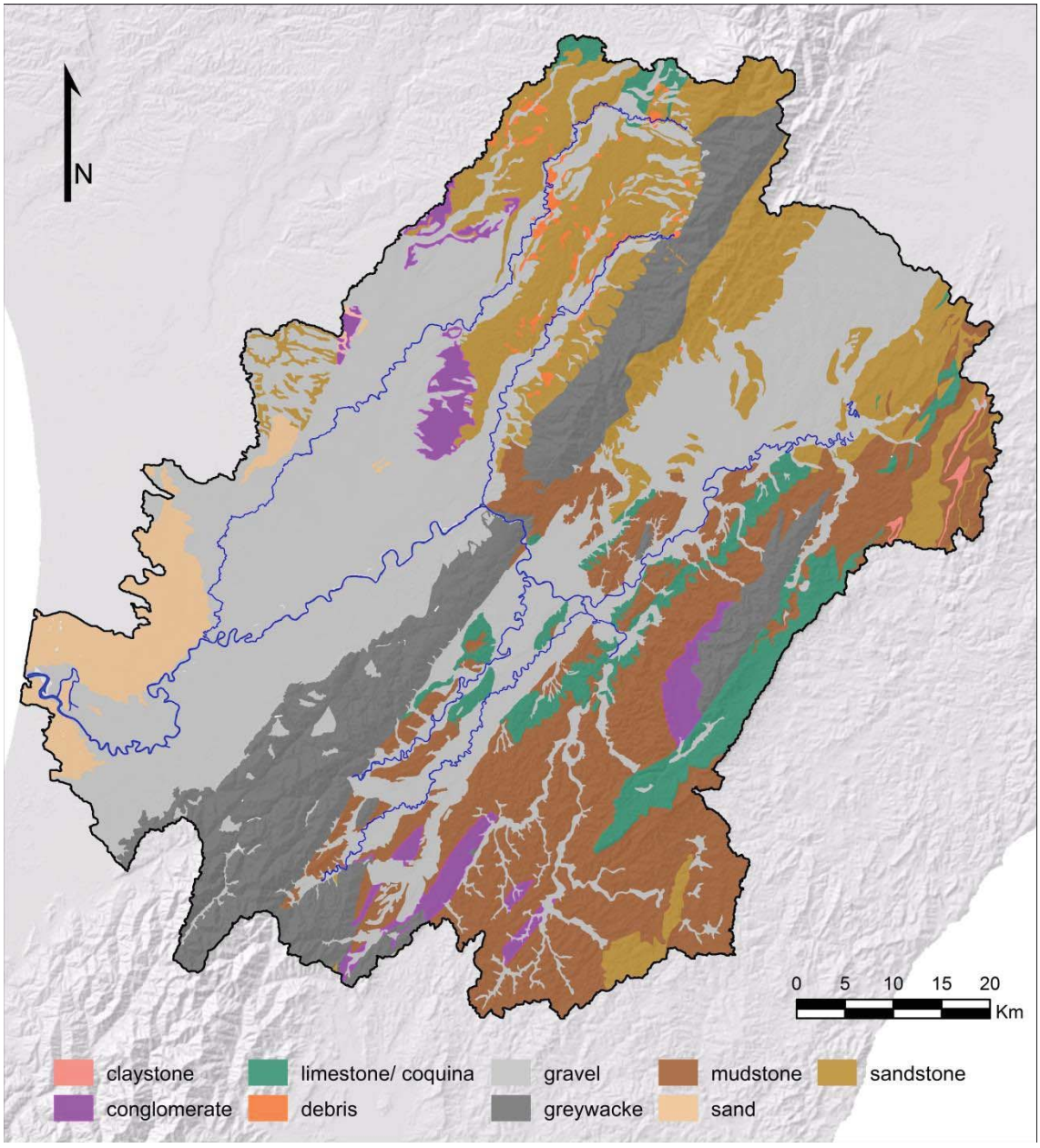

Fig. 2: *Geological map of the Manawatu Catchment*

New Zealand rivers show a large range in suspended sediment concentrations (Fig. 3) with particularly high sediment concentrations found in mudstone catchments (Hicks and Griffiths, 1992) while rainfall simulated experiments have shown increased sediment run-off post-

grazing in hill-country areas (Adams and Elliott, 2006). Both of these conditions are commonplace throughout the Manawatu catchment and agricultural intensification over the past 20 years has coincided with negative environmental trends. This has caused the local Regional Council to identify unsustainable land-use in the hill country as a major environmental issues (Gibbard, 2006, Dymond *et al.*, 2006a). In contrast, while the steep slopes and fractured greywacke composition of the mountain ranges generate significant quantities of material to the bedload of the Manawatu River (Mosley, 1978, Fuller *et al.*, 2016), a combination of more resistant greywacke, dense vegetation cover and thin soils likely impede the ability to generate fine sediment from this source.

Table 1: *River Classification of the Manawatu Region after Ausseil and Clark (2007)*

WMZ Class	Source of flow	Geology	Typical river type	Examples
Lowland Sand	Lowland	Windblown sand dominant	Western coastal streams. A large proportion of these streams flow either into or out of coastal lakes	West coast zones
Lowland Mixed	Lowland	No dominant geology, generally a mix of sand, loess, alluvium and soft sedimentary	Medium to slow flowing streams/rivers. Bed material a mix of gravel and soft sediments	lower Manawatu
Hill Mixed	Predominantly Hill	Hill country zones with no dominant geology class. Geology is generally a mix of alluvium, SS, HS and loess	Rivers have a gravel/cobble bed, receiving base flow from the Tararua or Ruahine Ranges, but is also influenced by soft sedimentary geology, impacting on water clarity/bed saltation	Upper and middle Manawatu, Pohangina, Mangatainoka
Upland Hard Sedimentary	Predominantly Hill with some Mountain	Predominantly greywacke	Typically streams flowing from the Tararua and Ruahine Ranges	Tamaki, Turitea, Kahuterawa, Mangahao, Mangatainoka, Pohangina and Oroua
Upland Limestone	Hill	Predominantly limestone	Streams flowing from the Puketoi Range	Makuri River
Hill Soft Sedimentary	Hill	Predominantly soft sedimentary	Zones dominated by soft sedimentary geology	Tiraumea

Land-use in the Manawatu Catchment is dominated by exotic grassland used for agricultural farming (≈ 75 %), comprising mostly sheep and beef farming, as well as dairy farming in the flatland. Indigenous vegetation comprises ≈ 17 % of areal land coverage (Table 2; Fig. 4). The majority of this is from indigenous forest and broadleaf indigenous hardwoods located on the flanks of Tararua and Ruahine ranges as well as the Puketoi Range. Zonation of vegetation

species clearly exists in relation to the elevation and associated temperature and moisture (Marden, 1984).

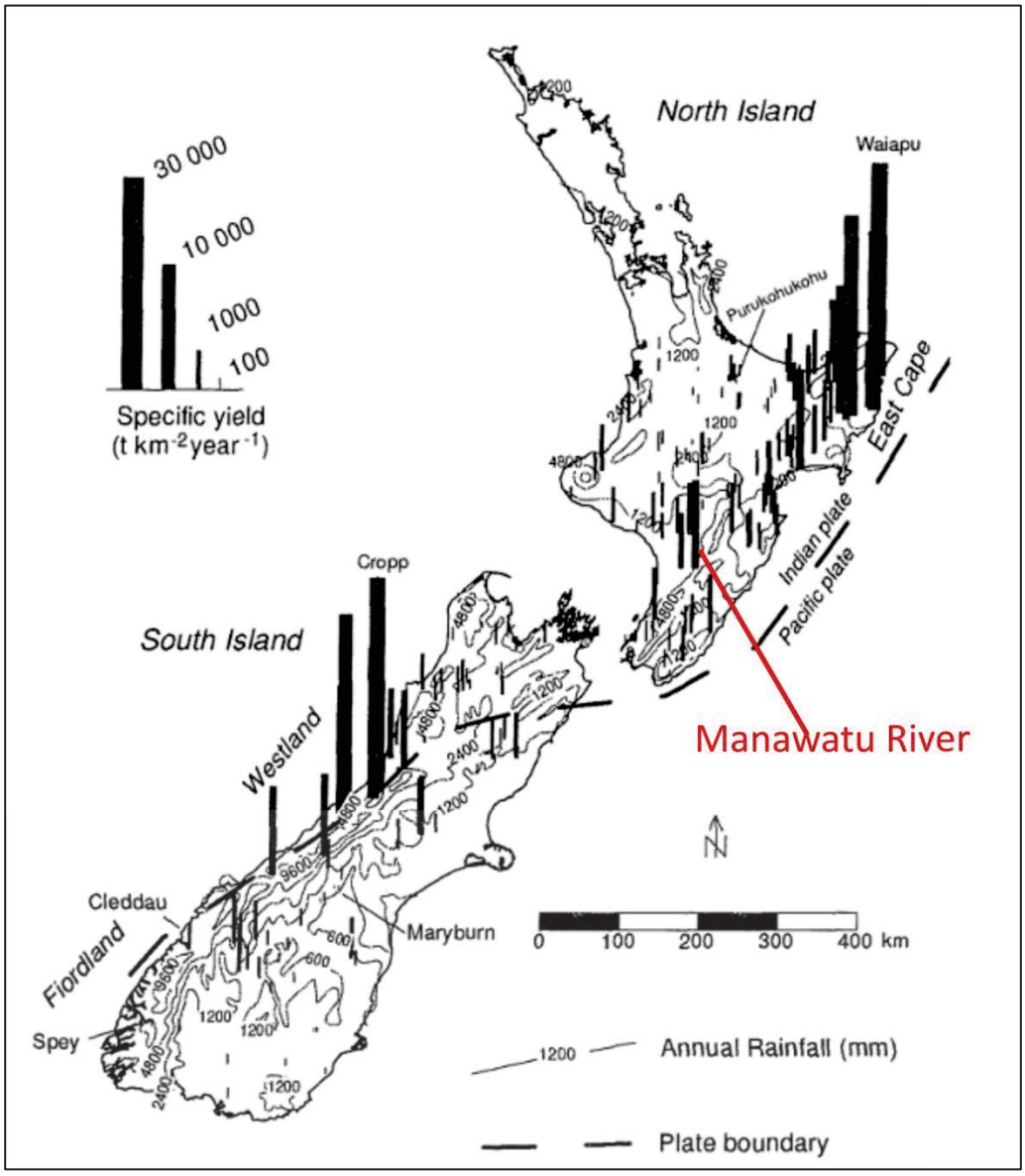

Fig. 3: *Map of New Zealand showing suspended sediment yields at gauging stations and mean annual rainfall isohyets after Hicks et al. (1996). Bar areas are proportional to sediment yield*

Moving from a podocarp/hardwood dominated forest to a kamahi dominated zone through to leatherwood and a finally a sub-alpine zone. Mānuka and kanuka along with other grey scrub (dark coloured vegetation typically composed of small-leaved, highly branched shrubs) and introduced gorse and broom occupy pockets of land particularly in the Tiraumea sub-catchment associated with marginal land often associated with disturbed land, regenerating land types or poor soil fertility. Short-rotation agricultural crops occupy small pockets in the western Manawatu Catchment.

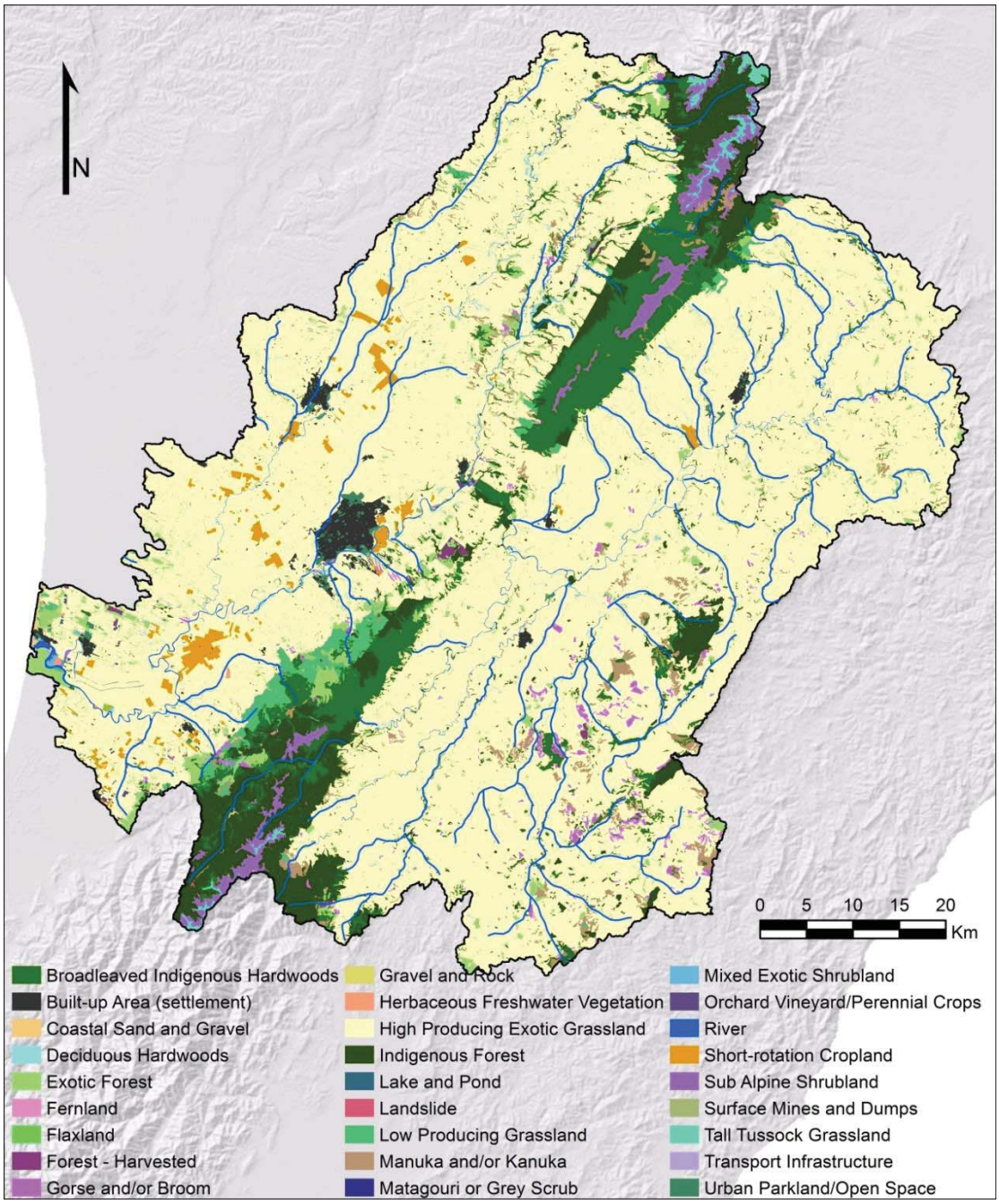

Fig. 4: *Spatial pattern of land-use in the Manawatu Catchment*

Table 2: *Areal percentage cover of the main land cover in the Manawatu derived from the Landcover Database (LCDB) v3 after Landcare Research NZ Ltd (2012).*

Land-use	Area (Km^2)	Area (%)
High Producing Exotic Grassland	4346.3	74.0
Indigenous Forest	403.7	6.9
Broadleaved Indigenous Hardwoods	397.6	6.8
Exotic Forest	172.7	2.9
Manuka and/or Kanuka	98.5	1.7
Sub Alpine Shrubland	86.6	1.5
Low Producing Grassland	72.7	1.2
Short-rotation Cropland	68.0	1.2
Built-up Area (settlement)	57.2	1.0
Gorse and/or Broom	43.1	0.7
Other	124.5	2.1
Total	**5870.9**	**100**

1.4 Aims and Objectives

The aim of this thesis was to investigate sediment source differentiation and quantification using sediment fingerprinting techniques within a New Zealand setting, particularly within a large, homogenous catchment such as the Manawatu, as well as understand some of the ongoing challenges in sediment fingerprinting research.

The objectives of this study were to:

a. provide a comprehensive review of sediment fingerprinting techniques, applications and challenges

b. investigate the feasibility of sediment fingerprinting within the Manawatu catchment and gain a better understanding of the challenges and procedures involved through a sub-catchment based study

c. apply sediment fingerprinting to assess:

    i. key sediment sources within the Manawatu catchment

    ii. change in catchment contributions to the suspended sediment load of the Manawatu during a flood event

d. evaluate these observations, assessing the reliability (conservativeness) of key geochemical tracers, and identify key areas of focus for future research.

1.5 Thesis Organization

The first chapter introduces the general topic of sediment research providing a brief background to the importance of understanding sediment erosion, transportation and deposition, before introducing the characteristics of the Manawatu River Catchment to provide a context for the subsequent review. A review of sediment processes is provided in Chapter 2 as well as in Vale, S. (2013). *Sediment Fingerprinting review and application to Manawatu River Catchment* which was prepared for the Clean Water Productive Land research Programme (C10X1006) and published by Landcare Research, New Zealand as Report No.: LC 1644. This review outlines the physical, chemical and ecological impact fine sediment has on river systems as well as the range of processes which can deliver fine sediment to the channel system and move it downstream. The review goes on to give a comprehensive overview of sediment fingerprinting research, including the origin, key developments and ongoing challenges with the technique and is accompanied by Appendix A: A comprehensive summary of sediment fingerprinting literature.

Chapter 3 investigates the application of sediment fingerprinting to major river confluences in the Manawatu catchment as a broad-scale approach to characterizing sub-catchment sediment contributions for a sedimentary catchment dominated by agriculture. This was primarily to resolve whether there is enough geochemical variability in suspended sediment deposits throughout the catchment to distinguish sediment sources. This chapter was also published in the manuscript: Vale SS, Fuller IC, Procter JN, Basher LR, Smith IE., Application of a confluence-based sediment-fingerprinting approach to a dynamic sedimentary catchment, New Zealand, which was first published in *Hydrological Processes*, 30: 812-829. DOI: 10.1002/hyp.10611.

Chapter 4 presents geochemical analysis of 8 geological and geomorphological sources; Mudstone, Hill Subsurface, Hill Surface, Channel Bank, Mountain Range, Gravel Terrace, Loess and Limestone. The geochemical suite was analysed using Discriminant Function Analysis and sediment mixing models to derive the best suite of variables to differentiate each sediment sources, upon which estimated proportions of fine sediment sources were derived using two mixing models, each with two optimization techniques for comparison. Differentiation of the sediment sources, mixing model comparison and evaluation in relation to the geomorphological understanding is discussed. This chapter is also published in the manuscript: Vale SS, Fuller IC, Procter JN, Basher LR, Smith IE., Characterization and quantification of

suspended sediment sources to the Manawatu River, New Zealand first published in *Science of the Total Environment* 2016; 543: 171-86. This chapter

Chapter 5 estimates sediment source proportions at hourly intervals over a 53 hour storm event to capture changes in relative proportions in relation to sub-catchment flow throughout the duration of the storm flow. This involved geochemical differentiation of eight geomorphological source groups, and synchronization of sub-catchment flows with the arrival at the Manawatu River sample site. The relationship between sub-catchment flow, and changes in sediment source are discussed in relation to the catchment characteristics.

Chapter 6 explores the variability of the geochemical data for each source group in order to evaluate more thoroughly the suitability of individual elements. The average percentage standard deviation is presented for individual elements as well as source groups as a whole before applying a 40 and 35 % standard deviation limit for individual elements and removing these elements from a revised geochemical suite. Sediment mixing models are re-executed using the revised geochemical suite and the changes in source estimation are discussed in relation to uncertainty and variability.

Chapter 7 provides the synthesis of discussion which revolves around the main research concepts drawn together into a single discussion followed by Chapter 8 which provides the final concluding remarks and perspective for future research.

1.6 Summary

Suspended sediment origin and flux is an important component to the fluvial system and wider catchment environment, influencing the physical, chemical and ecological character of the fluvial channel. Human activity can have profound influences on suspended sediment delivery to the active channel so sound knowledge of sediment dynamics and spatial origin is important in order to effectively manage rates of sediment movement throughout a catchment. Sediment fingerprinting provides a means to differentiate fine sediment sources and estimate relative source proportions. This research focuses on providing a comprehensive review of sediment fingerprinting literature, investigation to the feasibility of sediment fingerprinting in the Manawatu, the relative fine sediment source proportions and an evaluation of uncertainty associated with geochemical variability within the catchment. The Manawatu catchment is also introduced as the study site providing context for the following chapter, covering the literature review of sediment processes and sediment fingerprinting research.

Chapter 2

Literature Review: Sediment Fingerprinting

2.1 General Introduction

Before applying sediment fingerprinting techniques to understand sediment dynamics in the Manawatu River, it is important to understand the process of sediment movement throughout a catchment. This chapter introduces fine sediment and the importance it has to the river catchment and then provides an overview of sediment movement throughout a catchment and the specific processes which deliver sediment to the active channel. The chapter then introduces sediment fingerprinting including the background and key developments in the technique as well as some of the main challenges facing the research. The chapter is published as Vale, S. (2013). *Sediment Fingerprinting review and application to Manawatu River Catchment* which was prepared for the Clean Water Productive Land research Programme (C10X1006) from Landcare, Report No.: LC 1644

2.2 Introduction

Research into the quantification and modelling of sediment movement through a wide range of Earth's surface processes has increased substantially in recent decades. However, catchment-scale identification of erosion processes and geomorphically active areas contributing to sediment yield has often been poorly understood and quantified. Increased realization of the impact sediment has on the health of the aquatic environment and the surrounding landscape has intensified the need for improved understanding. Small changes in the input of fine sediment due to modifications in land-use can have significant downstream

implications, adversely affecting river health (Walling *et al.*, 2013, Collins and Walling, 2004). To mitigate these issues all aspects of sediment movement, production, transport, and deposition need to be understood. This includes how our landscape was formed and also how it will continue to change in response to natural and anthropogenic pressures (Warburton, 2011, Hicks and Griffiths, 1992). Traditional field-based techniques for sediment source identification are typically qualitative, time consuming, and difficult to apply to larger catchment scales. Sediment fingerprinting provides an alternative approach to quantifying sediment sources that allows increased focus on fine sediment, large catchments scales, and the use of pre-existing tracers (Walling *et al.*, 2013).

2.3 Catchment Sediment Processes

2.3.1 Introduction

The suspended sediment component in a fluvial environment is arguably one of the most important components of the sediment cascade (Collins and Owens, 2006, Bracken, 2010). With global sediment discharge estimates ranging from 8.3 billion to 51.1 billion tonnes per year and realistically probably around 15–20 billion tonnes per year (Walling, 2006a) it represents a significant, globally important process. Fine sediment production, with commensurate erosion, transport and deposition processes, directly influences the form and character of river channels and surrounding riparian environments, including a range of physical, chemical and ecological effects that are typically negative (Collins and Owens, 2006, Kemp *et al.*, 2011, Walling, 2006b, Owens *et al.*, 2005). The intensive nature of human activities such as arable farming and associated poor management and exposure of topsoil from vegetation removal, all have a significant effect on erosion rates (Collins *et al.*, 1997, Walling *et al.*, 1999, Owens *et al.*, 2005). Erosion causes the loss of agriculturally important land through removal of nutrient rich soil, a growing medium to almost all agricultural dependent activities, and poses some significant issues to agricultural production and flow-on effects to global issues of food production and agriculturally dependent economies (Collins and Owens, 2006). The introduction of fine sediment into the channels can also cause morphological changes, altering channel navigability, increasing flood risk, and infilling dams and reservoirs, which decrease the capacity of hydroelectric schemes (Collins *et al.*, 2011).

Aquatic life is adapted to distinctive habitats; however, elevated fine sediment fluxes cause environmental changes in river morphology and hydrology that affect the characteristics of the aquatic ecosystem. Changes in turbidity, light attenuation, sedimentation of channels and

estuaries, impoundment of flow regimes can all influence food availability, foraging efficiency, physiology, dissolved oxygen concentration, pH levels, and habitat, which more often than not have an adverse impact on the aquatic environment (Walling and Fang, 2003, Bilotta and Brazier, 2008, Wood and Armitage, 1997, Owens *et al.*, 2005, Kemp *et al.*, 2011). Suspended sediment contains a variety of material (Fig. 5), each impacting the fluvial system in specific mechanisms. Nonpoint source (NPS) pollution can occur due to the spate of associated contaminants, nutrients, pathogens and heavy metals that can be contained within the suspended sediment fraction (Owens *et al.*, 2005, Davis and Fox, 2009). Agricultural land-use is often identified as a key contributor due to intensification in the application of fertilizers and pesticides that increase nutrient concentrations in the river. Urban areas give rise to point source inputs in the way of sewage solids, road dust, and higher levels of sediment generation during construction processes that are often associated with concentrations of contaminants increasing downstream of urban areas (Owens *et al.*, 2005, Owens *et al.*, 2001).

In order to address the issues posed by elevated and/or contaminated suspended sediment flux, there must be an understanding of the origin and source of sediment as well as the transport process, and fate of sediment within a catchment scale (Davis and Fox, 2009). Identifying the actual spatial distribution of these sediment sources is important, as is identifying the dominant processes generating the sediment. Sediment source identification and quantification is the principal concern of sediment fingerprinting, but understanding sediment sources is not a straightforward task. Each catchment is unique in its particular pattern of sediment movement due to the complex arrangement of variables such as climate, vegetation, topography, soil type, and, notably, human disturbances, all of which influence the source, transport, and fate of sediment movement (Davis and Fox, 2009). Therefore, all aspects of sediment movement, production, transport, and deposition need to be understood in order to understand not only how our landscape was formed but also how it will continue to change in response to natural and anthropogenic pressures (Warburton, 2011, Hicks and Griffiths, 1992).

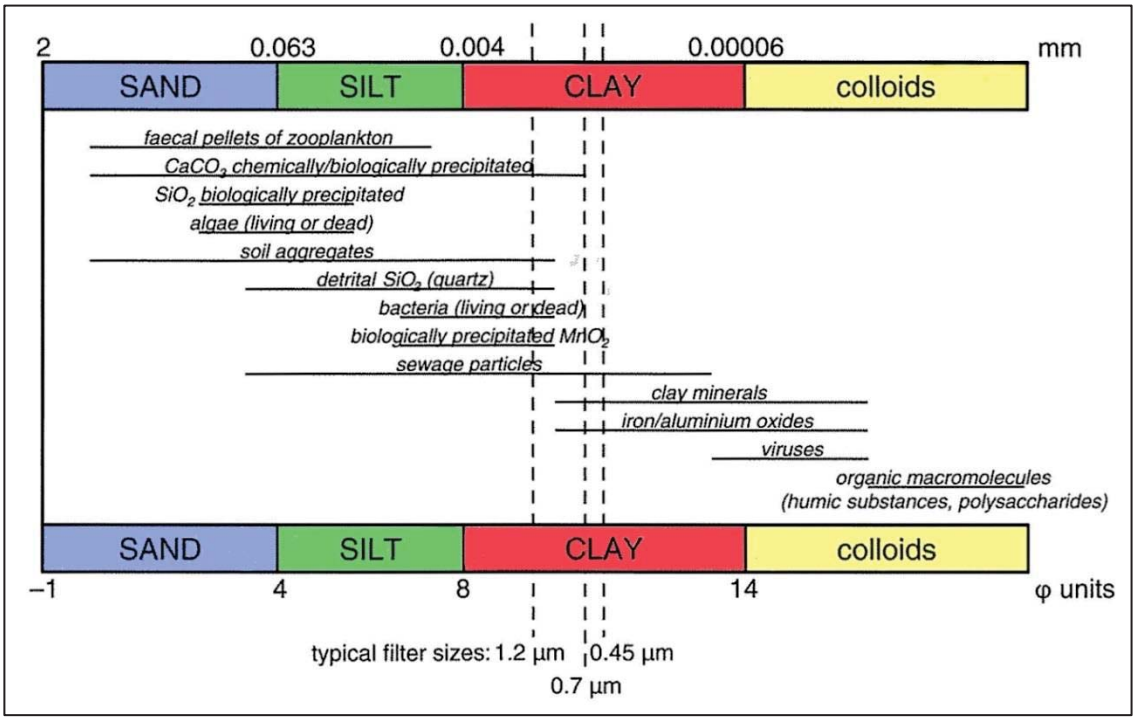

Fig. 5: *Fine sediment size characteristics including organic and colloidal ranges from Naden (2010), although does not include silicates.*

2.3.2 Sediment Cascade

A catchment or drainage basin forms the basic boundary of a connected fluvial system, consisting of both water and sediment transfer through slope, channel and floodplain environments. This provides the context for properly understanding the dynamics of the aptly termed '*jerky conveyor belt*' (Ferguson, 1981) of sediment transport, which includes sediment (dis)connectivity mechanisms which disrupt the transport of sediment, sometimes referred to as "buffers, barriers, and blankets" (e.g. Fryirs *et al.*, 2007). The "source-mobilisation-delivery" model also conceptualized the movement of sediment throughout a river system incorporating impacts as part of the model (Haygarth *et al.*, 2005). The discipline is not new, but steeped in many pseudonyms; 'sediment delivery', 'sediment yield', 'sediment storage', 'sediment erosion', 'sediment transport', 'sediment cascade', 'sediment budget' (Burt and Allison, 2010), all of which target the same issue – understanding sediment behaviour within a catchment. Researchers have used a diverse range of techniques, including empirical understanding, direct measurements, imagery, and modelling, to explain and better understand sediment behaviour and generation.

Sediment movement is of course inherently a natural process, intrinsic to the structure and form of a fluvial environment. Fundamental variables such as bedrock geology, topography,

basin size, climate (particularly rainfall), vegetation cover, and anthropogenic influence all contribute to controlling sediment supply and transport. Milliman and Farnsworth (2011) and Syvitski and Milliman (2007) concluded that geological factors such as basin relief, area and lithology explain the majority of variation (64%) in suspended sediment yields globally. Climate (temperature and rainfall) explains 14% of variation, and 16% of variation is explained by anthropogenic influences. This is a simplified approach that becomes increasingly complicated when considering spatial and temporal patterns which introduce factors such as seasonal rainfall, storm events, sediment storage, vegetation cover, and hysteresis. All these factors introduce complexity and present challenges for extrapolating between local and short-term research and long-term averages (Brunsden, 1974, Dietrich and Wilson, 1978, Trimble, 1981).

The sediment cascade exists as a conveyance of sediment from origin to destination (Fig. 6) normally separated into three components: 1) erosion, the initial supply of available sediment; 2) transport, the entrainment of sediment from source including alternating deposition and re-entrainment; and 3) deposition or net yield, the removal of sediment from the system through outflow or deposition.

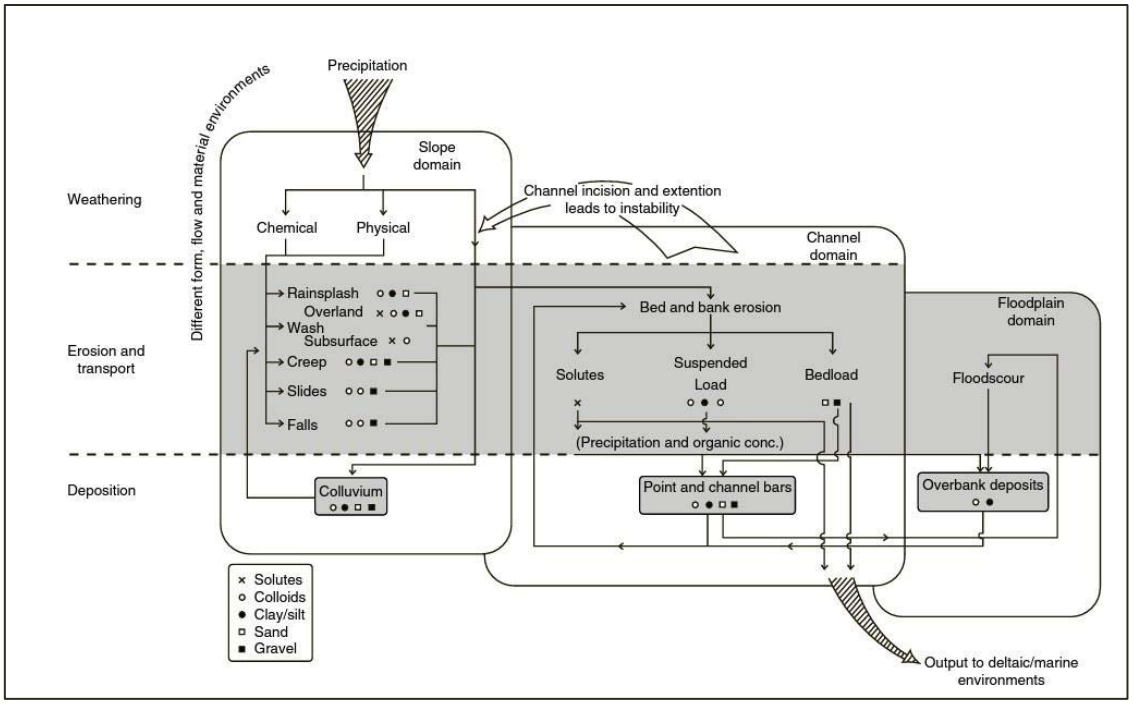

Fig. 6: *Overview of erosion, transport, and deposition processes operating in a slope, channel, and floodplain domain (Warburton, 2011)*

Sediment generation begins in the upper catchment slope environment of hills and mountains through erosion and weathering. Weathering is strongly related to temperature and moisture, with overlying drivers including climate, geology, topography, and organic activity (Robinson and Moses, 2011). Topography determines water availability and characterizes the slopes and gravity influence, while geology exerts a direct control on the rate of weathering which reflects differences in geological composition (Fig. 7). Stable minerals like quartz and zircon weather more slowly than unstable minerals like feldspars and mafic minerals, causing different quantities in the availability of minerals, which result in relative enrichment and depletion patterns (Weltje and von Eynatten, 2004). Climate, geology, and basin morphology/topography are also primary variables for erosion, acting to remove sediment from its origin. Basin morphology (including basin size, shape, and slope) and climate particularly determine patterns of water flow and erosivity. Available sediment is eroded through water action, mobilized into the fluvial channel through a number of different mechanisms and, alternating between deposition/storage and remobilization, is progressively transported towards the sea.

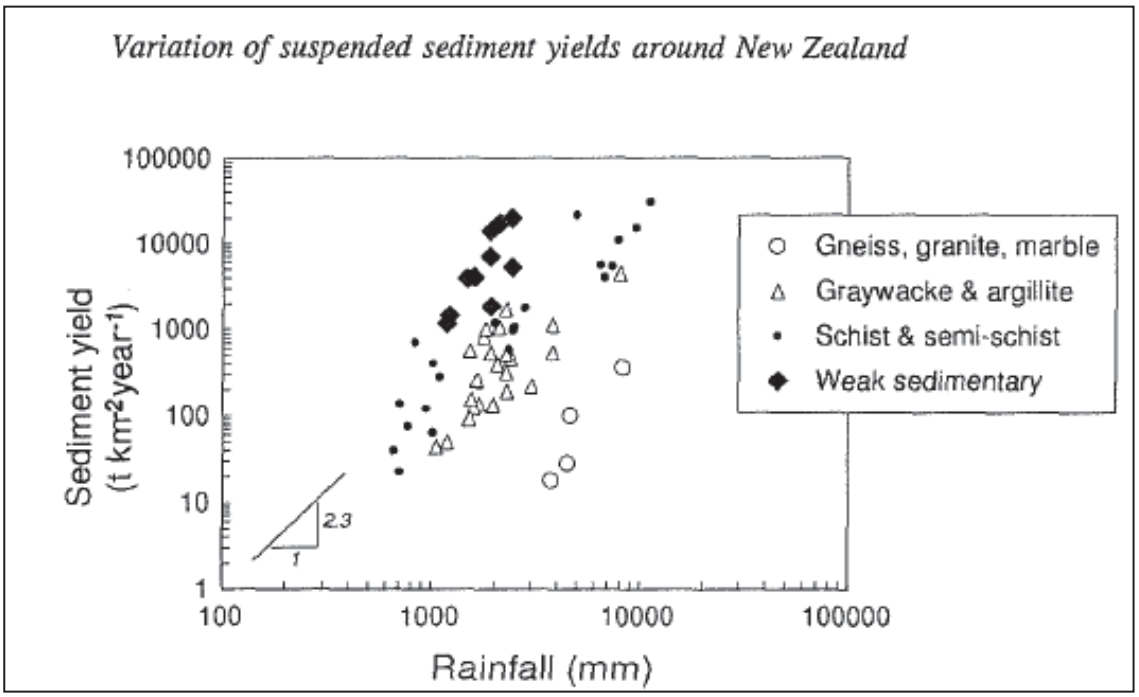

Fig. 7: *Difference in sediment yield based on rainfall and geology; weak sedimentary rocks yielded more sediment in comparison to gneiss, granite and marble rock (Hicks et al. 1996)*

The main processes for erosion consist of surface erosion, gully erosion, bank erosion, earthflows, and landslides (mass movements), which take place under different conditions and mechanisms. Surface or sheet erosion occurs in the topmost layer of the surface soil due to overland water flow and rain-splash (Fig. 8) particularly in agricultural fields where soils may be

exposed and allow the formation of rills. Gully erosion occurs in deeper erosion channels that cannot be removed by cultivation and can refer to permanent gullies, ephemeral, bank gullies and complex gully systems consisting of multiple erosion processes. Gully erosion represents a significant mechanism of sediment delivery through increased connectivity of upland hillslopes to the main stream channel often initiated after vegetation loss and may remain active for extended periods. Complex gully erosion has been well demonstrated in New Zealand through widespread forest clearance from the 19th century, and exists in soft-rock hill country commonly found on east-coast North Island catchments (Hicks *et al.*, 1996) e.g. Weraamaia (Kasai *et al.*, 2005), Te Weraroa (Gomez *et al.*, 2003), Mangawhairiki (Betts *et al.*, 2003), Waipaoa (Marden *et al.*, 2005), Waiapu (Parkner *et al.*, 2006).

Landslides can refer to a number of different but related processes under the banner of mass movements which are fully outlined in a classification by Varnes (1978) and include falls, topples, slumps, slides (rotational and translational), spreads, flows, and complex failures. The typical processes involve a threshold-based mechanism where the shear strength of the slope is exceeded by the shear stress along a plane of failure, which results in movement. This is most often triggered by rainfall events but also by earthquakes, erosion and weathering, groundwater level, and human activity and as a result is sporadic in nature (Sassa *et al.*, 2009). In New Zealand shallow landslides are a common process in the soft-rock hill country triggered by high intensity rainfall; the Waipaoa River, for example, receives approximately 15 ± 5% of the suspended sediment yield from shallow landslides, 75% of which occurs during storms with a recurrence interval of < 27 years (Reid and Page, 2003). A particularly relevant event in the Manawatu occurred during a major storm in February 2004. Dymond *et al.* (2006b) identified over 62,000 individual landslides covering an area of 190 km^2. This was not unsurprising with 58 % of landslides occurring in land considered susceptible to land sliding.

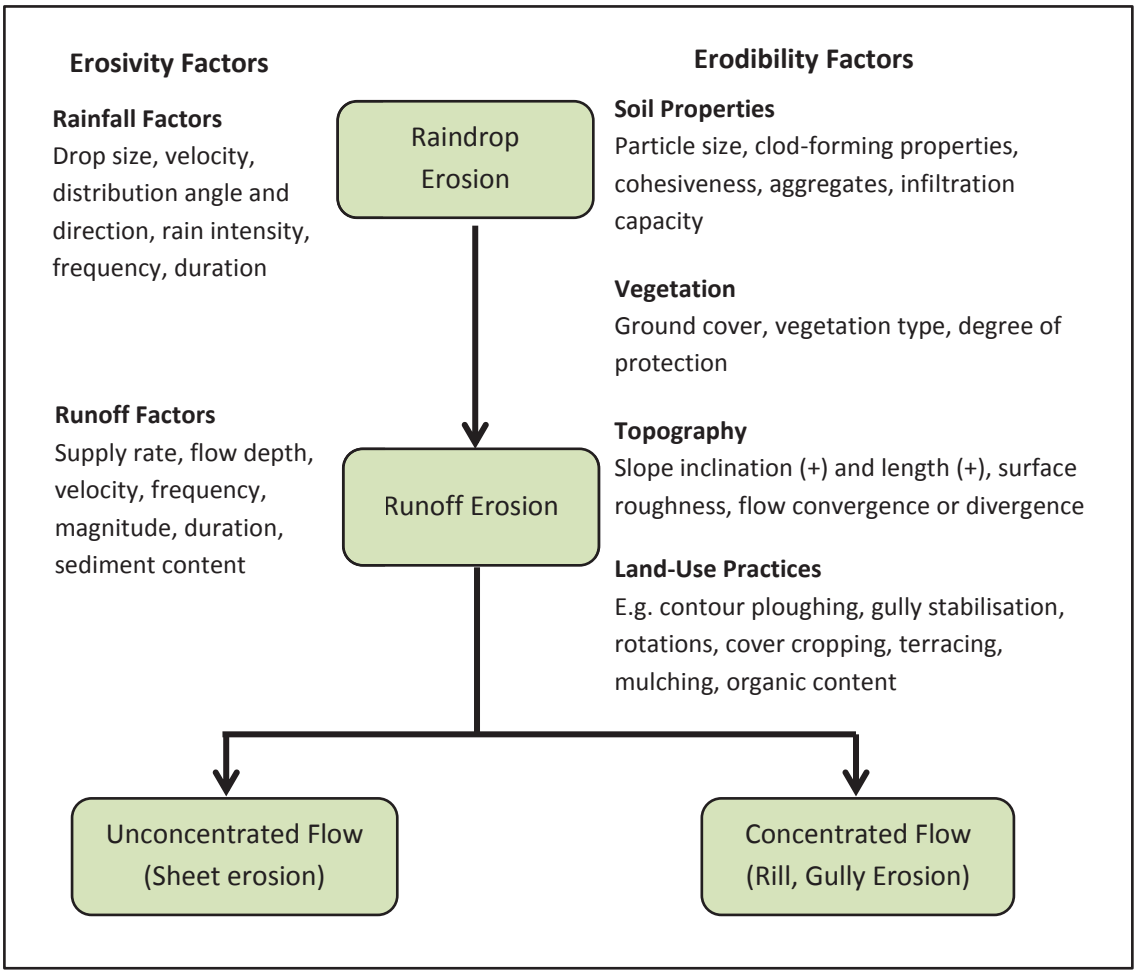

Fig. 8: *Summary of principal factors controlling water erosion on hillslopes and sedimentary yield to rivers, after Charlton (2008)*

Bank erosion is characteristically defined by immediate proximity to the channel and is a primary sediment generation mechanism in the floodplain environment where areas of unconsolidated material are available for transport. There are many variables that influence bank erosion (Table 3); cohesiveness, for example, is a significant conditioning feature of bank erosion, along with pore-water-pressure changes during repeated wetting and drying causing cracking and exfoliation. One such mechanism occurs during hydrograph recession when bank material becomes submerged during the high flow, but then loses the buttressing effect following receding flows while the material is still saturated, resulting in bank failure (Lawler *et al.*, 1997). Fluvial forces acting directly on the bank material cause lift and drag to occur, resulting in erosion and undercutting. Bank erosion can be greatly increased during such higher flows and flood events as have been documented in the Manawatu catchment during record-breaking rainfall, leading to wide-scale volumes of bank erosion in tributary rivers (Fuller and Heerdegen, 2005).

Table 3: *Factors influencing bank erosion (Lawler et al., 1997)*

Key processes	Factor
Subaerial processes	Microclimate – temperature
	Bank composition – silt/clay percentage
Fluvial processes	Stream power
	Shear stress – distribution due to primary currents
	Secondary currents
	Local slope
	Bend morphology – cross section, curvature
	Bank morphology
	Vegetation
	Bank moisture content
Mass failure	Bank height
	Bank angle
	Bank composition
	Bank moisture content – pore water pressure

Fine sediment (< 63 µm) will remain in transport for extended periods of time as '*suspended load*' since settling velocities decrease with grain size. The fine sediment will remain in suspension at very low velocities according to Stokes' Law, while sediment at very small grain sizes (< 1 µm) may not settle at all due to Brownian diffusion. Cohesiveness and inter-particle forces are increased in finer sediments and give rise to flocculation and accumulation, modifying deposition processes. This *washload* is regarded as having no interaction with the bed and channel form as it moves through the system, typical of clays; *throughput load* is material that moves through the system with some bed interaction; and *bed material load* is material that exchanges between bedload and suspension during movement (Naden, 2010).

Sediment storage increases downstream through reduction in stream power and provides a modulating effect on sediment transfer through the catchment (Davies and Korup, 2010). Storage occurs through the means of bars and bed storage within channel, as well as floodplain storage outside the channel. Remobilization of this material through scour and further erosion eventually transports sediment to discharge from the catchment, either dispersed into the ocean or deposited in estuarine or marine environments (Burt and Allison, 2010). Sediment will be deposited in the lee of morphological features like channel and point bars where shielding from the main current is sufficient. Development of pools and other flow features that produce dead zones allow settling out of sediment, and small-scale features such as pebble clusters, cobbles and vegetation provide spaces that allow for trapping of sediment (Cotton *et al.*, 2006, Naden, 2010). In gravel-bed channels, fine sediment often becomes trapped below an armour layer within the interstices of gravels and pebbles. In regard to the

washload, settling rates will allow fine sediment to remain entrained for a considerable time after threshold levels have lowered.

The falling limb of large flow events also gives rise to depositional features. As the water level recedes, sediment remains in thin veneers and localized puddles left from overwashing on bars and features not normally submerged. Higher flows additionally allow for significant deposition of sediment beyond the channel boundaries when the channel bank is breached in overbank flow, allowing the floodplain to be inundated with drapes of sediment that can vary in thickness significantly throughout the catchment (Trimble, 2010, Belyaev *et al.*, 2013). Storage times of sediment are highly variable and can occur for substantial lengths of time. Some may even be trapped in upstream sinks that effectively remove it from sediment transport. This occurs in environments such as lakes and dam reservoirs as well as floodplain storage, where it may remain for millennia. Sediment loss to the catchment occurs at or near the coastal zone by depositing in a delta, harbour or estuary, or moving out into the coastline and wider marine environment (Burt and Allison, 2010). Sediment loss from the catchment can also be referred to as the sediment yield and be derived from measurement and or estimation. This can have significant effects on the channel network.

Understanding this sediment transfer system, especially for a whole catchment, is difficult to determine accurately through traditional techniques. In-stream measurement techniques such as suspended sediment samplers fail to yield information on spatial distributions of erosion sources and processes contributing to the quantities. They are also difficult to extrapolate to whole system approaches without substantial increases in resource investment. Modelling techniques are very good for whole system approaches but still require the use of accurate measurements to calibrate and determine that the model is conceptually correct. Imagery techniques provide very good information for spatial contributions of some erosion sources, i.e. landscapes, but present significant issues of cost of up scaling and quantification of volumetric information without ‘on-the-ground’ measurements of depths across a variety of terrains. Alternative methods are required for application for whole system catchments and these are required to provide quick, efficient information, not only about spatial contribution and critical source areas of erosion, but also on the types of processes contributing to sediment erosion, and to provide that information at increasing resolutions.

2.4 Sediment Fingerprinting

2.4.1 Introduction

Sediment fingerprinting has developed as an alternative means of providing quantitative information on sediment providence and movement through a catchment (Walling, 2005). Development was stimulated by the limitations of traditional direct and indirect methods to provide the necessary information to understand sediment movement within a catchment. Indirect methods (e.g. mapping, erosion pins, photogrammetry) provide important information on sediment mobilization and erosion but do not necessarily relate to sediment flux downstream, while direct methods (e.g. sedigraphs and hysteretic loops) link sediment source and flux (Collins and Walling, 2004). Sediment fingerprinting represents a direct approach which developed momentum through the 1970s utilizing soil properties in the form of tracers to provide sediment source information (Walling, 2005).

Sediment fingerprinting relies on inferring the sediment source using multiple diagnostic properties that are inherent in each sediment type or source location and remain as a tracer of that sediment source through transport, providing the ability to distinguish and identify the locations where sediment is being supplied within catchments (Davis and Fox, 2009, Collins and Walling, 2002, Peart and Walling, 1986). The technique is therefore based on the following assumptions, which underly accurate quantitative ascription of sediment sources:

- The fingerprint is transported and deposited in association with sediment
- A fingerprint property should be able to distinguish between sediments derived from different source areas (e.g. topsoils and subsoils, different rock types, or land-uses) and/or different erosion processes (primarily distinguishing processes affecting surface or sub-surface materials)
- Selective erosion does not change the properties of the fingerprint, or if it does, only in a way that can be measured
- For a given source of sediment, which does not change through time, a sediment fingerprint signal must also be constant
- For a given source of sediment, which does not change along the transport pathway, a sediment fingerprint signal must also be constant along this pathway (i.e. there is no transformation along the transport pathway or after deposition).

Implementation of a quantitative source ascription is composed of several fundamental steps: first, selecting one or more properties that uniquely characterize sediment from a particular source; second, comparing these properties with samples from sediment deposited and actively transported downstream; finally using a mixing model to determine source contributions (Foster and Lees, 2000, Collins *et al.*, 1998, Walling, 2005). Implementing these steps requires a variety of tools including field collection of samples, laboratory preparation and analysis, followed by statistical work to render and resolve valid information (Davis and Fox, 2009). Sediment fingerprinting presents itself then as a powerful tool that can be rapidly applied for a range of time scales and use a mix of different tracers. The development of sediment fingerprinting has extended to numerous geochemical tracers and at a wide range of sedimentary environments at varying spatial and temporal scales (Foster and Lees, 2000, D'Haen *et al.*, 2012). These applications have consisted of atmospheric and hydrological tracers, soil erosion and hillslope processes, fluvial sediments, coastal transport, and palaeo-environmental (Foster and Lees, 2000). The following review centres mainly on tracers used in fluvial sediments. For this, it is important to get an appreciation of the large suite of tracers that have been employed throughout literature and their various applications for each environment.

Sediment fingerprints have included colour, mineralogy, geochemistry, mineral magnetism, radionuclides, stable isotopes, and biogenetic properties as the most prominent to date (Foster and Lees, 2000, D'Haen *et al.*, 2012). Physical tracers were some of the earliest tracers used for identifying sources and have also been some of the simplest. These studies used colour (e.g. Grimshaw and Lewin, 1980, Peart, 1993) and clast characteristics such as lithology, morphology, and grain-size distributions, the latter more commonly for coarse deposits (D'Haen *et al.*, 2012). These early tracers are not commonly used in today's sediment fingerprinting research but geochemical (e.g. Wall and Wilding, 1976, Grigsby, 1992), mineralogical (e.g. Klages and Hsieh, 1975), and mineral magnetic tracers (e.g. Walling *et al.*, 1979, Oldfield *et al.*, 1978, Oldfield *et al.*, 1979, Caitcheon, 1993) used in early work have all provided successful sediment source ascriptions and continue to be among the main tracers still used today.

Tracer selection is highly site specific as there is no globally applicable tracer or composite fingerprint (Collins and Walling, 2002). Tracer selection will depend on the objective of the study, the specific environment being studied, the array of processes operating in the catchment and, of course, the resources available (time, money, equipment, etc.). A focus on spatial patterns, for example, is likely to require a different set of tracers compared with a

study focused on the key processes producing sediment. The wide range of tracers that have been employed for sediment fingerprinting studies internationally is too large to cover within this review; however, a summary of each study, the types of sediment sources, tracers, and analyses employed, as well as the key outcomes, is tabulated in Appendix A.

In most cases, geology will be the key underpinning variable that will determine the sediment properties and the tracers used in a fingerprint. Mineralogy is considered relatively stable and robust for distinguishing sediment sources based on geology (Koiter *et al.*, 2013b). Sub-catchments that have distinct geologies will likely show discrimination using mineralogy and, by extension, geochemical analysis, due to the base signals originating from these distinct geological components. Mineralogy has typically been used for coarser sediment fractions applied at bulk, specific mineral, and individual grain analysis (e.g. Arribas *et al.*, 2000, Ergin *et al.*, 2007, Sabeen *et al.*, 2002). Heavy mineral analysis (HMA) is widely used due to its advantages in providing a wide spectrum of specific minerals (e.g. garnet), allowing for greater constraints on source provenance, particularly for sedimentary environments, and focuses on 20 μm – 200 μm fraction where heavy minerals are most highly concentrated (Dill, 1998, Morton and Hallsworth, 1999, von Eynatten and Gaupp, 1999).

In finer sediment fractions clay minerals provide the opportunity for differentiation (e.g. Klages and Hsieh, 1975, Gingele and De Deckker, 2005). Successful mineralogy source determination relies on a strong relationship between mineralogy and the parent geological source, and quantitative determination is based on both the ability of source rocks to produce consistent detrital grain assemblages and the degree to which climate dilutes some minerals, i.e. carbonate rocks (Arribas *et al.*, 2000). Gingele and De Deckker (2005) used clay because the $^{87}Sr/^{86}Sr$ ratios indicated the clays were inherited from the diverse rock formations in the catchment headwaters. Their work identified four types of clay; smectite, illite, kaolinite, and chlorite, as well as geochemical analysis that corroborated the identity of clay minerals (Fig. 9). Klages and Hsieh (1975) used a clay analysis to deduce that erosion sources had remained the same over a long time due to similarity of the clays to the floodplain material. Potential issues relate to extremely mature mineral associations, preferential weathering and erosion, mechanical breakdown, hydraulic processes, and burial digenesis, which may overprint the original provenance signal (Morton and Hallsworth, 1999, von Eynatten and Gaupp, 1999, Rhoton *et al.*, 2008).

Geochemical analysis of minor element constituents of minerals has become a widely used fingerprinting technique (Grigsby, 1992, D'Haen *et al.*, 2012, Minella *et al.*, 2008, Collins and

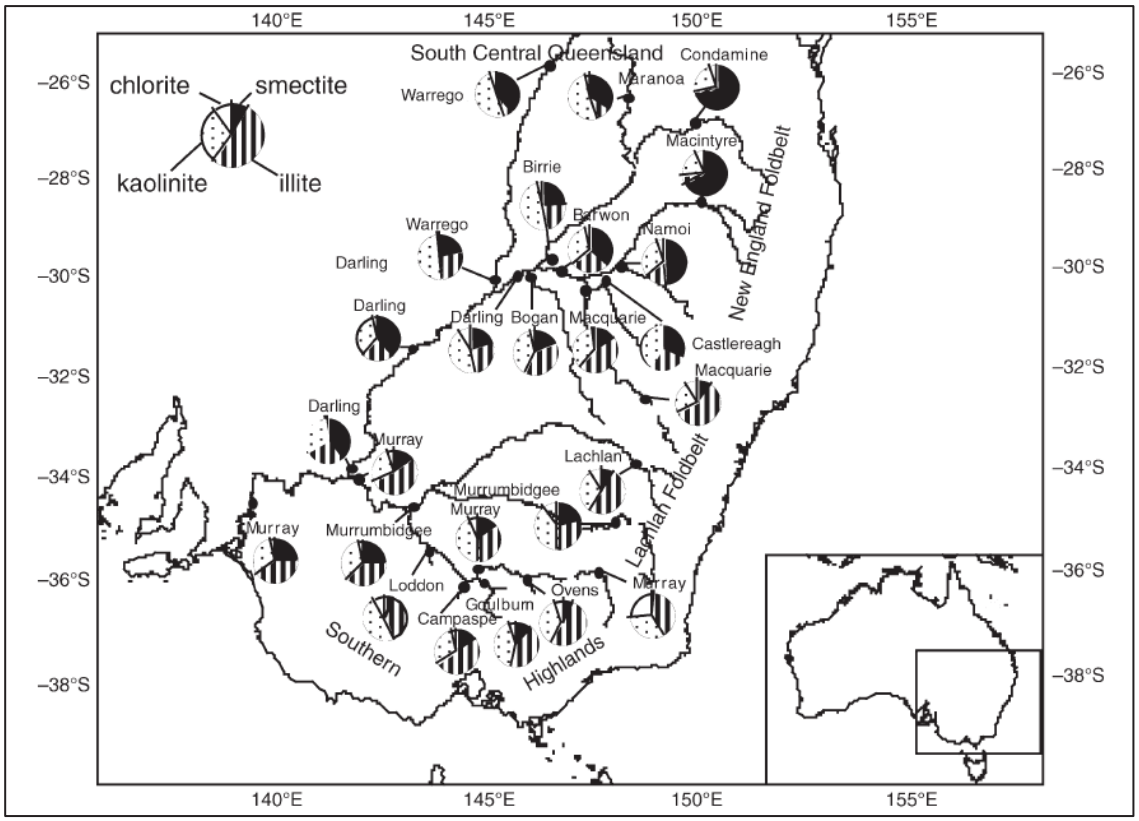

Fig. 9: *Location of investigation area and clay mineral compositions of sediments in the major tributaries of the Murray-Darling Basin from Gingele and De Deckker (2005)*

Walling, 2002). Geochemical analysis can allow minerals to be further differentiated beyond simple mineral classification. Major, minor, and Rare Earth Elements (REE's) can potentially be used as a tracer for fingerprinting; the exact elements will depend on specific catchment properties. Elements typically targeted include Ag, Al, As, Ca, Ce, Co, Cr, Cu, Fe, K, La, Mg, Mn, Na, Ni, Pb, S, Si, Sr, Ti, Y, Zn, as well as inorganic C, N, and P (Davis and Fox, 2009). Different igneous rocks comprise different minerals and geochemical composition as a result of different parental magmas and crystallisation histories and therefore provide potential for geochemical fingerprinting. Sedimentary rock types will also show variations and can be differentiated by the ratios of trace elements such as Th/U, La/Sc, Sc/Th, Cr/Th, Co/Th, Eu/Eu* for their respective geochemical behaviours (Kasanzu *et al.*, 2008). The large number of possible elements allows this approach to be the basis of multivariate approaches utilizing a large suite of tracers and employing statistics to render the most appropriate elements as opposed to relying on specific soil-environmental approaches to target particular elements (Davis and Fox, 2009). The geochemical compositions can be looked at as a bulk analysis, particle-size fractions, specific geochemical compositions of light or heavy minerals, or looking at ratios of specific element combinations (D'Haen *et al.*, 2012, Morton and Hallsworth, 1999).

Isotopic ratios (e.g. $^{87}Sr/^{86}Sr$) also provide information on geologic sources e.g. Douglas *et al.* (1995) and Gingele and De Deckker (2005). Isotope ratios can vary based on the environment in which they were formed, and can remain stable, be produced from fractionation processes in the soil, or be radiogenic, derived from radioactive decay of radionuclides but may not be radioactive themselves (Davis and Fox, 2009, Gingele and De Deckker, 2005). Radiogenic isotopes are influenced by the source igneous rock genesis; the most common radiogenic isotopes include $^{87}Sr/^{86}Sr$, $^{208}Pb/^{204}Pb$, and $^{143}Nd/^{144}Nd$, while the most common stable isotope ratios include $\delta^{18}O$, $\delta^{15}N$, $\delta^{13}C$, and $\delta^{66}Zn$. Radioactive decay of ^{87}Rb produces ^{87}Sr which when compared to naturally occurring ^{86}Sr can give a unique signature based on different mineral ages. Isotopes of N and P are associated heavily with the organic content, so $\delta^{15}N$ and $\delta^{13}C$ are well suited to changes in land-use (Alt-Epping *et al.*, 2009, Fox and Papanicolaou, 2008a).

Often geology is not exclusively defined within sub-catchments or catchments contain relatively homogeneous geologies. It has been suggested that mineralogy and geochemical signals based on geology may not be sufficient to discriminate sources in this context. Mineral magnetism has been proposed to be a possible solution by Hatfield and Maher (2009). Mineral magnetism is primarily controlled by mineral components but possibly allows for a greater sensitivity to subtle differences. Greater sensitivity, together with a capability to analyse in several dimensions through a simple suite of mineral magnetic scans could give mineral magnetism tracers a capacity to resolve geologies that are too homogeneous for mineralogy and geochemical analysis, (Hatfield and Maher, 2009, Hatfield and Maher, 2008, Caitcheon, 1998).

The suite of common magnetic analysis includes magnetic susceptibility (χ), frequency dependent susceptibility (χ_{fd}), and isothermal remanent magnetisation (IRM) for sediment fingerprinting (Walden *et al.*, 1997, Caitcheon, 1993, Walling *et al.*, 1979, Oldfield *et al.*, 1979). The main controls exerted on a mineral magnetic signature relate to primary magnetic mineralogy, magnetic grain size, the particle size of the transported sediment, diagenitic changes in source materials and deposited sediments, in addition to a range of effects attributed to anthropogenic inputs, all of which can be non-destructively analysed in several of the dimensions (Foster *et al.*, 1998, Hatfield and Maher, 2009). Using mineral magnetism, Zhang *et al.* (2008) demonstrated clear discrimination between sediment sources from the Yellow and Yangtze rivers. Compared with the Yellow River, the Yangtze River typically contained higher ferrimagnetic mineral contents and ferrimagnetic to antiferromagentic ratios, which were attributed to lithology and weathering effects. Issues still need to be addressed concerning unknown effects of mechanisms that could complicate the interpretation of the

results, i.e. hydrodynamic sorting, post-depositional diagenesis, and authigenesis, which make derivation of definitive results difficult (Zhang *et al.*, 2008).

Land-use differentiation provides a second major variable for discrimination sources, which is overprinted on geological source signals. Specific geochemical tracers can indicate these post-formation signals and provide a wide range of elements for consideration. Agriculture practices can vary significantly, which can allow good fingerprinting signals for discrimination. Practices such as the application of manure or fertiliser can cause elevated concentrations of P, K, Ca, and Na, generating relatively higher concentrations in cultivated soils compared with uncultivated soils and even more so than with sub-soils. In some instances, elevated concentrations of Ca have been used to distinguish particularly poorly managed soils due to heavy applications of lime (Minella *et al.*, 2008). Fe, Zn, and Cu also exhibit significant contrasts in land-use studies, and saturated soils tend to have an accumulation of Mn, which is thought to be an indicator of soils derived from channel banks (Minella *et al.*, 2008). Regardless, the binding strength of fertilizer derived elements to sediment particles and their subsequent influence on sediment fingerprinting is poorly understood. The exact land-use units used will vary between studies, as they can be specific to the study catchment or the tracer being employed. Generally, despite the varied land-uses, categories commonly employed in literature include uncultivated agriculture (pasture), cultivated agriculture (crops) subsurface (channel banks, gully walls), forest, road sediments, and urban influences (Table 4). Owens *et al.* (2001) have shown the increase in urban and industrial influences by increasing associated contaminants such as P, Cr and PCBs downstream of urban centres. Some research using mineral magnetism has even shown promise in discriminating sediment influences from burnt soil following wildfires, known to increase soil magnetic susceptibility (Blake *et al.*, 2006, Oldfield and Crowther, 2007).

Biogeochemical fingerprinting relies primarily on organic C, N, and P as key indicators of influences on organic matter variables, which are highly spatially variable, in part as a result of land-use practices (fertilizer, tillage, water content, livestock inputs) (Davis and Fox, 2009, D'Haen *et al.*, 2012). This high spatial variability increases the tracers' discriminating potential for higher resolution studies. However, enrichment, depletion, and decomposition issues are the main causes of concern because microbial activity can significantly alter the tracer property. Isotopes of C, N, and P (e.g. $\delta^{15}N$ and $\delta^{13}C$) can also indicate agricultural management practices that offer sensitivity to differences in nitrogen and carbon cycles (Fig. 10), and processes that break up aggregates and expose labile organic matter (Davis and Fox, 2009, Fox and Papanicolaou, 2008a). Fox and Papanicolaou (2008a) reported that 63.5% of the

isotopic variability was attributed to land management and practices involving fertilizers, plant harvest, and mineralization processes. Recent research (e.g. Gibbs, 2008, Blake *et al.*, 2012, Hancock and Revill, 2013) has focused on the use of compound-specific stable isotopes in the form of fatty acid biomarkers, which have the potential to show very high land-use-specific discrimination.

Table 4: *Common land-use categories in fingerprinting studies*

Study	Land-use categories
Carter *et al.* (2003)	Forested, uncultivated agriculture, cultivated agriculture/cropping, channel banks
Minella *et al.* (2008)	Cultivated agriculture, fallow cultivated agriculture, pasture agriculture, eroding channel banks, unpaved roads
Collins *et al.* (2001)	Surface soils and subsurface soils, communal and commercial agriculture, stream banks and gullies
de Boer and Crosby (1995)	Agricultural (cereal grain) and forest
Gruszowski *et al.* (2003)	Top soil, subsoil, channel banks, roads
Krause *et al.* (2003)	Pasture agriculture, eroding gully walls, roads
Motha *et al.* (2002),	Gravel-surfaced-roads, un-gravelled roads, pasturelands, cultivated lands, and undisturbed forests
Wallbrink *et al.* (1998)	Forest, pasture agriculture, cultivated agriculture, and eroding gullies/ streambanks

Radionuclides, particularly the Fallout Radionuclides (FRN's) Caesium-137 (^{137}Cs), Berrylium-7 (^{7}Be), and Lead-210_{ex} ($^{210}Pb_{ex}$), have possibly been one of the most powerful additions to the tracer repertoire and have proved very useful indicators for differentiating between surface and subsurface sources and between cultivated and uncultivated land types (Wallbrink *et al.*, 1998, Walling, 2005). They are effective for source discrimination because of the unique origin of their signal. Radionuclides are radioactive isotopes of elements that emit radiation in a process known as radioactive decay. Radioactive decay rates vary depending on the radionuclide and type of radiation emitted which in turn influences the measured radionuclide concentrations and resultant daughter isotopes. Radionuclides – primordial, secondary, and cosmogenic – can occur naturally. Primordial radionuclides were formed from the beginning of time, and exist today due to their extremely long half-lives, i.e. Uranium – 238 (^{238}U). Secondary radionuclides are formed from radioactive decay from primordial radionuclides, i.e. $^{210}Pb_{ex}$, which is a product of the uranium decay series from the decay of escaped Radon-222 (Rn^{222}) gas in the atmosphere and subsequently washed out of the atmosphere and incorporated into young sediments. Cosmogenic radionuclides form from cosmic rays

bombarding the earth and causing 'cosmic ray spallation' when they collide with isotopes, i.e. colliding with oxygen or nitrogen can produce ^{7}Be. Radionuclides can also be produced artificially from thermonuclear activities, for example, atmospheric nuclear testing, particularly during the 1960s and the 1986 Chernobyl incident have resulted in ^{137}Cs signatures in sediments (Mabit *et al.*, 2008, Nichols *et al.*, 2002).

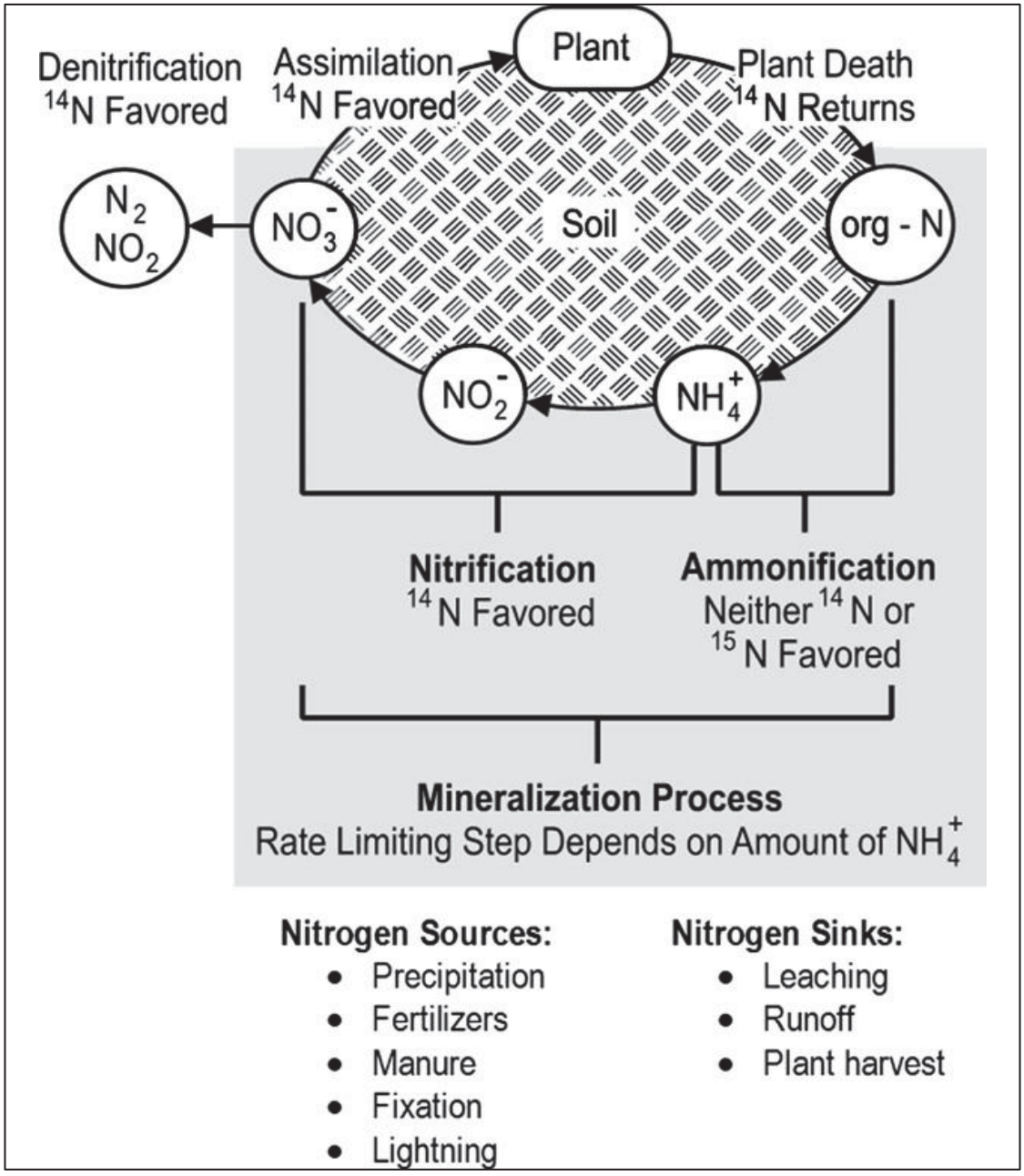

Fig. 10: *δ15N cycle for soil–plant–atmosphere system (Fox and Papanicolaou, 2008a)*

These characteristics allow radionuclides to be largely independent from source geology and soil composition, meaning their deposition has strong spatial patterns linked to precipitation and their surface deposition, strong adhesion to soil particles, varying half-lives, and penetration depth that allows for significant soil profile variability (Mabit *et al.*, 2008, Roddy, 2010, Wallbrink *et al.*, 1998, Davis and Fox, 2009, Nichols *et al.*, 2002). FRN are the most extensively utilized radionuclides for sediment fingerprinting research, particularly ^{137}Cs, but also $^{210}Pb_{ex}$ and ^{7}Be, with 30.2 years, 22.3 years and 53.3 days respectively (Mabit *et al.*, 2008).

Applications have focused both on bulk quantities and on particular concentrations in specific grains, size fractions or by ratios between samples. The appropriate radionuclide used will depend on the research site, as FRN's can vary strongly with rainfall and immediate atmospheric patterns following production. For example, ^{137}Cs, exhibits a strong latitudinal distribution due to the location of the atomic activities. The time frame of study will determine the radionuclide that is targeted, in that ^{7}Be is very short so is often limited to < 6 months analysis, whereas ^{10}Be and ^{26}Al can be used for 10^3 to 10^5 year time-scales (Mabit *et al.*, 2008, Nichols *et al.*, 2002). Other radionuclides that have been commonly used include ^{226}Rn, ^{226}Ra, ^{228}Rn ^{207}Pb, ^{208}Pb, and ^{90}Sr. Wallbrink *et al.* (1998) have illustrated that the highest surface

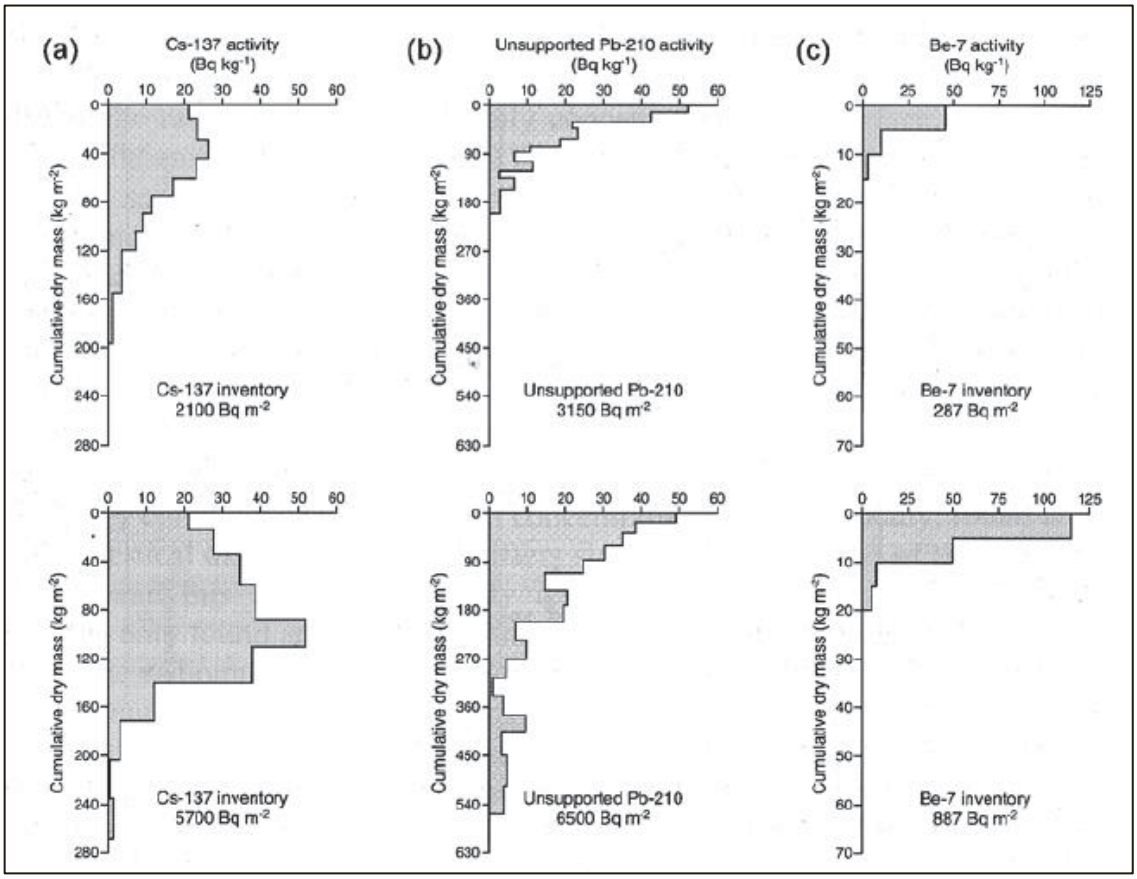

Fig. 11: *Example of depth penetration characteristics down a soil profile (as measured by cumulative dry mass) of ^{137}Cs, ^{210}Pb, and ^{7}Be in undisturbed (top row) and cultivated (bottom row) soils (Walling 2002)*

concentrations of ^{137}Cs and ^{210}Pb have been in uncultivated soil, followed by cultivated soil, with very low concentrations occurring in the sub-surface sediments (Fig. 11). The cultivated land values were higher than imagined but were attributed to the type of ploughing common in the area causing relatively little vertical mixing. A potential issue however relates to agricultural rotation which can diminish the ability for FRN's to discriminate land-use. ^{137}Cs has provided the best use as a medium-term tracer, along with $^{210}Pb_{ex}$ and its parent ^{226}Ra (Mabit *et al.*, 2008).

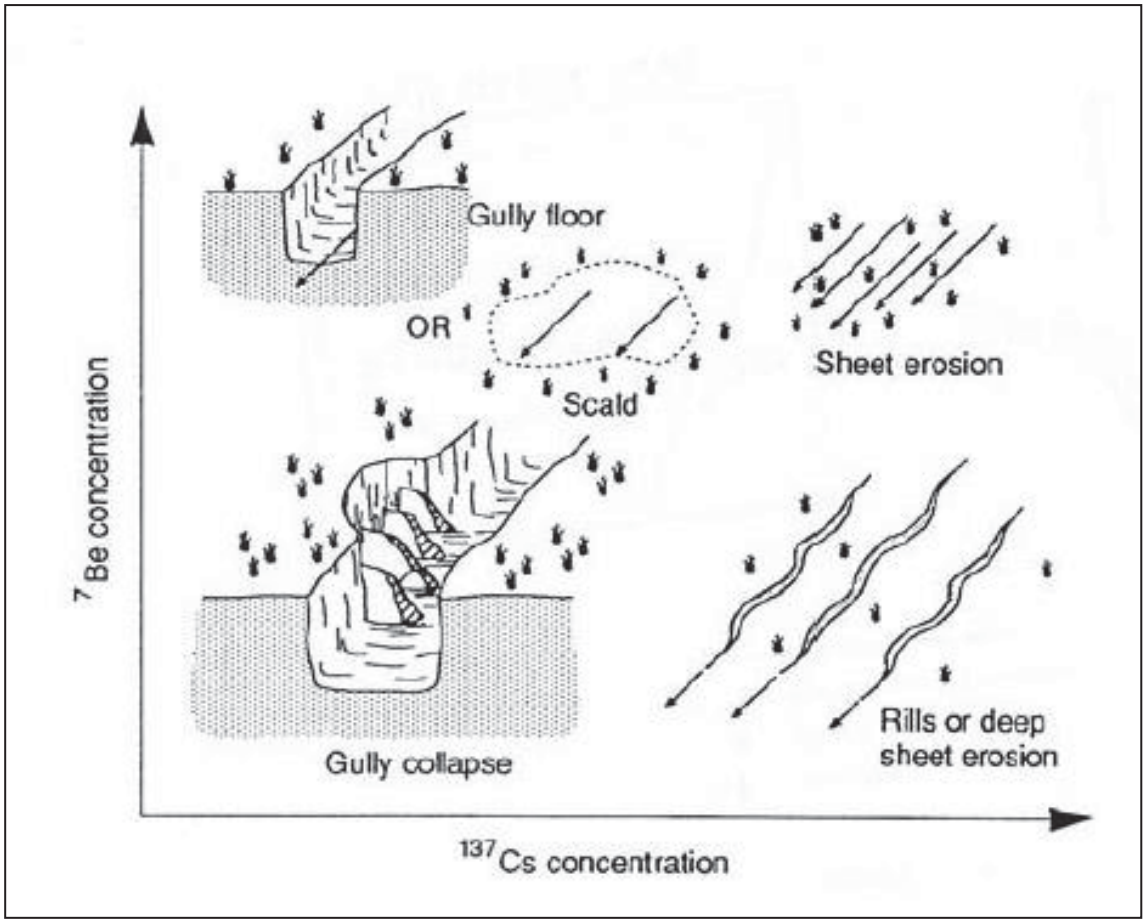

Fig. 12: *Sediment source labelling from ^{137}Cs and ^{7}Be depth ratios (Wallbrink and Murray, 1993)*

^{7}Be provides a very good short-term tracer of single events due to its short half-life, which precludes it from penetrating the soil profile (Mabit *et al.*, 2008, Walling, 2013). Used in conjunction with other radionuclides it is possible to be able to differentiate the subsurface-derived sediment through the lower concentrations in the subsurface material (Fig. 12). This has allowed some studies to identify which processes contribute most sediment. This is even more useful when strong connections between process and land-use or geology occur. The ability to identify subsurface material has also been shown to differentiate material during

flood events, as illustrated by Wallbrink et al. (1998), who found lower concentrations of ^{137}Cs in flood sediments compared with sediments from low flow events. Other studies have indicated that during the winter season and associated flood events, sediment sources located further from streams are active, while in summer low flow conditions, in-channel sources are of greater significance (Krein *et al.*, 2003). Belmont *et al.* (2014) also used ^{10}Be, $^{210}Pb_{ex}$, and ^{137}Cs to distinguish between and estimate channel–floodplain exchange.

2.4.2 Quantitative Sediment Fingerprinting

Development in sediment fingerprinting undertook a significant shift when it moved from qualitative to quantitative source ascription and the ability to differentiate multiple sources (Krause *et al.*, 2003, Collins *et al.*, 1997, Walling, 2005, Walling *et al.*, 1993). This shift saw the introduction of vital developments in the fingerprinting approach: the introduction of multivariate or composite fingerprints; the use of quantitative mixing models; and a heavy reliance on statistical discrimination and optimization (Walling, 2005). Early sediment fingerprinting work was optimistic about finding a single property that would be universally applicable, but the realization that quantitative source ascription was unlikely in this manner shifted focus to using several combined sediment properties (Walling, 2005, Peart and Walling, 1986, Collins and Walling, 2002). Single tracers amplify a significant problem – if the tracer signature matches two difference sources, or the combination of two sources is similar to a third source, source ascription is problematic (Collins and Walling, 2002, Small *et al.*, 2002). It is very difficult to know whether this is occurring but by increasing the combination of tracers, unsuitable tracers are more readily identified.

The composite of tracers used will frequently vary between studies, due to the highly site-specific nature of discriminatory tracers, and can be either a subset of properties (e.g. inorganic elements) or, often, a combination of different properties, e.g. inorganic elements, magnetic signals, radionuclides, and biogenic properties (Collins *et al.*, 1998, Collins and Walling, 2002). Therefore recent fingerprint studies generally analyse a large suite of tracers, which means the ability to detect and analyse a large range of tracers has become particularly useful. Inorganic tracers have recently benefited particularly well in this area; XRF, and more recently ICP-MS, have made it possible to scan a full suite of 70+ elements in a matter of seconds. Precision has increased significantly and detection limits of parts per billion (ppb) are comfortably achieved; for many elements even parts per trillion (ppt) are now achievable. Sample preparation for these analyses has traditionally been a lengthy process involving acid

digestions to dissolve samples. However, ICP-MS can add a laser ablation unit (LA-ICP-MS) to analyse solid samples directly, greatly improving the time efficiency of the procedure and allowing for more direct analysis of materials.

The ability to rapidly obtain large arrays of geochemical concentrations can generate too much information to directly comprehend and creates a statistical problem whereby data reduction techniques are required to avoid over-determination and multi-collinearity issues. To begin data reduction, a few statistical approaches have been used to assess the variance of individual tracers: the Tukey test has been used for normal distributed data; the Mann-Whitney U-test for use between two sources (e.g. Carter *et al.*, 2003); and the Kruskal-Wallis H test for multiple-source variations (Collins *et al.*, 1998). The objective of these discrimination approaches is to determine whether the tracer provides any discriminatory power for an optimal tracer suite (Davis and Fox, 2009, D'Haen *et al.*, 2012), after which suitable tracers undergo discriminant function analysis (DFA) to minimize the number of tracers. This has become an important step in determining source estimations for multivariate fingerprinting. Principal component analysis (PCA), can also be used to explore tracer suitability and is based on the same functions as DFA, however does not incorporate prior knowledge of the source groups, but instead will provide information on variability within the data set and their relationship to the variables. However, a purely statistical approach to tracer selection does not in itself provide selection criteria to take into account actual sediment and behaviour from a geochemical perspective, an area which needs further attention.

Source ascription is the final step in sediment fingerprinting, which has been restricted to a qualitative assessment of sediment sources for the mainstay of sediment fingerprinting research (Walling, 2005). Binary and ternary plots provide useful indications and are particularly effective as a visual aid in identifying key sources of sediment (Fig. 13). However, quantifiable information is much more beneficial, and an increased amount of information (sources and tracers) to process makes visual appraisal much more difficult. Although these qualitative forms are still useful, particularly for early explorative investigation, sediment mixing models have become the dominant tool for apportioning sediment sources employing a variety of Bayesian and frequentist approaches (Cooper *et al.*, 2014).

Frequentist mixing models commonly rely on minimization of the sum of squared residuals for a combination of linear equations created for each tracer variable in order to arrive at the most likely estimations which satisfy geochemical concentrations. The mixing model will

determine the proportion of sediment (*P*) with source tracer concentration (*S*) that causes the sample tracer concentration (*C*). The basic component is

$$C_i = P_j S_{ij} + E \quad \text{(Eq. 1)}$$

where *i* and *j* are the tracer and source type respectively and (*E*) is an error correction (D'Haen *et al.*, 2012, Small *et al.*, 2002). Collins *et al.* (1998) employed the following mixing model, which also included correction factors for organic matter (O) particle size (Z) and a weighting (W) that applied to each unique tracer (i) based on its precision:

$$\sum_{i=1}^{n} \left\{ \left(C_i - \left(P_{g1} S_{ig1} Z_{g1} O_{g1} + P_{g2} S_{ig2} Z_{g2} O_{g2} + P_{g3} S_{ig3} Z_{g3} O_{g3} \right) \right) / C_i \right\}^2 W_i \quad \text{(Eq. 2)}$$

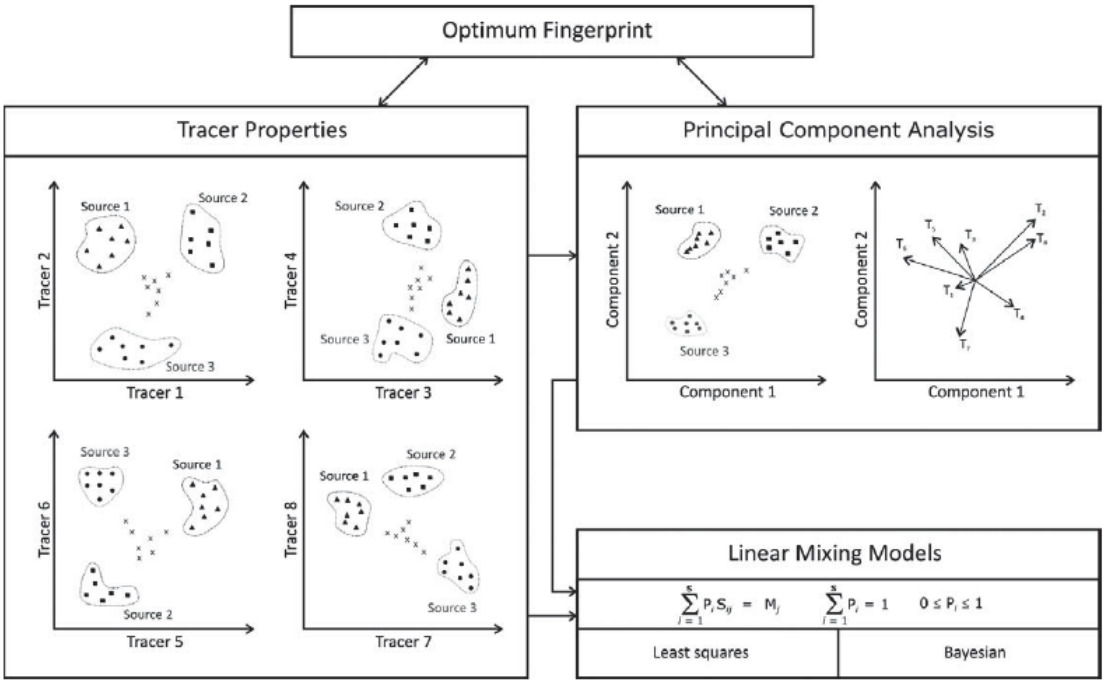

Fig. 13: *Overview of approaches used to gain provenance information from tracers (D'Haen et al., 2012)*

These mixing models are required to obey two key constraints: 1) each source input (P_g) must be positive; 2) the sum of the source contributions must total to one. Some models have incorporated correction factors to address enrichment and depletion which has been caused as a result of organic and particle size effects. There are concerns that some of these correction factors are causing unexplored errors and result in a reduction of model accuracy (Smith and Blake, 2014, Laceby and Olley, 2015), e.g. particle corrections that assume a linear

relationship of surface area between sediment and source samples (Koiter *et al.*, 2013b, Russell *et al.*, 2001). Conversely, recent research by Pulley *et al.* (2015) has also shown that incorporation of these correction factors does not necessarily increase uncertainty .

Techniques such as Monte Carlo (e.g. Blake *et al.*, 2012, Krause *et al.*, 2003, Wilkinson *et al.*, 2013) and Markov Chain Monte Carlo (MCMC) simulations (e.g. Fox and Papanicolaou, 2008b) can be used to improve quantitative estimate uncertainties. Small *et al.* (2002) addressed this uncertainty by using MCMC to explore the sampling procedure. Sampling procedures can easily fail to characterise the true variability, and present issues for multivariate mixing models which use mean/median values. This has given rise to recent increase in the range of models and model variations being investigated. In addition to the well-used Collins model (Collins *et al.*, 2010a) which uses calculated trace values derived from mean and standard deviations, other models have included; the modified Hughes model (Hughes *et al.*, 2009) which utilizes measured fingerprint properties of replicated samples, a correlated distribution model which re-incorporates correlations between tracer concentrations in order to handle correlations during Monte Carlo sampling (Laceby and Olley, 2015); the Landwehr model (Devereux *et al.*, 2010, Gellis *et al.*, 2009) which operates similar to the Collins model (Haddadchi *et al.*, 2014). Haddadchi *et al.* (2014) found that the distribution model after Laceby and Olley (2015) provided the most accurate estimates when applied to artificially mixed sediment samples with a Mean Absolute Error (MAE) = 10.8% and standard error (SE) = 0.9%), followed by the Modified Hughes (MAE = 13.5%, SE = 1.1%), Landwehr (MAE = 19%, SE = 1.7) and Collins models (MAE = 29%, SE = 2.1%). Despite this, the Modified Hughes was the most accurate source contribution predictor with 5.4% error followed by the Distribution model (MAE = 6.1%), Landwehr model (MAE = 7.8%) and the Collins model (MAE = 28.3%) (Haddadchi *et al.*, 2014). The advantage of the Laceby distribution model is the reintroduction of the correlations between elements which are lost in standard distribution modelling (Laceby and Olley, 2015).

Alternatively, studies can employ the use of Bayesian statistics which are able to incorporate known and residual uncertainties into a mixing model a lot more consistently than frequentists approach and have provided valuable information on the uncertainties. Cooper *et al.* (2014) was able to use 13 versions of a Bayesian mixing model to demonstrate the sensitivity of the mixing model for different error assumptions and model structures. The models all attributed the subsurface material as the dominant contributor, but did vary by as much as 21% for some source proportions between model versions. Nosrati *et al.* (2014) also showed significant uncertainties of 2–24% for rangeland, 1–26% for orchards and 66–83% for stream banks respectively.

2.4.3 Challenges within Sediment Fingerprinting

Regardless of the research focus or tracers selected, there are many challenges common to all fingerprinting research which needs to be carefully considered. Most of these issues have been around since early studies using colour (e.g. Moore, 1961, Grimshaw and Lewin, 1980, Peart, 1993), magnetism (e.g. Walling *et al.*, 1979, Oldfield *et al.*, 1979, Peart and Walling, 1986) and geochemistry (e.g. Peart and Walling, 1986). Although early work showed great potential, that early research recognized a need for more sophisticated techniques to reach higher levels of precision and resolution in discrimination (Grimshaw and Lewin, 1980), and also a need for an increased standardization of the technique. Many of these issues relate to the ability of tracers to represent the soil fraction by their tracer behaviour and accounting for unknown behaviours which are outlined in Table 5.

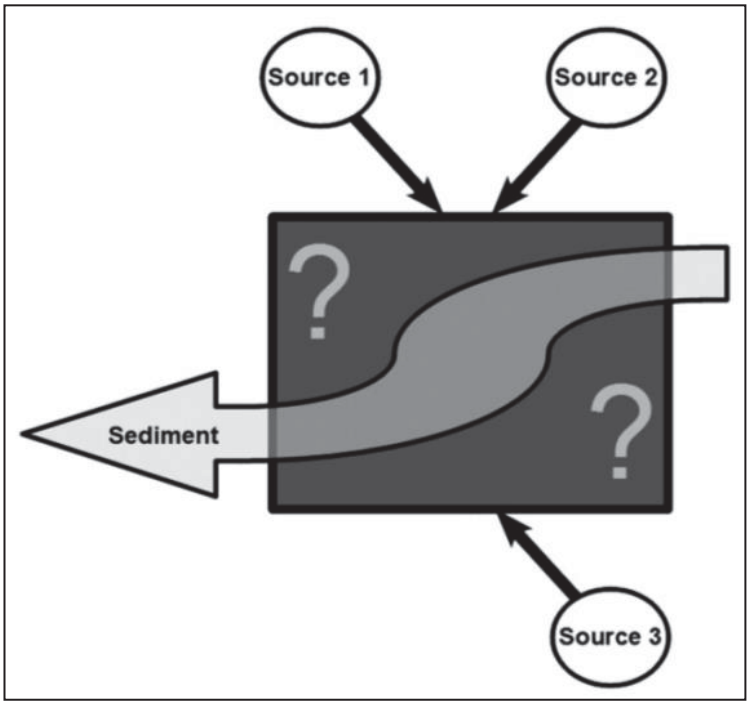

Fig. 14: *Black box approach demonstrating gap of understanding in the processes between source and sediment and how they may alter sediment tracer values (Koiter et al., 2013b)*

Uncertainties can be dealt with under the broad area of tracer conservativeness, which is essential for quantitative source ascription. Failure to address these issues adequately may compromise the accuracy of sediment fingerprinting studies in agricultural catchments (Smith and Blake, 2014). Conservativeness may be subject either to how the tracer itself is applied or used in the research, or to the conditions surrounding it, which may influence the signal. The conservativeness of the fingerprint therefore relates primarily to how the tracer(s) behaves, interacts or is influenced by the environment it is in and how well the original signal is retained through transport (Motha *et al.*, 2002). This is an essential consideration during method development and selection of sediment fingerprint tracers, yet it is one of the most poorly understood areas of sediment fingerprinting. Koiter *et al.* (2013b) illustrates this with a 'black-box' approach: while the sediment source inputs and collected sediment outputs are understood, there is very little

understanding of the processes occurring in between (the black-box) that may change or modify sediment properties (Fig. 14). If the behaviour of a tracer within the transport environment is not known or understood, the credibility of the conclusions can be compromised. Some tracers that received attention in early studies lost favour when it was realized they exhibited a non-conservative behaviour, a behaviour likely to be repeated by other apparently conservative tracers selected in future studies. Physical tracers in particular (i.e. colour, density, and particle size) were more prone to being non-conservative and are examples of less-used tracers today (Davis and Fox, 2009). Colour was used optimistically in early work as a tracer, but was found to change due to the moisture content of the sediment and interaction with tracers (Davis and Fox, 2009).

Ideally, tracer concentrations do not change over time; however, many tracers will have some degree of change that must be evaluated and accounted for when comparing source and sediment (Motha *et al.*, 2002). Sediment signatures can change through chemical and biological influences as the tracer interacts with the surrounding environment, particularly when there are significant changes to the environment which expose the sediment to new chemical influences e.g. movement from the hillslope to the fluvial channel (Koiter *et al.*, 2013b). Water chemistry changes, for example, can cause pH and redox conditions, ion exchange, dissolution, and microbial activity (Peart and Walling, 1986). Variations in a tracer's signal can occur at all stages of transport – at source, during transport, or during the post-deposition phase (D'Haen *et al.*, 2012, Motha *et al.*, 2002), and each stage must be assessed for what direct or indirect effects could disturb the signal. If that tracer is to be used, identification of the changes must then be measured or somehow accounted for (Davis and Fox, 2009). Many geochemical tracers, i.e. P, K, Na, Ca, Mn, Zr, Ti, Hf, Sn, Cs, and Rb have an advantage of a close association with clay minerals and are often regarded as conservative (Gingele and De Deckker, 2005, Minella *et al.*, 2008). However, the exact association provides relevant information for evaluating how conservative the tracer behaves. Phosphorus can be heavily affected by biochemical processes and influence the concentration through inputs from sewage treatment works, but is very stable within mineral formation (Withers and Jarvie, 2008, Koiter *et al.*, 2013b). Solubility of trace elements and Rare Earth Elements (REE) are often relatively low, so the effect of weathering is negated to a degree, and bolstered by use of ratios that have been noted to typically match source rocks (Kasanzu *et al.*, 2008). It has also been suggested that even though weathering takes place, losses and gains to the system do not actually occur, so REE patterns stay relatively the same from source rock to soil (Lee *et al.*, 2008). There is a lack of understanding regarding the source of the observed geochemical

signatures, especially from sedimentary material, which limits conclusive explanations. Thorough knowledge of the mineral assemblages which give rise to the geochemical concentrations may provide necessary information in order to justify and qualify the geochemical sediment signatures (Vale *et al.*, 2016b).

Whether change to a tracer concentration is significant will depend on the focus of the research, including the time period of interest and the spatial extent, which impose different requirements for geochemical conservativeness. The sediment transport route presents a particular issue because it causes temporal disparity. Sediment transport times are considered to be relatively quick when compared with post-deposition residence times (D'Haen *et al.*, 2012) but multiple stages of storage may occur through transport, extending the transport time and stretching the linkage between source and sediment yield by providing preferential transport. Depending on the length of time sediment remains in storage, it may present itself as a new sediment source as is identified in the floodplain environment where alluvial sediment deposited from previous high flow events becomes the same sediment eroded from channel banks. This is useful for distinguishing contemporary sediment sources, but presents an issue when the geochemical change is not sufficient to provide clear demarcation of the sources, sometimes referred to as 'legacy' sediments, which impair discrimination (Mckinley *et al.*, 2013).

In addition to this, disparate routing times for sediment sources proximal and distal to the active channel complicate direct relationships between erosion source and sediment transport. Wilkinson *et al.* (2013) suggested this was the cause of higher suspended sediment concentrations in the rising limb of high flow events compared to the falling limb, attributing it to a dominance of sources in close proximity to the channel. This also likely complicates the ability to determine relationships between sediment sources and individual storms as they may not include the temporal aspects of the sourced sediments (Gellis and Noe, 2013). Research has identified the need for greater emphasis on sediment redistribution as opposed to sediment outputs, with the former able to provide a lot more information related to soil degradation and mobilization. In this instance, ^{137}Cs and $^{210}Pb_{ex}$ provide information related to sediment budgets and quantification of both erosion and sediment redistribution (Porto *et al.*, 2013). In other occurrences, $^{210}Pb_{ex}$ decay rates have shown residence times of deposited material are likely to be a mix of short-term and long-term time frames. This has been evidenced by Wallbrink *et al.* (1998) in the Murrumbidgee River, Australia where $^{210}Pb_{ex}$ decay rates indicated 10 ± 5 year residence times but ^{137}Cs indicated time frames of weeks to months.

Table 5: *Principal sources of uncertainty within sediment fingerprinting schemes (Small et al., 2002)*

Nature of Uncertainty	Key issues (and assumptions)	Solutions
Problem formulation, i.e. how many source groups can be distinguished	Too few source groups compromises utility of approach, too many leads to problems of source group discrimination and spurious numerical solutions	Good experimental design; field experience
Discriminating power of tracers to distinguish between source groups	Depends partially on number, location and types of source groups to be distinguished, and laboratory resources available to the research team	Optimize analysis through *a priori* appreciation of the problem; obtain broadest array of property measurements possible
Tracer bias	Order of magnitude variations in tracers	Normalization procedures in mixing models
Characterisation of source group variability	Discrimination between source groups depends on 'within group' variance relative to 'between group' variance	Requires sound characterization of 'source groups' and appropriate sample numbers to adequately capture variability
Measurement uncertainty of tracer properties	Radiometric measurements, i.e. ^{137}Cs associated with intrinsic uncertainties ±5%, clay mineralogy typically only semi-quantitative	Good laboratory practice and quality controls
Tracer transformation	During transport and particularly sediment deposition diagenetic transformations may occur, i.e. synthesis of biogenic greigite in lake sediments	Ensure only conservative tracers are employed in analysis
Linear additivity	Some properties, such as mineral magnetic measurements, present nonlinear additivity problems	Combine range of sediment properties i.e. radiometric geochemical and magnetic (multi-parameter approach)
Enrichment	Preferential enrichment/selective deposition of fine/coarse fractions of the mineral sediment fraction and organic matter	Repeat measurements across selection fractions. Examine only specific fraction i.e. 'heavy silts' following extensive sample preparation and particle size corrections.
Mixing models	Constrained linear programming (optimization based) – problems of equifinality in prediction of estimated source contributions	Further development of 'likelihood based' modelling approaches

The most appropriate selection of tracers is going to vary between study sites and research focus, but generally if the a tracer's concentration changes significantly slower relative to movement through the catchment then suitability increases, however, for longer time frames geochemical stability increases and the same tracer may be rendered unsuitable. Examples include; biogenic tracers, such as organic C, N and P, which are often considered to have non-conservative issues beyond contemporary studies (50 years) due to enrichment and depletion associated with the organic matter fraction (D'Haen *et al.*, 2012); and fallout radionuclides which are restricted to the last 50–100 years based on when they were first released into the environment (D'Haen *et al.*, 2012, Mabit *et al.*, 2008). The exact tracer selection has also been demonstrated to have significant influence on source estimates, as Pulley *et al.* (2015) demonstrated, a mean difference of 24.1 % was observed between estimates for channel bank sources, and 8% and 11%,for urban dust sources when using different tracer groups.

The same conceptual approach needs to be applied when considering catchment scale processes in order to determine which tracers show the required degree of variability. In small catchments (<10 km^2), some tracers might not vary significantly. However, for larger scale regional studies those same tracers may show the variation required. The task of ascribing sediment sources for intermediate-sized catchments (10–10 000 km^2) becomes increasingly difficult, and for significantly large catchments (> 10 000 km^2) is considered to be nearly impossible (e.g. Hardy *et al.*, 2010) due to the increasing number of sources and residence times of old sources that are not present today. Some alternative approaches to address larger catchments have targeted a 'compositional evolution' (e.g. Hardy *et al.*, 2010) or stepwise analysis of catchments at confluences (e.g. Caitcheon, 1998, Rustomji *et al.*, 2008) through the length of the river. The difficulties of ascribing sediment sources for large catchments can also be overcome through using isotopes ratios such as Nd, Sr, and Pb; one of their main advantages is that they remain conservative over large temporal and spatial scales (Gingele and De Deckker, 2005, D'Haen *et al.*, 2012). Many authors employ a range or bracket test in an attempt to confirm there are no major transformations of tracer properties (e.g. Haddadchi *et al.*, 2013, Gellis and Noe, 2013). The exact rules of the test differ between studies but provide an important step in screening out non-conservative behaviour, although do not rule out non-conservative behaviour at all (Collins *et al.*)

One of the fundamental issues that affect the conservativeness of many tracers is the strong influence of particle size on sediment tracer signals. Varying particle-size distributions are formed by preferential weathering, erosion, and the sorting effects that occur through transport. Weathering will cause weaker grains to decompose preferentially into smaller

particles, such as the relative decrease in SiO_2/Al_2O_3 ratios with decreasing grain size and higher concentrations of heavy minerals in larger grain size fractions (Weltje and von Eynatten, 2004, Nesbitt *et al.*, 1996). The more weathered particles are likely to retain less information about the parent rock and, due to increasing specific surface area and binding of constituents, are also likely to reflect aspects of the processes acting on them, which may include aggradation and disaggregation occurring during transport (D'Haen *et al.*, 2012, Peart and Walling, 1986). The nature of the transport pathway after sediment production and environmental constraints will influence particle selectivity accordance to factors such as connectivity between the hillslope and channel and energy of the erosive force (Koiter *et al.*, 2013b). Higher energy flow moves a greater range of particle sizes with less selectivity, e.g. gully flow; whereas light rainfall and low slopes can lead to enrichment of fine grains. Within the channel, hydraulic sorting results in downstream fining and dissimilar settling rates, which cause spatial fining over within-channel morphological features, e.g. point bars, particularly from receding water levels. Preferential entrainment of finer sized particles causes the initial grain-size variation of suspended sediment. However, it is thought that the preferential deposition of coarser particles during transport is more significant for suspended load and therefore has implications for sediment fingerprinting (Walling and Moorehead, 1989).

The most common approach to addressing size-selectivity issues is to adopt targeted size fractions or specific minerals for analysis, e.g. Hatfield and Maher (2009), Caitcheon (1998), Gingele and De Deckker (2005). The size fraction itself directs how the sample can be analysed. Heavy Mineral Analysis (HMA) can be used to determine provenance information in sand-sized particles, i.e. Arribas *et al.* (2000) used the particle-size range 250–500 µm for bulk analysis and then used analysis of specific heavy minerals for the 250–63 µm fraction. These studies are able to target specific minerals and their compositions, which are often strongly related to the parent rock (Weltje and von Eynatten, 2004, Abu-Zeid *et al.*, 2001). Weathered particles tend to constitute the majority of suspended sediment load, in the <63 µm fraction. Unlike the larger grain sizes, individual minerals are hard to analyse individually in the silt and clay-sized fraction, which leaves bulk analysis of those fractions as the main method of analysis (Weltje and von Eynatten, 2004). Undertaking bulk analysis means that size fractions are even more important for better discrimination, and direct comparisons between sediment samples often cannot occur until sediment-size separation has occurred. For this reason, many studies may divide the <63 µm fraction further, into divisions at 32 µm, 10 µm (e.g. Roddy, 2010) 2 µm (e.g. Wallbrink *et al.*, 1998) depending on the focus e.g. Gingele and De Deckker (2005) separated the fraction into <2 µm to characterize the clay, and 2–63 µm to characterize the

silt. The appropriate grain size selection should be based on analysis of target sediment from the study catchment in order to minimize potential errors associated with grain size selectivity.

In many cases, given particle size and tracer conservativeness issues, alternative methods are needed to circumvent these problems, which may involve the use of correction factors and ratios focused on adjusting properties of surface area concentrations, or alterations to the analysis of the actual tracer (Collins *et al.*, 1997, Collins *et al.*, 1998, Gruszowski *et al.*, 2003, He *et al.*, 1996, Russell *et al.*, 2001, Motha *et al.*, 2002). The extent of these effects are partially dependent on particle size where enrichment issues are thought to pose the biggest problems for the <10 µm fraction, with enrichment factors of the order of 1.5 (Peart and Walling, 1986). Corrections using ratios have been employed to address organic matter enrichment which affects organic C, N and P and is closely related to the enrichment of fines and is assumed to be accounted for through particle-size selection (D'Haen *et al.*, 2012, Collins *et al.*, 1997, Collins *et al.*, 1998, Motha *et al.*, 2002, Walling, 2005). However, many correction factors have assumed a linear relationship between particle size and tracer value which may not hold true. Russell *et al.* (2001) have highlighted the variation of correction factors for each trace value across a small catchment in relation to particle size while Smith and Blake (2014) have emphasised the use of correction factors can cause additional large issues due to the inadequacy for corrections to represent each tracer sufficiently. Correction factors may need to be applied in a property-dependent approach to account for these discrepancies in future research, especially for larger catchments. Relative to other uncertainties such as tracer selection, some studies have also shown that organic matter content and particle size may actually have negligible effect on the final source predictions (Pulley *et al.*, 2015).

Magnetic properties are strongly affected by particle sizes, where the signals arise either from the mineral components themselves or due to an increase in surface area that results in more the surface-bound Fe oxides (Caitcheon, 1998). This can cause diagenetic effects and in situ bacterial magneitite grains and magnetosomes to provide a contribution to tracer signals (D'Haen *et al.*, 2012, Zhang *et al.*, 2008, Oldfield, 2007). Zhang *et al.* (2008) overcame this issue by lessening the specific surface area by not analysing sediment with grain size below 4 µm in order to avoid magnetosomes and the diagenetic influences. Oldfield (2007) however, addressed the issue by using magnetic susceptibility at two frequencies of magnetic remanence generated by direct and alternating currents. This allowed the generation of bi-logarithmic plots, through which it is possible to discriminate between assemblages dominated by magnetic minerals formed through pedogenesis and those arising from the presence of magnetotactic bacteria that use chains of magnetic particles to seek optimum environments in

surface. Sediments. A mineralogical approach may choose to isolate a particular mineral or magnetic inclusion (Foster *et al.*, 2007, Owens *et al.*, 1999). Secondary ferromagnetic minerals can be formed along with reductive transformation of iron-bearing minerals, both of which contribute to the bulk magnetic signal. Isolation of the magnetic inclusions, therefore, can provide a more pure signal of the source (D'Haen *et al.*, 2012, Hounslow and Morton, 2004, Maher *et al.*, 2009). Isolating distinct aspects of a tracer has also been demonstrated in geochemical tracers, where certain stable phases can be isolated and used as opposed to other less stable phases, which are leached away. An example of this is using carbonate-free signals when the carbonate fraction behaves non-conservatively due to its solubility (D'Haen *et al.*, 2012) or the different way of analysing colour. Martínez-Carreras *et al.* (2010a) employed a method using 24 colour parameters derived from colour space models that were able to differentiate land-use types and surface and sub-surface sources; however, this was less effective in larger catchments where intra-source variabilities overlap.

Source group variability and the number of samples must be considered as key influences effecting uncertainty and are major limitations to sediment fingerprinting research (Pulley *et al.*, 2015). Employing statistical techniques can reduce uncertainties but part of the issue relates to inherent tracer variability, as tracer concentrations can be highly variable both between groups and within source groups which means high replication numbers are needed to give quality results for quantitative calculations. This reinforces the need for increasing sampling density and resolution which could off-set or decrease uncertainty, but may exceed feasible and realistic resource limitations. It has also been demonstrated that different groups of tracers can yield significantly different source estimates for the same data, creating significant uncertainty in model estimates for catchments with similar geochemically sources (Pulley *et al.*, 2015). One approach to limit the variability encountered is to use the sediment from the geologically distinct river tributaries, which possess less-variable geochemistry than soils, allowing for more straightforward spatial source discrimination (e.g. Wilkinson *et al.*, 2013, Vale *et al.*, 2016a)

Evaluation of the sediment source predictions provided by sediment mixing models is another fundamental challenge facing sediment fingerprinting. There are two main approaches used; the first is a goodness–of-fit (GOF) (e.g. Motha *et al.*, 2004, Motha *et al.*, 2003) which compare source-weighted predicted sediment chemistry and measure chemistry for the target sediment; and the second approach uses artificial mixtures to test model predictions. These two approaches are important but may be conflicting in that GOF estimators encourage a reduction of the number of tracers used in order to minimize errors, whilst recent research is

showing more accurate results are often produced from larger composite signatures when tested with artificial mixtures. A variety of different weightings have also been applied in recent research to improve mixing models. These have included weightings based on spatial variation (e.g. Wilkinson *et al.*, 2015), tracer discrimination (e.g. Collins *et al.*, 2010a, Haddadchi *et al.*, 2013) and prior information of typical contributions (e.g. Haddadchi *et al.*, 2013).

A sound understanding of the geomorphological context and geochemical explanation would add great value to sediment fingerprinting knowledge, especially for process-based applications (Belmont *et al.*, 2014). A more thorough appraisal of sediment mixing model selection would also be of great benefit due to the significant influence model selection can have on sediment apportionment (Nosrati *et al.*, 2014, Haddadchi *et al.*, 2014, Laceby and Olley, 2015). Results also need to be interpreted appropriately so as not to distort their legitimacy or the application of the findings in the context of the uncertainties inherent in the technique and any quantitative analysis can benefit greatly from additional lines of evidence in order to build a strong case from accurate crosschecking and validation Koiter *et al.* (2013b).

2.5 New Zealand Research

There have been two significant studies implemented in the New Zealand environment. Gibbs (2008) applied sediment fingerprinting approaches based on Compound-Specific Isotope Analysis as naturally occurring biomarkers (CSIA). This was applied to a 117 Km^2 catchment on the east coast of the North Island of New Zealand which drains the Mahurangi River system into the Mahurangi Harbour. This is a predominantly agricultural catchment (70 %) with native forest (20 %) located in the steep-sided gullies. The method used $\delta^{13}C$ isotopic values of the bulk soil and each individual fatty acid as different "isotopes" including; $\delta^{13}C$, Decanoic (C10:0), Lauric (C12:0), Myristic (C14:0), Pentadecanoic (C15:0), Palmitic (C16:0), Stearic (C18:0), Oleic (C18:1), Linolenic (C18:2), Arachidic (C20:0), Behenic (C22:0), Lignoceric (C24:0) and Abietic. The results indicated measureable differences in the $\delta^{13}C$ isotopic values for individual organic compounds extracted from soils from different land-uses. Thus, the percent of sediment from pine forest land-use area was estimated to be three times greater than the percent land-use area of the pine forest and was coming from smaller areas of exposed soil. Roddy (2010) applied sediment fingerprinting to a 110 km^2 catchment in the Coromandel, North Island, New Zealand. This is known as the Whangapoua catchment draining into the Whangapoua Harbour

and is composed of steep slopes with short first order streams subject to intense rainfalls. The geology is composed of andesitic and dacite built on a greywacke basement and alluvium found in the lowland areas. Over 85 % of the study area has slopes of more than 20°. Roddy (2010) analysed the < 10 µm size fraction including variables such as Co, Ni, Ga, Ge, Se, Br, Nb, Mo, Ag, Cd, In, Sn, Sb, Te, I, Cs, Pr, Nd, Hf, Ta, W, Hg, Ti, Bi, Li, Na, Mg, Al, Si, P, S, K, Ca, V, Cr, Fe, Mn, Cu, Zn, As, Sr, Ba, Pb, B, and U, as well as radionuclides including ^{137}Cs, ^{210}Pb, ^{228}Ra, and ^{226}Ra. This research indicated that sediment fingerprinting can distinguish between landscape units with 62 % of sediment delivery attributed to native forest, 23 % to exotic pine forests and 15 % to agriculture, and this was predominantly subsoil erosion (79 %), followed by stream banks (13 %), and surface soils (8 %).

2.6 Summary

Fine sediment has been demonstrated to represent an important component to the active channel and wider catchment environment through physical, chemical and ecological influences. Erosion processes provide the source of fine sediment which can be delivered into the active channel and transported downstream through successive storage and remobilization processes. The production, transport and deposition of fine sediment need to be understood in order to address sediment related issues of which sediment fingerprinting can provide differentiation of sediment sources and provide quantification of relative proportions. Some challenges exist within the technique such as the ability to differentiate sediment sources within a large catchment dominated by similar sedimentary landscapes throughout. The following chapter investigates whether differentiation of sediment sources within the Manawatu catchment is possible by focusing on sub-catchment sediment sources at the major tributary confluences.

Chapter 3

Application of a confluence-based sediment fingerprinting approach to a dynamic sedimentary catchment, New Zealand

3.1 General Introduction

Chapter 2 introduced the basic concepts of sediment processes operating within a river channel and wider catchment as well as the key concepts underlying sediment fingerprinting and ongoing challenges relating to clear discrimination of sediment sources within larger catchment areas. Thus, the following chapter explores the ability of a confluence-based sediment fingerprinting approach to differentiate sub-catchment sediment sources within a larger catchment dominated by similar sedimentary geological terrains.

Chapter 3 has been published as Vale SS, Fuller IC, Procter JN, Basher LR, Smith IE., Application of a confluence-based sediment-fingerprinting approach to a dynamic sedimentary catchment, New Zealand, which was first published in *Hydrological Processes*, 30: 812-829. DOI: 10.1002/hyp.10611. The chapter covers collection and analysis of the sediment samples, data analysis techniques employed and geochemical indicators used to aid interpretation of results. Results and discussion cover the discrimination ability of sediment sources within the Manawatu Catchment, along with interpretation of the results in relation to the geomorphological processes occurring in the catchment before some final conclusions.

3.2 Abstract

Fine sediment is a dynamic component of the fluvial system, contributing to the physical form, chemistry and ecological health of a river. It is important to understand rates and patterns of

sediment delivery, transport and deposition. Sediment fingerprinting is a means of directly determining sediment sources via their geochemical properties, but it faces challenges in discriminating sources within larger catchments. In this research, sediment fingerprinting was applied to major river confluences in the Manawatu catchment as a broad-scale application to characterizing sub-catchment sediment contributions for a sedimentary catchment dominated by agriculture. Step-wise discrimination function analysis and principal component analysis of bulk geochemical concentrations and geochemical indicators were used to investigate sub-catchment geochemical signatures. Each confluence displayed a unique array of geochemical variables suited for discrimination. Geochemical variation in upstream sediment samples was likely a result of the varying geological source compositions. The Tiraumea sub-catchment provided the dominant signature at the major confluence with the Upper Manawatu and Mangatainoka sub-catchments. Subsequent downstream confluences are dominated by the upstream geochemical signatures from the main stem of Manawatu River. Variability in the downstream geochemical signature is likely due to incomplete mixing caused in part by channel configuration. Results from this exploratory investigation indicate that numerous geochemical elements have the ability to differentiate fine sediment sources using a broad-scale confluence-based approach, and suggest there is enough geochemical variation throughout a large sedimentary catchment for a full sediment fingerprint model. Combining powerful statistical procedures with other geochemical analyses is critical to understanding the processes or spatial patterns responsible for sediment signature variation within this type of catchment.

3.3 Introduction

The suspended sediment component in a fluvial environment is arguably one of the most important components of sediment transport, influencing the character of alluvial environments through physical, chemical and ecological processes (Owens *et al.*, 2005, Collins and Owens, 2006, Bracken, 2010, Walling, 2006a, Kemp *et al.*, 2011). Impacts from intensification and poor management of human activities such as farming can lead to loss of agriculturally productive land (Collins *et al.*, 1997, Walling *et al.*, 1999, Owens *et al.*, 2005, Collins and Owens, 2006), while increasing sediment delivery to the river channel and influencing aquatic ecosystems negatively (Wood and Armitage, 1997, Walling and Fang, 2003, Owens *et al.*, 2005, Bilotta and Brazier, 2008). To mitigate these issues, catchment-scale identification of sediment production, transport, and deposition need to be understood, although identification of geomorphically active areas contributing to fine sediment flux is still

often poorly understood and quantified (Slattery *et al.*, 1995, Collins and Walling, 2004). Traditional indirect methods such as aerial photography, erosion pins and erosion plots provide information on sediment mobilization but not the extent to which the sediment is transported downstream (Walling, 2005), and conversely downstream sediment gauging stations provide information on the quantity of sediment transport but do not directly provide information on the nature of the sediment mobilization.

Sediment fingerprinting provides the possibility of directly quantifying sediment sources that allows increased focus on fine sediment, larger catchments, and the use of pre-existing tracers (Walling *et al.*, 2013). Early sediment fingerprinting research successfully used mineralogy (e.g. Klages and Hsieh, 1975, Wall and Wilding, 1976) and mineral magnetism (e.g. Oldfield *et al.*, 1978, Walling *et al.*, 1979), but has since undergone considerable development. The establishment of composite fingerprints aided by availability of an increased range of sediment analytical techniques, discriminant statistical tests and numerical mixing models (e.g. Collins *et al.*, 1997) have provided enhanced discrimination techniques using a wide range of usable sediment properties and applications. The following properties have been seen in recent research; mineralogy (e.g. Arribas *et al.*, 2000, Gingele and De Deckker, 2005), mineral magnetic properties (e.g. Caitcheon, 1998, Blake *et al.*, 2006, Foster *et al.*, 2007), geochemical compositions (e.g. Collins *et al.*, 1998, Jin *et al.*, 2006, Lee *et al.*, 2008, Singh, 2009, Hardy *et al.*, 2010, Zhang *et al.*, 2012, Collins *et al.*, 2013), isotopic ratios (e.g. Douglas *et al.*, 1995, Gingele and De Deckker, 2005), radionuclides (e.g. Wallbrink and Murray, 1993, Walling *et al.*, 1999, Olley and Caitcheon, 2000, Brigham *et al.*, 2001, Carter *et al.*, 2003, Rhoton *et al.*, 2008), organic elements (e.g. Fox and Papanicolaou, 2008a) and compound specific isotopes (e.g. Gibbs, 2008, Blake *et al.*, 2012).

However, there are many challenges that still require attention in order for sediment fingerprinting to advance as a robust quantitative tool for sediment source research. A considerable emphasis in recent research has focused on uncertainties surrounding mixing models, tracer selection, and the variability encountered within source group tracer concentrations. Pulley *et al.* (2015) found an average of ~24 % difference in predictions from different tracer groups and as high as 100 % for specific samples. Koiter *et al.* (2013b) refer to geochemical uncertainty issues as the 'black box' whereby the sediment source inputs and outputs are well defined, but, what occurs during the transport process to the geochemical signature of the sediment is not well understood. Sediment geochemistry can change substantially due to chemical, biological and physical processes thereby jeopardising the

conservativeness of the geochemical sediment fingerprint. Furthermore, sediment transport pathways cannot be assumed to directly connect source and sink, but instead comprise a series of buffers, barriers, and blankets, which disrupt the transport of sediment (Fryirs *et al.*, 2007) providing good reason for Ferguson (1981) to refer to sediment transport as a *'jerky conveyor belt*'. Haddadchi *et al.* (2014) showed different sediment proportion results were exhibited for different mixing models which processed the same data set, concluding that source attribution was often dependent on model selection. Several studies have cautioned the use of correction factors in mixing models. Laceby and Olley (2015) showed element corrections did not improve model performance while Smith and Blake (2014) found that organic matter and particle size corrections result in unquantified errors and should be used with caution.

Complex catchments face challenges to clearly discriminate between sediment sources due to duplication or blurring of sediment source signatures. Smith and Blake (2014), for example, found difficulty discriminating between sources in their study because the cultivated source signature resembled a mix of pastures and channel bank sources. This issue is compounded in larger catchments where the task of ascribing sediment sources for intermediate-sized (10–10 000 km^2) and large-sized catchments (> 10 000 km^2) becomes increasingly difficult due to the greater number of sources and sediment residence times (Hardy *et al.*, 2010). This leads to increases in variation and uncertainty encountered in source sample signatures and provides challenges for conventional source sampling techniques which rely on point source sampling from soils. Wilkinson *et al.* (2013) for instance, found greater uncertainty in the soils from geological units. The soils displayed greater confidence intervals in larger catchments than source areas defined using sediment from geologically distinct river tributaries, concluding the latter sampling of source sediment from geologically distinct tributaries to river confluences as the best way to identify spatial patterns in larger catchments. Hardy *et al.* (2010) also used stream sediment for analysing a large catchment, but employed sampling through a compositional evolution approach to distinguish changes through the sediment continuum of that large catchment. Koiter *et al.* (2013a) and Lamba *et al.* (2015) also indicate differences in source composition between suspended sediment and fine sediment deposited on the stream bed, suggesting a requirement to analyse both.

The present study has been carried out in the 5870 km^2 Manawatu River catchment, New Zealand with the intention of calibrating SedNetNZ, an adaptation of the Australian SedNet model after Prosser *et al.* (2001). This type of model is considered a means to providing

ongoing information and prediction of sediment discharges at a range of spatial scales without relying on increasing resolution of empirical information i.e. gauging stations (De Rose and Basher, 2011b). Accuracy of sediment discharge estimates need to be verified and calibrated; sediment fingerprinting can provide parallel estimates for tested SedNetNZ results. Sediment fingerprinting itself, has had limited application in New Zealand catchments (e.g. Gibbs, 2008, Roddy, 2010). Through this research the Manawatu River Catchment will be the largest New Zealand catchment in which sediment fingerprinting has been applied to date and subsequently raises questions of how effective the technique is within a New Zealand catchment of this scale and geological configuration.

The main aims of this paper are to investigate:

(i) the application of sediment fingerprinting within a significant New Zealand catchment and whether there is indication of enough geochemical variation for source provenance

(ii) a confluence-based application of sediment fingerprinting whereby upstream sediment samples are taken as a proxy for sub-catchment sediment signatures in order to evaluate relative source contributions for a larger catchments with minimal outlay of resources

(iii) incorporation of wider geochemical indicators to provide deeper understanding to the processes occurring beyond direct statistical interpretation of Discrimination Function Analysis (DFA) and Principal Component Analysis (PCA)

3.4 Study Area

The Manawatu River Catchment lies within the central North Island, New Zealand with headwaters rising on both the eastern and western flanks of the Tararua and Ruahine Range (Fig. 15). The eastern catchments flow east to west cutting through the main drainage divide forming the Manawatu Gorge before arriving at the Tasman Sea on the west coast. Average discharge in the lower Manawatu is c.110 $m^3 s^{-1}$ and contributions from main sub-catchments, Upper Manawatu (c. 27 $m^3 s^{-1}$) , Tiraumea (c. 16 $m^3 s^{-1}$), Mangatainoka (c. 18 $m^3 s^{-1}$), Mangahao (c. 15 $m^3 s^{-1}$), Pohangina (c. 17 $m^3 s^{-1}$), and Oroua (c. 13 $m^3 s^{-1}$) (Henderson and Diettrich, 2007). The morphology ranges from semi-braided to pseudo-meandering over gravel and sand-bedded alluvium. Many of the lower reaches have undergone straightening and narrowing of

the channel, transitioning from multi-thread braided channels to a laterally-confined single thread channel as evidenced in the Pohangina River (Fuller, 2009). Middle reaches are often semi-confined through contact with bedrock cliffs or alluvial terraces.

Catchment geology comprises almost exclusively sedimentary material, predominantly mudstone, greywacke and sandstone interspersed heterogeneously throughout the catchment with limestone and alluvial gravels (Fig. 15). Eastern catchments are dominated by soft hillslope terrains underlain primarily by mudstone e.g. Tiraumea sub-catchment, which is also common throughout some western catchments (Table 6). Upper Manawatu, Pohangina and Oroua hillslopes consist of mixed geology i.e. commonly sandstone in varying proportions with poorly or well bedded siltstone and mudstone with additional shellbeds and conglomerates. The Tararua and Ruahine Ranges are predominantly greywacke.

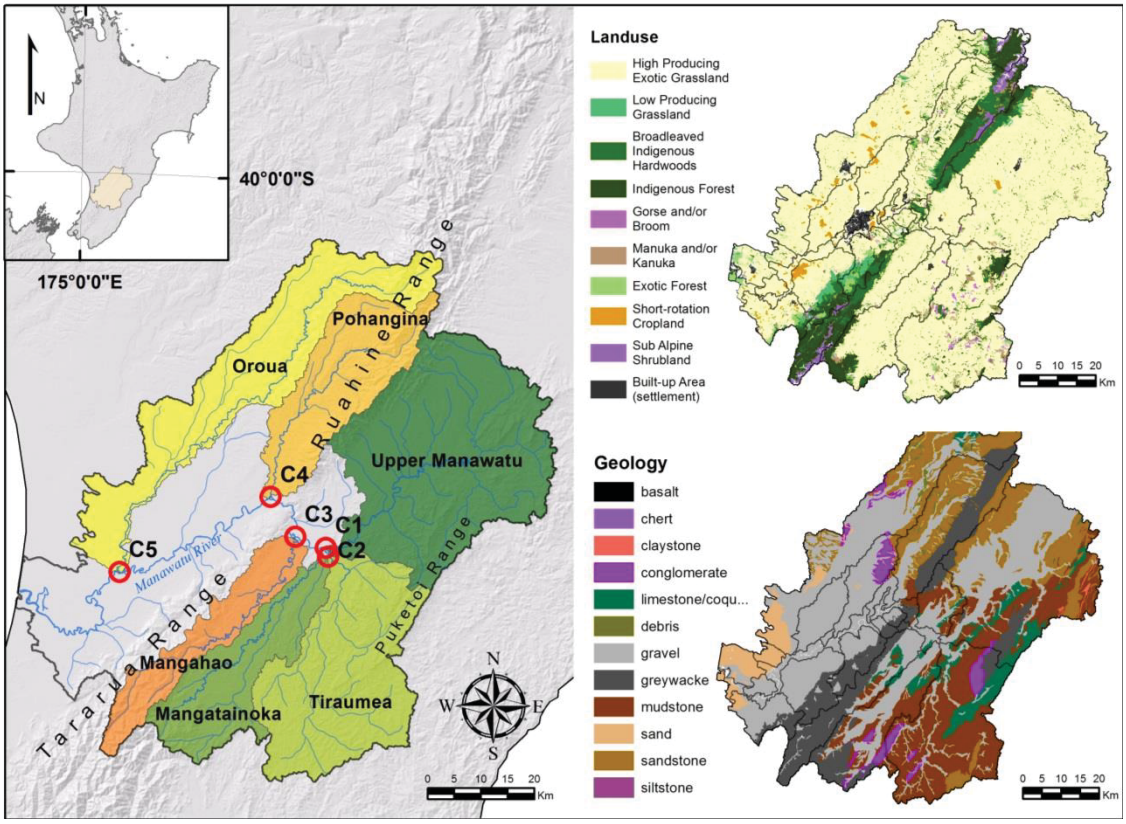

Fig. 15: *Manawatu sub-catchments showing confluences with small insets of land-use and geology*

The Puketoi Range includes a significant amount of limestone. Lowland areas consist of alluvial floodplains of gravels and sands and nearer to the west coast the introduction of coastal wind-blown sands begins to dominate. The New Zealand Soil Classification (NZSC) after Hewitt (1998) states the soils in region consist predominantly of orthic/firm brown soils, consisting of mica/illite, across the catchment with limited distributions of allophanic brown

soils associated with the flanks of the greywacke range. Argillic pallic soils are found in eastern catchments, particularly Puketoi Range, with immature pallic soils common in both the eastern catchments as well as in the Pohangina. Perched-Gley pallic soils are also found on the western flanks of the Tararua Range, and in the lowland areas surrounding the Oroua and north of Palmerston North. Recent alluvial soils are found on extensive floodplains following the channel outlines. Limited melanic soils are found in the limestone regions.

Exotic grassland dominates the majority of the catchment owing to agricultural farming (≈ 75 %), comprising mostly sheep and beef farming in the hillslopes, as well as dairy farming in the lowland floodplain areas. Indigenous vegetation comprises ≈ 17 % in land coverage. The majority of this is from indigenous forest located on the flanks of Tararua and Ruahine and Puketoi Range. Exotic forest contributes to ≈ 3 % of land-use. Mānuka and kanuka along with other grey scrub, introduced gorse and broom occupy pockets of land particularly in the Tiraumea sub-catchment associated with marginal, disturbed and regenerating land types or poor soil fertility. Short-rotation agricultural crops occupy small pockets in the lowland areas.

Table 6: *Sub-catchment geological composition derived from the Qmap - Geological Map of New Zealand (see Rattenbury and Isaac, 2012)*

Geological Material	Percent of sub-catchment underlain by geology					
	Upper Manawatu	Tiraumea	Mangatainoka	Mangahao	Pohangina	Oroua
Greywacke	5.9	3.1	21.2	59.0	30.9	3.4
Mudstone	22.8	63.8	29.5	7.3	2.3	-
Sandstone	24.0	3.9	0.1	0.0	44.6	27.3
Gravel	39.7	11.8	37.8	28.0	19.7	52.6
Limestone	7.4	11.3	6.3	5.6	-	2.6
Conglomerate	0.1	6.1	5.1	-	0.1	2.4
Sand	-	-	-	-	-	9.7
Debris	-	-	-	-	2.3	2.0

3.5 Material and methods

3.5.1 Sample Collection

The research was conducted through an exploratory approach purposed to provide an overall appreciation on the effectiveness of sediment fingerprinting to differentiate source material at a very broad-scale before the outlay of further resources. The most direct way was to break the catchment down into sub-catchments and key confluences. This simplifies the sediment

sources by isolating upstream sediment from a given confluence and allows the assumption to be made that the sediment flowing out of a given confluence is a proportionally representative upstream signal of the entire sub-catchment at a given point in time. The sub-catchment tributaries utilized are the Upper Manawatu, Tiraumea, Mangatainoka (C1-2), Mangahao (C3), Pohangina (C4) and Oroua sub-catchments (C5) (Fig. 15).). The sub-catchments that drain to the five confluences cover a significant area of the Manawatu Catchment, Upper Manawatu (1301 Km^2), Tiraumea (876 Km^2), Mangatainoka (481 Km^2), Mangahao (339 Km^2), Pohangina (551 Km^2) and Oroua sub-catchment (903 Km^2) with each sub-catchment containing a unique composition of geology, albeit all sedimentary in nature.

The confluences of the six major sub-catchments were selected as sample site locations. For each confluence, upstream and downstream samples were collected from fine drapes over bars within the channel during a period of low flow. Upstream samples were collected as close to the confluence point as possible. Downstream of the confluence, attempts were made to collect samples approximately 500 m to 1 km downstream to provide distance for mixing to occur but limiting the introduction of new sediment sources. Five samples were initially collected for each location on one occasion. A trowel was used to collect multiple (typically 5) point grabs/scrapings from the immediate area (≈ 10 m^2). Deposits that clearly contained fine sediment were targeted over larger clast material and samples near the bank edge or where the sediment was clearly a direct input from the channel bank were avoided. Fine sediment was found in three key positions: around the fringes of point bars, particularly on the lee side and after receding waters; trapped in semi-dried-out pools following receding waters; and caught within the interstices of larger clasts and objects (Fig. 16). Sampling occurred at the culmination of the winter season, following a period of increased rainfall across the catchment, common for the time of year. Repeated sampling was not undertaken due to initial resource constraints and was beyond the purpose of the exploration which poses important limitations to the study and the ability to evaluate temporal information.

Fig. 16: *Typical in-channel fine sediment deposits: point bar deposition (left); trapped in the interstices of larger clasts on a bar (right); and deposited in semi-dry to dried-out pools on bars (middle)*

3.5.2 Sample Preparation and Analysis

Samples were washed through a plastic sieve stack on a sieve shaker; fractions < 63 µm were retained and larger fractions were discarded. Deionized water was rinsed through when needed but used sparingly. The samples were collected in plastic containers and dried at 40°C. XRF preparation consisted of crushing the dried samples with a tungsten carbide grinder and weighing into crucibles. The samples were and left overnight at 105°C, re-weighed and left in a furnace at 850°C overnight to combust any organics. 2 g of sample was mixed with 6 g of lithium tetraborate and fused into glass discs. The glass discs were analysed using Siemens SRS 3000 Sequential XRF Spectrometer for elements SiO_2, TiO_2, Al_2O_3, Fe_2O_3, MnO, MgO, CaO, Na_2O, K_2O, P_2O_5, Ba, Rb, Sr, Pb, Th, Zr, Nb, Y, V, Cr, Ni, Cu, Zn, La, and Ce. Concentrations were all above the Limit of Quantitation (LoQ) with several trace elements displaying values close to their limits (Table 7).

Table 7: *Limits of Quantification (LoQ) from XRF analysis for the major and minor elements*

Element	Mean (%)	LoQ (ppm)	Element	Mean (ppm)	LoQ (ppm)
SiO_2	63.5	295.4	**Ba**	478.4	27.3
TiO_2	0.7	42.6	**Rb**	108.1	4.2
Al_2O_3	15.3	193.5	**Sr**	234.2	3.2
Fe_2O_3	4.8	23.1	**Pb**	20.4	10.3
MnO	0.1	13.8	**Th**	9.0	6.1
MgO	1.4	102.2	**Zr**	260.2	3.4
CaO	1.4	70.4	**Nb**	11.2	3.2
Na_2O	2.8	121.5	**Y**	23.9	3.3
K_2O	2.5	23.8	**V**	94.1	10.2
P_2O_5	0.2	26.8	**Cr**	54.1	11.6
			Ni	17.9	8.2
			Cu	14.2	9.2
			Zn	77.4	6.2
			La	31.8	15.9
			Ce	50.9	43.1

The glass discs were retained and analysed on a Agilent Technologies 7700 Series LA-ICP-MS for Sc, V, Cr, Co, Ni, Cu, Zn, Ga, Rb, Sr,Y, Zr, Nb, Cs, Ba, La, Ce, Pr, Nd, Sm, Eu, Gd, Tb, Dy, Ho, Er, Tm, Yb, Lu, Hf, Ta, Pb, Th, U. The LA-ICP-MS used BCR-2G chemical standard every 10 samples to check accuracy and precision. Since the glass discs are what are being ablated and measured, Ca is used as an internal standard to calibrate the LA-ICP-MS values against the XRF values.

3.5.3 Data Analysis

Recent sediment fingerprinting approaches have encouraged the use of a combination of independent statistical techniques to explore sediment source discrimination (e.g. Collins *et*

al., 2012). In this instance, exploration of the fingerprint data consisted of two statistical approaches. The first approach followed Collins *et al.* (1998) for tracer selection using a two stage statistical selection procedure. This involved statistical discrimination using non-parametric statistical tests of Kruskal-Wallis and Mann-Whitney tests to verify the ability of an individual tracer to provide statistical discrimination between sources. The second stage used a stepwise minimization of Wilk's lambda multivariate discriminant analysis to deduce the final selection of variables that could discriminate between sources. The second approach utilized Principal Component Analysis (PCA) to explore the relationship and significance of the variables accounting for the variance of sediment sources. PCA is a data reduction technique that allows multiple correlated variables to be reduced to a set of uncorrelated variables called principal components. This is done through the use of a transformation that establishes the axis in the direction of the greatest variation, the first component. Due to the close proximity and lack of sample locations C1 and C2 were combined into one 3-junction confluence.

3.5.3.1 Statistical Discrimination

Mann-Whitney tests were used for C3, C4 & C5 and Kruskal-Wallis H test were used for C1-2. These tests were carried out for each analysed element concentration to develop a rank order that would indicate the statistically significant discriminants for subsequent analysis. The null hypothesis was that the upstream sediment sources group at each confluence were the same while the alternative hypothesis accepted upstream sediment sources to be different. A 95.0 % confidence interval or an α level of 0.05 was chosen for the critical p-value. Discriminant function analysis (DFA) allows for prediction of group membership based on linear combinations of predictor variables (Eq. 3)

$$D = v_1X_1 + v_2X_2 + v_3X_3 + \ldots v_iX_i + a \qquad \text{(Eq. 3)}$$

Where D = discriminant function

v = the discriminant coefficient

a = a constant

i = the number of predictor variables

Discriminant analysis was conducted using SPSS using stepwise discriminant analysis applying a minimization of Wilks' Lambda. Wilk's Lambda is a measure of the between group variability to within group variability whereby minimizing the value reduces the sample grouping. It is guided by '*F*' values which determine the entry and removal of variables as a measure of the

extent to which an individual variable contributes to group prediction. Default values of 3.84 (probability = 0.5) and 2.71 (probability = 0.1) are used for F to enter and F to remove respectively. These values provided and adequate number of selected elements the purposes of this study without the need to alter the F values. However for C4 the F values were lowered to allow additional tracers to be employed in the final solution.

3.5.3.2 Principal Component Analysis

Principal component analysis was carried out using SPSS version 21.0 (IBM Corp., 2012). A correlation matrix was used to standardize the variable measurements. Component extraction was limited to eigenvalues greater than 1 unless the percentage of variation accounted for was low, in which case additional components were added. An oblique rotation of direct oblimin was used for the rotation method as a standard method for allowing factors to be correlated. Coefficients for the PCA components were applied to the original samples for visual display as well as well as rotated loading plots for the variables

3.5.4 Geochemical indicators

In order to evaluate sediment fingerprint data a collection of geochemical analyses and displays was performed. Multi element normalised diagrams for Major, Trace and REEs were constructed to show trends in average sediment geochemistry. Major and trace elements were normalized to Upper Continental Crust (UCC) using McLennan (2001) values revised from Taylor and McLennan (1985). Post-Archean Australian Shale (PAAS) values after McLennan (2001) were also used for comparison. Rare Earth Element (REE) values were normalized using average CI chondrite values from McDonough and Sun (1995). Plots were constructed using *PetroGraph* from Petrelli *et al.* (2005).

Major element geochemistry was explored through Chemical Index of Alteration (CIA) (Nesbitt and Young, 1982), Index of Compositional Variability (ICV) (Cox *et al.*, 1995) and K_2O/Al_2O_3 values to give an indication of the major element character. CIA measures the conversion of feldspars to clays by measuring the depletion of CaO, Na_2O and K_2O relative to Al_2O_3 in the silicate portion. CIA values typically range from <50 for fresh material to 100 for fully weathered material.

$$CIA = (100)\left[\frac{Al_2O_3}{Al_2O_3+CaO^*+Na_2O+K_2O)}\right] \quad \text{(Eq. 4)}$$

CaO* only refers to the CaO incorporated into the silicate portion so a correction was applied according to McLennan (1993) to approximate the CaO* value devoid of the carbonate fraction. ICV is similarly a measure of the major cation composition relative to Al_2O_3 using wt%. Values <1 are typical of clay minerals and > 1 is more indicative of plagioclase and feldspars.

$$ICV = \left[\frac{(Fe_2O_3+K_2O+ Na_2O+CaO+MgO+TiO_2)}{Al_2O_3}\right] \quad \text{(Eq. 5)}$$

K_2O/Al_2O_3 ratios from 0.0 – 0.3 suggest clay minerals, and 0.3 – 0.9 suggest plagioclase (Cox *et al.*, 1995). Sorting and sediment recycling effects can be reflected in plots of Th/Sc and Zr/Sc, whereby, high Zr/Sc values indicate zircon enrichment associated with sediment recycling as Sc preserves provenance signatures whereas Zr is strongly associated with mineral zircon which is subject to sorting due to the high mineral density. $(La/Yb)_N$ is used as a measure of LREE/HREE enrichment and low Eu/Eu* ratio a measure of depletion of plagioclase, which is enriched in Eu^{2+}. TotREE is the sum of all REE concentrations (in ppm) to show variation in total REE concentrations across sediment source groups. Particle size analysis was undertaken on the upstream and downstream sediment samples using a Horiba Partica LA-950v2 laser scattering particle size distribution analyser.

3.6 Results

3.6.1 XRF and LA-ICP-MS

The XRF and LA-ICP-MS concentrations were generally in good agreement. Most of the elements displayed similar patterns for high and low sample concentrations. The LA-ICP-MS results exhibited between ≈ 10 % to ≈ 25 % lower mean concentration for Ba, Rb, Sr, Th, Zr, Nb, Y, V, Cr, Ni, Cu, La and Ce, with Pb and Zn displaying ≈ 34 % and ≈ 11 % higher mean concentration (Table 8). Closer inspection of the Pb and Zn values showed that the first LA-ICP-MS batch exhibited significantly elevated levels of Pb and Zn. These were attributed to the polishing agent used in glass slide preparation causing surface contamination. The contamination only influenced Pb and Zn concentrations and exclusion of the polishing agent in the second batch also removed the contamination effects. Therefore the XRF values of Pb and Zn were favoured over the LA-ICP-MS values for all samples. Preference was given to the LA-ICP-MS values for remainder of the elements Ba, Rb, Sr, Th, Zr, Nb, Y, V, Cr, Ni, Cu, La and Ce.

Table 8: *Comparison between the XRF and LA-ICP-MS concentrations values*

Element	XRF			LA-ICP-MS		
	Mean (ppm)	Standard Error (ppm)	Standard Deviation (ppm)	Mean (ppm)	Standard Error (ppm)	Standard Deviation (ppm)
Ba	514.4	5.8	46.6	440.5	3.4	27.5
Rb	110.3	1.2	9.6	82.5	0.8	6.7
Sr	256.4	3.6	29.1	206.0	3.8	30.6
Pb	20.4	0.4	3.5	27.4	1.9	15.5
Th	11.0	0.4	3.1	9.8	0.1	0.7
Zr	353.3	19.5	156.8	295.7	17.1	138.0
Nb	11.4	0.1	1.1	8.9	0.1	0.6
Y	25.9	0.4	2.9	19.3	0.2	1.8
V	95.9	1.1	8.6	85.7	1.0	7.8
Cr	57.3	0.6	5.1	50.3	0.8	6.3
Ni	20.0	0.6	4.7	16.5	0.3	2.5
Cu	13.4	0.6	5.1	13.2	0.5	3.7
Zn	80.3	1.5	12.2	89.4	4.8	38.4
La	33.1	0.4	3.6	25.0	0.3	2.3
Ce	60.2	1.4	11.1	53.3	0.6	5.0

3.6.2 Step-wise discrimination analysis of confluences

Statistical analysis of geochemical data showed clear differentiation of the upstream sediment samples from downstream. This was achieved through a 2-step statistical procedure that firstly involved removing variables that are not statistically different and then applying DFA using minimization of Wilks' Lambda to test the sample classification. Case-wise statistics of all the confluence coefficient combinations enabled 100 % classification of group membership of the upstream sources and was possible even with relatively low sample replications. Statistical significance tests of individual element concentrations displayed unique arrays for each confluence (Table 9). Three variables, CaO, Cu, P_2O_5, showed successful discrimination tests within all sampled confluences. C3 and C5 have over double the amount of successful statistically significant variables than C1-2 and C4 confluences. The difference can mainly be accounted for by successful significance tests for the REE earth elements (Sc, Y, La, Ce, Pr, Nd, Pm, Sm, Eu, Gd, Tb, Dy, Ho, Er, Tm, Yb, and Lu) which generally have similar chemical properties.

Table 9: *Summary table of elements that showed successful discrimination for each confluence location with elements common to each confluence indicated in bold.*

Confluence	Number	Elements
C1-2	13	**CaO**, Sr, Sc, Pb, , Zn, Cr**, Cu**, Al_2O_3, MnO, **P_2O_5**, Ni, K_2O, Tm
C3	35	Pb, **P_2O_5**, SiO_2, TiO_2, Al_2O_3, Fe_2O_3, **CaO**, Na_2O, K_2O, Sc, V, **Cu**, Ga, Rb, Sr, Y, Nb, Cs, La, Ce, Pr, Nd, Sm, Eu, Gd, Tb, Dy, Ho, Er, Ta, Th, Zn, MnO, Co, Tm
C4	12	TiO_2, Co, Hf, MgO, Na2O, **P_2O_5**, **Cu**, Zr, Al_2O_3, K_2O, Cr, **CaO**,
C5	34	Na_2O, **P_2O_5**, Zn, Fe_2O_3, MgO, **CaO**, Co, **Cu**, Sr, Y, Zr, La, Ce, Pr, Nd, Sm, Eu, Gd, Tb, Dy, Ho, Er, Tm, Yb, Lu, Hf, Ta, Th, U, Al_2O_3, SiO_2, K_2O, V, Ni,

DFA of successful tracer elements produced assorted tracer combinations for each confluence (Table 10). DFA analysis of the geochemistry showed a clear discrimination of C1-2 reaching a Wilks' Lambda value of 0.000 with 5 variables used in the final solution. C3 required 4 variables in the final solution achieving a Wilks' Lambda value of 0.001. The initial C4 solution only required two tracers to provide correct classification of the upstream sub-catchment signals but the Wilks' Lambda value remained relatively high in comparison to the other confluences, indicating adding additional tracers may be beneficial. Reducing the 'F' to enter threshold allowed Cu, Cr and TiO_2 to be added, reducing the Wilks' Lambda value from 0.095 to 0.006, providing a more optimal discriminant function. C5 required 5 variables to achieve a Wilks' Lambda value of 0.001.

Table 10: *Summary of stepwise Discriminant function analysis Wilks' Lambda value indicated by* ***λ.***

Step	C1-2				C3				C4			C5		
	Ent	λ	Coeff. 1	Coeff. 2	Ent	Rem.	λ	Coeff.	Ent	λ	Coeff.	Ent	λ	Coeff.
1	CaO	.040	31.97	8.91	Ce		.078		Hf	.292	5.54	Er	.145	74.66
2	Cu	.008	.02	1.21	Sr		.020	1.05	MgO	.095	134.36	V	.033	-3.47
3	Ni	.003	-.42	-1.39	K_2O		.011		Cu	.073	1.90	Al_2O_3	.012	73.20
4	Pb	.001	-.89	.51	SiO_2		.006	-9.15	Cr	.038	2.44	SiO_2	.004	24.25
5	Cr	.000	.94	.04	Nd		.002	-10.32	TiO_2	.006	-455.9	Tb	.001	104.44
6						Ce	.002							
7						K_2O	.002							
8					Cu		.001	1.42						
	constant		-64.79	-18.51	constant			635.08	constant		-29.39	constant		-2758.3

The downstream discriminant scores can be related to the upstream sub-catchment source providing indications of their relative contributions to downstream sediment samples. Downstream samples from the C1-2 confluence indicate a similar geochemical character to the

Tiraumea sub-catchment and a minor signature contribution from the Mangatainoka and the Upper Manawatu sub-catchments (Fig. 17). Samples downstream of C3 are closest to the upstream sediment signature of the Manawatu. Downstream samples from C4 showed the most variation in the signature, ranging from a close similarity with Upstream Manawatu to a similarity that lies somewhere in between Upstream Manawatu and Upstream Pohangina. C5 indicates dominant sediment signature from the upstream Manawatu with minor influences from the Oroua sub-catchment.

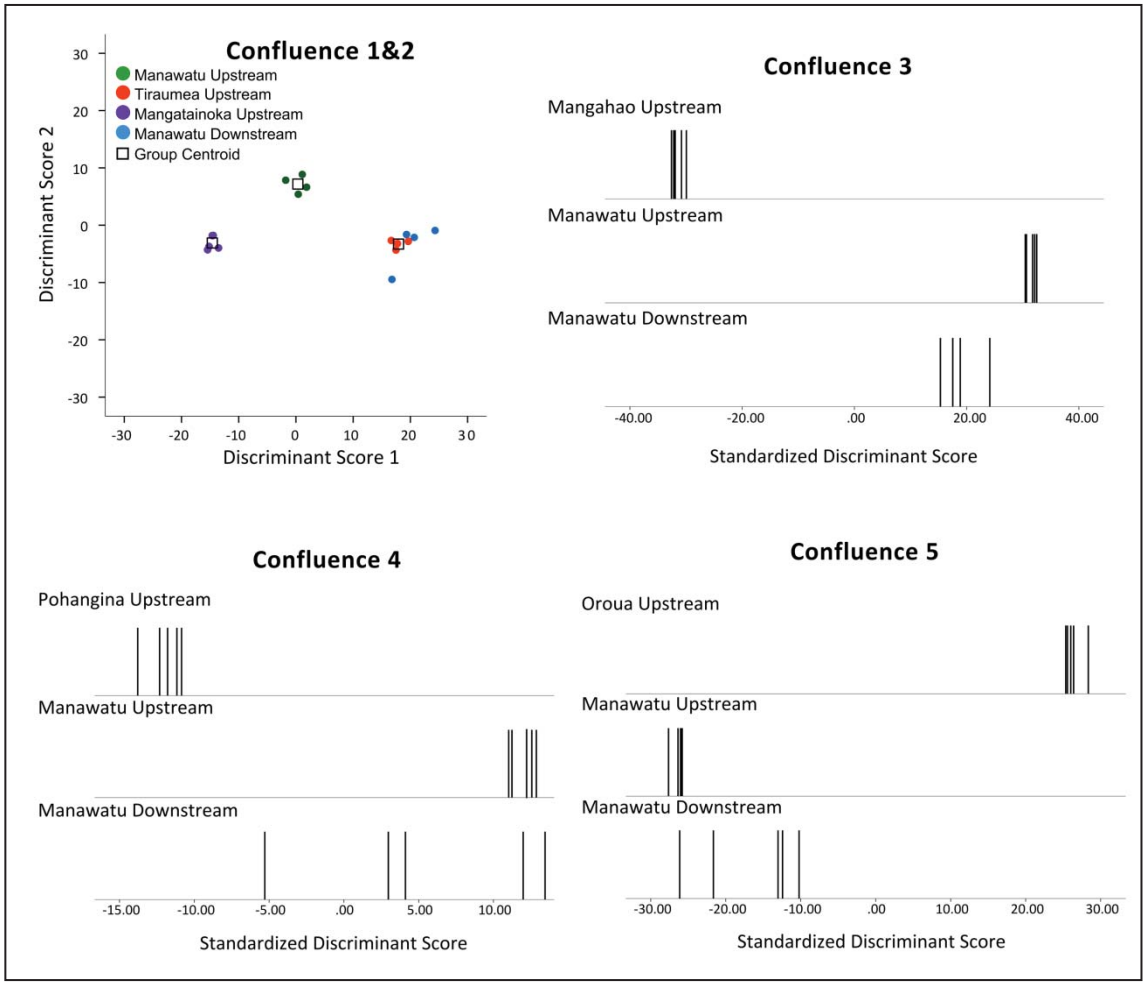

Fig. 17: *Display of discriminant function results for each confluence showing upstream and downstream discriminant scores. C1-2 has 3 variables so can have both x and y axis, C3, C4 and C5 only have 2 variables.*

3.6.3 Principal Component Analysis

The first two components account for the majority of variance for all the confluences, however, the extent varies for each sub-catchment (Table 11). C1-2 has a low first component variance of ≈ 54 %. C1-2 involves an additional sub-catchment which adds an extra degree of freedom. C1-2 & C4 confluences used fewer variables within their component analysis and the first component accounted for less of the total variance. In order to raise the percent of variance account for, C4 required an additional component with an eigenvalue below the initial cut-off value of 1. Percentage of variance account at C3 and C5 was ≈ 94 – 96 % for the first 2 components which provided the strongest values of all the confluences.

The pattern matrix (Table 11) and loading plots (Fig. 18) provide information on how the variables or tracers associate with the sediment source groups. The first component of C1-2 separates the Tiraumea and Mangatainoka sub-catchments attributed to higher concentrations of Zn, Al_2O_3, Pb, MnO and P_2O_5 in Mangatainoka Upstream, and lower concentrations of Sr and CaO. Component 2 provides the differentiation of Manawatu Upstream from Tiraumea and Mangatainoka sub-catchments, attributed to Sc, K_2O and Tm.

Component 1 of C3 can be attributed to REE's producing a positive loading on the Mangatainoka with CaO providing negative loading associated with Manawatu Upstream. Component 2 is dominated by major elements. Negative values are associated with Mangatainoka and positive values of Na_2O, Sr and SiO_2 associated with the Manawatu Upstream. Component 1 of C4 can be attributed to the major element composition with major elements except Na_2O providing the positive loading for the Manawatu Upstream also supported by higher concentrations of Zr and Hf in component 2. Component 1 of C5 is attributed to REEs, associated with positive loading of the Oroua Upstream loading while P_2O_5 can be attributed to the Manawatu Upstream loading. Component 2 could be attributed to major elements, alkali metal and alkaline earth elements exhibiting positive values associated with the Manawatu Upstream.

Table 11: *Principle Component Analysis results showing total variance account for and the associated pattern matrix of contributing elements*

Confluence 1-2				Confluence 3		Confluence 4				Confluence 5		
Eigenvalue	Component			Component		Component				Component		
	1	2	3	1	2	1	2	3		1	2	
Total	7.05	3.14	1.70	26.41	6.18	8.5	1.8	0.8		29.06	2.90	
% Variance	54.26	24.18	13.05	77.66	18.17	70.8	15.0	6.9		85.46	8.52	
Cumulative %	54.26	78.44	91.49	77.66	95.83	70.8	85.8	92.7		85.48	93.99	
Pattern Matrix for Principle Component Analysis												
Variable	1	2	3	Variable	1	2	Variable	1	2	3	Variable	1	2
Zn	1.00	-.06	.07	Tm	1.08	0.31	K_2O	1.05	-0.15	0.01	Sm	1.09	0.16
Al_2O_3	.97	.19	.03	Er	1.03	0.16	MgO	1.02	-0.04	0.06	Ta	1.08	0.18
MnO	.96	.11	.05	Th	1.02	0.05	Al_2O_3	1.00	-0.02	0.11	Gd	1.07	0.14
Pb	.93	-.13	.05	Ho	1.01	0.07	Na_2O	-0.98	-0.03	-0.05	Th	1.04	0.07
P_2O_5	.90	.21	-.07	Pr	1.01	0.04	TiO_2	0.94	0.10	0.08	Nd	1.04	0.07
Sr	-.75	.47	.26	Nd	1.01	0.05	P_2O_5	0.94	0.06	0.09	Pr	1.02	0.04
CaO	-.70	.55	.26	Ta	1.00	0.06	CaO	0.81	0.04	-0.23	Tb	1.02	0.09
Sc	-.27	.92	.20	Nb	1.00	0.00	Cr	0.69	0.21	-0.52	Eu	1.00	0.06
K_2O	.49	.76	-.21	Y	0.98	-0.02	Zr	-0.08	1.01	0.08	Ce	1.00	-0.01
Tm	.56	.72	-.09	La	0.98	-0.01	Hf	-0.06	1.01	0.06	La	0.97	-0.04
Cu	.07	.70	-.52	Dy	0.97	-0.05	Co	-0.33	-0.58	0.26	Dy	0.96	-0.04
Ni	.14	-.18	.95	Sc	0.97	-0.01	Cu	0.37	0.39	0.70	Er	0.95	-0.07
Cr	-.08	.29	.90	Sm	0.95	-0.06					Tm	0.92	-0.02
				Ce	0.93	-0.12					Ho	0.92	-0.10
				Eu	0.89	-0.17					Y	0.92	-0.12
				Tb	0.89	-0.18					Yb	0.88	-0.15
				Rb	0.88	-0.19					U	0.80	-0.26
				Gd	0.84	-0.19					P_2O_5	-0.80	0.17
				CaO	-0.80	0.20					Lu	0.79	-0.28
				Ga	0.72	-0.39					Sr	0.76	-0.30
				V	0.62	-0.47					CaO	0.68	-0.38
				Cs	0.57	-0.55					Na_2O	0.62	-0.44
				MnO	-0.25	-1.10					Co	-0.61	0.24
				Zn	-0.09	-1.03					Zn	-0.60	0.49
				P_2O_5	-0.10	-1.02					Hf	0.55	-0.54
				Fe_2O_3	0.02	-0.99					Ni	0.13	1.00
				SiO_2	-0.06	0.97					V	0.14	1.00
				Co	0.04	-0.95					SiO_2	0.11	-0.89
				Na_2O	-0.10	0.94					Al_2O_3	-0.13	0.89
				Al_2O_3	0.12	-0.93					K_2O	-0.18	0.86
				Sr	-0.12	0.93					MgO	-0.41	0.68
				TiO_2	0.25	-0.85					Cu	-0.32	0.67
				Cu	0.31	-0.75					Fe_2O_3	-0.40	0.67
				K_2O	0.50	-0.62					Zr	0.52	-0.57

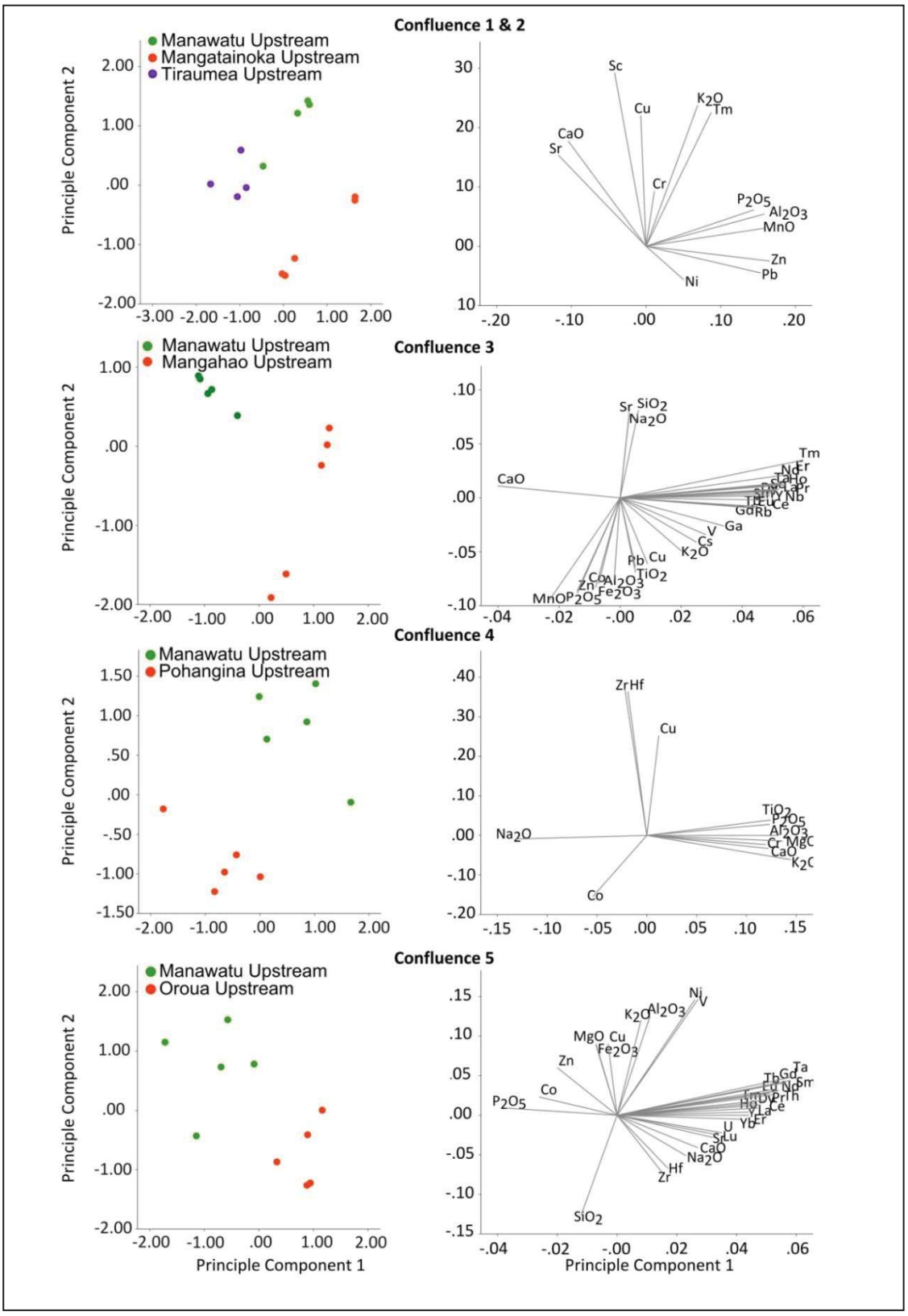

Fig. 18: *Display of principal component analysis data using biplots (left) showing the sample variation and loading plots (right) showing element loading pattern for each confluence*

3.6.4 Geochemical Summary

Major elements show similar trends for the average upstream catchment samples. SiO_2 abundance ranges from ≈ 65 – 72 % with the highest values in the Oroua and lower values in the eastern sub-catchments. The concentrations for the major elements, TiO_2, Al_2O_3, Fe_2O_3 and MnO display similar values to UCC and slightly lower values than PAAS, with the exception of the upstream Oroua sediment samples where MnO display an elevated value (Fig. 19).

CIA values range from ≈ 58 – 65, higher than the UCC values of ≈ 48 but lower than PAAS values of ≈ 70. ICV values range from 0.84 – 0.94 relative to UCC and PAAS values of ≈1.3 and≈ 0.89 respectively (Table 12). K_2O/Al_2O_3 ratios for the upstream sub-catchment samples lie between 0.14 – 0.17, compared to 0.22 and 0.20 for UCC and PAAS respectively. These three measures indicate a mixture of clays and feldspars. CIA values indicate low degree of total cation depletion, mostly from a loss of CaO opposed to Na_2O or K_2O.

Table 12: *Geochemical Indices for average upstream sediment data plus UCC and PAAS values for comparison*

Confluence	C1 Upstream Manawatu	C2 Upstream Mangatainoka	C2 Upstream Tiraumea	C3 Upstream Mangahao	C4 Upstream Pohangina	C5 Upstream Oroua	UCC	PAAS
K_2O/Al_2O_3	0.17	0.15	0.16	0.15	0.16	0.16	0.22	0.20
Th/Sc	0.77	0.79	0.72	0.81	0.78	0.92	0.79	0.91
Zr/Sc	14.93	13.70	14.40	23.32	17.74	45.56	13.97	13.13
Eu/Eu*	0.66	0.67	0.68	0.67	0.64	0.66	0.64	0.63
$(La/Yb)_N$	8.35	8.69	8.34	8.33	8.53	8.07	9.78	9.72
TotREE	125.55	118.20	114.56	145.42	122.98	146.14	146.37	184.77
ICV	0.89	0.86	0.94	0.84	0.89	0.93	1.28	0.89
CIA	62.82	65.44	60.66	65.23	61.28	58.85	47.93	70.39

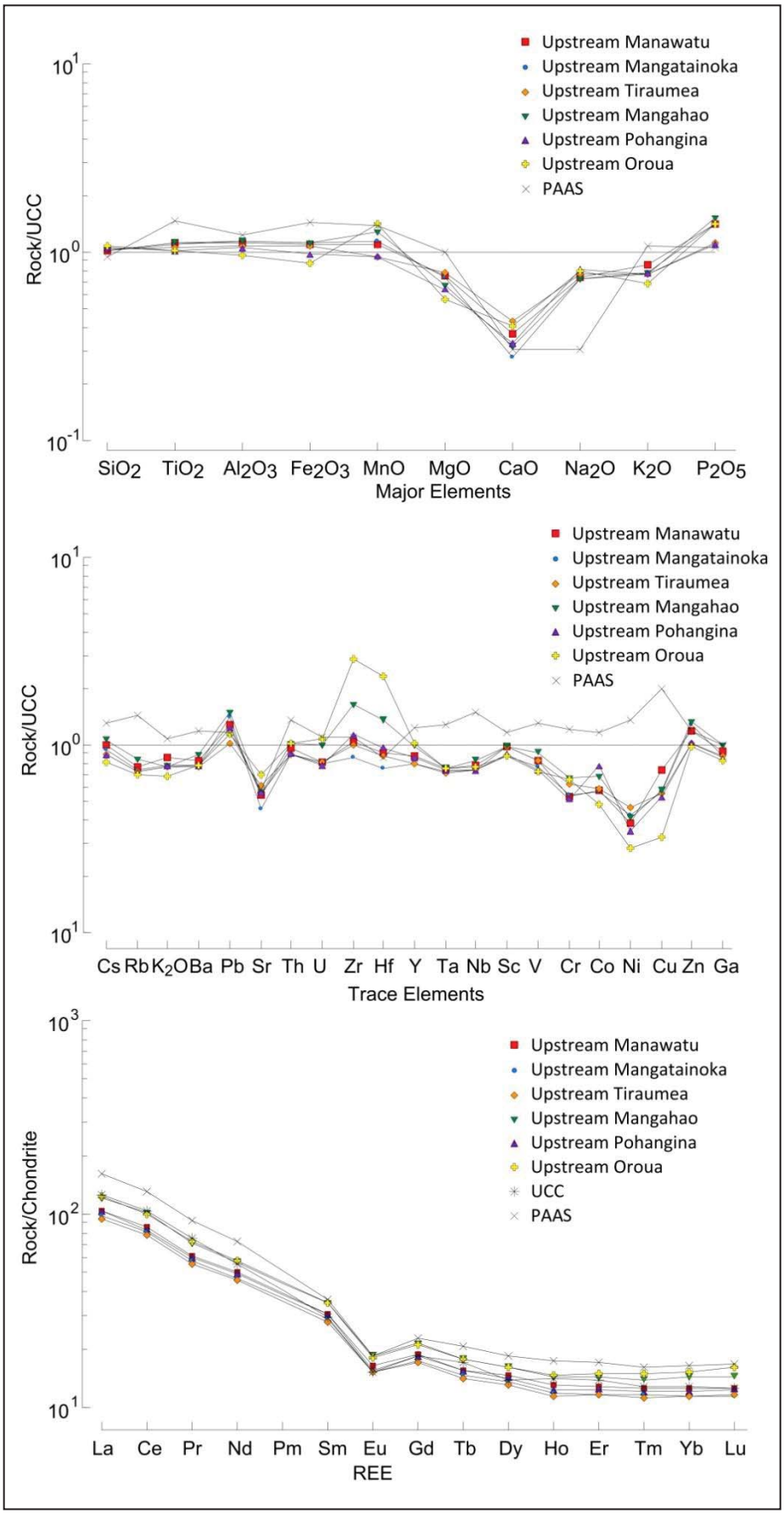

Fig. 19: *Multi-element plots of major (top), trace (middle) and REE (bottom)*

LIL elements, Rb, Cs, K_2O and Ba, display lower values relative to UCC and PAAS, likely related to lower CIA values. Sr values are analogous CaO depletion. The HFS elements particularly Zr and Hf are enriched in Oroua and Mangahao sub-catchments relative to the other sub-catchments as are Th, U, Nb and Y to a lesser extent (Fig. 19). Transition elements V, Cr, Co, Ni, Cu display depletion relative to UCC and PAAS. The Oroua displays the lowest trace element values compared to other sub-catchments, most evident for Ni and Cu. Values for Co in the Pohangina depart from the other sub-catchment trends, showing much higher values. Total REE (TotREE) values exhibit lower values than PAAS with the highest values observed within the Upstream Oroua and Mangahao sub-catchment sediment (146.1 & 145.4 respectively) (Table 12). LREE/HREE fractionation indicated by $(La/Yb)_N$ shows a LREE enrichment which is more pronounced in Mangatainoka (8.7) and Pohangina (8.5) and lowest LREE/HREE values for Upstream Oroua (8.1). Negative Eu/Eu* anomalies characterized all upstream sub-catchment sediment samples. Upstream Tiraumea displayed the weakest (0.678) average negative Eu/Eu* anomaly, whereas the Pohangina displayed the strongest (0.645) of the upstream sub-catchment sediment samples. A bivariate plot of Zr/Sc vs Th/Sc indicate significant zircon enrichment in the Oroua sub-catchment, and some enrichment occurring in the Mangahao sub-catchment (Fig. 20) when compared to other upstream sediment source groups which can also be seen directly in the Zr concentrations.

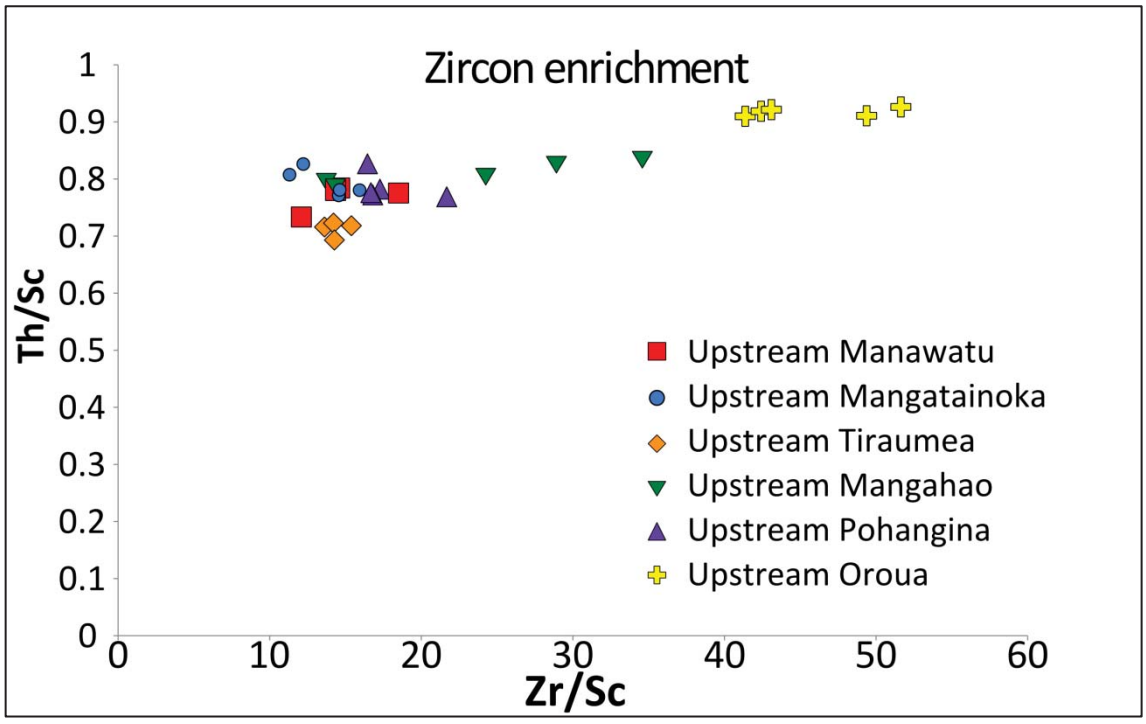

Fig. 20: *Th/Sc versus Zr/Sc indicating zircon enrichment for each upstream sub-catchment*

Particle size values for D_{50} ranged from 16 to 44 µm across all sample groups. The C1-2 upstream and downstream samples all showed D_{50} values of 16 µm. The C3 Upstream and Downstream Manawatu D_{50} values was 22 µm while the Upstream Mangahao D_{50} had value of 44 µm; the coarsest D_{50} across all confluences. The C4 samples showed D_{50} values for Upstream Manawatu of 16 µm and a coarser 22 µm for the Pohangina and Downstream Manawatu samples. The C5 showed a D_{50} of 16 µm for Upstream and Downstream Manawatu and a coarser D_{50} of 22 µm for the Upstream Oroua (Fig. 21).

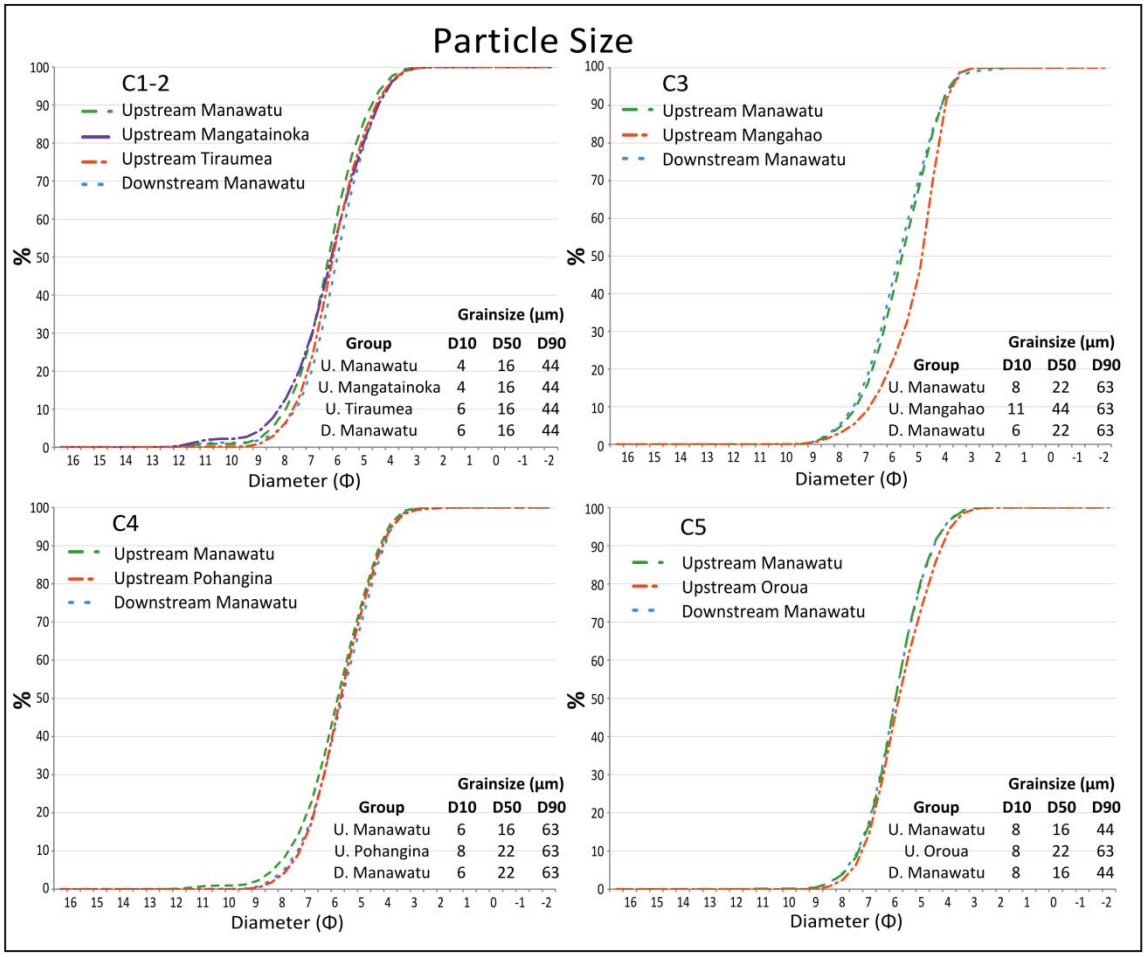

Fig. 21: *Particle size analysis for upstream and downstream samples including D10, D50 and D90*

3.7 Discussion

3.7.1 Statistical limitations of data analysis within large catchments

Large / intermediate sized catchments present complex challenges involving too many potential sources for a standard sediment fingerprinting technique. A solution to this issue may lie in alternative approaches such as a 'compositional evolution' (e.g. Hardy *et al.*, 2010) whereby sources as well as transported sediments are sampled throughout the river length. This study employs confluence-based sampling around confluence mixing zones as a coarse approach to understanding the variation in sediment character.

Step-wise discrimination for each confluence examined in this approach was able to select a set of variables that accurately classified the upstream signatures on a per confluence basis, even with low sample replication. There are several explanations as to why this is possible. A confluence-based approach simplifies the sediment transport connections by reducing the distance between the classically termed 'source' and 'sink' concept of a sediment fingerprint approach. This is achieved by sampling immediately upstream of the confluence, which provides a proxy for upstream sediment source geochemical signatures. The short distance between upstream and downstream sediment samples limit the effect that non-conservative behaviour has on geochemical signature uncertainty. Variables that prove successful with a confluence approach will not necessarily be suitable for a whole catchment mixing model purposed for attributing sediment sources. This is because the whole catchment will involve a greater number of sources that need to be characterized from each other and remain unaltered through a longer transport route. They do however provide useful information to the nature of the geochemical behaviour taking place during transport.

The results indicate that such an approach can provide knowledge of proportional sediment contributions for sub-catchment sources, and with greater sample replication, sub-catchment sediment sources could be quantified. A limitation of this approach is the lack of information it provides on specific sediment sources within sub-catchments, which is important for catchment management strategies. Source-specific sediment information is however limited in providing spatial information by the degree in which the processes and specific sources are spatially distributed or confined. A large catchment that experiences similar processes and geological/pedological sources across multiple sub-catchments, even if sufficiently mapped, would be limited in the ability to specify the unique contribution between two mudstone

sources in different locations. Therefore both lines of information would be ultimately beneficial.

DFA by minimization of Wilks' Lambda is designed to use the least number of variables as possible but may not always provide the most suitable variable selection from a geochemical perspective. Statistically, including multiple variables which are linearly related provide no additional information to account for variance and would actually inhibit reliable results by causing collinearity issues to arise. Collinearity is minimized from the dataset during the stepwise minimization of Wilks' Lambda and using the minimum variables possible as well as only utilizing variables that account for variance in a new dimension. This is evidenced with C3 and C5 where, although there are a suite of REE elements available for inclusion in DFA, only Nd is eventually included in the C3 solution, and Er and Tb included in the C5 solution. The initial 2-variable DFA solution of C4 highlights the issue of relying on a statistical technique. This makes statistical sense; however, when evaluated within the context of a dynamic fluvial catchment, it does not seem wise to rely on two elements to discriminate the confluence sediment source. This increases the susceptibility to outlier values or single element contamination. Collins *et al.* (1998) experienced a similar issue when characterizing the Severn sediment fingerprinting signature using only 3 tracers but added 3 additional tracers to increase the reliability. There is also high variability in the association of tracers with sediment sources (Fig. 18) which places emphasis on the importance of tracer selection and source classification in determining quantitative sediment source estimates.

3.7.2 Geomorphic effects at confluences

Variability between downstream sediment signatures possibly reflects the dissimilar extent of transverse sediment mixing that occurs at each confluence which would have direct implications on the heterogeneity of the sample. The degree of transverse mixing that occurs is dependent on the confluence flow structure and planform geometry, including channel width and confluence angle, bedform morphology, hydrological conditions such as high and low flows, and the differences in flow between main-stem and tributary channels (Best, 1988, Kenworthy and Rhoads, 1995, Rhoads and Sukhodolov, 2008). These factors influence secondary flow and lateral advection characteristics which determine the distance and efficacy for sediment contributions from each respective confluence to become homogenously mixed. An assumption of this field study was that sediment mixing occurs within a relatively short distance of the confluence which may not hold true, as evidenced by the C4 confluence. The difference in channel width and the complexity of the confluence planform geometry through

the presence of mid-channel bars and multiple channels may be responsible for the variability of the downstream sediment signature of the C4 confluence (Fig. 22). These channel features are not as evident in the C1-2, C3 and C5 confluences. C3 and C5 reflect tributaries entering the mainstem of the Manawatu River with respective channel widths of the Mangahao and Oroua Rivers being considerably narrower and representing a single sinuous channel with fewer morphological bar units. The two components of the C1-2 each display relatively simple confluences with the Tiraumea, void of depositional features while the Upper Manawatu enters as a single sinuous thread channel.

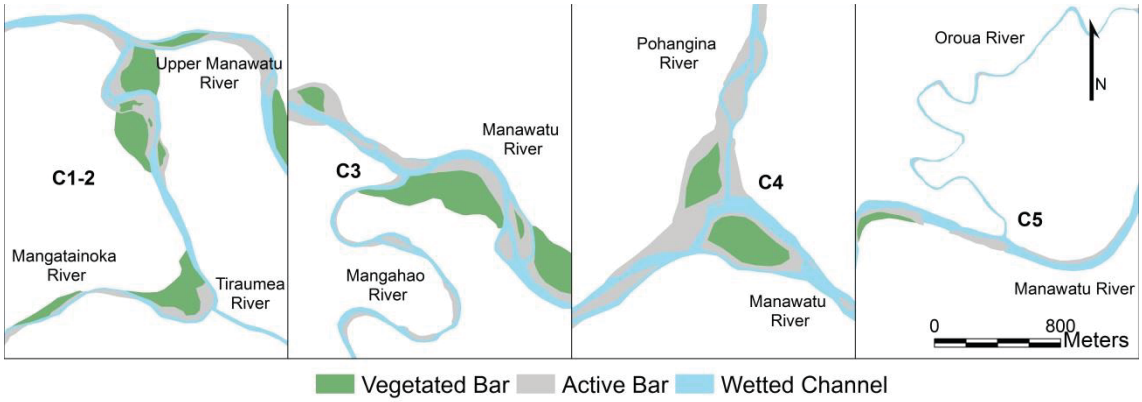

Fig. 22: *Simplified map showing confluence morphology*

The variations could also be explained by a limitation in the sampling method to account for the inherent spatial variability that can occur within short distances and temporal sediment fluxes. Sediment deposition patterns change during different stages of a flood hydrograph which reflect changing sub-catchment flow contributions. This typifies the challenge of any point sampling method to adequately represent the phenomena targeted. Thus, it is important to caution against extrapolating results for each individual confluence beyond the spatial and temporal constraints in which the sampling method permits. Localized high rainfall events and rainfall anomalies which affect one sub-catchment more than another are likely to prime the confluence with sediment from that respective sub-catchment so that the sampled channel sediment is inevitably influenced by the antecedent hydrological and sediment conditions prior to sampling. The extent of these conditions on each confluence has not been explored in this investigation but is likely to be less influential downstream as the Manawatu main stem becomes progressively dominant in total sediment load.

3.7.3 Changing geological influences of sub-catchments

Regardless of how well the stepwise DFA is able to classify sources, it is advantageous to explore the geochemical patterns for all elements in order to fully understand the nature of the geochemical environment. Statistically, PCA has provided a complimentary set of data and the ability of visually displaying the weighting and correlations of element concentrations. It provides a simple way to identify substitute elements if modification of the discriminant function is required in the event of contamination or unreliable data of a selected element or the requirement to add more variables to the discriminant analysis. An understanding of geochemical processes needs to be coupled clearly with the statistical tools to avoid the discriminant scores becoming arbitrary and disconnected from the 'on-the-ground' implications. Smith and Blake (2014) also point out the importance of understanding the physical and chemical basis for tracer selection and the causes of patterns observed for successful sediment fingerprinting application. Exploring the geochemical trends and particular array of elements providing discrimination can provide further understanding as to the type of processes or spatial variation responsible for the trends observed. It is not possible to cover every element and its' associated geochemistry but some observations can be made.

A clear difference for discriminating the upstream sediment samples for the Oroua and Mangahao sub-catchments is the increased number of variables that provide discrimination attributed to the addition of REE's. Enrichment of Zr and Hf in the sediment samples indicates the presence of the mineral zircon which possibly also explains the lower LREE/HREE ratio found in the Oroua sediment samples compared to the other Manawatu sub-catchments (Table 6). This is due to zircon progressively favouring substitution of higher atomic number REEs due to their decreasing ionic radii producing a lower LREE/HREE ratio. The overall REE trend for the bulk sediment sample is relatively unaffected and is still very much enriched in LREE, indicative of felsic derived minerals due to zircon's relatively low total abundance. In explanation for the Upstream Oroua sediment values is quite straightforward. Zircon is resistant to weathering and exhibits a high specific gravity meaning that Zr is susceptible to sorting effects, concentrating in coarser material such as sand (Taylor and McLennan, 1985). The Oroua confluence is situated in sand-dune landscape and provides a barrier to further dune movement eastward. The elevated Zr and Hf concentrations are therefore likely due to an external source not from the Manawatu River. The elevated Zr possibly provides a tracer to distinguish where dune sand contribution into the Oroua and Manawatu Rivers initiates.

Elevated Zr and Hf concentrations are less pronounced in the Mangahao sediment samples, but are still likely related to a zircon influence for several reasons. The Zr and Hf are elevated

more than other HFSE elements indicating enrichment beyond expected felsic composition. The particle size of the Mangahao sediment samples was slightly coarser than the other upstream sediment samples (Fig. 21) providing a sediment sorting explanation for the increase of Zr concentration. Another possibility is the retention of the geological source signal responsible for the Zr influence within the Mangahao sub-catchment, namely the clastic greywacke which typically has higher Zr concentrations than sandstone, shale or mudstone (Salminen *et al.*, 2005). The sub-catchment is underlain by a higher proportion of the greywacke range (59.0 %) compared with other sub-catchments in the Manawatu (Table 6). Sediment originating from this sub-catchment is likely to be dominated less by the lowland (low relief) agricultural grassland and proportionally more from the sediment originating from the Tararua Range, where steep valley sides and sheared rock matrix is prone to failure. This implies retention of a 'clearer' or 'undiluted' greywacke geological signal, less affected by other geological sources (i.e. mudstone cliffs) and agricultural regimes.

Within the C1-2 confluence, Ca presents a strong discriminating variable, exhibiting the highest concentrations from Tiraumea followed by the Upper Manawatu and Mangatainoka sediment samples. These differences likely arise due to the variation in the source composition. The Tiraumea drains the largest extent of mudstone (63.8 %) and limestone (11.3 %) terrain of all the sub-catchments (Table 6). The weathered limestone gives rise to melanic soils occurring more widely than in the Mangatainoka and Upper Manawatu sub-catchments, with the remainder overlain by various brown and pallic soils covering most of the remaining catchment area. The Upper Manawatu drains similar mudstone and limestone landscapes but also contains a high proportion underlain by gravelly alluvial floodplain (39.7 %) and predominant drainage originates from the greywacke range overlaid by allophanic brown and pallic soils. The Mangatainoka also consists of greywacke headwaters (21.2 %) but is also dominated by gravelly alluvial floodplain (37.8 %). Although the Manawatu catchment as a whole is depleted in Ca, the limestone and derived detritus within the Tiraumea may provide high enough Ca concentrations to influence the Tiraumea sub-catchment geochemical signature. The ability to extend the use of Ca concentrations as a viable sediment property for whole catchment differentiation is however dependent on whether the Ca concentrations are conservative during transport, especially through a larger catchment. This depends on whether residence time is relatively short compared to enrichment or depletion effects caused by the aquatic geochemistry, which is beyond the scope of this preliminary research and the subject of ongoing investigation.

3.7.4 Geomorphic evaluation with sub-catchment characteristics.

The source differentiation of sub-catchment sediment is generally in agreement with the characteristics of the catchment geology and catchment size. The Tiraumea sub-catchment, which is predominantly soft sedimentary mudstone hill country, was identified as the main contributor to downstream sediment supply from C1-2, and is recognized to have very high suspended sediment loads, draining 36 % of the total erosion prone land in the Manawatu (Horizons Regional Council, 2011). Measured and modelled SedNetNZ suspended sediment loads attribute the highest contributions coming from Upper Manawatu, Pohangina and the Tiraumea (Table 13). The measured loads suggest the Upper Manawatu is a much greater source of sediment than that Tiraumea. This is not reflected in the DFA results for C1-2, but could be explained by the variability of fluvial sediment in both the sampling of this study and in the annual measured suspended sediment loads which have been found to have a coefficient of variation ranging from 42 % to 176 % (Hicks and Hoyle, 2012).

Table 13: *Comparison of mean annual suspended sediment yields estimates for Manawatu sub-catchments*

Sub-catchment	Hicks and Hoyle (2012) Measured		Basher *et al.* (2012) Measured		Dymond *et al.* (2014) SedNetNZ		Horizons Regional Council (2011)
	$t\ y^{-1}$	%	$t\ y^{-1}$	%	$t\ y^{-1}$	%	%
Upper Manawatu	600,444	32.0	569,879	31.9	478,346	28.4	29
Tiraumea	338,014	18.0	323,694	18.1	411,068	24.4	34
Mangatainoka	50,400	2.7	55,695	3.1	148,771	8.8	6
Mangahao	163,833	8.7	175,560	9.8	130,014	7.7	5
Pohangina	508,356	27.1	451,689	25.3	232,505	13.8	11
Oroua	215,100	11.5	210,374	11.8	282,699	16.8	10

Additionally, there is evidence for considerable errors with the measured data arising from calibration errors, extrapolation uncertainties, and point source vs cross-section sampling (Basher *et al.*, 2012). The SedNetNZ sediment values, incidentally, show a greater contribution from the Tiraumea which would agree more with the DFA scores for C1-2 and may suggest measured data is underestimating sediment source contribution from the Tiraumea. Downstream, the effect of drainage size becomes more evident as the total Upstream Manawatu catchment size, at successive downstream confluences (C3, C4 and C5), represents a greater proportion of catchment area, which dominate the downstream signatures. Lower sub-catchment sizes for the Mangahao, Oroua and Mangatainoka are an important factor in their lower total sediment contributions, despite the Mangahao and Oroua having higher

suspended sediment yields (SSY) than the Tiraumea and Upper Manawatu (Basher *et al.*, 2012). Substantial measured suspended sediment loads from the Pohangina (Table 13) do however appear to be represented in the confluence results, with some samples displaying similar signatures to the Pohangina sediment.

3.8 Conclusions

Given the challenge of assessing large/intermediate sized catchment sediment fingerprints, 'compositional evolution' approaches may be necessary to address the increasing complexity. The Manawatu is a dynamic catchment with a heterogeneously interspersed geology which is spatially unconfined for many geological sources. Results from this exploratory investigation indicate that numerous geochemical elements have the ability to differentiate fine sediment sources using a broad-scale confluence-based approach and suggest there is enough geochemical variation throughout the Manawatu catchment for a full sediment fingerprint model of the Manawatu catchment. An increase in sample replication would dramatically increase the robustness of this approach, providing useful information necessary for evaluating a greater number of sources over larger distances.

The Tiraumea sub-catchment provides the dominant signature for the first major confluence (C1-2), although major contributions from the Upper Manawatu are likely but not evident in this study. These two larger sub-catchments provide the majority of the sediment signature to downstream confluences. The Pohangina sub-catchment contributes a significant proportion of sediment at C4, but much less than upstream Manawatu contributions. C4 sediment signatures also indicate only partial mixing. Despite the limitations associated with point sampling, it has nevertheless been useful in characterising the nature of sediment sampled, and indicates the dominant sub-catchment inputs from fluvial transport. In order to undertake quantitative calculations of the relative sediment inputs, sample replication will need to be increased with a temporal component.

Combining powerful statistical procedures with other geochemical analyses is critical to understanding the processes or spatial patterns responsible for the sediment signature variation produced. Statistical approaches by themselves can only provide limited understanding. Geochemistry is influenced by source geology and subsequent diagenetic processes, and weathering which can enrich or deplete geochemical elements, therefore an improved understanding of the degree of conservativeness behaviour and suitability of

individual elements within this catchment is necessary for subsequent sediment fingerprint research to provide quantitative information.

3.9 Acknowledgements

We would like to acknowledge funding support from Landcare Research by way of the Murray Jessen PhD Scholarship.

3.10 Summary

This chapter has concluded that geochemical differentiation is possible for broad-scale confluence-based sediment fingerprinting approach in the Manawatu Catchment. This justifies the outlay for a significantly more extensive sampling programme of unique sediment sources in the catchment which is provided in the following chapter.

Chapter 4

Characterization and quantification of suspended sediment sources to the Manawatu River, New Zealand

4.1 General Introduction

Chapter 3 showed that despite being underlain by similar geological terrains, there is enough geochemical variability with the catchment to provide differentiation of sub-catchment sources when using a confluence-based approach. Chapter 4 includes the published manuscript: Vale SS, Fuller IC, Procter JN, Basher LR, Smith IE., Characterization and quantification of suspended sediment sources to the Manawatu River, New Zealand first published in *Science of the Total Environment* 2016; 543: 171-86, expands on the initial research through an extensive sampling scheme focusing on unique fine sediment sources within the catchment. This is achieved in categorizing the sediment sources into eight distinct geomorphological sources and geochemically analysing the sediment using XRF and LA-ICP-MS analysis to determine major, minor and rare earth element bulk concentrations. Discriminant function analysis is employed to derive the best set of geochemical variables to characterize the unique sources. This is followed up by the implementation of two mixing models, each with two optimization techniques, to estimate relative source proportions which are evaluated in context to the Manawatu Catchment characteristics.

4.2 Abstract

Knowledge of sediment movement throughout a catchment environment is essential due to its influence on the character and form of our landscape and relates to agricultural productivity and ecological health. Sediment fingerprinting is a well-used tool for evaluating sediment sources within a fluvial catchment but still faces areas of uncertainty for applications to large

catchments that have a complex arrangement of sources. Sediment fingerprinting was applied to the Manawatu River Catchment to differentiate 8 geological and geomorphological sources. The source categories were Mudstone, Hill Subsurface, Hill Surface, Channel Bank, Mountain Range, Gravel Terrace, Loess and Limestone. Geochemical analysis was conducted using XRF and LA-ICP-MS. Geochemical concentrations were analysed using Discriminant Function Analysis and sediment mixing models. Two mixing models were used in conjunction with GRG non-linear and Evolutionary optimization methods for comparison. Discriminant Function Analysis required 16 variables to correctly classify 92.6 % of sediment sources. Geological explanations were achieved for some of the variables selected, although there is a need for mineralogical information to confirm causes for the geochemical signatures. Consistent source estimates were achieved between models with optimization techniques providing globally optimal solutions for sediment quantification. Sediment sources was attributed primarily to Mudstone, ≈ 38 – 46 %; followed by the Mountain Range, ≈ 15 – 18 %; Hill Surface, ≈ 12 – 16 %; Hill subsurface, ≈ 9 -11 %; Loess, ≈ 9 -15 %; Gravel Terrace, ≈ 0-4 %; Channel Bank, ≈ 0 - 5 %; and Limestone, ≈ 0 %. Sediment source apportionment fits with the conceptual understanding of the catchment which has recognized soft sedimentary mudstone to be highly susceptible to erosion. Inference of the processes responsible for sediment generation can be made for processes where there is a clear relationship with the geomorphology, but is problematic for processes which occur within multiple terrains.

Keywords: sediment fingerprinting; suspended sediment; New Zealand; geochemistry

4.3 Introduction

Suspended sediment is one of the most important components of the sediment transport system (Collins and Owens, 2006, Bracken, 2010). Elevated suspended sediment loads reflect enhanced erosion processes, land instability, and often a loss of productive soils within a catchment (Owens *et al.*, 2005, Walling and Fang, 2003). Sediment influx can also impact channel morphology, water quality and aquatic ecosystems (Wood and Armitage, 1997) which is often considered a pollutant where elevated levels of nutrients bind to sediment (Calmano *et al.*, 1993, Horowitz and Elrick, 1987). It is therefore important to identify the key source areas responsible for sediment generation as the first step towards minimizing sediment delivery into the fluvial system. This is especially true for erosion-prone areas where erosion rates have been exacerbated due to human activity and poor land management.

A variety of direct and indirect techniques have been developed to assess suspended sediment source information, including aerial photography (e.g. Marzolff and Poesen, 2009), erosion pins (e.g. Haigh, 1977, Lawler, 1986), sediment gauging stations (e.g. Hicks *et al.*, 2000, Wang *et al.*, 2007), turbidity sensors (e.g. Lewis, 1996, Hicks *et al.*, 2004), sediment fingerprinting (e.g. Collins *et al.*, 1997, Walling *et al.*, 1999) and modelling (e.g. Prosser *et al.*, 2001, Merritt *et al.*, 2003). However, the spatial and temporal variability of suspended sediment load, coupled with the financial limitations for full catchment system monitoring, compromise the ability of many studies to provide meaningful information (Collins and Walling, 2004).

Sediment fingerprinting provides a means of directly quantifying sediment contribution from unique sources within catchments. This is achieved by sampling a range of sediment sources throughout the catchment system, differentiating the sources using inherent properties, and then quantifying the relative contributions to the suspended sediment load from the identified sources. A considerable range of tracers has been employed in sediment fingerprinting research, including; mineralogy (e.g. Eberl, 2004, Gingele and De Deckker, 2005), mineral magnetic signatures (e.g. Caitcheon, 1998, Blake *et al.*, 2006), geochemical compositions (e.g. Collins *et al.*, 1998, Collins *et al.*, 2013, Lamba *et al.*, 2015, Hardy *et al.*, 2010, Zhang *et al.*, 2012), isotopic ratios (e.g. Douglas *et al.*, 1995, Gingele and De Deckker, 2005), radionuclides (e.g. Wilkinson *et al.*, 2013, Olley *et al.*, 2013, Porto *et al.*, 2013), organic elements (Fox and Papanicolaou, 2008a, Evrard *et al.*, 2013), and compound-specific isotopes (e.g. Gibbs, 2008, Hancock and Revill, 2013, Blake *et al.*, 2012).

Sediment fingerprinting research has expanded dramatically, advancing from early studies, which employed a limited array of tracers (e.g. Peart, 1993, Walling *et al.*, 1979), to comprehensive geochemical suites relying on statistical analysis and mixing models for sediment source evaluation (e.g. Haddadchi *et al.*, 2014, Laceby and Olley, 2015, Cooper *et al.*, 2014). Despite the increasing use of sediment fingerprinting, there have been a number of ongoing challenges within the approach. Recent research has drawn attention to uncertainties with sediment mixing models (e.g. Haddadchi *et al.*, 2014), tracer selection (e.g. Pulley *et al.*, 2015), source classification and within-source geochemical variability (e.g. Collins *et al.*, 2010a).

Changes in sediment geochemistry can occur from chemical, biological and physical modification throughout transportation. The extent of these changes is often poorly understood and has been referred to as a 'black-box' by Koiter *et al.* (2013b) due to the uncertainties. These uncertainties raise implications for how accurately sediment source

signatures are retained during transport. Furthermore, typical sediment fingerprinting approaches assume a directly connected transport pathway from source to sink, which is not the case in many circumstances as sediment is transported as periodic storage and release, sometimes referred to as a 'jerky conveyor'(Ferguson, 1981). Belmont *et al.* (2014), explored the nature of some of these changes through measuring and modelling $^{210}Pb_{ex}$ and ^{137}Cs decay through floodplain storage and understanding the geomorphic processes that fractionate sediments, concluding that there is a need to better understand the relationships between the processes and geochemical signature of the sediment. The specific suite of geochemical variables employed also generates significant uncertainty, as most sediment fingerprinting approaches use a different array of tracers and select the ones which provide the best discrimination between sources. This was demonstrated by Pulley *et al.* (2015), who identified a mean difference of ≈ 24 % between predictions arising from different tracer groups.

Quantitative mixing models have also come under scrutiny as the number of mixing models to choose from increases. Some models use local optimization techniques, while others use global optimization, the latter, in theory, is more likely to produce an appropriate solution but can also take considerably longer to run (Frontline Systems Inc., 2010). In addition, the use of Genetic or Evolutionary Algorithms have been used in recent studies (e.g. Collins *et al.*, 2010b) as a form of global optimization. Haddadchi *et al.* (2014) tested different models using the same dataset and showed that source contribution displayed a dependence on the selected mixing model. Incorporation of weighting and correction factors has been used in some studies to improve performance (e.g. Collins *et al.*, 2010a), however, Laceby and Olley (2015) found incorporation of some of these factors in mixing models does not necessarily improve the model performance. Pulley *et al.* (2015) also highlight this point, finding that organic matter and particle size distribution were not likely causes for uncertainties. This highlights the need to carefully consider using adjustments within mixing models as they can generate unquantifiable errors (Smith and Blake, 2014).

In this study a sediment fingerprint is applied to a New Zealand sedimentary rock dominated catchment with a variety of geological and geomorphological sources. The aim is to identify discrete fine-sediment sources within the catchment and identify the geochemical variables that provide source differentiation, identify and relate the geological and geomorphological processes with the statistical outcomes and variable selection, and compare optimization techniques for the two mixing models applied.

4.4 Study Site

The Manawatu River drains a ≈ 5870 km^2 catchment situated in the lower North Island, New Zealand (Fig. 23) which is underlain by a sedimentary geology consisting of mudstone and sandstone. The headwaters drain the eastern flanks of the uplifted greywacke block forming the Tararua and Ruahine Ranges before flowing west through the main drainage divide via the Manawatu Gorge, incorporating flow from the western flanks of the mountain range before continuing through to the Tasman Sea (Fig. 23). Steep hillslopes are common throughout the eastern sub-catchments e.g. Tiraumea (Table 14) and underlain primarily by soft mudstone while the middle reaches are semi-confined within mudstone bedrock cliffs and alluvial terraces. The lower reaches flow through extensive alluvial floodplains and range from wandering to pseudo-meandering. Many of the channels have undergone straightening and narrowing of the channel , transitioning to laterally-confined single thread channels as evidenced in the Pohangina River (Fuller, 2009).

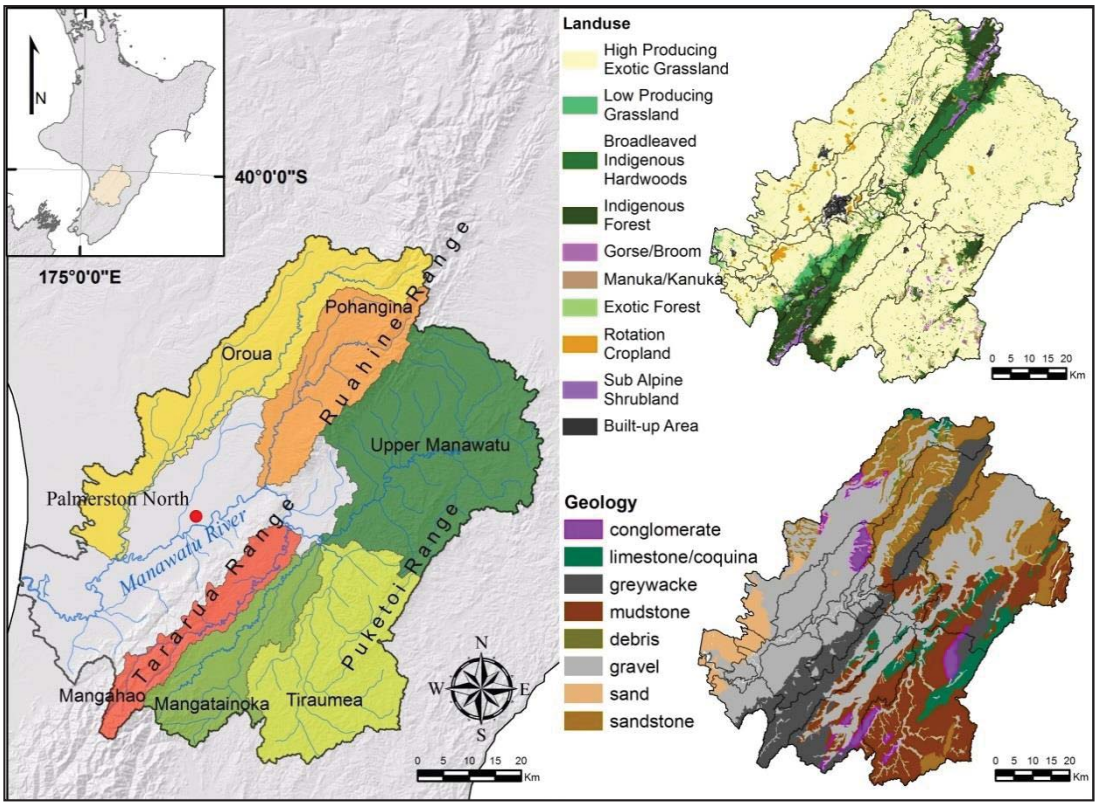

Fig. 23: *Manawatu Catchment, Land-use and Geology*

Table 14: *Geological composition by sub-catchment*

Geological Material	% of area						
	Main Sub-catchment						Total Catchment
	Upper Manawatu	Tiraumea	Mangatainoka	Mangahao	Pohangina	Oroua	
Greywacke	5.9	3.1	21.2	59.0	30.9	3.4	14.6
Mudstone	22.8	63.8	29.5	7.3	2.3	-	18.5
Sandstone	24.0	3.9	0.1	0.0	44.6	27.3	14.7
Gravel	39.7	11.8	37.8	28.0	19.7	52.6	40.3
Limestone/ Coquina	7.4	11.3	6.3	5.6	-	2.6	4.8
Conglomerate	0.1	6.1	5.1	-	0.1	2.4	2.4
Sand	-	-	-	-	-	9.7	2.8
Debris	-	-	-	-	2.3	2.0	0.5

The New Zealand Soil Classification (NZSC) after Hewitt (1998), classifies most the soils as Orthic/Firm Brown Soils with Allophanic Brown Soils found on the flanks of the axial range while Argillic Pallic Soils are found in the Puketoi Range, along with limited Melanic Soils found in the limestone regions. Immature Pallic Soils are common throughout the eastern sub-catchments as well as the Pohangina, Perched-Gley Pallic Soils are found on the western flanks of the Tararua Range, in the lowland areas in the Oroua and north of Palmerston North (Fig. 23) and recent Alluvial Soils are found on extensive floodplains proximal to the channels.

Mean annual discharge for Manawatu River is c.110 m^3 s^{-1} with contributions from the following main sub-catchments, Upper Manawatu (c. 27 m^3 s^{-1}), Tiraumea (c. 16 m^3 s^{-1}), Mangatainoka (c. 18 m^3 s^{-1}), Mangahao (c. 15 m^3 s^{-1}), Pohangina (c. 17 m^3 s^{-1}), and Oroua (c. 13 m^3 s^{-1})(figures derived from Henderson and Diettrich, 2007).

Land-use in the Manawatu Catchment is predominantly agriculture, with vegetation consisting of ≈ 75 % exotic grassland (cf. Fig. 23). Sheep and beef farming occurs in the steeper terrain and dairying in the lowlands. The Tararua, Ruahine and Puketoi Range contain most of the catchment's indigenous vegetation (≈ 17 %). Exotic forest only accounts for ≈ 3 % of catchment area. Minor pockets of mānuka and kanuka, grey scrub, and short-term rotation crops occur in the catchment.

4.5 Materials and Methods

4.5.1 Sediment Sample Collection

Sampling aimed to characterize the processes responsible for sediment inputs to the fluvial system e.g. landslides, bank erosion, cliff erosion, surface erosion. However, it became evident that a process-only sampling classification does not adequately categorize the full range of distinct sources and therefore these initial classifications were reclassified to represent a combination of spatial location, processes and geological landscape units (Table 15). Sampling consisted of 5-10 samples taken to form a composite sample for the sediment source at each specific location. Surface sediment samples were taken from the top 4 cm of material, while the remaining source samples were taken at various depths depending upon where that source material lay within the sample profile. The sink sediment sample was collected by placing PVC pipes in the Manawatu River for a period of 4 months at monitoring site known as Teachers College (T-Col) in Palmerston North (Fig 24). The sink sample location does omit capture of the Oroua confluence which accounts for an estimated ≈ 10 % of suspended sediment.

Table 15: *Sediment source characteristics for each of the sediment source classifications (cf. Fig. 25)*

Sediment Source	Characteristic
Mountain Range	Mountain Range Sediment was sampled from the Ruahine and Tararua Range from landslide and debris avalanche material originating from the greywacke dominated terrain.
Mudstone	Mudstone samples were taken throughout the catchment, typically from exposed mudstone cliffs. Due to safety limitations, sampling consisted of grab samples taken from sediment deposits at the foot of the cliffs. This represents the most readily available sediment entering the channel.
Hill Subsurface	Hill Subsurface samples were taken from subsurface scrapings typically consisting of the B horizon (but not bedrock material) of the steeper hill country terrain to represent a proxy for shallow translational landslide material.
Hill Surface	Hill Surface samples were taken from the upper 4 cm of the steeper hill country terrain to represent surface material originating from the steep slopes.
Limestone	Isolated limestone deposits were sampled as grab samples to represent a limestone signature.
Loess	Unconsolidated material, mostly in the form of loess, was sampled both from cliff material as well as some horizons in bank sediment
Channel Bank	Samples were collected from scrapes of subsurface sediment channel banks proximate to active channel erosion. Multiple subsurface samples were taken if there were multiple subsurface horizons.
Gravel Terrace	Alluvial gravel terraces were sampled from exposures found throughout the catchment typically next to the active channel forming part of the bank or cliff sequence.

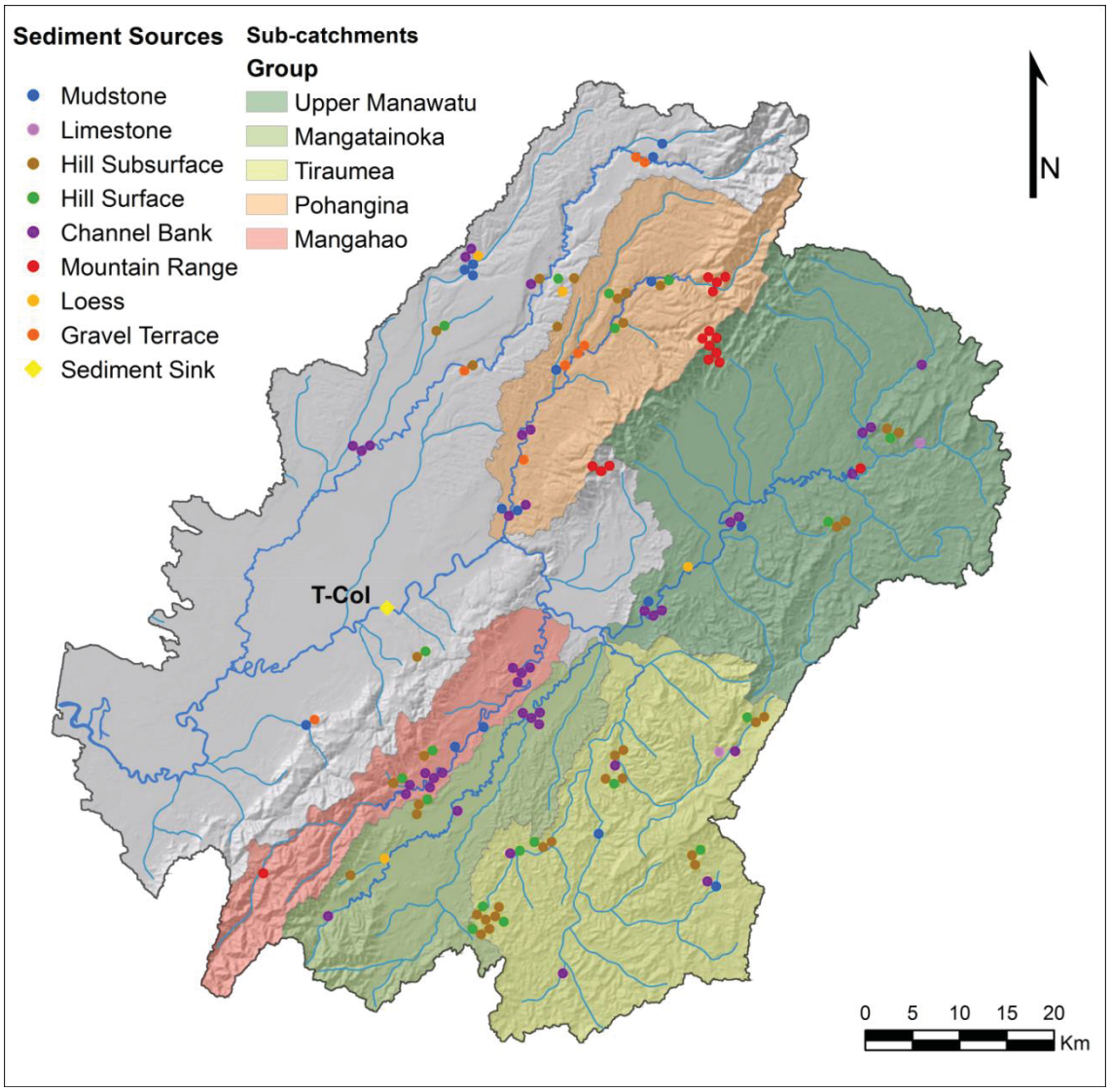

Fig 24: *Manawatu River Catchment showing source sampling spatial distribution and key sub-catchments*

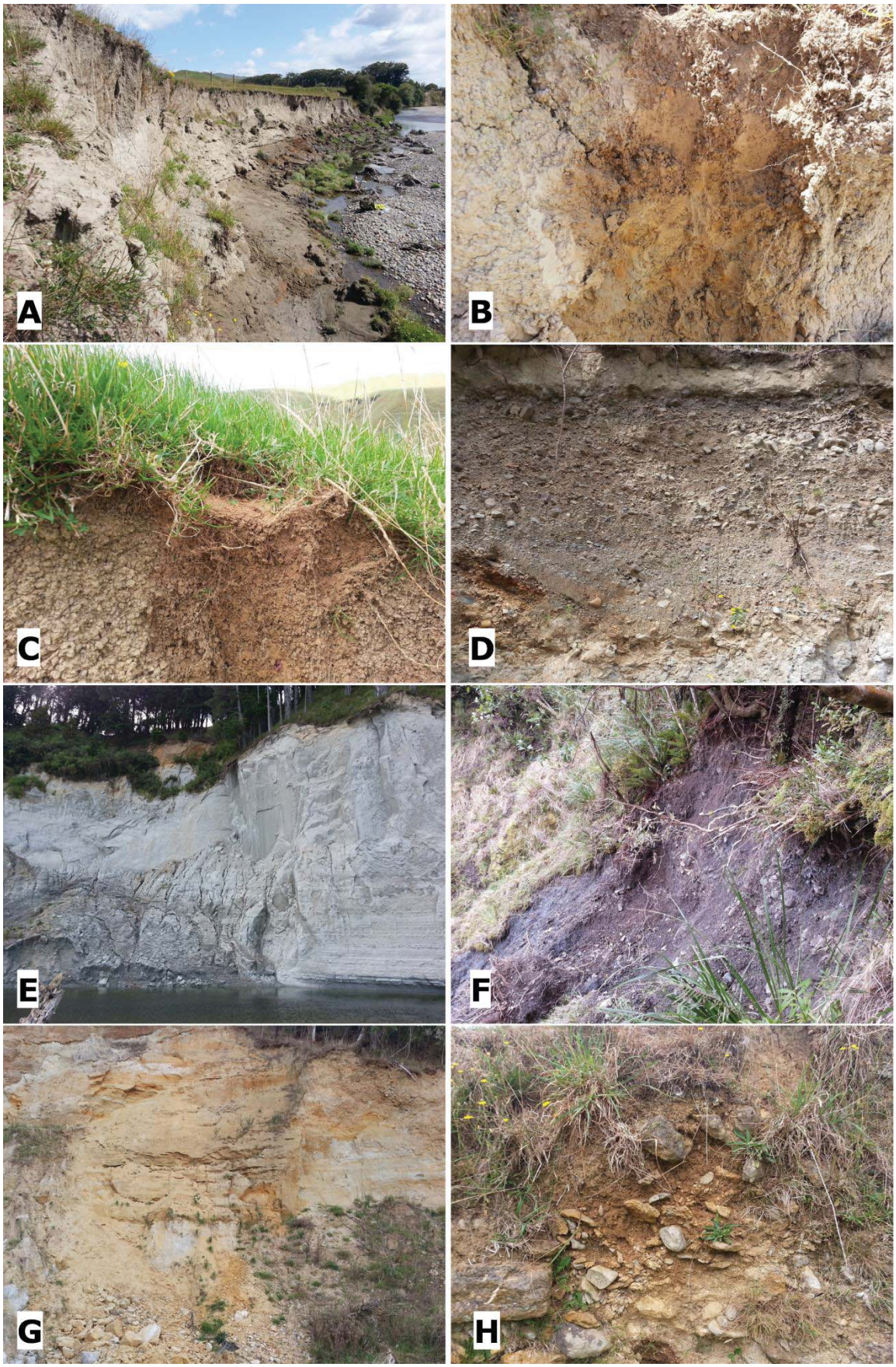

Fig. 25: *Sediment sources; (A) Channel Bank; (B) Hill subsurface; (C) Hill Surface; (D) Gravel Terrace; (E) Mudstone; (F) Mountain Range; (G) Loess; (H) Limestone*

4.5.2 Sample Preparation & Analysis

Sample preparation involved drying at 40°C, light disaggregation and sieving to retain the < 63 µm size fraction. Samples where then weighed into crucibles for XRF analysis and combusted 850°C overnight to oxidize combust any organic material. 2 g of sample was then mixed with 6 g of lithium tetraborate and fused into glass discs. The glass discs were analysed using a Panalytical Axios 1kW X-ray Fluorescence Spectrometer for SiO_2, TiO_2, Al_2O_3, Fe_2O_3, MnO, MgO, CaO, Na_2O, K_2O, P_2O_5, Ba, Rb, Sr, Zr, Nb, Y,V, Cr, and Ni concentrations. The glass discs were retained and also analysed using an Agilent 7700 Series Inductively Coupled Plasma-Mass Spectra with an attached Laser Ablation unit (LA-ICP-MS). LA-ICP-MS elements analysed included Sc, V, Cr, Co, Ni, Cu, Zn, Ga, Rb, Sr,Y, Zr, Nb, Cs, Ba, La, Ce, Pr, Nd, Sm, Eu, Gd, Tb, Dy, Ho, Er, Tm, Yb, Lu, Hf, Ta, Pb, Th, U. XRF data was given preference over LA-ICP-MS values where elements were analysed using both systems because the XRF values provided more consistent results.

4.5.3 Geochemical Indicators

A range of geochemical indicators were derived from the data and used in statistical analysis. Multi-element diagrams were constructed for Major, Trace and Rare Earth Elements (REE's), to express geochemical trends for source group means. Upper Continental Crust (UCC) values, after McLennan (2001) revised from Taylor and McLennan (1985), were used for normalization of the major and trace element diagrams as it showed more comparable geochemistry than PAAS and was visually clearer. REEs were normalized using average CI chondrite values from McDonough and Sun (1995). Post-Archean Australian Shale (PAAS) values after McLennan (2001) were also plotted for reference. Diagrams were constructed using *PetroGraph* from Petrelli *et al.* (2005).

The chemical Index of Alteration (CIA) after Nesbitt and Young (1982), Index of Compositional Variability (ICV) after Cox *et al.* (1995), and K_2O/Al_2O_3 were used as an indication for major element weathering patterns. CIA indicates conversion of feldspars to clays by measuring the depletion of silicic CaO, Na_2O and K_2O relative to Al_2O_3. Higher CIA values typically reflect more weathered material, often values < 50 reflect fresher material while a value of 100 would indicate a much higher degree of weathering. However there can be significant variation in these values depending on the minerals involved.

$$CIA = (100)\left[\frac{Al_2O_3}{Al_2O_3+CaO^*+Na_2O+K_2O)}\right] \quad \text{(Eq. 6)}$$

A correction was applied to approximate the Silicate CaO* values excluding the carbonate according to McLennan (1993). ICV measures the major cation composition relative to Al_2O_3 in wt%. Values < 1 are typical of clay minerals and > 1 are more indicative of plagioclase and feldspars.

$$ICV = \left[\frac{(Fe_2O_3 + K_2O + Na_2O + CaO + MgO + TiO_2)}{Al_2O_3}\right] \quad \text{(Eq. 7)}$$

K_2O/Al_2O_3 ratios for clay minerals occur from 0.0 – 0.3, and values between 0.3 – 0.9 indicate plagioclase (Cox *et al.*, 1995). Eu/Eu* ratio provides information on plagioclase occurrence due to preferential enrichment of Eu^{2+} in plagioclase crystallization. Zircon enrichment is indicative of sediment recycling and can be illustrated by high Zr/Sc ratios, e.g. when plotted against Th/Sc. $(La/Yb)_N$ is used as a measure of Light-REE (LREE) enrichment over Heavy-REE (HREE).

4.5.4 Statistical Discrimination

Analysis of the geochemical concentrations involved several statistical approaches. Fluvial tracers must show conservative behaviour from source to the sampling point. The bracket test provides a basic test that each fluvial tracer falls within the geochemical range of the potential sources. If they do not pass this test (within a 10 % measurement error) they are removed. Next, a widely used method after Collins *et al.* (1998) was applied, which employs a two-step approach for selecting appropriate tracers. The first step uses the Kruskal-Wallis non-parametric test to statistically evaluate significant differences of individual tracers between two or more groups. Normal distribution criteria were met for most source group tracers, but not for all, so non-parametric tests are used as a conservative approach. The second stage uses a stepwise minimization of Wilk's Lambda multivariate discriminant function analysis to distinguish the most suitable subset of variables that can provide discrimination.

Kruskal-Wallis H test was carried out for each geochemical concentration to determine the statistically significant discriminants for subsequent analysis. A 95.0% confidence interval or an α level of 0.05 was chosen for the critical p-value. Discriminant function analysis (DFA) allows for prediction of group membership based on linear combinations of predictor variables (Eq. 8)

$$D = v_1X_1 + v_2X_2 + v_3X_3 + \ldots v_iX_i + a \quad \text{(Eq. 8)}$$

Where D = discriminant function

v = the discriminant coefficient

a = a constant

i = the number of predictor variables

Stepwise discriminant analysis was conducted using SPSS 21 (IBM Corp., 2012). The analysis used minimization of Wilks' Lambda, where Wilk's Lambda is a measure of the between-group variability compared with within-group variability, whereby minimizing the value reduces the sample grouping. It is guided by '*F*' values which determine the entry and removal of variables as a measure of the extent to which an individual variable contributes to group prediction. Default values of 3.84 (probability = 0.5) and 2.71 (probability = 0.1) are used for F to enter and F to remove respectively.

4.5.5 Multivariate Mixing Model

The tracers selected from the discriminant function analysis in order of significance were CaO, Lu, Cs, Sr, Tm, Na_2O, P_2O_5, Fe_2O_3, Pb, U, Hf, MnO, Zn, MgO, Nb, and Y. These tracers were incorporated into several multivariate mixing models and optimization techniques to estimate the relative proportions of sediment source contributions to the sink sample. This was achieved following the approach outlined by Collins *et al.* (1997) whereby equations are created for each element which relate the source proportions to the sediment sink element concentration. The relative proportions of each source group are estimated through minimizing the sum of the residual (objective function) of the element concentrations through least squares. A variety of mixing model variations exist, two of which are utilized in this research for comparison. The first is the basic mixing model after Collins *et al.* (1997), Walling *et al.* (1999), Owens *et al.* (1999) illustrated in Eq. 9:

$$R_{es} = \sum_{i=1}^{n} \left(\frac{C_i - \sum_{j=1}^{m} X_j \bar{S}_{ij}}{C_i} \right)^2 \quad \text{(Eq. 9)}$$

R_{es} = the sum of squares of the residuals

n = the number elements in the composite fingerprint (e.g. P_2O_5)

C_i = the concentration of element (i) in the sediment sink sample

m = the number of source groups (e.g., mudstone, hill surface etc.)

X_i = the relative proportion from source group (j) to the sediment sink sample

$\bar{S}_{ij}$ = the mean concentration of element (i) from the sample in source group (j). The mean was used in the basic model as there was not a significant difference observed between medians and mean data and thus minimal effect from outliers.

The second follows the approach of Hughes *et al.* (2009) as illustrated in Eq.10:

$$R_{es} = \sum_{i=1}^{n} \left(\frac{\sum_{i=1}^{1000} \sum_{j=1}^{m} X_j S_{i,j,l} / 1000 - C_i}{C_i} \right)^2 \quad \text{(Eq. 10)}$$

R_{es} = the sum of squares of the residuals

C_i = Concentration of fingerprint property (i) in sediment samples

n = the number elements in the composite fingerprint (e.g. P_2O_5)

m = the number of source groups (e.g., mudstone, hill surface etc.)

$S_{i,j,l}$ = concentration of fingerprint property (i) in source (j) and iteration (l)

X_j = percentage contribution from source category (j)

Both models adhere to two constraints that must be satisfied to produce realistic values; the first constrains each source group proportion to being a positive value between 0 and 1, i.e.

$$0 \leq P_i \leq 1 \quad \text{(Eq. 11)}$$

The second constraints the sum of all source group contributions to being equal to 1, i.e.

$$\sum_{i=1}^{n} P_i = 1 \quad \text{(Eq. 12)}$$

The main differences between the models were that Collins-Model (Collins) uses calculated values based on the mean or median and standard deviation of each source group to employ a Monte Carlo approach for the desired number of replications. Hughes-Model (Hughes) employs the actual sample values randomly selected for and summed over 1000 iterations. A tracer specific weighting was not deemed necessary in this instance due to the large tracer suite being employed.

The optimization of these models was conducted using the solver extension on Microsoft Excel and was based on an initial setup from Roddy (2010). Two solving methods were employed across the models; 'Generalized Reduced Gradient (GRG) Nonlinear' and 'Evolutionary'. Both optimizations were employed for each model (Table 16). The GRG-Nonlinear method was employed using the multi-start parameter to improve likelihood of a globally optimal solution. The multi-start method automatically runs repeated iterations using different random starting values for the decision variables, thereby providing a selection of locally optimal solutions of which the best can be selected as a likely globally optimal solution. The Evolutionary optimization is based on a Genetic algorithm approach employing random sampling and mutation to determine the solution.

Table 16: *Parameters used in the mixing model optimization*

Parameters	Mixing Model			
	Collins-GRG	Collins-Evo	Hughes-GRG	Hughes-Evo
Equation	$R_{es} = \sum_{i=1}^{n} \left(\frac{C_i - \sum_{j=1}^{m} X_j \overline{S}_{ij}}{C_i} \right)^2$		$R_{es} = \sum_{i=1}^{n} \left(\frac{\sum_{i=1}^{1000} \sum_{j=1}^{m} X_j S_{i,j,l} / 1000 - C_i}{C_i} \right)^2$	
Method	GRG nonlinear	Evolutionary	GRG nonlinear	Evolutionary
Auto-scaling	Yes	Yes	Yes	Yes
Constraint Precision	0.0001	0.0001	0.0001	0.001
Differencing	Central	-	Central	-
Multi-start	Yes	-	Yes	-
Mutation Rate	-	0.5	-	0.5
Population size	200	200	200	200
Convergence	0.00001	0.00001	0.00001	0.00001
Random Seed	Yes	Yes	Yes	Yes
Iterations	5000	5000	1000	1000

4.6 Results and Discussion

4.6.1 Geochemical Indicators

Differences in major geochemistry patterns reflect different sediment sources (Table 17; Fig. 26). The most prominent is the higher CaO values from Limestone due to calcite content, as well as generally lower values for the remaining major elements, except MgO and P_2O_5. MnO values for both Gravel Terrace and Mountain Range sediment are significantly elevated and to a lesser extent so are TiO_2, Al_2O_3, Fe_2O_3, and P_2O_5 values relative to the other sediment sources. Mountain Range sediment also displays higher values of MgO and K_2O, while Hill Subsurface sediment shows depleted values of P_2O_5.

CIA values range from ≈ 53 – 67 and indicate a relatively high ratio of clay/feldspars for Gravel Terrace and Mountain Range sediment, compared with Limestone and Mudstone sediment. ICV values range from 0.78 – 0.92 across source groups, with the exception of Limestone, which has a value of 10.14 due to the presence of $CaCO_3$. Hill Subsurface and Hill Surface values indicate the most weathering, with less weathering evident in Mudstone and Loess values. K_2O/Al_2O_3 ratios range from 0.12 -0.19, suggesting the dominance of clay minerals over feldspars.

Table 17: *Geochemical indicators for sediment sources with * Indicating the influence of an outlier.*

	Sediment Sources									
Indicator	Mudstone	Hill Subsurface	Hill Surface	Channel Bank	Mountain Range	Gravel Terrace	Loess	Limestone	UCC	PAAS
K_2O/Al_2O_3	0.162	0.127	0.117	0.154	0.180	0.136	0.140	0.187	0.22	0.20
Th/Sc	0.81	0.74	0.69	0.81	0.82	0.80	0.83	0.80	0.79	0.91
Zr/Sc	40.08	51.36	57.19	72.26	37.91	53.91	54.12	25.15	13.97	13.13
Eu/Eu*	0.67	0.71	0.73	0.68	0.68	0.69	0.66	0.73	0.64	0.63
$(La/Yb)_N$	7.56	7.14	6.96	6.62	6.33	6.96	7.72	9.55	9.78	9.72
TotREE	130.2	86.2	73.8	116.8	150.5	204.1*	171.7	98.1	146.4	184.8
ICV	0.92	0.78	0.78	0.86	0.86	0.85	0.92	10.14	1.28	0.89
CIA	57.06	63.39	62.27	59.31	66.59	67.00	61.29	52.67	47.93	70.39

Generally, the trace elements display higher values in Mountain Range and Loess, and lower values in the Hill Subsurface and Hill Surface sediments due to the effects of weathering (cf Fig. 26). This is consistant with other studies (e.g. Lamba *et al.*, 2015, Smith and Blake, 2014) where comparatively lower trace element values are observed in Hill Surface and Hill Subsurface due to weathering, compared to less weathered bank-derived sediment. Large-Ion Lithophile (LIL) elements, Rb, Cs, K_2O and Ba values are lowest in Limestone sediments and highest in the Mountain Range sediment, particuarly for Cs values. The Sr pattern reflect the CaO pattern which exhibit highest concentrations in the Limestone sediment. High Field Strength Element (HFSE), Zr and Hf are highest in the Loess, Channel Bank and Gravel Terrace while the remaining HFSE elements (Th, Ta, U, Nb, Y) are highest in the Mountain Range and Loess sediment. Transition elements, V, Cr, Co, Ni, Cu display depletion, relative to UCC and PAAS standards, with Mountain Range sediment maintaining the highest values. Limestone shows notably higher values for Co and Ni. TotREE values are highest for the Gravel Terrace (204.1) and remain high for Loess (171.2) and Mountain Range sediment (150.5) respectively. However the Gravel Terrace value is inflated due to abnormally high Ce concentration in one of the samples and as a precaution was removed from the DFA. The lowest values for TotREE occur in the Hill Surface (73.8) and Hill Subsurface (86.2) sediment sources. LREE enrichment relative to HREE (indicated by $(La/Yb)_N$) is more pronounced in Limestone (9.6), Loess (7.7) and Mudstone (7.6) sediment sources and less pronounced in Mountain Range (6.3) and Channel Bank (6.6) sediment sources, but are all below the UCC and PAAS standards. Tm depletion is evident in Limestone, Channel Bank, Gravel Terrace, Hill Subsurface and Hill Surface sediment sources. Eu/Eu* ratios show a weak negative anomaly ranging from 0.66 to 0.73; the highest ratio coming from Limestone and Hill Surface and lowest from Loess sediment sources.

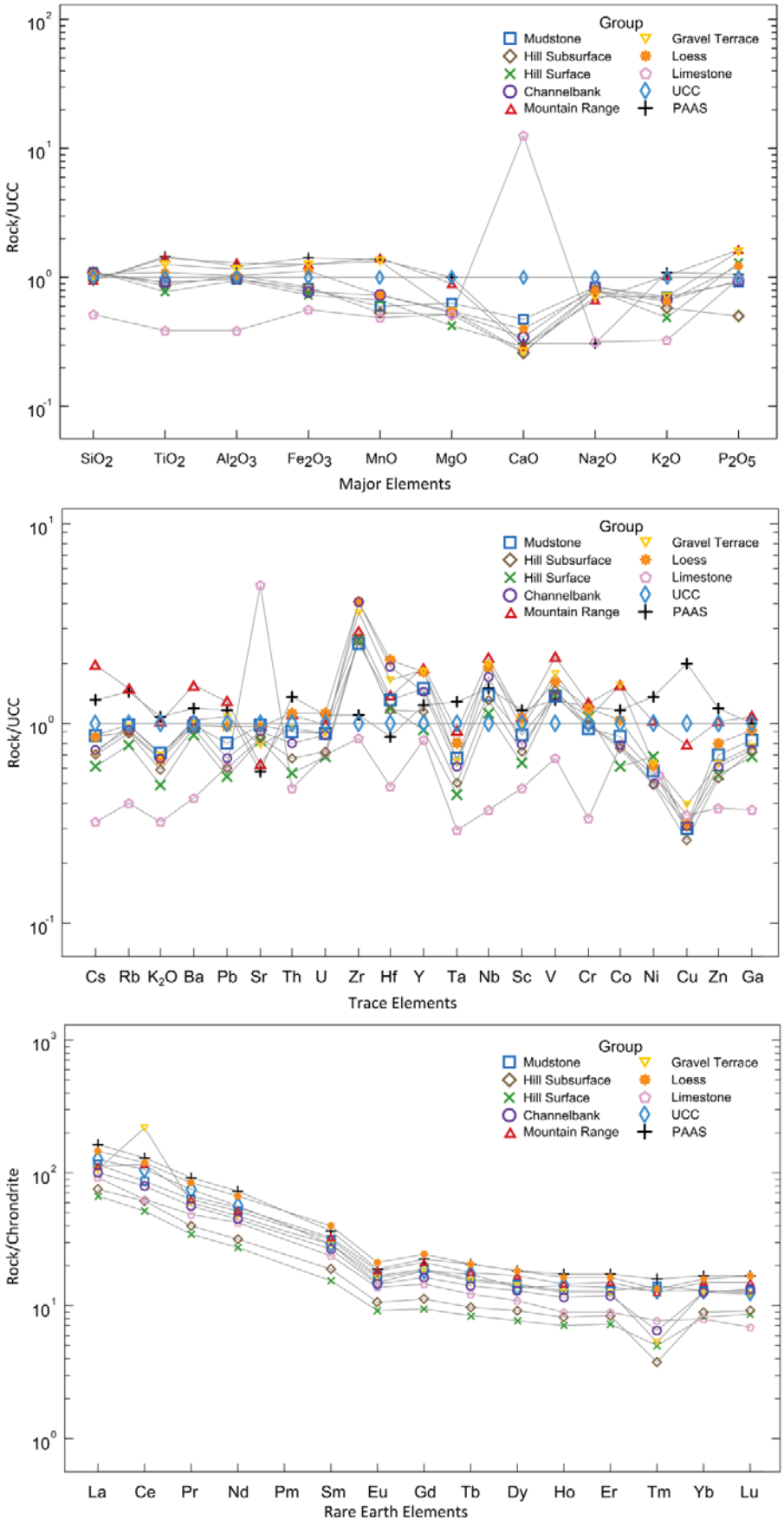

Fig. 26: *Normalized multi-element diagrams for Major elements (top); trace elements (middle) and Rare Earth Elements (bottom)*

4.6.2 Statistical Differentiation

The study illustrates several implications for differentiation when using an increasing number of source groups. All tracers passed the bracket test and fall comfortably within source values (illustrated for selected tracers in Fig. 27, Fig. 28, Fig. 29) and as such no tracers were removed. The large number of sources and large geochemical range encountered across these sources (even if Limestone is removed) provided a wide range for the fluvial tracers to occur within.

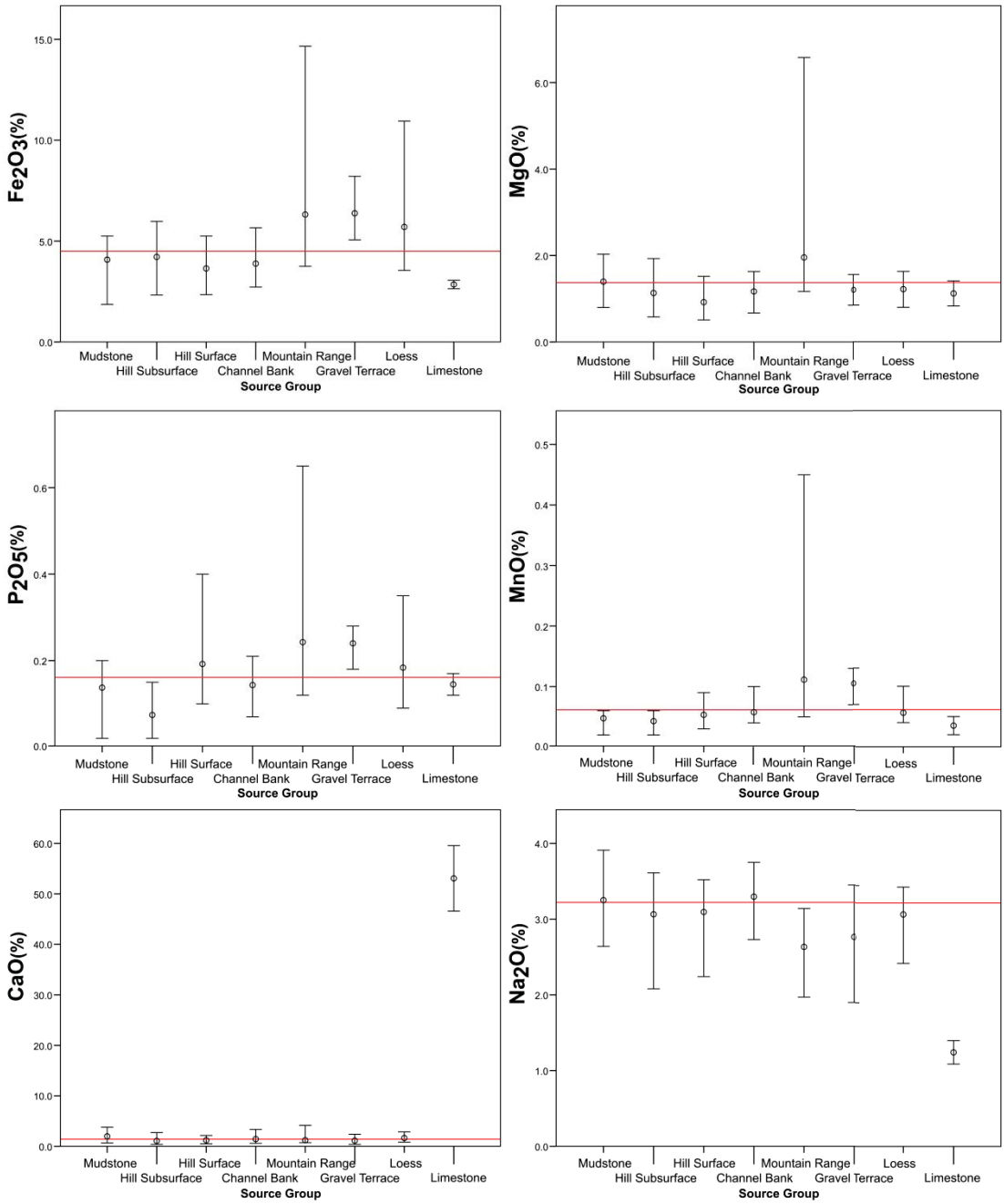

Fig. 27: *Bracket test showing maximum and minimum tracer values by source group for selected tracers with the fluvial values indicated by the red line.*

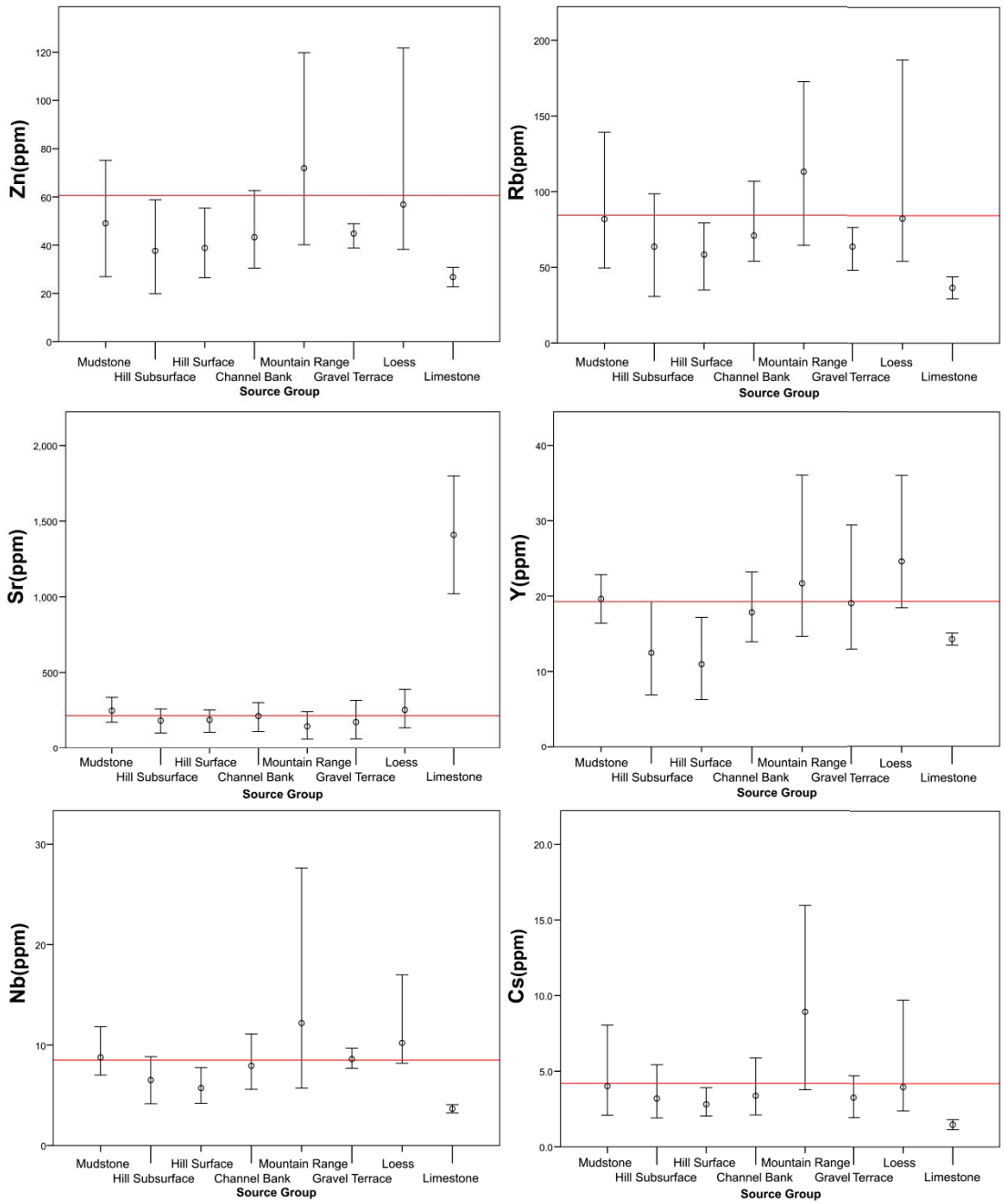

Fig. 28: *Bracket test (cont'd) showing maximum and minimum tracer values by source group for selected tracers with the fluvial values indicated by the red line.*

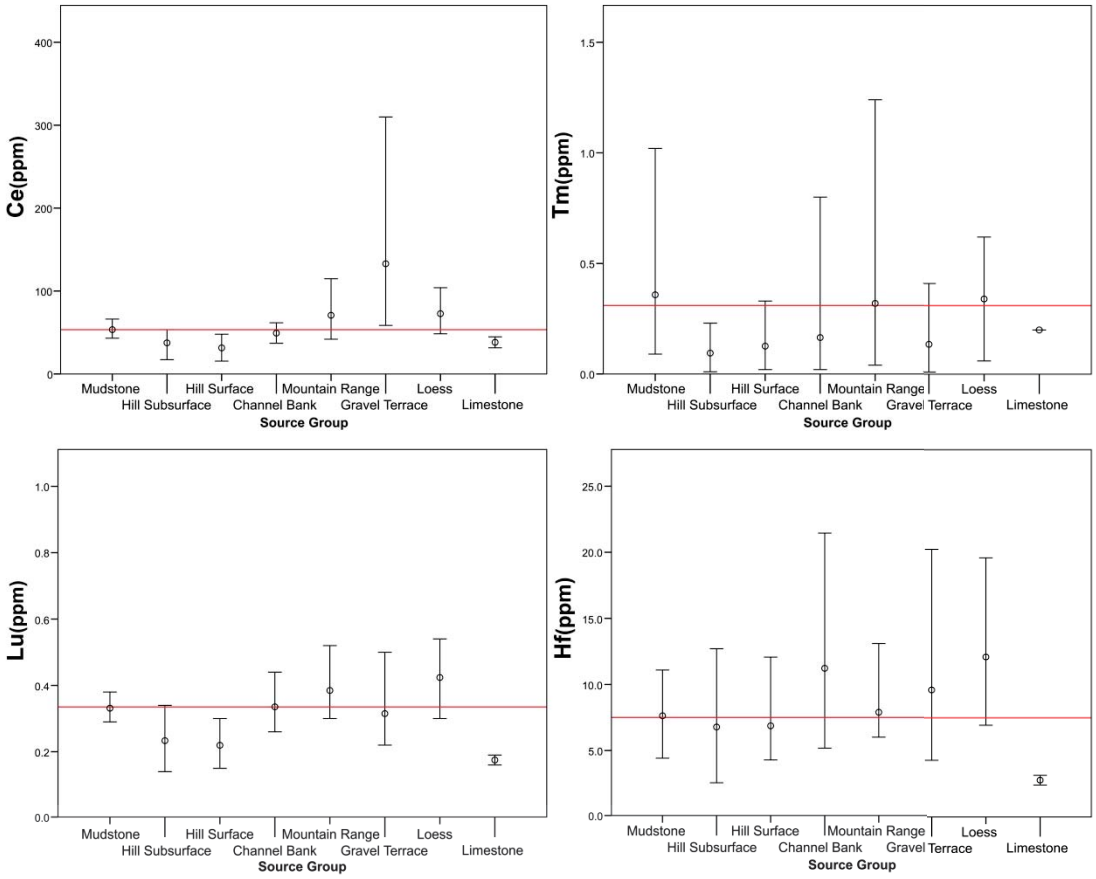

Fig. 29: *Bracket test (cont'd) showing maximum and minimum tracer values by source group for selected tracers with the fluvial values indicated by the red line.*

The Kruskal-Wallis test rejected the null hypothesis that sediment concentrations were the same between upstream sediment sources, in favour of the alternative for all tracer concentrations measured. This indicates that each element distribution showed significant difference between at least two of the source groups. With 8 source groups, the value of using the Kruskal-Wallis test becomes less important. The Kruskal-Wallis test aims to identify variables that do not show statistical significance between any source groups in order to remove them from further analysis, however, in this study the test did not rule-out any tracer. The relatively high numbers of sources, as well as the unique geochemistry of limestone are probable explanations. With increasing number of sources, the chance of an element being statistically different between at least 2 sources also increases. Similarly, the $CaCO_3$ based limestone significantly reduces the possibility of finding non-statistically significant differences between at least two sources. It is unclear what number of sources would be regarded as too many to differentiate. The appropriate number of source groups will vary for each catchment

site, based on catchment size, sample size and geochemical variation. In this case the Discriminant Function Analysis (DFA) produced a high level of explanation of variance within the data and predicted group membership relatively well.

Table 18: *Variables Entered for Stepwise Discriminant Function analysis displaying Wilks' Lambda statistic (λ)*

Step	Entered	λ Statistic
1	CaO	0.02331
2	Lu	0.0085
3	Cs	0.00406
4	Sr	0.0023
5	Tm	0.0011
6	Na_2O	0.00056
7	P_2O_5	0.00033
8	Fe_2O_3	0.00021
9	Pb	0.00014
10	U	0.0001
11	Hf	0.00007
12	MnO	0.00006
13	Zn	0.00004
14	MgO	0.00003
15	Nb	0.00002
16	Y	0.00002

DFA produced a 16 element solution which included, in order of the elements entered into the function; CaO, Lu, Cs, Sr, Tm, Na_2O, P_2O_5, Fe_2O_3, Pb, U, Hf, MnO, Zn, MgO, Nb and Y. Through the 16 variables, Wilk's lambda was minimized to 0.00002 (Table 18). Seven functions were used in the analysis. The first function accounted for 98.3 % of the variance followed by 0.7 % of the variance for the second function, cumulatively accounting for 99.0 % of variance across the first two functions (Table 19). The group centroids provide multivariate means, delivering information on the separation of the source groups relative to the functions (Table 19). Function 1 separated the Limestone source (177.0) from the rest of the source groups (≈ -2 to ≈ - 4) but also allowed some differentiation for the Mountain Range and Gravel Terrace sources. Function 2 provided differentiation of Mountain Range sediment (≈ 4.4) sources from Hill Subsurface (≈ -1.7) and Hill Surface sediment (≈ -1.4). Function 3 provided separation of the Loess (≈ 3.0) and Mudstone sediment (≈ 2.0) from the Hill Surface (≈ - 1.9) and Mountain Range sediment (≈ - 1.6). The remaining functions are of minor significance overall but do help to accentuate discrimination of some of the sources as displayed in Table 19.

Table 19: *Variance explained by each function (top), and centroid values for each source and group function (bottom)*

Discriminant Function % of Variance explained							
Variable	Function						
	1	**2**	**3**	**4**	**5**	**6**	**7**
Eigenvalue	485.904	3.435	1.847	1.186	1.041	0.618	0.246
% of Variance	98.3	0.7	0.4	0.2	0.2	0.1	0.0
Cumulative %	98.3	99.0	99.4	99.6	99.8	100	100
Group Centroids Functions							
Group	Function						
	1	**2**	**3**	**4**	**5**	**6**	**7**
Mudstone	-2.329	0.605	1.908	0.316	-1.46	-1.03	-0.567
Hill Subsurface	-2.128	-1.721	-0.274	1.295	0.588	-0.231	0.117
Hill Surface	-2.855	-1.407	-1.878	-1.523	-1.071	-0.499	0.302
Channel Bank	-2.306	-0.125	0.391	-0.424	0.017	1.047	-0.237
Mountain Range	-4.367	4.365	-1.631	0.874	-0.085	0.009	0.167
Gravel Terrace	-3.807	1.254	-0.494	-2.511	3.997	-1.721	-1.187
Loess	-1.95	1.216	2.966	-1.075	0.825	-0.321	1.441
Limestone	177.015	0.379	-0.217	-0.022	0.012	-0.036	-0.011
Unstandardized canonical discriminant functions evaluated at group means							

Classification from the 7 functions allowed for 92.1 % total correct classifications (Table 20) with some source groups displaying clear discrimination, while others of more similar geochemistry proved more difficult to provide a clear signal. The main misclassifications were related to the Channel Bank, Hill Subsurface and Mudstone sources. Hill Subsurface and Channel Bank showed the lowest correct classifications of 85.7 % and 87.8 % respectively. Hill Subsurface was misclassified as Hill Surface (8.6 %) and Channel Bank (5.7 %) while Channel Bank was misclassified as Mudstone (2.4 %), Hill Subsurface (4.9 %) and Gravel Terrace (4.9 %). Mudstone classified 93.8 % with 6.3 % misclassified as Gravel Terraces. A plot of the DFA functions show the Channel Bank sediment is positioned centrally to all other sediment sources and likely reflects the mixed origin of floodplain deposits and depositional links between primary and secondary sediment sources. The level of retention of the original sediment character in the secondary source is dependent on the degree of weathering and alteration since deposition, which varies among catchment Channel Bank sources. The advantage of a similar geochemical signature is that it can provide a means to determine historical sediment sources deposited in the floodplain, but the same tracer can also be

problematic for clear differentiation of contemporary sediment sources. Belmont *et al.* (2014) has also highlighted the usefulness of tracers which are non-conservative during longer time periods and their ability to provide useful information, on the sediment routing timeframes.

However, for contemporary sediment sources, the long term conservative tracers open up the possibility of source sediment signatures from the Channel Bank being somewhat obscured by upstream sediment sources signatures. The same phenomena could also be in effect with the Gravel Terrace source, which is a depositional source and has some discrimination issues with Mudstone and Channel Bank sediment. Given that the Gravel Terraces are mostly composed of greywacke clasts, it could be expected that there would be some masking effect occurring between the Gravel Terrace and the Mountain Range sediment. However, it is possible this effect is not observed due to either a significant chemical alteration in the Gravel Terrace since deposition, or the small amount of fine sediment present in the terrace being derived from a different origin to the larger clasts i.e. mudstone. The explanation for Hill Subsurface sediment being misclassified as Hill Surface sediment is likely, either due to the same geological or mineral origin. Alternatively, it is possible there was not clear differentiation between surface and subsurface layers in a subset of the sediment samples. If sediment sources cannot be clearly differentiated, it can create issues during mixing, as identified by Smith and Blake (2014), referring to cultivated sediment sources possibly representing a mixture of channel bank and pasture surface soils. The Hill surface, Range, Gravel Terrace, Loess and Limestone sediment sources all classified 100 % correctly. This reflects the presence of more distinguishable geochemical signals relative to other sediment sources and ties into the conclusions of Pulley *et al.* (2015), which notes that uncertainly is lower in catchments where a larger contrast between source group tracers exists.

The most easily differentiated source was Limestone, being the only non-siliceous sediment source. This is displayed in Function 1 where CaO displays the strongest correlation (r = 0.29), although it falls short of the 0.3 cut-off normally observed when evaluating predictor variable contributions (Table 22). Limestone is composed primarily of $CaCO_3$, and therefore has significant CaO, and is also echoed by Sr, which behaves similarly to Ca (Fig. 26). A lower Na_2O concentration is also observed to be contributing to the differentiation of the Mountain Range sediment in the first function. Mountain Range sediment has the dominant differentiation in the second function, and to a lesser extent Loess and Gravel Terrace, which display similar geochemical patterns of the Mountain Range sediment. These sources are characterized by lower concentrations of SiO_2,and CaO, and generally higher concentrations of trace elements, transition metals and REE. This is represented by the strengths and positive correlations with

Pb (r = 0.60), Cs (r = 0.58), Lu (r = 0.55), Y (r = 0.54), as well as significant correlations with Zn, Nb, P, U, Fe, Mn and Mg and Tm in the second function. This is reflective of both the high proportion of rock fragments and muddy matrix inherent within the greywacke underlying the Ruahine and Tararua Ranges. The Mountain Range sediment also reflects the weathering profile found in the soils on greywacke ranges encountered in a study from Anderson *et al.* (2002) who observed depletion of Si, Ca and Na within the soil horizon compared to the underlying greywacke bedrock.

Table 20: *Predicted group membership of samples based on discriminant function analysis values*

Group	Predicted Group Membership							
	Mudstone	Hill Subsurface	Hill Surface	Channel Bank	Mountain Range	Gravel Terrace	Loess	Limestone
Mudstone	93.8	-	-	-	-	6.3	-	-
Hill Subsurface	-	85.7	8.6	5.7	-	-	-	-
Hill Surface	-	-	100	-	-	-	-	-
Channel Bank	2.4	4.9	-	87.8	-	4.9	-	-
Mountain Range	-	-	-	-	100	-	-	-
Gravel Terrace	-	-	-	-	-	100	-	-
Loess	-	-	-	-	-	-	100	-
Limestone	-	-	-	-	-	-	-	100
92.1 % of selected original grouped cases correctly classified								

Contributions from Lu, Tm, and Y represent the role of REEs in differentiating between Mountain Range, Gravel and Loess sediment from the other sources in the second DFA score, and follow general trends of increased REE concentration with decreasing SiO_2 concentration (Salminen *et al.*, 2005). Selection of Lu and Tm (as well as Y) out of the REEs also reflects the slightly higher HREE enrichment indicated by the $(La/Yb)_N$ ratio of the Mountain Range sediment, compared to other source groups, which is attributed to retention of more resistant minerals, rock fragments and muddy matrix of the greywacke. Differentiation between Loess, Gravel Terrace and the Mountain Range sediment is achieved through magnifying differences in specific elements. The Loess displays higher concentrations of TotREE which accounts for Function 3 being mostly weighted with Lu (r = 0.46) and U (r = 0.31) concentrations which can be attributed to greater retention of resistant minerals within the Loess deposit. Zircon is the likely mineral responsible, indicated by the very high concentrations of Zr and Hf found in the Loess deposits. A similar characteristic is also used to distinguish Gravel Terrace from the Mountain Range sediment due to the Hf-Zircon and P_2O_5 (r = - 0.46) correlation with Gravel Terrace and the correlation of Cs (r = 0.33) with the Mountain Range sediment within Function 4.

The Hill Subsurface and Surface sediment plot closely in the function scores (Fig. 30) and show similar geochemical patterns (Fig. 26) due to weathering from the same geological material. They are distinct from Mountain Range sediment, Mudstone, Loess and Gravel Terrace due to generally lower concentrations of REE and Trace elements, which is observed in Function 2. The key differentiation between Hill Surface and Hill Subsurface occurs from the higher concentrations of P_2O_5 in the Hill Surface, due the biologically active behaviour of P_2O_5 in top soil compared with Hill Subsurface. Differentiation of the remaining source groups can be observed in Functions 4, 5, 6 and 7, however contribute low significance to the DFA so are not explored in detail. These include differentiation of the Mudstone in Function 5 attributed to Lu and U, Channel Bank in Function 6 attributed to Nb and Fe_2O_3, and Loess and Gravel Terrace in Function 7 attributed to Fe_2O_3, Zn and Na_2O.

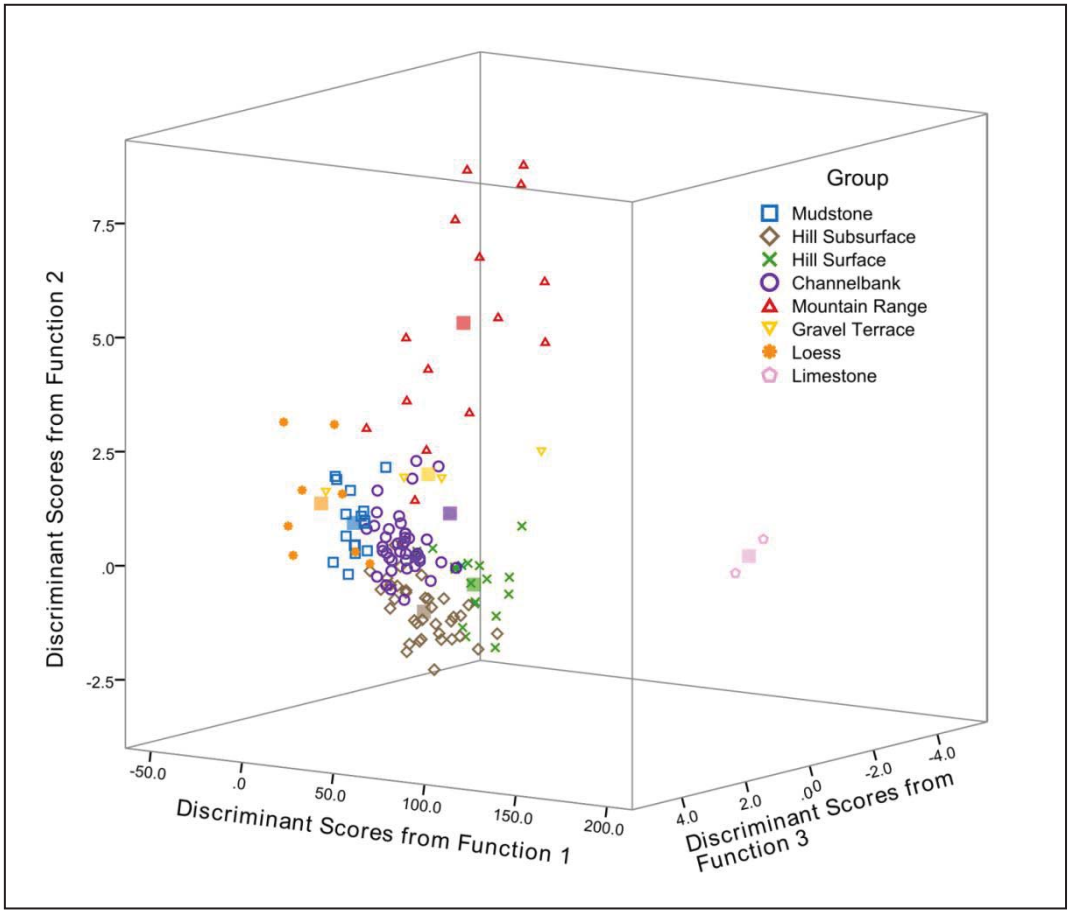

Fig. 30: *Visualization of sediment sources discriminant scores for the first 3 functions.*

It is clear that mineral analysis would have added considerable value by providing greater certainty and detail to the geochemical explanations for the sediment source associations with specific elements. Although this does not detract from the validity of a geochemical concentrations association with a sediment source group, it does inhibit the ability to map the mineral responsible for the geochemical signature in some of the sources.

4.6.3 Model Comparisons

The sediment source estimates generally showed good agreement between each model, suggesting globally optimal solutions were achieved (Table 21) and that model estimates in this research were possibly more dependent on variables used than on the model to run them. Frequency distributions of the Monte Carlo simulations show the most variation occurring within mudstone sediment source estimates (Fig. 31; Fig 32). This amounted to a standard deviation of ≈ 10 % for the Collins-GRG and Collins-Evo models, ≈ 7.8 % for Hughes-Evo model and ≈ 1.7 % for Hughes-GRG model (Table 21) which is considerable, but still places the mudstone firmly as the dominant sediment source. The agreement between model results could also reflect the advantage of using grouped sediment samples rather than composited sub-samples of sediment sources emphasizing the importance of source characterization being able to accommodate natural within-source geochemical variability.

Table 21: *Mean source estimates with associated standard error plus standard deviation*

Source Type	Model Collins – GRG		Model Collins – Evo		Model Hughes – GRG		Model Hughes – Evo	
	Mean % ± SE	SD	Mean % ± SE	SD	Mean % ± SE	SD	Mean % ± SE	SD
Mudstone	46.6 ± 0.2	10.7	45.8 ± 0.2	10.6	45.9 ± 0.1	1.7	37.8 ± 0.3	7.8
Hill Subsurface	10.2 ± 0.1	6.9	9.2 ± 0.1	7.3	9.4 ± 0.0	1.3	10.8 ± 0.1	3.9
Hill Surface	13.7 ± 0.1	6.5	13.2 ± 0.1	7.1	16.3 ± 0.0	0.8	12.1 ± 0.1	4.0
Channel Bank	1.2 ± 0.0	2.8	1.5 ± 0.1	3.4	0.0 ± 0.0	0.0	4.3 ± 0.2	5.2
Mountain Range	15.6 ± 0.1	3.9	15.9 ± 0.1	3.8	17.5 ± 0.0	0.5	16.6 ± 0.1	2.2
Gravel Terrace	3.6 ± 0.1	4.3	3.5 ± 0.1	4.3	0.2 ± 0.0	0.4	2.0 ± 0.1	3.1
Loess	9.1 ± 0.1	7.6	10.2 ± 0.1	7.7	10.7 ± 0.0	1.0	15.2 ± 0.2	5.2
Limestone	0.0 ± 0.0	0.0	0.0 ± 0.0	0.0	0.0 ± 0.0	0.0	0.00 ± 0.0	0.0

Table 22: *Structure matrix showing function contributions of selected and unselected variables*

Structure Matrix							
Variable	Function						
	1	2	3	4	5	6	7
CaO	.293	.132	.071	-.076	-.133	-.072	-.174
Er	-.015	.605	.421	-.117	.078	.226	.077
Pb	-.005	.602	-.005	.074	.217	-.251	.122
Dy	-.008	.594	.403	-.116	.100	.119	.041
Yb	-.046	.588	.401	-.138	.066	.333	.104
Gd	-.009	.583	.401	-.090	.105	.100	-.012
Nd	.013	.582	.444	-.119	.102	.084	.028
Cs	-.011	.580	-.218	.334	-.062	-.031	.236
Pr	.012	.573	.460	-.130	.093	.087	.054
Sm	.022	.572	.447	-.100	.101	.069	.013
Tb	-.016	.565	.388	-.123	.098	.109	.020
Ho	-.020	.561	.423	-.151	.072	.173	.051
Lu	-.014	.553	.461	-.170	.060	.444	.139
Y	-.012	.543	.268	-.009	.275	.099	-.093
Ta	-.037	.540	.174	.083	.016	.085	.115
Th	.002	.521	.286	.082	.142	.018	.188
Eu	.011	.473	.375	-.127	.050	.052	.021
SiO_2	-.047	-.464	.049	-.200	-.196	.114	-.124
Zn	-.010	.452	.002	.074	-.052	-.050	.306
Ga	.006	.450	.073	.190	.056	-.137	.338
Nb	-.021	.439	.098	-.063	.346	.415	.041
Sc	-.008	.433	.200	.052	.056	-.007	.175
Rb	-.069	.409	-.087	.379	.069	.053	-.005
La	.059	.399	.345	-.182	.117	.033	.116
K_2O	-.093	.398	-.020	.348	.048	.083	-.091
Al_2O_3	-.048	.392	-.107	.294	.266	-.128	.213
TiO_2	.002	.390	-.040	.073	.184	-.030	.042
V_2O_5	.050	.333	-.070	.156	.234	-.208	.230
U	-.005	.318	.314	-.094	.088	.122	.234
BaO	.216	.318	.090	.239	-.012	.122	-.019
MnO	-.005	.302	-.176	-.068	.150	.003	-.088
CoO	-.068	.295	-.135	.016	.215	-.210	.127
Cu	-.081	.289	-.058	-.021	-.021	.061	.048
MgO	-.002	.266	-.020	.194	-.019	-.035	-.070
Tm	.000	.258	.212	-.013	-.215	-.191	.056
Cr	-.029	.174	.024	-.021	-.047	.087	.002
NiO	-.096	.165	-.013	-.023	-.064	.006	.023
SrO	.102	-.091	.235	-.101	-.095	.029	-.139
P_2O_5	-.001	.359	-.185	-.459	-.063	-.105	.142
Zr	.008	.021	.185	-.275	.231	.618	-.035
Hf	-.011	.090	.267	-.296	.151	.603	.004
Na_2O	-.031	-.216	.264	-.132	-.207	.338	-.325
Fe_2O_3	-.008	.312	-.033	.071	.324	-.248	.332

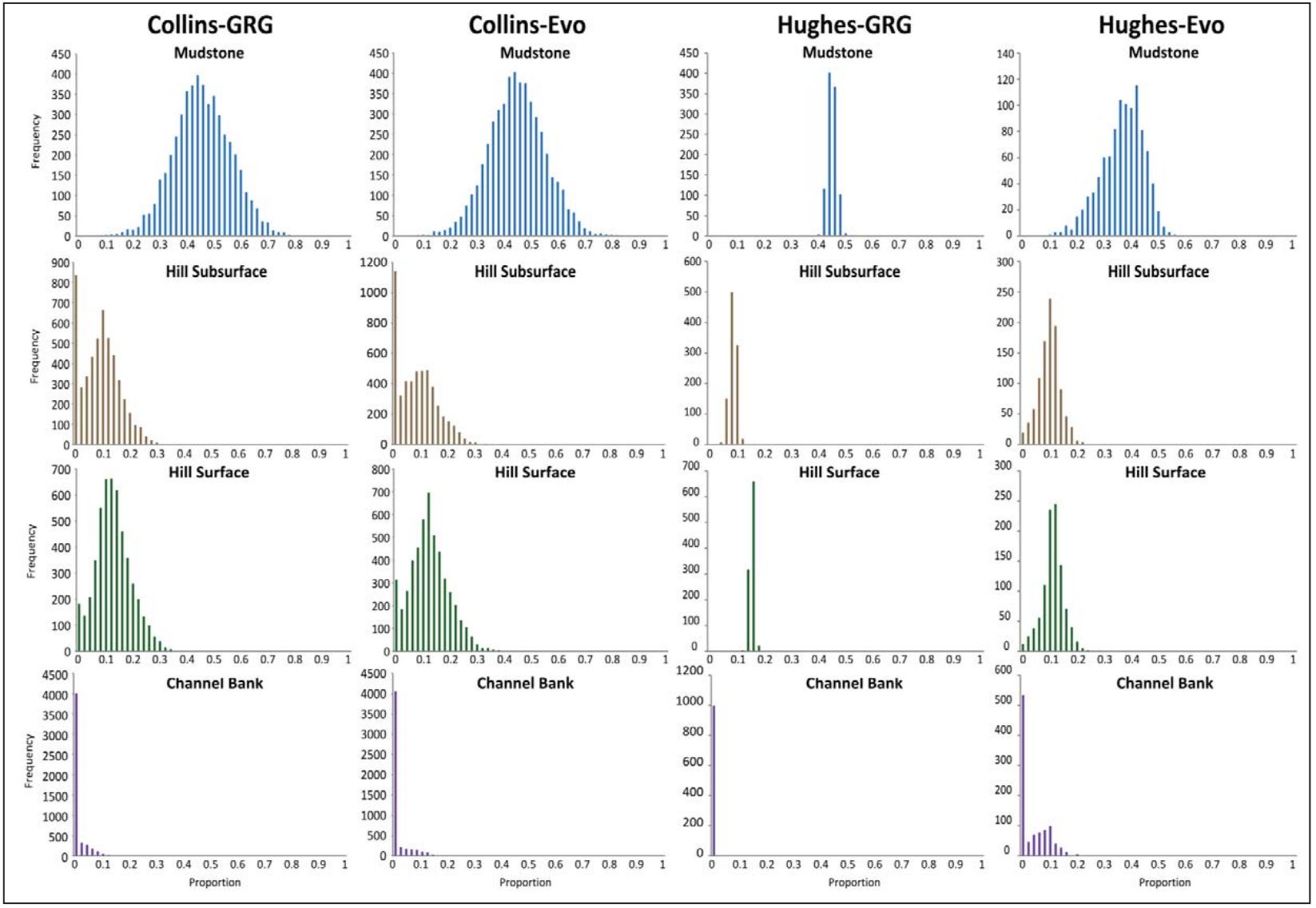

Fig. 31: *Frequency distributions from mixing model outputs for each sediment source group from each of the four mixing models; Collins-GRG,*

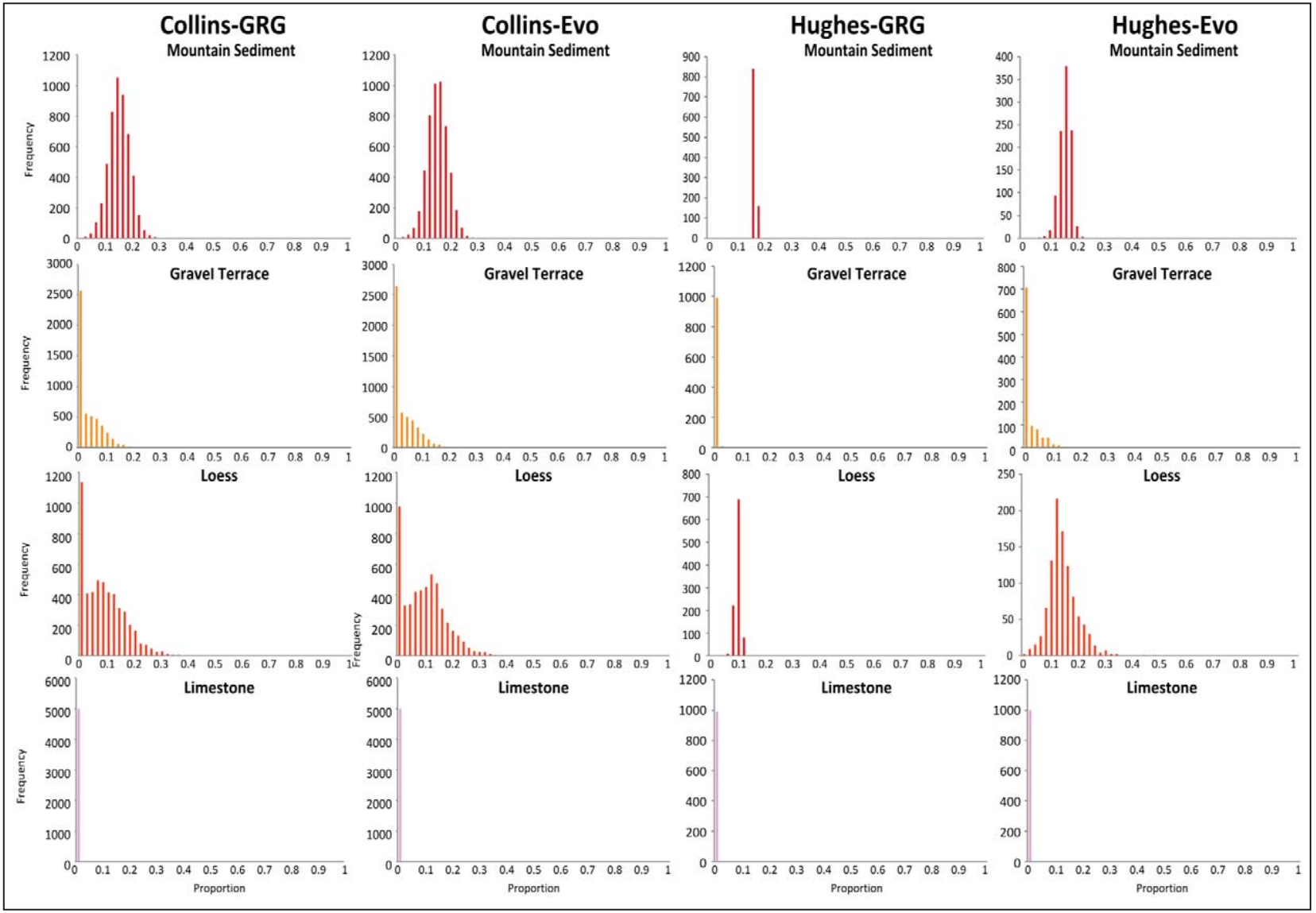

Fig 32: *Frequency distributions from mixing model outputs for each sediment source group from each of the four mixing models; or Collins-GRG, Collins-Evo, Hughes-GRG and Hughes-Evo*

The Mean objective functions were consistent across the models. Hughes-GRG showed a noticeably lower mean value of 0.070 compared to 0.087 for the remaining models (Table 23). Hughes-GRG also had the lowest standard deviation of 0.002 compared to Collins-GRG which displayed a standard deviation of 0.032. Collins-GRG and Collins-Evo display the highest and lowest objective function values, exhibiting a considerable range. Despite containing some relatively high objective functions (> 0.30), they have a negligible impact given their infrequency (Fig. 33). Differences in source sediment attribution are shown in the high and low objective functions. The higher objective functions arise from a greater difference between the data and the model. The main difference in contribution occurs from the Mudstone and Loess sediment; high objective functions provide lower values of Mudstone and higher values of Loess, whereas the opposite is seen in the lower functions. Hughes-GRG shows little difference between high and low objective functions given the low variation.

Table 23: *Summary of Objective Function statistics from each sediment mixing model as well as source contributions from the 30 top-most and bottom-most sediment objective functions*

Mixing Models Objective Functions								
Model	Model Collins-GRG		Model Collins-Evo		Model Hughes-GRG		Model Hughes-Evo	
Mean	0.087		0.087		0.070		0.086	
S.D.	0.032		0.032		0.002		0.019	
Min	0.020		0.017		0.066		0.065	
Max	0.316		0.326		0.075		0.199	
Proportions from 30 highest and lowest Objective Functions								
	High	Low	High	Low	High	Low	High	Low
Mudstone	39.1	52.0	39.3	53.3	45.4	46.3	19.9	45.2
Hill subsurface	7.8	8.0	7.7	5.2	10.4	8.6	12.5	7.8
Hill Surface	18.5	12.2	14.3	12.5	15.8	16.9	13.2	13.9
Channel Bank	3.8	1.3	4.4	1.0	0.0	0.0	11.9	0.0
Mountain Range	15.7	16.4	15.7	15.4	17.8	17.2	14.8	17.4
Gravel Terrace	2.0	3.6	2.7	2.3	0.1	0.1	5.1	0.8
Loess	13.0	6.5	15.0	10.2	10.5	10.9	21.5	13.0
Limestone	0.0	0.0	0.0	0.0	0.0	0.0	0.0	0.0

Collins-GRG required the least time to calculate due to the relative simplicity of the model combined with the GRG-Nonlinear optimization, whereas Hughes-GRG using the same optimization technique, took considerably longer to complete the iterations, but did provide the most consistently low objective function. This is a result of optimization being based on 1000 randomly selected sample values which would cause the tracer concentrations used for

optimization to start from similar starting values for each iteration. This narrows the variability as evidenced in Fig. 31, Fig 32, and Fig. 33. Haddadchi *et al.* (2014) showed that a Modified-Hughes model performed better than a Modified-Collins model, the point of difference being the Modified-Hughes uses the measured property of replicated samples compared to calculated values derived from the samples. Hughes-Evo uses the same equation as Hughes-GRG, but displays a much wider range of objective functions due to the mutation effects of the evolutionary optimization approach, providing additional randomness to the equation. The evolutionary optimizations initially provided lower proportions of mudstone, however this was found to be a limitation caused by the length of time the model was allowed to run. Increasing the run-time made the estimates more comparable to the GRG-Nonlinear model but substantially increased overall duration of the model run-time. It is possible that the Hughes-Evo is still underestimating the Mudstone sediment contributions and overestimating the Loess sediment source as indicated by the slight skewness in the Mudstone distribution (Fig. 31); increasing the run-time further could increase parity with the other models. This is a drawback of the evolutionary technique as it does not recognize an optimal solution, but only whether the solution is better than the previous solution (Frontline Systems Inc., 2010).

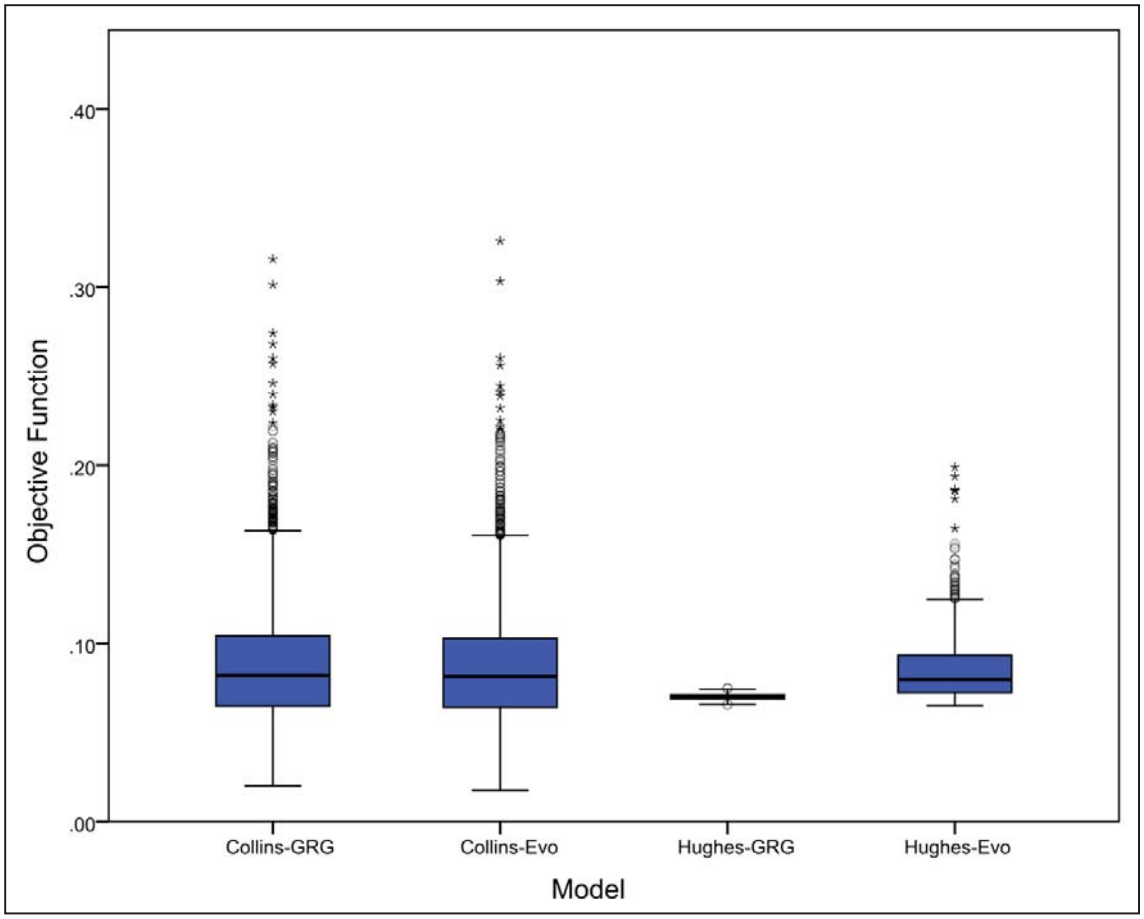

Fig. 33: *Boxplot showing comparison of Objective Function statistics*

4.6.4 Sediment Contributions

The model sediment source estimates present a number of considerations for catchment dynamics, which highlight the geological material and the ability of processes to deliver sediment into the channel system. All the mixing model estimates for relative fine sediment source contributions identified the dominant contribution to be coming from the Mudstone sources, ranging from 37.78 - 46.60 % (Table 21). This compares well with the conceptual understanding of the catchment, which postulates soft sedimentary hill country, with ubiquitous mudstone, to be a significant area of fine sediment generation (Dymond *et al.*, 2006a, Basher *et al.*, 2012).Tall exposed mudstone cliff faces are common throughout the mid to upper reaches of the Manawatu River tributaries. In these partly-confined and confined valley-floor settings, the channel often abuts against the cliff face which provides a delivery mechanism of mudstone sediment directly into the transport pathway via erosion of the cliff face and talus derived from debris falls. Deeply incised channel and gully systems of the mudstone bedrock are also common in the upper reaches of the Tiraumea and numerous tributaries. Similarly, this geomorphological setting provides a direct mechanism of sediment delivery into the channel transport. Shallow translational landslides are common throughout the catchment hill country, but typically involve just the soil horizon devoid of bedrock (Dymond *et al.*, 2006b) and therefore are not likely to be the dominant process for the delivery of mudstone derived sediment into the channel. Large mass failure landslides do exist within the catchment, and do comprise the mudstone bedrock layer but would not be a major mudstone sediment source, given their sporadic and highly localised occurrence.

Sediments derived from the Tararua and Ruahine Range account for 15.94 – 17.49 % of the Manawatu sediment contribution at T-Col, equating to about a third of the contribution from mudstone derived sediment, despite having comparable areal extent (14 %) with Mudstone (18 %). The steep slopes and fractured greywacke composition of the mountain ranges generate significant quantities of material to the bedload of the Manawatu River (Mosley, 1978, Fuller *et al.*, 2016), however a combination of more resistant greywacke, dense vegetation cover and thin soils likely impede the ability to generate fine sediment. Minor contribution of fine sediment was estimated to come from the Gravel Terraces (0.15 – 3.61 %). This is despite widespread occurrence throughout the catchment, and often in direct proximity to the channel via cliff-face and bank erosion in semi-confined channels. The minor contribution can be explained through the geological character which is similar to that of the Mountain Range sediment. The terraces themselves reflect a depositional feature or ‘temporary sink’ of a historic sediment source of the greywacke range and are also secondary

sediment sources for present day sediment generation. The terraces are unstable, and cliff collapse containing gravels is common, but as found from sample collection and processing, the original deposits contain very low quantities of fine sediment and likely generate minute quantities due to the resistance of the gravels to weathering. The Loess sediment source contribution estimate was between 9.10 – 10.23 %, attributed to the unconsolidated and high erodibility characteristics of this material.

Hill Surface and Hill Subsurface estimates ranged between 12.08 – 16.34 % and 9.2 - 10.78 % of source sediment respectively. Despite these values being lower than the Mudstone and Range sediment, they still suggest significant quantities of soil are being lost from the agricultural landscape through surface erosion and shallow translational landslides. The assumption with sampling surface sediments is that they will be geochemically similar, or at least relative to the other source groups. However, there is variability in soils within the Manawatu, and perhaps a sampling approach that took into account the variation would be more beneficial for providing spatially distributed surface erosion information but would require considerable resources and samples.

The estimated contribution of sediment derived from the Channel Bank is relatively minor, with 0.00 - 4.29 % of total contribution. This is quite different from findings put forward by Rosser *et al.* (2008), which concluded that bank erosion contributed 28 % of suspended sediment load in the Pohangina sub-catchment. The main explanation for this disparity is a difference in the Channel Bank classification. Rosser *et al.* (2008), classified bank erosion to include both alluvial banks as well as bedrock cliffs, whereas in this study the 'Channel Bank' is limited only to alluvial banks due to the significant geochemical difference between alluvial deposits and mudstone base rock. In addition, total suspended sediment yields from the Pohangina are estimated to be 11 – 27 % of the Manawatu River catchment. If the estimate is towards the lower value, then a high channel bank erosion value may not be represented throughout the whole catchment and thus represent a lower proportion for the whole of the Manawatu catchment. Low values demonstrate the nature of the floodplain environment as a primarily depositional feature and possibly also reflects widespread bank protection strategies implemented throughout the catchment. Bank protection measures in the form of vegetation planting and installing rip-raps for bank stabilization have been widespread. It is quite possible any sediment derived from bank erosion is simply overwhelmed from the sediment derived from the Mountain Range and Mudstone terrain. This is supported by estimated sediment yields from Basher *et al.* (2012) which attribute over half of the total sediment yield of the

Manawatu at T-Col (15,830 x 10^3 t) to the Upper Manawatu (5,813 x 10^3 t) and Tiraumea (2,673 x 10^3 t) sub-catchments, which drain significant portions of Mudstone and Mountain Range landscapes (Fig. 23). Even though bank erosion is demonstrated here as contributing a relatively minor source of sediment overall, it may still represent a significant issue in its own right, given the consequences for anthropogenic interests such as erosion of high production agricultural floodplains and proximity to urban centres and infrastructure. The Limestone Sediment source estimated was 0.0 % across all models, which is consistent with the high solubility of $CaCO_3$ material which would render very little material persisting through transport. This highlights a gap in the ability of this approach to measure erosion sources from limestone terrain.

4.7 Conclusion

The study deployed a sediment fingerprinting technique to a large sedimentary catchment with a varied assortment of geological and geomorphological process based sediment sources. Differentiating a greater number of sediment sources, in this case 8, added considerable complexity for model predictions to differentiate between sediment sources. Despite the complexity, a globally optimal solution was still achieved. This involved a DFA using 16 variables to correctly classify 92.6 % of sediment sources. Attributing the selected DFA variables to the sediment source geochemistry was achieved to a limited extent, but requires information on the mineral assemblages and compositions of each respective source to definitively associate geochemical values with specific minerals. This would add considerable understanding to the geochemical pathways responsible for the geochemical signatures. The sediment source apportionment fits well with conceptual understanding of the catchment, attributing greater sediment contributions to sources that are subject to more erosion and capable of delivering the eroded materials to the river. Although the relationship between geological or pedological source and geomorphological process can be made in many instances, some cannot be distinguished when coming from the same source terrain. Consistent optimal solutions were able to be achieved through two models run with two different optimization techniques. Both optimization techniques provided globally optimal solutions for sediment source apportionment while providing consistent sediment source estimates between each of the models which increases confidences in sediment source estimates, however the incorporation of artificial mixtures to test the model estimates would have been a useful addition to model certainty.

4.8 Acknowledgements

We would like to acknowledge funding support from Landcare Research by way of the Murray Jessen PhD Scholarship with which this research is made possible

4.9 Summary

Differentiation of eight sediment sources within a large sedimentary dominated catchment created a challenge for the sediment fingerprinting approach, although geomorphically consistent sediment source estimates were derived from the model solutions. These estimates were based on average sediment loads over several months and allowed the creation of the sediment mixing model for this catchment. This mixing model was then used in the following chapter which addresses event based sediment sources and temporal changes in sediment sources throughout the duration of a storm event.

Chapter 5

Sediment source characterization during a storm event, Manawatu, New Zealand

5.1 General Introduction

Chapter 5 extends the sediment research beyond looking at the prevailing dominant catchment sources of fine sediment and begins to look at temporal changes of fine sediment sources throughout the duration of a high flow event. Chapter 5 is reproduced as: Vale SS, Fuller IC, Procter JN, Basher LR, &. Dymond. J.R., Sediment source characterization during a storm event, Manawatu, New Zealand submitted for publication in *Hydrological Processes*. The chapter provides an introduction to sediment fingerprinting and the methods used to relate suspended sediment samples to the arrival of each sub-catchment flow. This involved the application of a time-delay to align the sub-catchment flow peaks to the sample site in the lower Manawatu River. The results of the sediment source proportions at 1 hour intervals is presented and discussed in context of the geomorphological characteristics of the catchment and the contribution of key sub-catchments.

5.2 Abstract

Suspended sediment can have negative influences on the riverine environment making it important to understand sediment sources and sediment movement through a river catchment. Sediment fingerprinting is a tool capable of characterizing and distinguishing

discrete sediment sources using geochemistry. In this investigation sediment fingerprinting was applied at a high temporal resolution to the Manawatu Catchment. This involved collecting hourly suspended sediment samples over 53 hrs of a storm event and employing a sediment mixing model to distinguish changes in relative proportions of sources over time. High variability was observed between adjacent hourly samples which could be due to either the highly variable nature of sediment transport dynamics or the high levels of uncertainty encountered in sediment fingerprinting studies. However, general changes in sediment proportions were observed in relation to switching of the dominant flows from the Pohangina sub-catchment to the Upper Manawatu sub-catchment, and hysteresis patterns observed for the Pohangina sub-catchment which relates rising and falling limbs to changes in sediment sources estimates. The main shifts observed were from higher to lower mean contributions of Mountain Range (≈ 40 % v. ≈ 30 %,), Mudstone (≈ 50 % v. ≈ 40 %) and Loess (0.4 % v. ≈ 0.1 %), and lower to higher mean contributions of Hill Subsurface (≈ 2.5 % v. ≈ 13.5 %), Hill Surface (≈ 2.5 % v. ≈ 10 %) and Gravel Terrace (≈ 1.0 % v. ≈ 3.5 %) sediment sources after twelve hours of sampling. Channel Bank and Limestone sediment contributions remained low throughout the storm. The shifts may give an indication of different erosion process behaviour between the two sub-catchments in response to high rainfall events. Regression between sub-catchment and sediment proportions revealed the highest correlations occurred for the Upper Manawatu with Mountain Range (0.83), Gravel Terrace (0.75) and Mudstone (0.69). It proved difficult to evaluate the modelled sediment without sub-catchment suspended sediment samples being taken throughout the storm event.

5.3 Introduction

Sediment loads in rivers reflect erosion and transport processes occurring upstream. When land becomes erosion prone, sediment loads will increase(Page *et al.*, 2000) and have associated negative impacts. When the sediment being lost is derived from fertile soils, there is a reduction in agricultural productivity. Negative consequences also extend to the channel where fine sediment and accompanying contaminants degrade water quality by increasing turbidity and smothering of ecological habitats (Wood and Armitage, 1997).

It is important to understand the spatial and temporal patterns of sediment generation to guide catchment management strategies and ensure effective expenditure of resources. A range of indirect and direct techniques are available for assessing the patterns of sediment transport throughout a catchment including aerial photography (e.g. Marzolff and Poesen,

2009), erosion pins (e.g. Haigh, 1977, Lawler, 1986), direct sediment monitoring via gauging stations (e.g. Hicks *et al.*, 2000, Wang *et al.*, 2007), turbidity sensors (e.g. Lewis, 1996, Hicks *et al.*, 2004), sediment fingerprinting (e.g. Collins *et al.*, 1997, Walling *et al.*, 1999) and modelling (e.g. Prosser *et al.*, 2001, Merritt *et al.*, 2003). However, the spatial and temporal variability of suspended sediment coupled with the high cost of high resolution full catchment monitoring usually limits the collection of meaningful information (Collins and Walling, 2004).

Sediment fingerprinting provides a means of directly quantifying sediment source contributions within fluvial catchments. This is achieved through sampling a range of sediment sources throughout the catchment system, differentiating the sediment source according to inherent properties, and then relating the properties of the suspended sediment back to the source as relative contributions. Early sediment fingerprinting research used a small selection of geochemical properties to distinguish sediment sources (e.g. Walling *et al.*, 1979, Peart, 1993) but now most studies use comprehensive geochemical suites in combination with complex statistical analysis and mixing models to derive sediment source proportions (e.g. Cooper *et al.*, 2014, Haddadchi *et al.*, 2014, Laceby and Olley, 2015). Current sediment fingerprinting techniques demonstrate a wide range of measureable characteristics capable of discriminating sediment sources. These include properties such as mineralogy (e.g. Eberl, 2004, Gingele and De Deckker, 2005), mineral magnetic (e.g. Caitcheon, 1998, Blake *et al.*, 2006), geochemical composition (e.g. Collins *et al.*, 1998, Collins *et al.*, 2013, Lamba *et al.*, 2015, Hardy *et al.*, 2010, Zhang *et al.*, 2012), isotopic ratios (e.g. Douglas *et al.*, 1995, Gingele and De Deckker, 2005), radionuclides (e.g. Wilkinson *et al.*, 2013, Olley *et al.*, 2013, Porto *et al.*, 2013), organic elements (Fox and Papanicolaou, 2008a, Evrard *et al.*, 2013), and compound specific isotopes (e.g. Gibbs, 2008, Hancock and Revill, 2013, Blake *et al.*, 2012).

Despite advancements in sediment fingerprinting, a number of uncertainties still present significant challenges to the validity of the technique and the capacity to produce a stand-alone evaluation of a given sediment problem. A significant amount of uncertainty relates to how well the measured property reflects the source sediment throughout sediment transport. Several authors (e.g. Motha *et al.*, 2002, Koiter *et al.*, 2013b) have reported on this issue and the compromised retention of the source's geochemical character. Storage effects and indirect transport pathways also present a significant problem for sediment fingerprinting applications, emphasising a pressing need to better understand the effects of sediment fractionation on the geochemical signature (Belmont *et al.*, 2014). Tracer selection for sediment source ascription can produce different estimates for different suites of selected tracers (e.g. Collins and Walling, 2002). A recent study has observed mean differences of c. 24

% between different tracer groups (e.g. Pulley *et al.*, 2015). The variability of within-source geochemistry and subsequent source classifications presents feasibility issues for acquiring adequate sampling at the desired resolution, especially for larger catchments (e.g. Collins *et al.*, 2010a). The assortment of sediment mixing models now available does not necessarily provide consistent estimates (Laceby and Olley, 2015, Pulley *et al.*, 2015, Smith and Blake, 2014, Haddadchi *et al.*, 2014). Each model and optimization technique has advantages and disadvantages, and selection has to be evaluated accordingly. Linear mixing models are the model of choice to date, some including weighting factors (e.g. Collins *et al.*, 2010a), and variations of local and global optimization techniques as well as genetic algorithms (e.g. Collins *et al.*, 2010b) for deriving the most probable estimates. More recently, Bayesian statistics have also been used as a means to provide source estimates (e.g. Cooper *et al.*, 2014).

Early research recognized that the application of sediment fingerprinting approaches to intra-storm variability had received little attention (Collins *et al.*, 1997), and is still the case. This is despite a significant number of studies identifying inter- and intra-storm variability as producing a dominant influence on any given sediment fingerprinting application. Several studies have looked at the topic. Slattery *et al.* (1995) observed a progressive increase in cultivated soil contribution in relation to discharge, while channel bank remained consistent throughout the rising limb, but increased within the receding limb. Similar patterns were encountered by Collins *et al.* (1997) where maximum pasture contributions coincided with the hydrograph peak and associated maximum rainfall intensities. Collins *et al.* (1998) also found consistent intra-storm results from composite fingerprinting when compared with flood routing times, but remobilization and storage may have an 'averaging' affect and complicate interpretation. Martínez-Carreras *et al.* (2010b) put forward an argument to use spectral-based sediment fingerprinting (involving visible and near-infrared diffuse reflectance spectroscopy) approach emphasizing the relatively low costs and labour requirements compared to traditional sediment fingerprinting. This highlights one of the challenges intra-storm variability investigations are faced with. Achieving adequate temporal resolution creates a significant obstacle within the resource constraints of most projects. In this study sediment fingerprinting is applied to a storm event that took place between 27th to 30th November in 2013 in the Manawatu Catchment, New Zealand. The aim was to identify sediment source changes throughout the duration of a storm and relate this to the flow contribution from upstream sub-catchments.

5.4 Study Site

Situated in the lower North Island of New Zealand, the headwaters of the Manawatu River drain the eastern and western flanks of the Ruahine and Tararua ranges; a total watershed of c. 5870 km^2 which is primarily an agricultural catchment underlain by sedimentary geology. The Upper Manawatu headwaters begin in the eastern Ruahine Range collecting additional flow from the Tiraumea, Mangatainoka and Mangahao before flowing through the Manawatu Gorge where it joins with the Pohangina River before eventually flowing into the Tasman Sea (Fig. 34). Mean annual discharge for Manawatu River from 2013 to 2014 taken from the Teachers College (T-col) site amounted to c.93 $m^3 s^{-1}$ with main contributions from the Upper Manawatu (c. 24 $m^3 s^{-1}$), Tiraumea (c. 15 $m^3 s^{-1}$), Mangatainoka (c. 16 $m^3 s^{-1}$), Mangahao (c. 12 $m^3 s^{-1}$), and Pohangina (c. 15 $m^3 s^{-1}$).

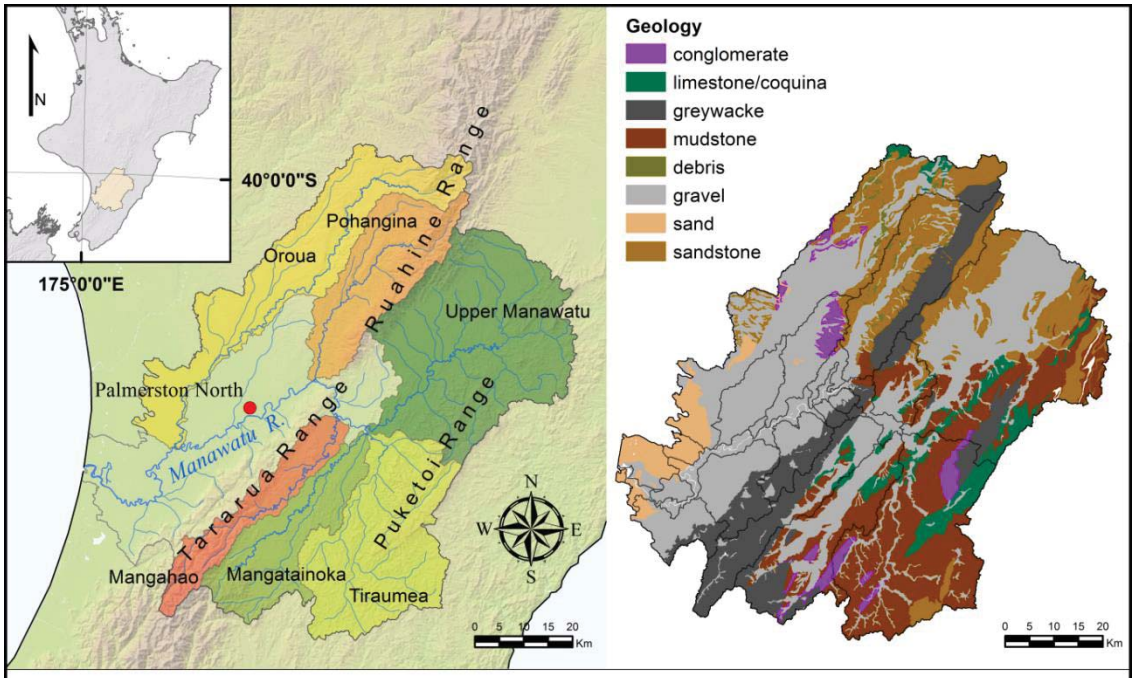

Areal Percentage

Geological Material	Upper Manawatu	Tiraumea	Manga-tainoka	Mangahao	Pohangina	Oroua	Total Catchment
Greywacke	5.9	3.1	21.2	59	30.9	3.4	14.6
Mudstone	22.8	63.8	29.5	7.3	2.3	-	18.5
Sandstone	24	3.9	0.1	0	44.6	27.3	14.7
Gravel	39.7	11.8	37.8	28	19.7	52.6	40.3
Limestone	7.4	11.3	6.3	5.6	-	2.6	4.8
Conglomerate	0.1	6.1	5.1	-	0.1	2.4	2.4
Sand	-	-	-	-	-	9.7	2.8
Debris	-	-	-	-	2.3	2	0.5

Fig. 34: *Study site and sub-catchment geological composition altered from Vale et al. (2016b).*

Steep slopes are prevalent throughout both the eastern and western sub-catchments which are typically underlain by soft sedimentary mudstone, as evidenced in the Tiraumea sub-catchment (Fig. 34). Mudstone cliffs, as well as alluvial gravel terraces, are exposed in semi-confined channels throughout the middle reaches of the catchment. The lower reaches of the Manawatu River, range from wandering to pseudo-meandering as the river flows through extensive alluvial floodplains. Many of the channels have undergone flood protection works in the form of levees, rock protection and channel straightening and narrowing, transitioning to laterally-confined single thread channels as demonstrated in the Pohangina River (Fuller, 2009). The dominantly agricultural catchment is primarily made up of exotic grassland (≈ 75 %) (cf. Fig. 34), which is mostly sheep and beef production on the steeper terrain and dairy farming in the lowland areas. Indigenous vegetation covers ≈ 17 % of the catchment area, mostly confined to the Tararua, Ruahine and Puketoi ranges. Exotic forest accounts for ≈ 3 % of catchment area with minor pockets of mānuka and kanuka, scrub, and small areas of short-term rotation crops also found within the catchment.

5.5 Methods

5.5.1 Sediment Sample Collection

Sediment sources were sampled from a range of geological and process based locations (cf. Vale *et al.*, 2016b). This involved 140 samples throughout the Manawatu River catchment (Fig. 35). The sediment sources were classified as Mudstone, Hill Subsurface, Hill Surface, Mountain Range, Channel Bank, Loess, Gravel Terrace and Limestone with descriptions outlined in Fig. 36. Sampling consisted of 5-10 samples taken to form a composite sample for the sediment source at each specific location. Surface sediment samples were taken from the top 4 cm of material, while the remaining source samples were taken at various depths depending where that source material lay within the sample profile. Hourly suspended sediment samples were taken from a site known as 'Manawatu at Teachers College' (Fig. 35) during a 53 hour storm event with a return period of approximately 1.3 years and stage of 4 m. This was achieved using an ISCO 6712 automatic sampler with an intake at 2 m to draw up a 1L suspended sediment sample using a peristaltic pump producing 53 suspended sediment samples.

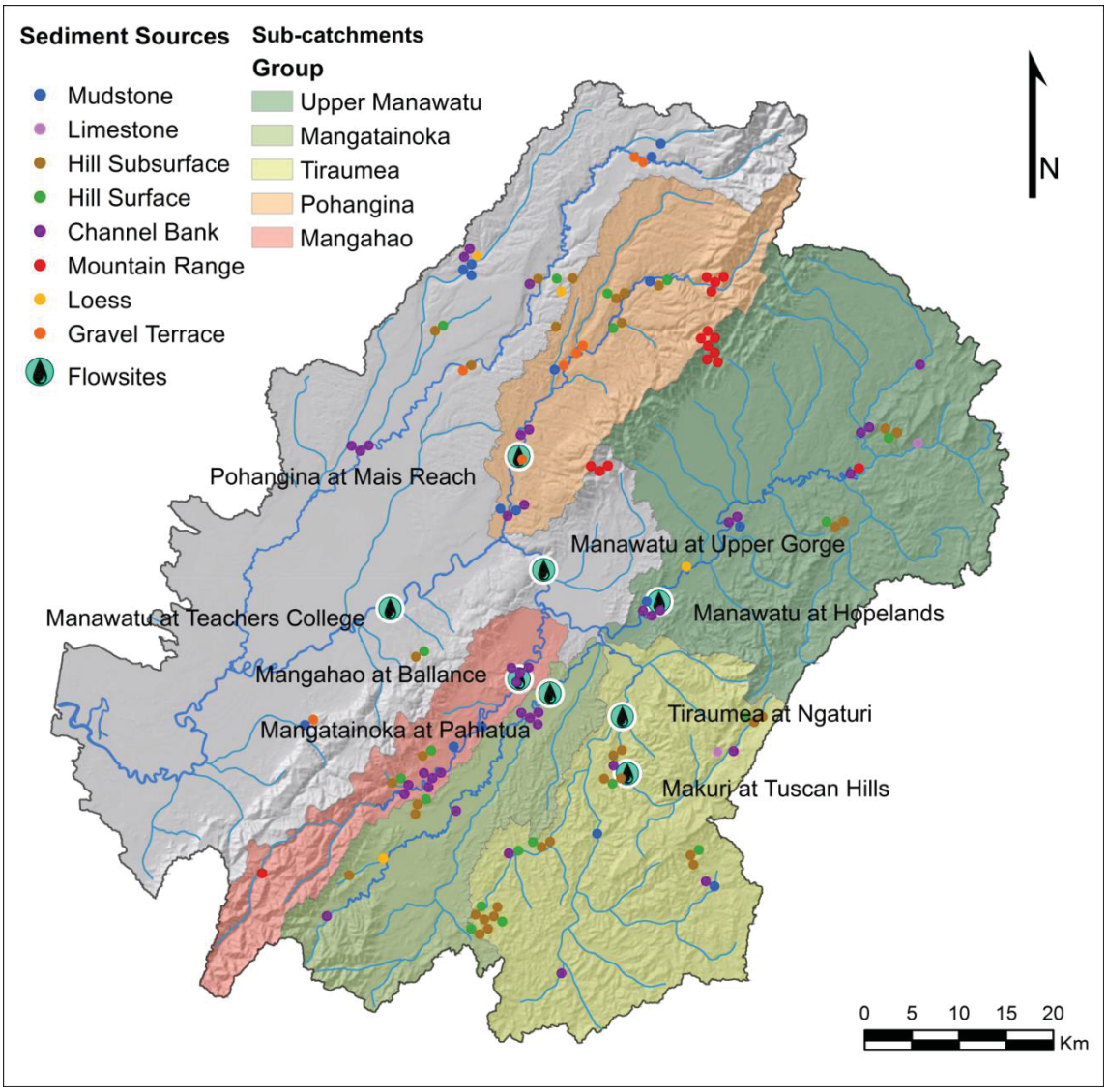

Fig. 35: *Manawatu River Catchment showing source sampling spatial distribution*

5.5.2 Sample Analysis

Sample preparation and statistical steps followed the same approach as Vale *et al.* (2016b). Source samples were dried at 40°C followed by light disaggregation and sieving to retain the < 63 µm fraction. Suspended sediment samples were wet sieved through to 63 µm, and then dried at 40°C. All samples were then weighed into crucibles for XRF analysis, and combusted at 850°C overnight to oxidize all elements and combust any organics. 2 g of the sample was mixed with 6 g of lithium tetraborate and fused into glass discs. Recovery of 2 g of sample was not possible for some of the suspended sediment samples, so in order to make up the necessary quantity, a measured quantity of purified SiO_2 was added as required. This allowed the

element sample concentrations to be derived after accounting for dilution. A straight SiO_2 disc was also made for analysis to quantify the introduction of any possible contaminations. The glass discs were analysed using a Panalytical Axios 1kW X-ray Fluorescence Spectrometer (XRF) for SiO_2, TiO_2, Al_2O_3, Fe_2O_3, MnO, MgO, CaO, Na_2O, K_2O, P_2O_5, Ba, Rb, Sr, Zr, Nb, Y,V, Cr, and Ni concentration. The glass discs were retained and a follow up analysis was conducted using a Agilent 7700 Series Inductively Coupled Plasma-Mass Spectra with an attached Laser Ablation unit (LA-ICP-MS) for Sc, V, Cr, Co, Ni, Cu, Zn, Ga, Rb, Sr,Y, Zr, Nb, Cs, Ba, La, Ce, Pr, Nd, Sm, Eu, Gd, Tb, Dy, Ho, Er, Tm, Yb, Lu, Hf, Ta, Pb, Th, and U. Where there are both XRF and LA-ICP-MS element concentrations the XRF data was given preference over LA-ICP-MS values because the XRF values provided more consistent results.

Fig. 36: *Sediment source Characteristics ; (A) Mudstone; (B) Hill subsurface; (C) Hill Surface; (D) Channel Bank; (E) Mountain Range; (F) Gravel Terrace; (G) Loess; (H) Limestone*

5.5.3 Statistical Discrimination

In order to select appropriate tracers the geochemical concentrations must show conservative behaviour from source to the sampling point. The bracket test provides a basic test that each tracer falls within the geochemical range of the potential sources. If they do not pass this test (within a 15 % measurement error) they were removed. The measurement error was larger for the flood samples than the samples from Section 4 since the lower sample yield resulted in greater uncertainty. Next, the two-step method after Collins *et al.* (1998) was employed. This first step relied on the non-parametric Kruskal-Wallis H test to evaluate statistically significant differences of individual tracers between the selected source groups. The test was carried out on the concentrations of each analysed element to identify the statistically significant discriminants for subsequent analysis. A 95.0% confidence interval (α level of 0.05) was used for the critical p-value.

The second step used Discriminant Function Analysis (DFA) which allows for prediction of group membership based on linear combinations of predictor variables (Eq. 13)

$$D = v_1X_1 + v_2X_2 + v_3X_3 + \ldots v_iX_i + a \quad \text{(Eq. 13)}$$

Where D = discriminant function

v = the discriminant coefficient

a = a constant

i = the number of predictor variables.

A stepwise minimization of Wilk's Lambda multivariate DFA was conducted using SPSS (IBM Corp., 2012). Wilk's Lambda is a measure of the between-group variability to within-group variability whereby minimizing the value reduces the sample grouping. It is guided by '*F*' values which determine the entry and removal of variables as a measure of the extent to which an individual variable contributes to group prediction. Default values of 3.84 (probability = 0.5) and 2.71 (probability = 0.1) are used for F to enter and F to remove respectively.

5.5.4 Multivariate Mixing Model

The successful elements from the discriminant function analysis were incorporated into a multivariate mixing model to estimate the relative proportions of sediment source contributions from the time-sequence of suspended sediment samples. This was done

following the approach outlined by Collins *et al.* (1997), whereby equations are created for each element which relate the source proportions to the sediment sink element concentration. The relative proportions of each source group are estimated through minimizing the sum of the residual (objective function) for the element concentrations through least squares. Previously, Vale *et al.* (2016b) employed several mixing model variations in the Manawatu Catchment, and found that mean estimates of sediment proportions were comparable between the models. However, given that the model was required to estimate for each hourly sample, a less time-dependent model was preferred and the Collins *et al.* model provided shorter run-times in comparison. The following mixing model after Walling *et al.* (1999), Collins *et al.* (1997), Owens *et al.* (1999) was selected:

$$R_{es} = \sum_{i=1}^{n} \left(\frac{C_i - \sum_{j=1}^{m} X_j \bar{S}_{ij}}{C_i} \right)^2 \quad \text{(Eq. 14)}$$

R_{es} = the sum of squares of the residuals

n = the number elements in the composite fingerprint (e.g. P_2O_5)

C_i = the concentration of element (i) in the sediment sink sample

m = the number of source groups (e.g., mudstone, hill surface etc.)

X_i = the relative proportion from source group (j) to the sediment sink sample

$\bar{S}_{ij}$ = the mean concentration of element (i) from the sample in source group (j). The mean was used in the basic model as there was not a significant difference observed between medians and mean data and thus suggesting minimal affect from outliers.

The model adheres to two constraints that must be satisfied to produce realistic values. The first constrains each source group proportion to being a positive value between 0 and 1, i.e.

$$0 \leq P_i \leq 1 \quad \text{(Eq. 15)}$$

The second constrains the sum of all source group contributions to be equal to 1, i.e.

$$\sum_{i=1}^{n} P_i = 1 \quad \text{(Eq. 16)}$$

The mixing model source estimates are calculated based on the mean and standard deviation of each source group employing a Monte Carlo approach over 5000 replications.

The optimization of the model solution was conducted using the solver extension in Microsoft Excel. The optimization method employed was the 'Generalized Reduced Gradient (GRG)

Nonlinear' using the 200 population size multi-start parameter. The multi-start method automatically runs repeated iterations using different random starting values for the decision variables thereby providing a selection of locally optimal solutions of which the best can be selected as a likely globally optimal solution. Auto-scaling was used to negate any significant differences in scales between variables. The Constraint Precision denotes value that cannot be exceeded between the constraint value and reference cell, which was set to 0.0001. The convergence value was set to 0.001 and outlines the limit of relative change which can occur during the last 5 iterations before the model is regarded as converging on the optimal solution.

5.5.5 Storm flow hydrograph

Stream flow and suspended sediment concentrations were obtained from Horizon's Regional Council's monitoring network. Flow data consisted of hourly measurements for 7 sites across the Manawatu (Fig. 35; Fig. 37). The Manawatu at Upper Gorge site was not used in the actual analysis except for confirming lag times between the sub-catchment flow peaks with the Manawatu at Teachers College site.

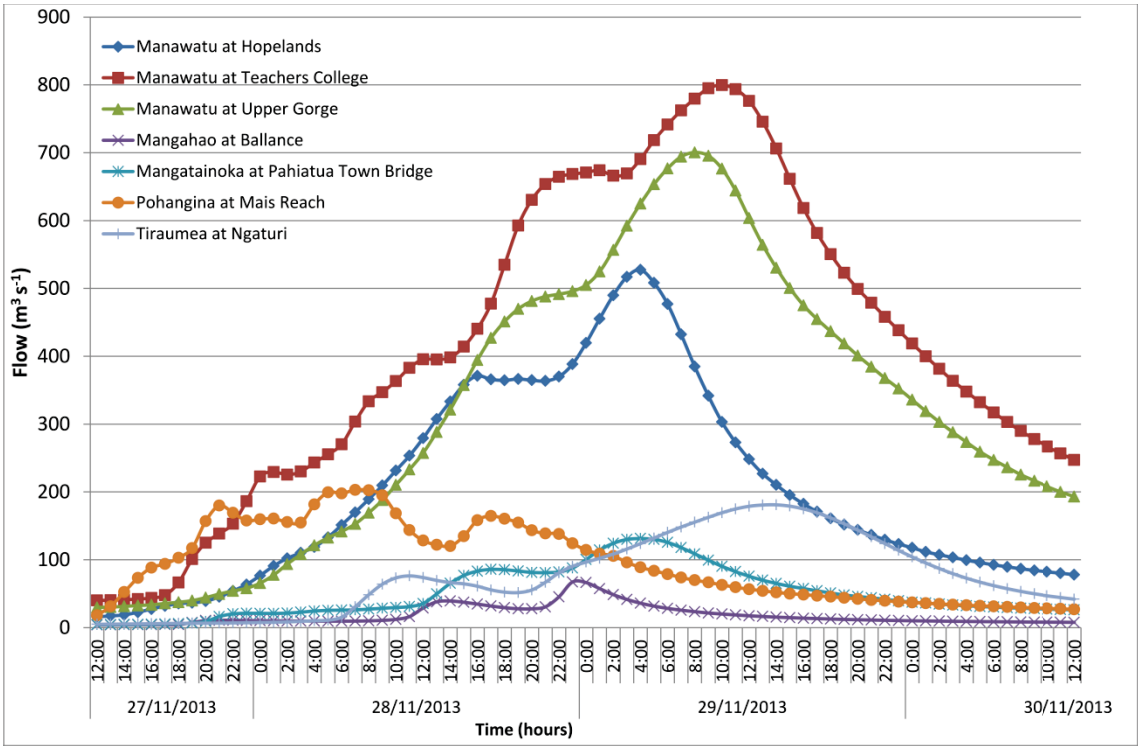

Fig. 37: *Flood Hydrograph showing sub-catchment flow curves in actual time*

Suspended sediment concentrations were derived from Horizons Regional Council turbidity measurements for each of the monitoring sites, which were converted to suspended sediment concentration using sediment concentration rating curves. Further information on this technique can be found in Hicks and Hoyle (2012). Suspended sediment concentrations from the Manawatu at Hopelands site were absent between 10:00 am 29/11/2013 and 10:00 am 30/11/2013 which corresponded to the falling limb of the flood hydrograph. Data for this time period was interpolated based on a power law curve line of best fit between flow and suspended sediment concentration.

In order to compare the sub-catchment flows with the suspended sediment samples taken at the T-Col monitoring site, the flow of each sub-catchment had to account for the lag-time for the sub-catchment flow to reach the T-Col site. This involved estimating lag times based on time differences between peak flows without taking into account flow peak smoothing experienced during travel. Horizon Regional Council provided estimates of the peak lag times in concordance with their monitoring equipment and arrival of the peak flows.

Table 24: *Lag-time estimates of each sub-catchment relative to Manawatu at Teachers College*

Monitoring Site	Time Delay
Manawatu at Hopelands	7 hrs
Manawatu at Upper Gorge	2 hrs
Mangahao at Balance Bridge	10 hrs
Mangatainoka at Pahiatua	6 hrs
Pohangina at Mais reach	4 hrs
Tiraumea at Ngaturi	12 hrs
Manawatu Teachers College	0 hrs

5.5.6 Relationship between sub-catchments and storm hydrograph

The relationships between the sub-catchment flow contribution and sediment sources was explored through multiple regression analysis and partial correlations. These were derived by selecting one sub-catchment and correlating it with the sediment source proportions estimated from the Manawatu Teachers College site, while controlling for the remaining sub-catchment sediment loads and repeated for each sediment source group.

A multivariate mixing model was applied to estimate the sediment source proportions for each sub-catchment for each time step. This was achieved by minimizing the R_{es} of the difference between the T-Col source proportions and the sub-catchment source proportions multiplied by

sub-catchment sediment loads and executed through the mixing model, after Collins *et al.* (1997), Walling *et al.* (1999), Owens *et al.* (1999),

$$R_{es} = \sum_{i=1}^{n} \left(\frac{S_i - \sum_{j=1}^{m} X_{ij} S_j}{S_i} \right)^2 \quad \text{(Eq. 17)}$$

R_{es} = the sum of squares of the residuals

n = the number source groups in the composite fingerprint (e.g. Mudstone)

S_i = the estimated sediment load of the source group (i) at T-Col

m = the number of sub-catchment groups (e.g. Pohangina)

X_{ij} = the relative proportion of the source group (i) for the sub-catchment (j)

S_j = the sediment load of sub-catchment sample (j).

The model adhered to three constraints which must be satisfied to produce realistic values. The first constrains the proportion of each sub-catchment source to being a positive value between 0 and 1, expressed as:

$$0 \leq X_{ij} \leq 1 \quad \text{(Eq. 18)}$$

The second constraint follows that the sum of all source group contributions for each sub-catchment are equal to 1, expressed as;

$$\sum_{i=1}^{n} X_i = 1 \quad \text{(Eq. 19)}$$

The third shows that the sum of each sub-catchment sediment load for a source is equal to T-Col sediment load for that sediment source assuming no channel or floodplain deposition has occurred, expressed as:

$$\frac{\sum_{j=1}^{m} X_{i,j} S_{i,j}}{S_{Tcol}} = X_{Tcol,i} \quad \text{(Eq. 20)}$$

The model was optimized using the solver extension on Microsoft Excel. The optimization method employed a 'Generalized Reduced Gradient (GRG) Nonlinear' with a multi-start parameter and population size of 1000 to improve the likelihood of a globally optimal solution. Auto-scaling was used to avoid any issues that could arise from different scales. Constraint Precision was set to 0.0001 with a convergence value of 0.001. Model and optimization selection favoured a less time-dependent model given that the model was run 5000 times for each hourly sediment sample.

5.6 Results and Discussion

5.6.1 Statistical Differentiation

Statistical differentiation is summarized and adapted from Vale *et al.* (2016b) as follows. All tracers from the storm sediment passed the bracket test and fall within sediment source values (illustrated for selected tracers in Fig. 38, Fig. 39, Fig. 40) and result in the removal of no tracers.

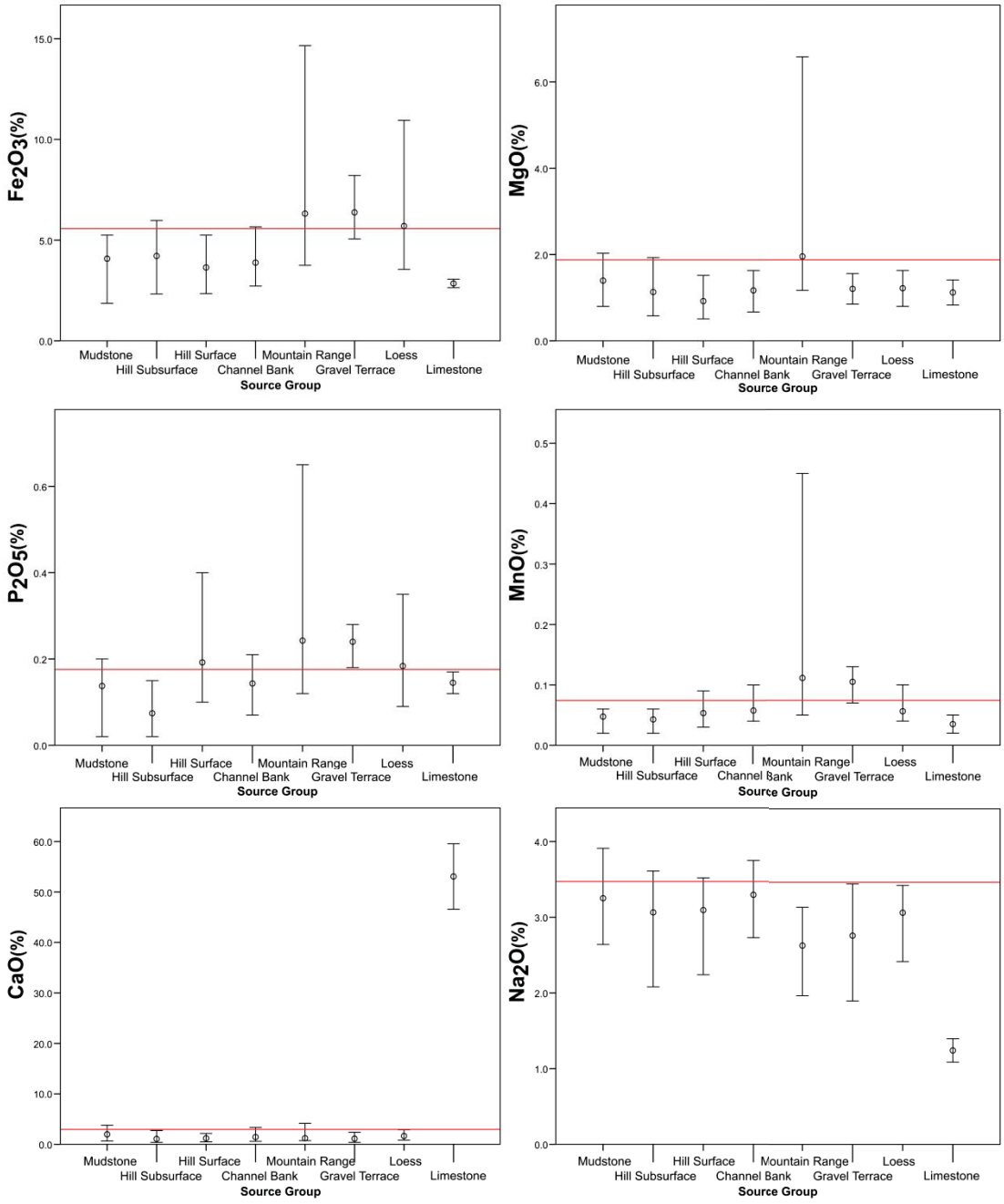

Fig. 38: *Bracket test showing maximum and minimum tracer values by source group for selected tracers with the mean from the storm sediment indicated by the red line.*

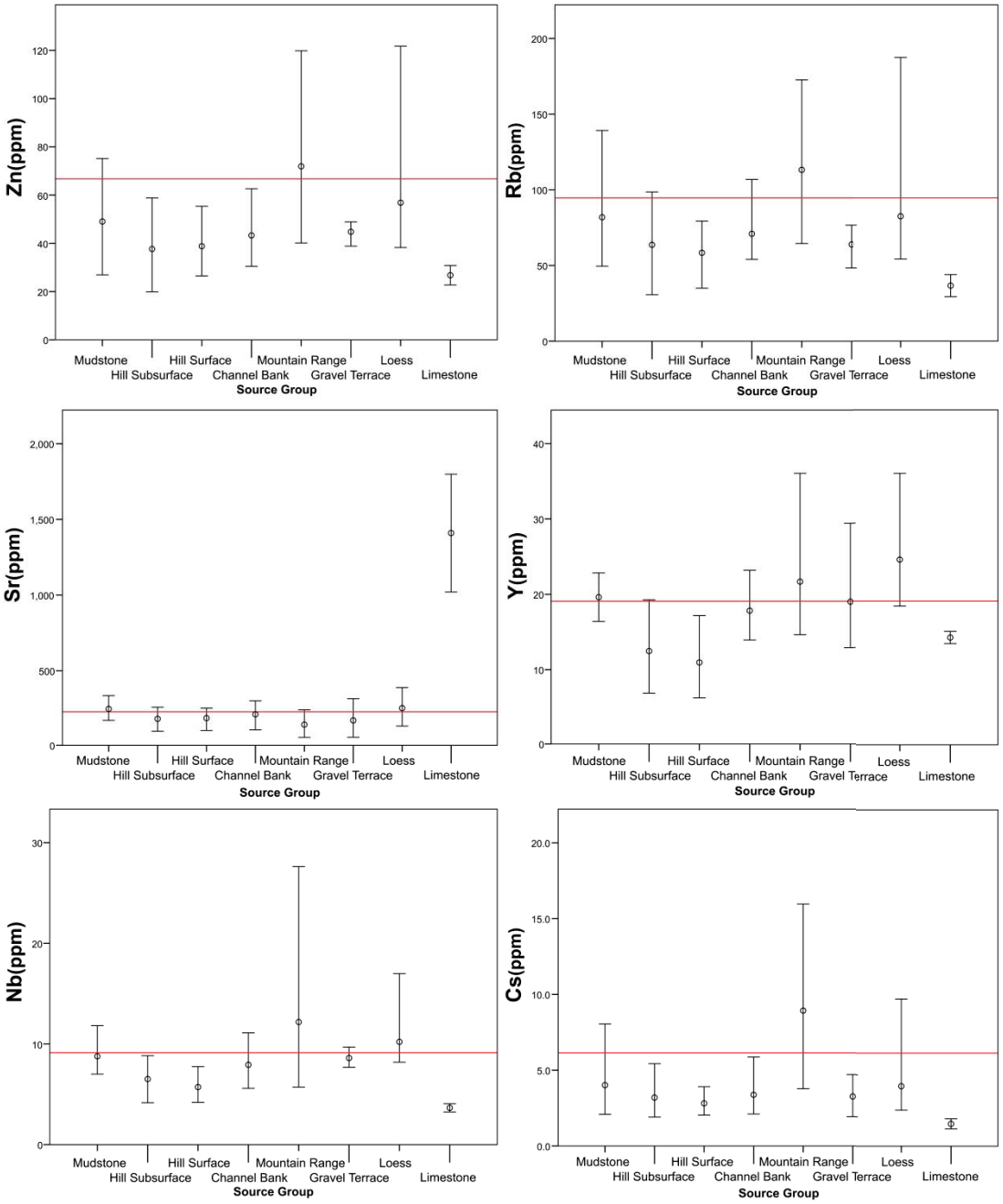

Fig. 39: *Bracket test (cont'd) showing maximum and minimum tracer values by source group for selected tracers with the mean from the storm sediment indicated by the red line.*

A successful Kruskal-wallis test permitted SiO_2, TiO_2, Al_2O_3, Fe_2O_3, MnO, MgO, CaO, Na_2O, K_2O, P_2O_5, Sc, V, Cr, Co, Ni, Cu, Zn, Ga, Rb, Sr,Y, Zr, Nb, Cs, Ba, La, Pr, Nd, Sm, Eu, Gd, Tb, Dy, Ho, Er, Tm, Yb, Lu, Hf, Ta, Pb, Th, and U to undergo discriminant function analysis (DFA). This narrowed the initial selection down to a group of 16 suitable tracers: CaO, Lu, Cs, Sr, Tm, Na_2O, P_2O_5, Fe_2O_3, Pb, U, Hf, MnO, Zn, MgO, Nb and Y. Seven functions were produced in the analysis with the first two functions accounting for 99.1 % of the variance (Table 25).

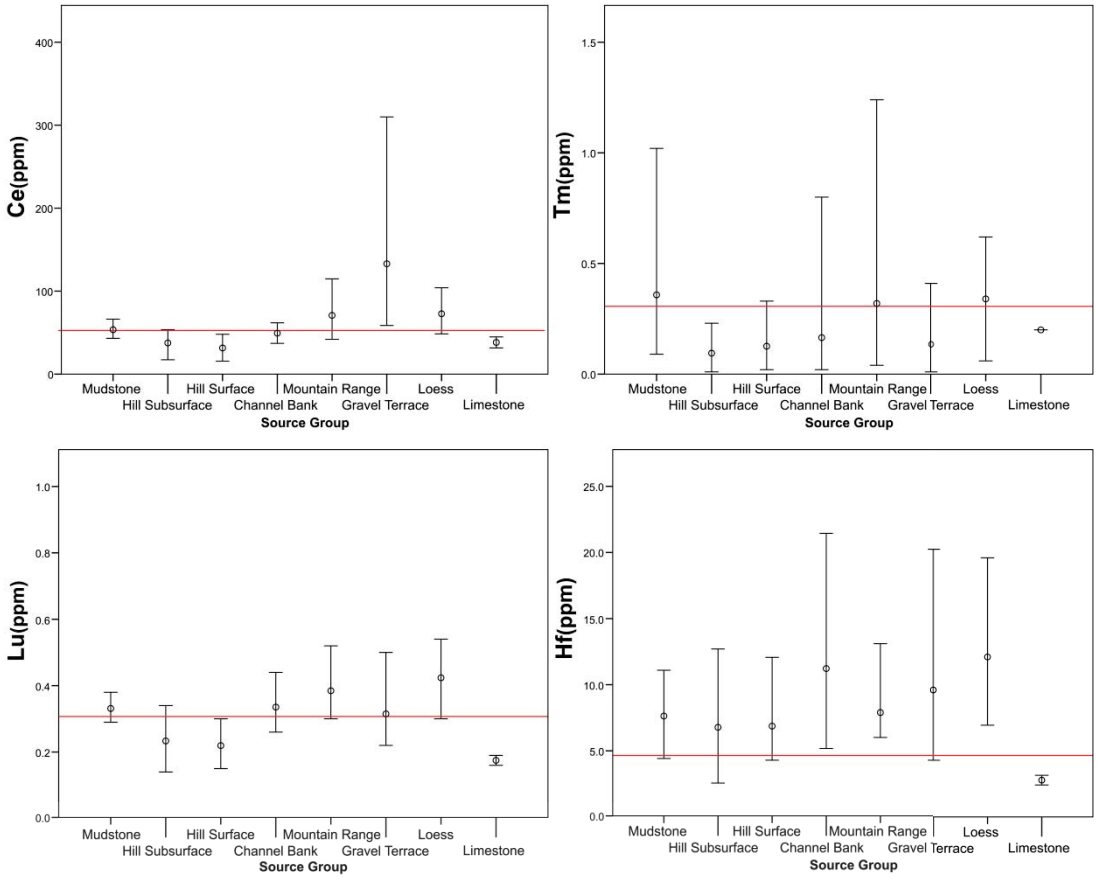

Fig. 40: *Bracket test (cont'd) showing maximum and minimum tracer values by source group for selected tracers with the mean from the storm sediment indicated by the red line.*

The group multivariate means show how the functions separate the source groups (Table 25; Fig. 42). Function 1 provided separation of the Limestone source (177.0) from the remaining groups (≈ -2 to ≈ - 4) but also provided some differentiation of the Mountain Range and Gravel Terraces. Function 2 provided differentiation of the Mountain Range (≈ 4.4) sources from Hill Subsurface (≈ -1.7) and Hill Surface sediment (≈ -1.4). Function 3 provided separation of the Loess (≈ 3.0) and Mudstone sediment (≈ 2.0) from the Hill Surface (≈ - 1.9) and Mountain Range sediment (≈ - 1.6). The remaining functions contribution minimal additional information for discrimination purpose but are displayed for results purposes (Table 25).

The 7 functions provided 92.1 % of total correct classifications (Table 26); Mudstone classified 93.8 % correct with 6.3 % misclassified as Gravel Terraces. Hill Subsurface and Channel Bank displayed the lowest correct classifications of 85.7 % and 87.8 % respectively. Hill Subsurface was misclassified as Hill Surface (8.6 %) and Channel Bank (5.7 %) while Channel Bank was misclassified as Mudstone (2.4 %), Hill Subsurface (4.9 %) and Gravel Terrace (4.9 %). Hill surface, Mountain Range, Gravel Terrace, Loess and Limestone all classified 100 % correctly.

Table 25: *Variance explained by each function (top), and centroid values for each source and group function (bottom)*

Discriminant Function % of Variance explained							
Variable	Function						
	1	**2**	**3**	**4**	**5**	**6**	**7**
Eigenvalue	485.904	3.435	1.847	1.186	1.041	0.618	0.246
% of Variance	98.3	0.7	0.4	0.2	0.2	0.1	0.0
Cumulative %	98.3	99.0	99.4	99.6	99.8	100	100
Group Centroid Functions							
Group	Function						
	1	**2**	**3**	**4**	**5**	**6**	**7**
Mudstone	-2.329	0.605	1.908	0.316	-1.46	-1.03	-0.567
Hill Subsurface	-2.128	-1.721	-0.274	1.295	0.588	-0.231	0.117
Hill Surface	-2.855	-1.407	-1.878	-1.523	-1.071	-0.499	0.302
Channel Bank	-2.306	-0.125	0.391	-0.424	0.017	1.047	-0.237
Mountain Range	-4.367	4.365	-1.631	0.874	-0.085	0.009	0.167
Gravel Terrace	-3.807	1.254	-0.494	-2.511	3.997	-1.721	-1.187
Loess	-1.95	1.216	2.966	-1.075	0.825	-0.321	1.441
Limestone	177.015	0.379	-0.217	-0.022	0.012	-0.036	-0.011
Unstandardized canonical discriminant functions evaluated at group means							

5.6.2 Storm Hydrograph Adjustment

The rainfall event was concentrated over the northern Pohangina and Upper Manawatu sub-catchments of the Manawatu, moving west to east across the mountain range. Measured rainfall reached 55 mm on the 29th November (Fig. 41) in the east of the catchment although rainfall levels could be significantly higher in the Ruahine mountain range. Adjusting the sub-catchment flows and sediment loads according to the respective sub-catchment lag-time provided cumulative flows comparable with the recorded T-Col site flow record (Fig. 43).

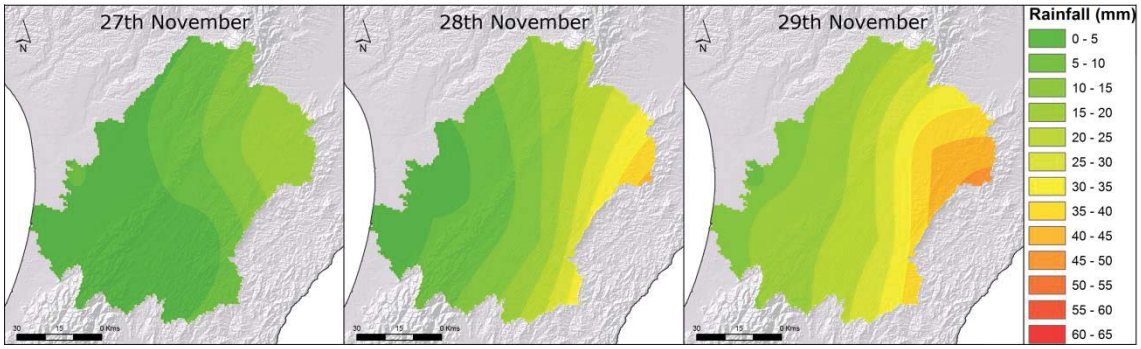

Fig. 41: *Interpolated daily rainfall (mm) from the 27th to 29th November 2013 showing highest levels to the east of the catchment.*

Table 26: *Predicted group membership of samples based on discriminant function analysis values*

	Predicted Group Membership							
Group	**Mudstone**	**Hill Subsurface**	**Hill Surface**	**Channel Bank**	**Mountain Range**	**Gravel Terrace**	**Loess**	**Limestone**
Mudstone	93.8	-	-	-	-	6.3	-	-
Hill Subsurface	-	85.7	8.6	5.7	-	-	-	-
Hill Surface	-	-	100	-	-	-	-	-
Channel Bank	2.4	4.9	-	87.8	-	4.9	-	-
Mountain Range	-	-	-	-	100	-	-	-
Gravel Terrace	-	-	-	-	-	100	-	-
Loess	-	-	-	-	-	-	100	-
Limestone	-	-	-	-	-	-	-	100
92.1 % of selected original grouped cases correctly classified								

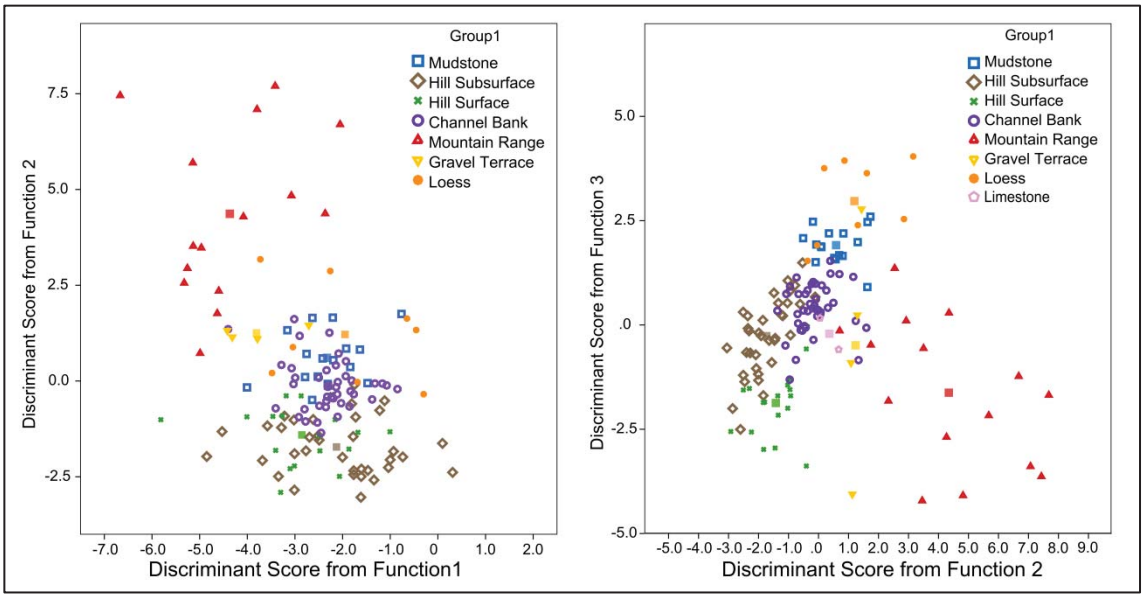

Fig. 42: *Visualization of sediment sources discriminant scores for function 1 and function 2 (Left) and function 2 and function 3 (right).*

The initial increase in flow came from the Pohangina sub-catchment as it is the most westward sub-catchment and presented a short lag time. The Upper Manawatu flow begins to rise in the early hours of Nov 28th, and becomes the most dominant flow throughout the majority of the storm with a major flow peak occurring at 11:00 on Nov 29th. Flow contribution from the Mangatainoka and Mangahao also start to increase at a similar time; experiencing several subsequent increases in flow which peak at approximately midnight on the 28th Nov and 10:00 on the 29th Nov. The Tiraumea has a minor peak in the final hours of 28th Nov, with the main peak occurring around 03:00 on Nov 30th.

Peak flow at the T-Col site was recorded as ≈ 800 m^3 s^{-1} at 10:00 29th Nov, whereas peak sediment loads experienced were close to 1 t s^{-1} at two occasions, 21:00 Nov 28th and 09:00 Nov 29th. The additive flow derived from the sub-catchments is greater than the measured flow taken at T-Col by almost 100 m^3 s^{-1}. Lower flow at the T-Col site compared with the cumulated sub-catchment total likely reflects surface water -groundwater interactions, namely loss of surface water through the zones of permeable alluvial and gravelly deposits which form much of the Manawatu floodplain (Roygard *et al.*, 2012, Vale, 2011). The discrepancy could also be influenced by over simplification of the time adjustment. In reality, the lag time is variable due to changes in temporal flow conditions and discharge peaks experiencing a flattening effect as they move downstream. This flattening of the discharge peaks is a downstream phenomenon of catchment flow and is observed quite clearly when comparing the T-Col site to the cumulative sub-catchment totals (Fig. 43). This likely contributes to discrepancies between the modelled sub-catchment flow and the T-Col site, which limits accurate mapping of the flow peaks as they move downstream.

The sediment load is characterised by the major flow contributions but is largely dominated by the Pohangina and Upper Manawatu sub-catchments. The first sediment load peaks arrive in the early hours of Nov 28th with a load of ≈ 0.46 t s^{-1} followed by a load of ≈ 0.48 t s^{-1} around midday on Nov 28th, both dominated by Pohangina sediment loads (Fig. 43). Introduction of the Upper Manawatu flow produces the two maximum sediment load peaks, reaching sediment loads of ≈ 0.97 t s^{-1} and ≈ 0.98 t s^{-1} at 21:00 Nov 28th and 10:00 Nov 29th respectively. Very minor sediment loads arise from the Mangahao and Mangatainoka sub-catchments. The Tiraumea begins to contribute sediment load towards the final stages of the storm, peaking around midnight 30th Nov. As with the flow, sediment loads differ between the T-Col measurements and the cumulative sub-catchment sediment loads. The T-Col values exhibit lower measured loads to the order of 0.3 t s^{-1} at the sediment peaks which is in-part related to the same discrepancy of the sub-catchment flow exhibiting lower values than measured T-Col flows. This is because the adjusted sediment loads are a function of the sub-catchment flows and suspended sediment concentrations (SSC) causing the flow discrepancies to propagate into the sediment loads. Additionally, it may reflect retention of suspended sediment upstream of the T-Col study through depositional features.

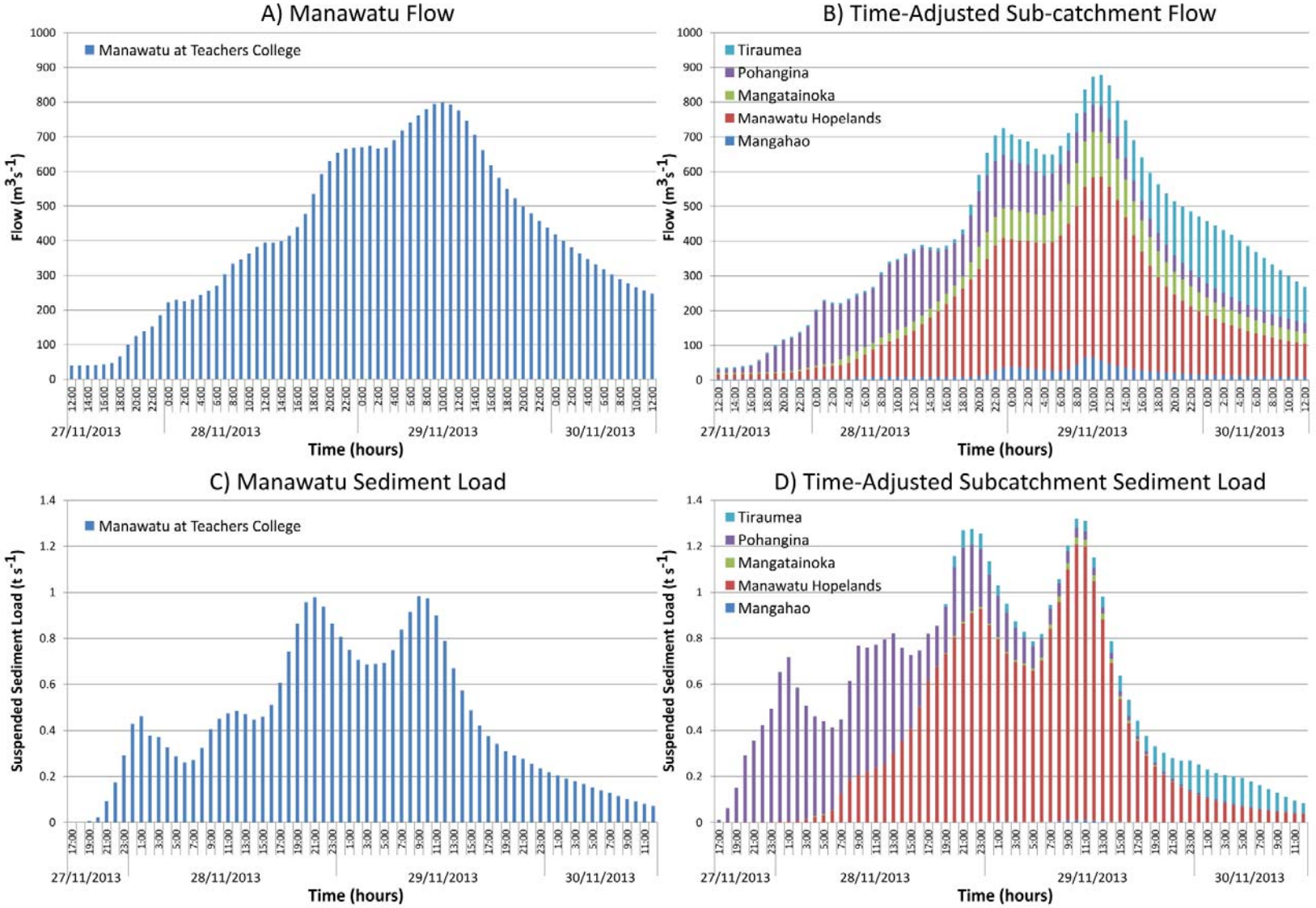

Fig. 43: *Hydrographs and Sedigraphs of; (A) Manawatu River Flow at Teachers College; (B) Time-adjusted cumulative sub-catchment flow; (C) Manawatu River Sediment load at Teachers College; (D) Time-adjusted cumulative sub-catchment sediment load (D)*

5.6.3 Sediment source proportions of hourly sediment samples

The mixing model was able to derive mean hourly sediment source contribution estimates throughout the storm hydrograph. This showed a number of fluctuations occurring throughout the flow hydrograph. Mean Mudstone source proportions fluctuated between ≈ 20 – 60 % throughout the storm duration while Hill Subsurface and Hill Surface both approached 0 % minimum, but upper limits of ≈ 23 % and ≈ 24 %. The Channel Bank sediment had the lowest proportions, remaining effectively 0.0 % throughout the storm. The Mountain Range sediment source fluctuated from ≈ 24 – 46 %. Gravel Terrace and Loess both have estimated contributions near 0 % but display maximums as much as ≈ 6 % and ≈ 0 % respectively. Limestone shows low sediment source contribution which range between ≈ 1 – 3 %. These hourly observations exhibit considerable variability, appearing as high frequency variations (Fig. 44). This variability could arise from uncertainties inherent in the current sediment fingerprinting technique. Several studies (Pulley *et al.*, 2015, Belmont *et al.*, 2014, e.g.Koiter *et al.*, 2013b) have identified issues arising from methodological assumptions and unconstrained factors connected to tracer and model selections. This limits the ability to interpret changes in suspended sediment source estimates between hourly observations, especially when source contribution changes are small.

Sediment transport mechanisms may also provide a geomorphological explanation for the observed variability. Bedload moves through the channel in pulses and waves (Nicholas *et al.*, 1995), and each pulse or wave of sediment can represent a distinct or unique combination of source sediments which may also apply to suspended sediment patterns. This provides different geochemical signatures, which incline the sediment source signals towards sporadic patterns. This has implications for achieving a desired temporal resolution, as not only is the sampling interval important, but the actual timing of the sample is important too. This study employed a one hour sample interval, which is relatively frequent considering the storm duration and the number of sediment samples collected as a result, but still may not fully capture the sediment dynamics occurring within the catchment. Sediment waves occur in different scales and require different lengths of time to move through a fluvial system, meaning that multiple superimposed patterns of variability occur within a single event, and the higher frequency sediment source contribution variations may in fact be missed altogether if the sediment waves are moving past the sample location faster than the sampling interval. The optimal time intervals required for adequate sampling warrant further consideration to reveal any patterns within the source variability and may require considerably more auxiliary information to provide better insights into sediment movement.

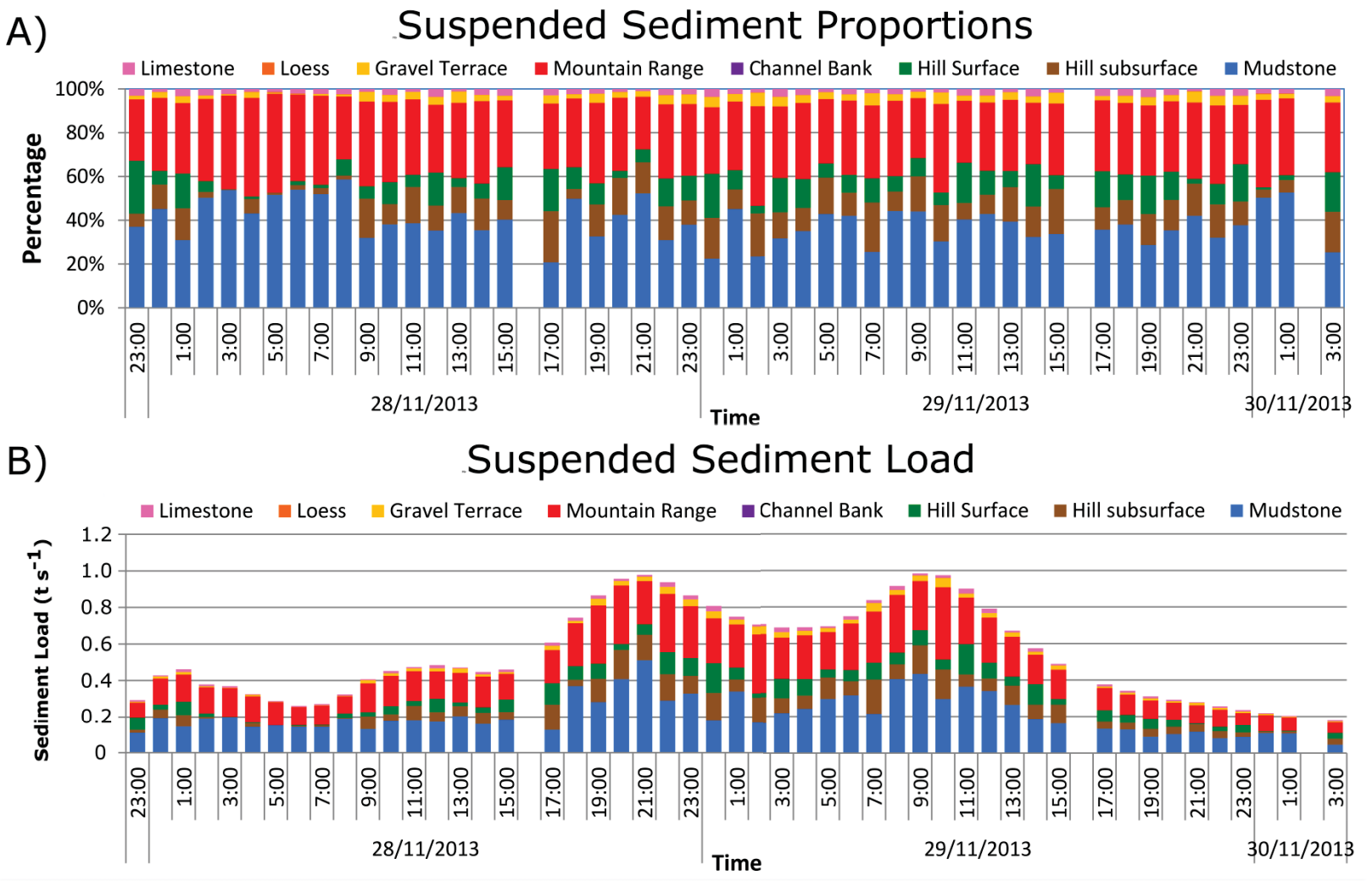

Fig. 44: *Mean hourly sediment source contributions during the storm event; percentage (top), sediment load (bottom)*

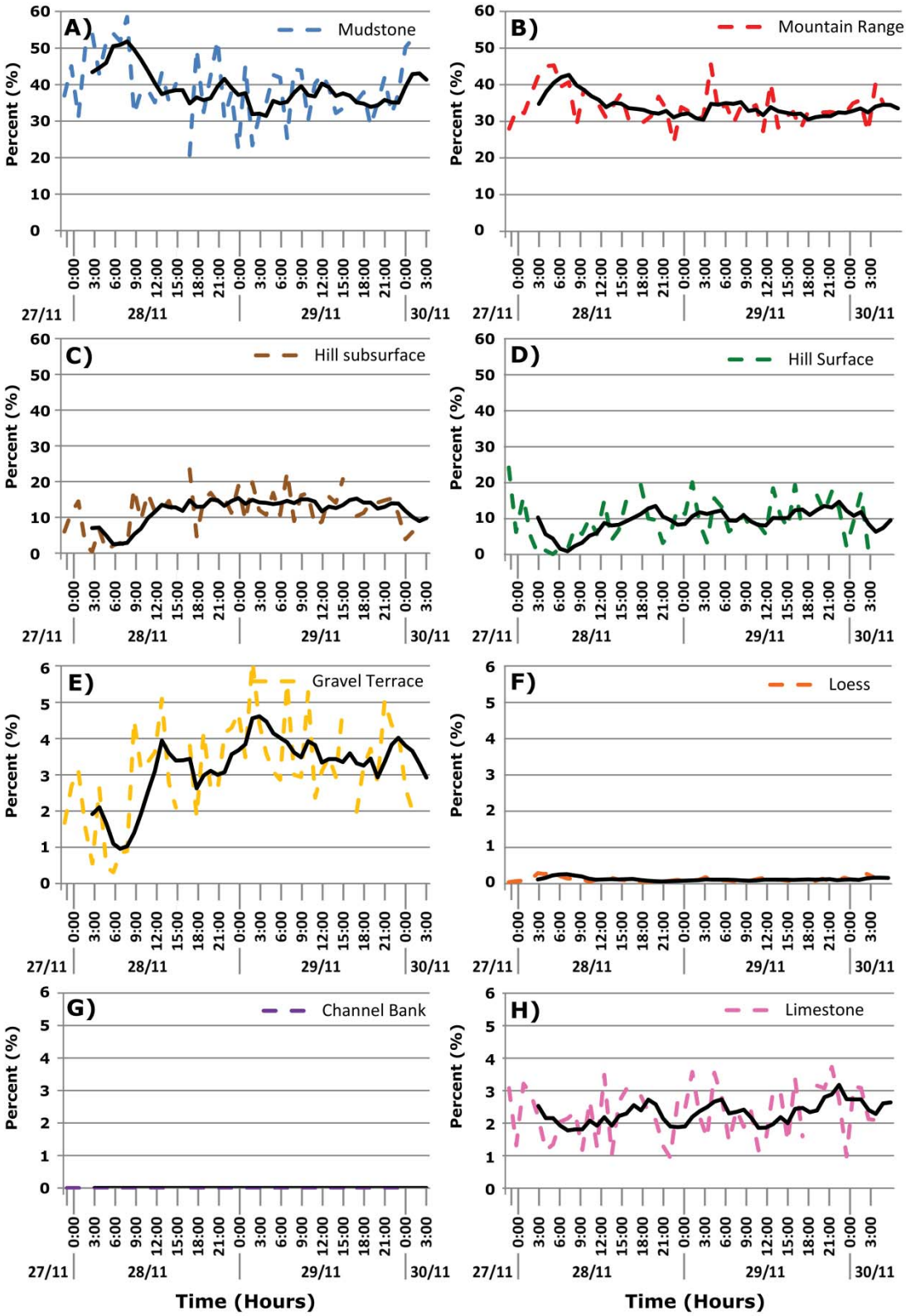

Fig 45: *Mean proportions of each sediment process throughout the storm event (dashed line) and a 5 point moving mean (bold line)*

Despite the high variability experienced between adjacent hourly samples, a moving average identifies some low-frequency patterns and switches in sediment source contributions. Five of the sources show a distinct shift occurring from the period between 2:00 and 8:00 hrs, 28th Nov, compared with the rest of the storm duration (Fig 45). Mean Mudstone source proportions were as much as ≈ 50 % between 2:00 – 8:00 hrs compared to contributions averaging closer to ≈ 40 % for the remaining duration. Similar elevated contributions between 2:00 – 8:00 hrs were also observed for Mountain Range and Loess derived sediment sources. The Mountain Range sediment exhibited contributions of ≈ 40 % in this heightened period compared to an average of ≈ 30 %, while Loess sediment almost reaches ≈ 0.4 %, compared to an average of ≈ 0.1 % throughout the remainder of the storm flow.

The inverse of this pattern is observed for Hill Subsurface, Hill Surface and Gravel Terrace, showing relatively low sediment contributions between 2:00 and 8:00 hrs, 28th Nov. Both the Hill Subsurface and Hill Surface contributions average ≈ 2.5 % compared to ≈ 13.5 % and ≈ 10 % for the remaining storm duration respectively. The Gravel Terrace contributes ≈ 1.0 % during the 2:00 – 8:00 hrs section and closer to ≈ 3.5 % sediment source contributions for the remainder of the storm duration. The Channel Bank and Limestone sediment sources do not display this pattern. In the case of the Channel Bank sediment, this is likely due to the contributions being effectively zero throughout (Fig 45).

Explanations for the difference between the 2:00 - 8:00 hrs phase and the rest of storm duration come from two factors. The first is the beginning of the shift between dominant sub-catchment flows, particularly the introduction and increase of the Upper Manawatu flow contribution (Fig. 43). This would lead to a relative decrease in flow contribution originating from the Pohangina sub-catchment and a shift in geochemical signature. However, the sedigraph shows that despite increasing flow contribution from the Upper Manawatu, the sediment load is almost exclusively still sediment originating from the Pohangina sub-catchment (Fig. 43). This indicates the changes here are less related to switches in sub-catchment flow and more likely reflect changes in suspended sediment either side of peak flow in the Pohangina sub-catchment occurring at approximately 1:00 hrs, Nov 28th (Fig. 43).

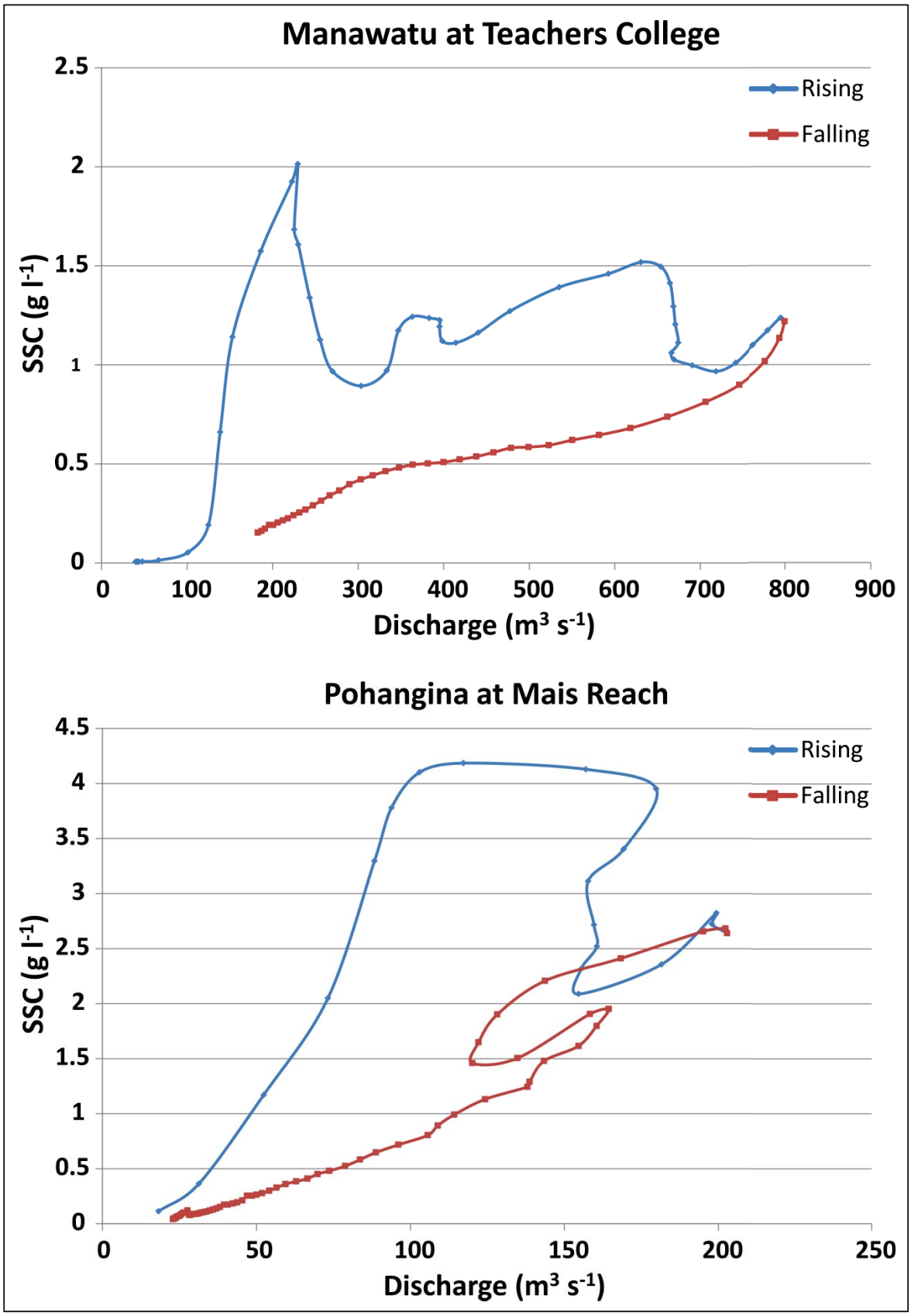

Fig 46: *Suspended Sediment Concentration (SSC) – Discharge hysteresis patterns for Manawatu River at Teachers college (top) and Pohangina at Mais Reach (bottom)*

Suspended sediment – discharge hysteresis for the Pohangina flow peak demonstrated an overall clockwise loop followed by a second counter-clockwise loop to reach the flood peak (Fig 46). Clockwise hysteresis patterns can reflect early sediment exhaustion which is often an indication of sediment sources occurring from within-channel causing an initial flushing of sediment or a significant sediment source close by (Lenzi and Marchi, 2000, Smith and Dragovich, 2009, Brasington and Richards, 2000, Klein, 1984). Alternatively, counter-clockwise hysteresis shows peak sediment concentration lags behind the flow peak. This potentially indicates a distal sediment source or the temporal difference in flood-wave celerity and mean flow velocity (Brasington and Richards, 2000, Klein, 1984, Smith and Dragovich, 2009, Lenzi and Marchi, 2000).

Thus, the initial clockwise loop in this storm indicates exhaustion of available sediment for transportation which coincides with the reduced influence of Hill Surface and Hill Subsurface sediment sources from the Pohangina sub-catchment (Fig 45, Fig. 47). It would appear that material from these two sediment sources is may be in storage within the channel, but are flushed through in the initial peak flow, while Mudstone and Mountain Range sources provide a more sustained and continuous supply of sediment throughout the storm. The Hill Surface and Hill Subsurface sediment sources reappear in the second peak flow, but this time a counter-clockwise hysteresis (Fig 46) is exhibited by a delayed sediment source arrival, reflecting the distal location and subsequent travel times of these sediment sources.

There is also an apparent shift in sediment contributions occurring towards the end of the storm event where an increase in Mudstone derived sediment occurs in the last few hours of the sampled storm event. This could be caused by similar hysteresis effects as observed for the Pohangina sub-catchment displayed in the final few hours of the Upper Manawatu sediment flow (Fig. 47), or it could be due to an increasing flow contribution from the Tiraumea River (Fig. 43) which is the last sub-catchment flow to reach the T-Col sampling station, at the end of the receding limb. The Tiraumea is strongly associated with a high mudstone composition as well as high suspended sediment concentrations (Basher *et al.*, 2012, Vale *et al.*, 2016a). In addition to the increase in Tiraumea flow reaching the T-Col site, the extent of the Mudstone proportion increase is likely enhanced by the recession of all the other major sub-catchment flows, particularly from the Upper Manawatu, allowing the Tiraumea sub-catchment sediment load to influence the source proportions more influentially.

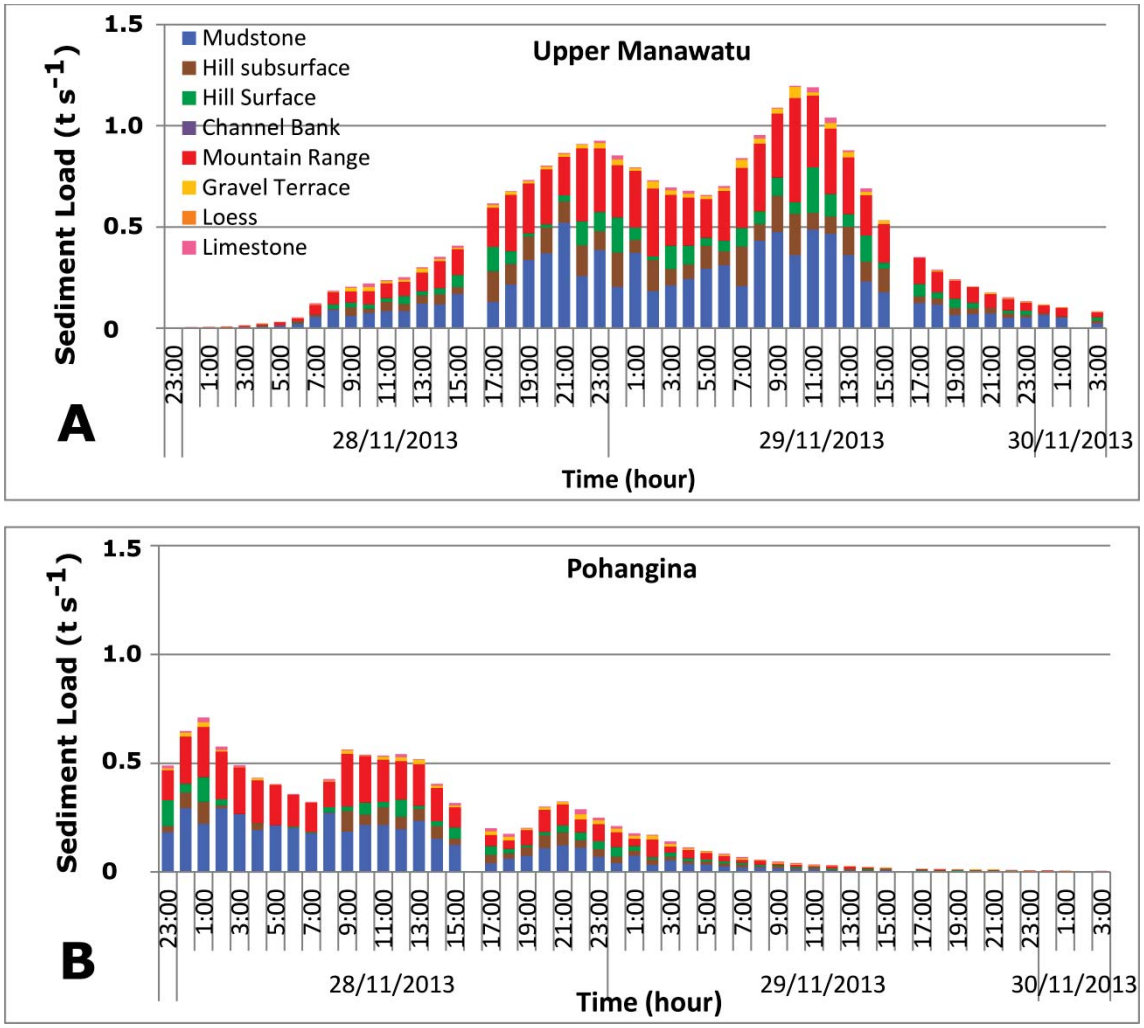

Fig. 47: *Differentiation of sediment sources from the two dominant sub-catchment flows; A) Upper Manawatu; B) Pohangina*

Regression analysis carried out in the sub-catchment sediment loads and the source proportions (Table 27). The strongest partial correlations were attributed to the Upper Manawatu and the Pohangina as these were the two most dominant sediment loads during this event. Despite controlling for each of the remaining sub-catchment sediment loads, the Mangahao, Mangatainoka and Pohangina do not display any strong partial correlations with any of the sediment sources, possibly reflecting the significantly lower sediment loads in those sub-catchments and an inability for the regression model to detect these correlations. The Upper Manawatu correlates high for all the sources except Channel Bank (0.282) and Loess (0.231), while exhibiting the greatest correlation with Mountain Range sediment (0.838). The proportion of Channel Bank sediment is effectively zero, removing any observable correlations. In addition, Vale *et al.* (2016b) identified Channel Bank sediment was the most difficult to

clearly distinguish geochemically because it is derived from other primary sediment sources, thus complicating any sediment correlations. Remobilization of in-channel fine-grained sediment also likely complicates the ability to associate storm related sediment source erosion with the suspended sediment sampled throughout the storm. The temporal and spatial pattern of sediment storage is dependent on previous storm events and processes. However an assumption is made that this stored sediment will still retain the signature of the primary erosion source during short time periods and still reflect original source locations which relate to their sub-catchments but may not be directly related to erosion from that storm. The higher partial correlations with Mountain Range sediment possibly indicate that the sources of sediment within that sub-catchment are relatively more sensitive to storm events. This would indicate the Mountain Range, Gravel Terrace, and Hill Subsurface are influenced more in the Upper Manawatu compared to the Pohangina sub-catchment where Mudstone (0.401) and Mountain Range (0.359) provide the largest partial correlation relative to Hill Surface (0.044) and Hill Subsurface (0.286), supporting the hysteresis effects observed in the Pohangina sub-catchment (Fig. 47).

Table 27: *Partial Correlations controlling for sub-catchment sediment loads derived from Regression analysis*

	Sub-catchment									
Sediment Load	**Upper Manawatu**		**Mangahao**		**Mangatainoka**		**Pohangina**		**Tiraumea**	
	Corr.	***p-value***	***Corr.***	***p-value***	***Corr.***	***p-value***	***Corr.***	***p-value***	***Corr.***	***p-value***
Mudstone	0.693	0.001	-0.199	0.184	0.187	0.214	0.401	0.006	0.092	0.544
Hill Subsurface	0.72	0.001	-0.284	0.056	0.133	0.378	0.286	0.054	0.18	0.233
Hill Surface	0.57	0.001	0.034	0.825	-0.109	0.469	0.044	0.773	0.001	0.997
Channel-bank	0.282	0.057	-0.169	0.262	0.096	0.525	0.246	0.1	0.189	0.207
Mountain Range	0.838	0.001	-0.146	0.333	0.053	0.726	0.359	0.014	-0.106	0.484
Gravel Terrace	0.748	0.001	-0.122	0.418	0.014	0.926	0.282	0.058	0.186	0.217
Loess	0.231	0.122	0.148	0.327	0.088	0.561	0.238	0.111	0.042	0.782
Limestone	0.633	0.001	-0.024	0.875	-0.101	0.503	0.042	0.782	-0.059	0.695

The differences in sediment source proportions between the Upper Manawatu and Pohangina sub-catchment are possibly attributed to disparate transport pathways between the Hill Surface/Hill Subsurface from the other remaining sediments sources. The Hillslope terrains are typically distal to the active channel, and therefore likely affected by intermittent and impeded

transport pathways. Kasai *et al.* (2005) noted, in a similar New Zealand terrain, decoupling of the channel and slopes subjected to shallow landslides can occur within 10 years, continually diminishing the average sediment yield. In contrast, sediment derived sources from Mountain Range and Mudstone have a much more direct transport pathway to enter the active channel. Additionally, a large influx of sediment from Mountain Range or Mudstone sources due to a storm event would also cause a relative reduction in contributions from the remaining source groups, specifically that of Hill Subsurface and Hill Surface sediment sources. A significant limitation is that only one storm was sampled in this study due to resource constraints, however the storm does represent a typical (but not extreme) flood event within the catchment displaying a return period of 1.3 years and was the 4th largest flood event in the Manawatu River in 2013.

5.7 Conclusion

This investigation explored the capacity for sediment fingerprinting techniques to be applied at a high temporal resolution for a large catchment. Suspended sediment samples were collected at hourly intervals for 53 hr of a storm event. High variability is observed between adjacent hourly samples which either relates to the highly variable nature of the sediment transport dynamics or the high levels of uncertainty encountered in sediment fingerprinting studies. However, general changes in the sediment source contributions were observed occurring in relation to the switching of dominant flows from the Pohangina to the Upper Manawatu sub-catchment, as well hysteresis patterns experienced within the Pohangina sub-catchment. This caused relatively higher contributions of Mountain Range and Mudstone, and lower contributions of Hill Subsurface, Hill Surface and Gravel Terrace sediment sources to occur within the first twelve hours of sampling. This may give some indication of different processes occurring in each of the two dominant sub-catchments and how they respond differently to high rainfall events. Channel Bank and Limestone sediment contributions remained low throughout the storm duration. Source contributions to each sub-catchment were modelled in order to provide information of relative inputs but are difficult to confirm actual measurements to critically compare between. Future sediment analysis needs to consider the interval at which sediment waves move downstream throughout a storm event.

5.8 Summary

Temporal fluctuations of suspended sediment sources taken at 1 hour intervals during a 53-hour storm event were investigated. Changes in sediment sources were observed throughout the event which relate to changes in sub-catchment flow and as well as storm flow hysteresis effects. This was despite encountering a high level of sporadic variability between adjacent hourly sediment samples. This high variability could arise from uncertainties and a high margin of error in the source estimation, which raises a concern regarding the individual source estimates and the level of confidence which can placed in them. The next chapter addresses the levels of uncertainty and geochemical variability encountered in the sediment sources.

Chapter 6

Sediment source variability and behaviour in the Manawatu River Catchment, New Zealand

6.1 General Introduction

Chapters 3 investigated the feasibility of applying sediment fingerprinting to a large sedimentary dominated catchment, which was then expanded in Chapter 4 to a full-scale sediment fingerprinting sampling initiative to characterize eight geomorphological sources within the Manawatu Catchment. Both of these chapters demonstrated sediment fingerprinting to be an effective tool for identifying and quantifying sediment sources in this catchment. Chapter 5 extended the technique to investigate temporal changes in sediment sources at 1-hour intervals throughout a 53-hour storm event. Chapter 6 is reproduced as: Vale SS, Fuller IC, Procter JN, & Basher LR. Sediment source variability and behaviour in the Manawatu River Catchment, New Zealand, in prep, revisits the sediment source data set to investigate the geochemical variability of individual element concentrations between and within sediment source groups and how this may influence overall uncertainty of the subsequent sediment source estimates.

6.2 Abstract

Understanding the nature of sediment movement throughout a river catchment is important to inform decision-making when assessing and managing river system health. Sediment fingerprinting is a tool used to determine and quantify the origin of sediment sources by comparing the geochemistry of suspended sediment to sediment sources within a river catchment. However, uncertainties exist in relation to the influence of geochemical variability on the ability to accurately differentiate sediment sources as well as assess the geochemical alterations occurring in the suspended sediment during transport. This research utilizes the dataset of 8 sediment sources throughout the Manawatu catchment, New Zealand, to investigate variability within the geochemical data and the changes in element concentration throughout transport of several source groups. Two thresholds based on the Standard Deviation (S.D. < 35 % and S.D. < 40 %) were applied to remove geochemical elements with a high variability. Mudstone, Hill Subsurface and Hill Surface sediment sources were submerged within the Manawatu River for 4 months to test geochemical alteration over time. Results indicate that there was considerable variation in concentrations between geochemical tracers and sediment source groups. The highest average variability was found within the Mountain Range sediment source, which had the highest average S.D. % of 39.4, followed by Gravel Terrace (S.D. % = 34.6), Loess (28.1), Hill Surface (S.D. % = 27.5), Hill Subsurface (S.D. % = 24.5), Mudstone (S.D. % = 19.6), Channel Bank (S.D. % = 18.3), and Limestone (S.D. % = 18.1). The highest variability within individual element concentrations was for transition elements such as Cu, Ni, Cr, and Mn, as well as Ca, and Tm. Mudstone sediment sources showed enrichment for most of the elements analysed, while Hill Surface sediment tended to show depletion and Hill Subsurface was relatively stable with the exception of several specific elements. A sediment mixing model was employed to estimate sediment source proportions using tracer suites that have the elements with the highest average variability removed. A threshold S.D. % < 40 was applied, resulting in the removal of Tm, Ni, Cu, and Ca while another threshold of S.D. % < 35 additionally removed P, Mn and Cr. The revised sediment source estimations using the S.D. % < 40 and S.D. % < 35 solutions produced the following values; Mudstone (59.3 % and 61.8 %) to be the dominant source followed by Mountain Range (12.0 % and 11.4 %), Hill Surface (11.5 % and 11.3 %), Gravel Terrace (7.3 % and 6.3 %), Hill Subsurface (6.6 % and 6.2 %), Loess (2.7 % and 2.7 %), and Channel Bank (effectively 0 %). These estimations showed notable differences from previous work and demonstrate the sensitivity mixing models have to changes to the specific geochemical suite.

Keywords: sediment fingerprinting; New Zealand; geochemistry variation; conservativeness

6.3 Introduction

Knowing the origin and nature of suspended sediment entering the active channel is important for understanding the patterns and causes of ongoing suspended sediment issues encountered in waterways. The effects that suspended sediment can have on waterways are well documented, particularly in regards to disturbance caused to aquatic ecosystems by altering turbidity and nutrient levels (e.g. Wood and Armitage, 1997, Calmano *et al.*, 1993). Detrimental effects associated with sediment removal from sources areas are also well identified, and mainly relate to issues of land instability and loss of agriculturally productive soils and landscapes (Owens *et al.*, 2005, Walling and Fang, 2003).

Sediment fingerprinting relies on differentiation of sediment sources in order to identify relative sediment contributions to the suspended sediment load. The technique is supported by a large body of literature which utilizes a common two-step approach, which typically involves first screening for variables with the highest discriminatory power using stepwise discriminant function analysis, and then compares the selected variables to downstream suspended sediment samples via a statistical mixing model to attain relative sediment source contribution estimates (e.g. Collins *et al.*, 1997, Walling and Amos, 1999, Smith and Blake, 2014). A considerable range of sediment tracers has been employed in sediment fingerprinting research. These tracers include; mineralogy (e.g. Eberl, 2004, Gingele and De Deckker, 2005), mineral magnetic (e.g. Caitcheon, 1998, Blake *et al.*, 2006), geochemical compositions (e.g. Collins *et al.*, 1998, Collins *et al.*, 2013, Lamba *et al.*, 2015, Hardy *et al.*, 2010, Zhang *et al.*, 2012), isotopic ratios (e.g. Douglas *et al.*, 1995, Gingele and De Deckker, 2005), radionuclides (e.g. Wilkinson *et al.*, 2013, Olley *et al.*, 2013, Porto *et al.*, 2013), organic elements(Fox and Papanicolaou, 2008a, Evrard *et al.*, 2013), and compound specific isotopes (e.g. Gibbs, 2008, Hancock and Revill, 2013, Blake *et al.*, 2012).

The technique depends on several key conceptual assumptions. Firstly, that the suspended sediment sources can be differentiated from each other by a combination of geochemical indicators; secondly, that the geochemical character of the original sediment source remains intact throughout sediment transport; and thirdly, that statistical mixing models can provide accurate estimates of sediment source contributions. Conservation of sediment geochemistry is a prevalent challenge concerning the uncertainties of geochemical behaviour during transport from 'source to sink' and the capacity of individual geochemical concentrations to be retained throughout transport. Geochemical concentrations display natural variability within and between sediment source groups. The degree of variability encountered for specific

tracers in the different sediment source groups may increase or decrease the appropriateness of that tracer to be used within sediment mixing models. Research in the Manawatu River catchment, New Zealand has shown that sediment sources in a large river system draining a largely homogenous sedimentary terrain can be discriminated by geochemistry (Vale *et al.*, 2016b, Vale *et al.*, 2016a). This paper addresses the extent to which tracer variability can have an influence on sediment source estimation by revisiting geochemical data from Vale *et al.* (2016b) and attempts to investigate the extent to which the geochemical character of the sediment sources in this catchment remain intact throughout fluvial transport by using an experimental approach designed to determine the conservativeness of Manawatu sediment geochemistry during fluvial transport.

6.4 Study Site

The Manawatu River drains a ≈ 5870 km^2 catchment situated in the lower North Island, New Zealand (Fig 48) which is underlain by sedimentary geology consisting of mudstone and sandstone. The headwaters drain the eastern flanks of an uplifted greywacke block forming the Tararua and Ruahine Ranges, before flowing west through the main drainage divide via the Manawatu Gorge, incorporating flow from the western flanks of the mountain range and continuing through to the Tasman Sea (Fig 48). Steep hillslope terrain is common throughout the eastern sub-catchments e.g. Tiraumea (Table 28), underlain primarily by soft mudstone while the middle reaches occur semi-confined due to contact with mudstone bedrock cliffs and alluvial terraces. The lower reaches flow through extensive alluvial floodplains ranging from wandering to pseudo-meandering. Many of the channels have undergone straightening and narrowing of the channel, with some transitioning to laterally-confined single thread channels as evidenced in the Pohangina River (Fuller, 2009).

Table 28: *Geological composition by sub-catchment*

Geological Material	% of area						
	Main Sub-catchment						Total Catchment
	Upper Manawatu	Tiraumea	Mangatainoka	Mangahao	Pohangina	Oroua	
Greywacke	5.9	3.1	21.2	59.0	30.9	3.4	14.6
Mudstone	22.8	63.8	29.5	7.3	2.3	-	18.5
Sandstone	24.0	3.9	0.1	0.0	44.6	27.3	14.7
Gravel	39.7	11.8	37.8	28.0	19.7	52.6	40.3
Limestone/ Coquina	7.4	11.3	6.3	5.6	-	2.6	4.8
Conglomerate	0.1	6.1	5.1	-	0.1	2.4	2.4
Sand	-	-	-	-	-	9.7	2.8
Debris	-	-	-	-	2.3	2.0	0.5

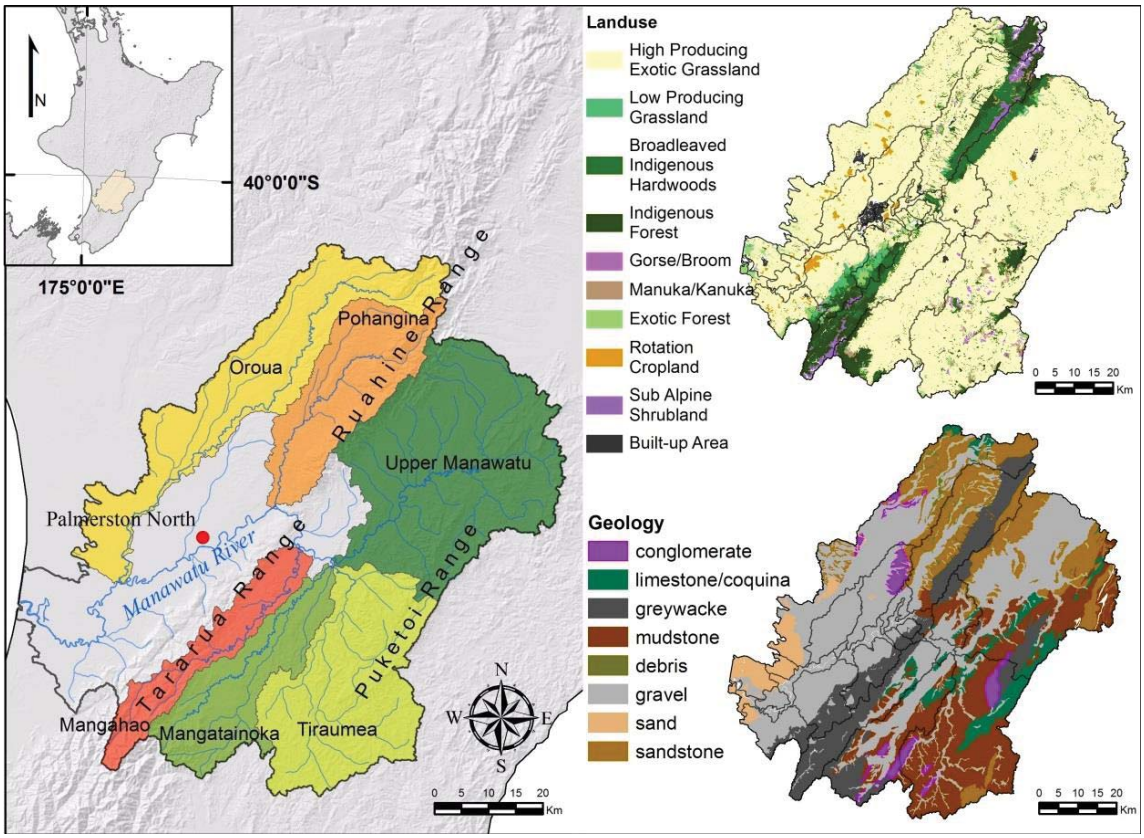

Fig 48: *Study site and sub-catchment geological composition altered from Vale et al. (2016b)*

The New Zealand Soil Classification (NZSC) after Hewitt (1998) classifies most of the Manawatu soils as Orthic/Firm Brown Soils with Allophanic Brown Soils found on the flanks of the axial range while Argillic Pallic Soils are found in the Puketoi Range along with limited Melanic Soils found in the limestone regions. Immature Pallic Soils are common throughout the eastern catchments as well as the Pohangina Perched-Gley Pallic Soils are found on the western flanks of the Tararua Range, in the lowland areas in the Oroua and north of Palmerston North (Fig 48) while recent Alluvial Soils are found on extensive floodplains proximal to the channels. Land-use in the Manawatu catchment is predominantly agricultural consisting of ≈ 75 % exotic grassland (cf. Fig 48) with sheep and beef farming occurring in the steeper terrain and dairy farming in the lowlands. Indigenous forest covers ≈ 17 % of the catchment and is mostly restricted to the Tararua, Ruahine and Puketoi Ranges, while exotic forest, mainly in the form of forestry, accounts for ≈ 3 % of catchment area. Minor pockets of mānuka and kanuka, grey scrub, and short-term rotation crops also exist in the catchment.

Mean discharge for the Manawatu River equates to c.110 $m^3 s^{-1}$ with contributions from main sub-catchments: Upper Manawatu (c. 27 $m^3 s^{-1}$), Tiraumea (c. 16 $m^3 s^{-1}$), Mangatainoka (c. 18 $m^3 s^{-1}$), Mangahao (c. 15 $m^3 s^{-1}$), Pohangina (c. 17 $m^3 s^{-1}$), and Oroua (c. 13 $m^3 s^{-1}$)(figures derived from Henderson and Diettrich, 2007).

6.5 Materials and Methods

6.5.1 Sediment Sample Collection

Sediment samples consisted of source samples collected throughout the catchment for characterization of original sediment sources, as well as sediment samples which underwent stream immersion in order to investigate geochemical changes occurring due to exposure to the aquatic environment. The sediment source samples characterized eight geomorphological sources in the Manawatu catchment (

Table 29) as in the approach of Vale *et al.* (2016b). The suspended sediment or 'sink' sample was collected using a time-integrated sediment sampler similar to Phillips *et al.* (2000). In this instance 200 mm diameter PVC pipes were used to account for the larger flow velocities (Fig 49). This sampler was placed within the Manawatu River at the Teachers College (T-Col) monitoring site for a period of 4 months (identified as 'sediment sink' in *Fig 50*.). The location of the suspended sediment sampler does omit capture of sediment from the Oroua River which accounts for an estimated ≈ 10 % of suspended sediment load from the Manawatu River (Basher *et al.*, 2012). However, the focus of this study is on the geochemical alteration of the sediment occurring through transport, rather than sediment flux *per se* so omitting the Oroua flow is not considered to be an important factor.

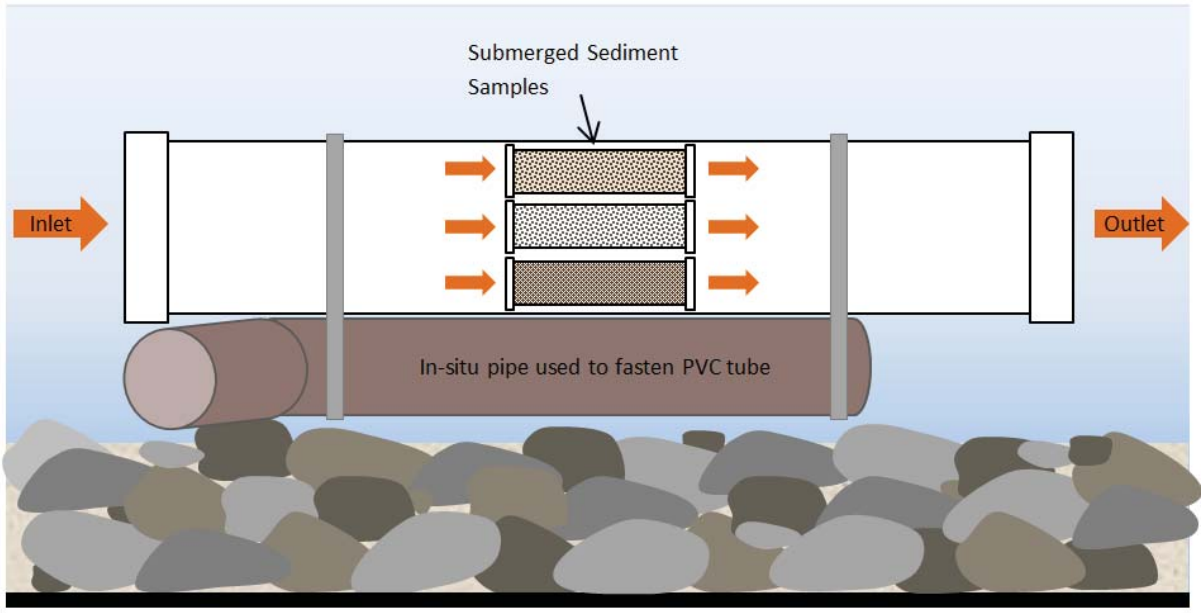

Fig 49: *Time integrated suspended sediment sampler and submerged sediment tube housing.*

In order to test the conservation of sediment geochemistry for individual elements, samples of Mudstone, Hill Surface, and Hill Subsurface sediment were placed within polypropylene screwcap containers, with both ends replaced with 1 µm sized mesh on each end to allow water to pass through while retaining sediment with grain size > 1 µm. Three PVC pipes were used to house 5 samples of each sediment source (Fig 49) and submerged within the Manawatu River for a period of 4 months to allow stream water to pass through the sediment sample. This approach is a simplified simulation and is not able to account for the range of conditions experienced throughout sediment transport. In some situations when sediment is intermittently retained in the channel bed the conditions may be reducing and conversely having sediment submerged in the water column continuously may expose the sediment to more oxygenated conditions.

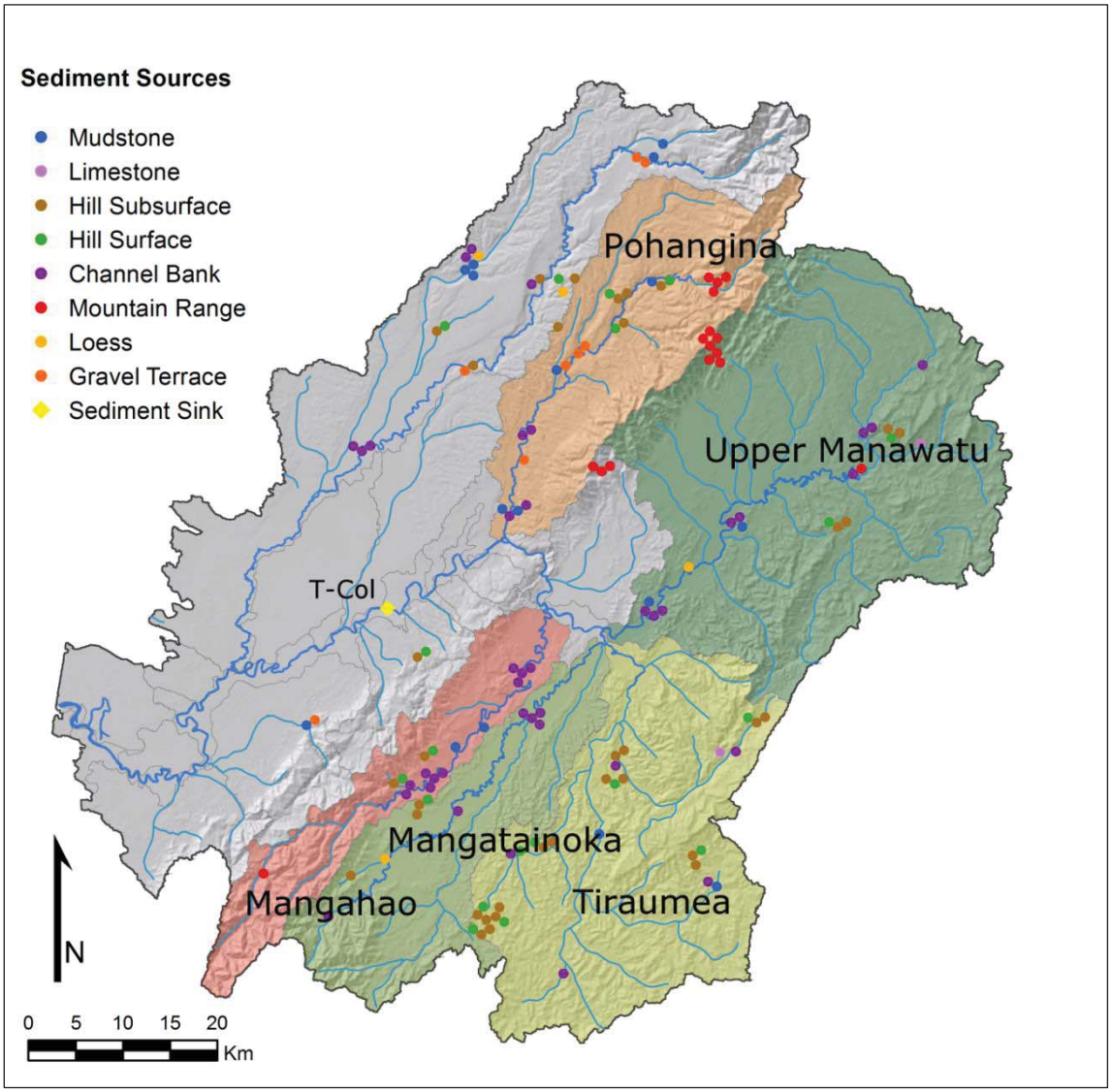

Fig 50: *Manawatu River Catchment showing spatial distribution of the sediment sources and location of the sediment sink. Shaded areas indicate sub-catchments as marked.*

Table 29: *Sediment source characteristics adapted from Vale et al. (2016b)*

Mudstone Mudstone samples were taken throughout the catchment typically from exposed mudstone cliffs. Due to safety limitations, sampling consisted of grab samples taken from sediment deposits at the foot of the cliffs. This represents the most readily available sediment entering the channel.		**Mountain Range** Mountain Range Sediment was sampled from the Ruahine and Tararua Range to target landslide and debris avalanche material originating from the greywacke dominated terrain.	
Hill Subsurface Hill Subsurface samples were taken from subsurface scrapings typically consisting of the B horizon (but not bedrock material) of the steeper hill country terrain to represent a proxy for shallow translational landslide material.		**Loess** Unconsolidated material mostly in the form of loess was sampled both from cliff material as well as some horizons in bank sediment.	
Hill Surface Hill Surface samples were taken from the upper 4 cm of the steeper hill country terrain to represent surface material originating from the steep slopes.		**Gravel Terrace** Alluvial gravel terraces were sampled from exposures found throughout the catchment typically next to the active channel forming part of the bank or cliff sequence.	
Channel Bank Samples were collected from scrapes of subsurface sediment channel banks proximate to active channel erosion. Multiple subsurface samples were taken if there were multiple subsurface horizons.		**Limestone** Isolated limestone deposits were sampled as grab samples to represent a limestone signature.	

6.5.2 Sample Preparation & Analysis

Source sediment samples were duplicated from Vale *et al.* (2016b) whereby sampling consisted of 5-10 samples taken to form a composite sample for the sediment source at each specific location. Surface sediment samples were taken from the top 4 cm of material, while the remaining source samples were taken at various depths depending where that source material lay within the sample profile. This was also applied to the submerged sediment samples. Sample preparation involved drying at 40°C, light disaggregation and sieving to retain the < 63 µm size fraction. Samples where then weighed into crucibles for XRF analysis and combusted at 850°C overnight to oxidize all elements and combust any organic material. 2 g of sample was then mixed with 6 g of lithium tetraborate and fused into glass discs. The glass discs were analysed using a Panalytical Axios 1kW X-ray Fluorescence Spectrometer for SiO_2, TiO_2, Al_2O_3, Fe_2O_3, MnO, MgO, CaO, Na_2O, K_2O, P_2O_5, Ba, Rb, Sr, Zr, Nb, Y,V, Cr, and Ni concentrations. The glass discs were retained and also analysed using an Agilent 7700 Series Inductively Coupled Plasma-Mass Spectra with an attached Laser Ablation unit (LA-ICP-MS). LA-ICP-MS elements analysed included Sc, V, Cr, Co, Ni, Cu, Zn, Ga, Rb, Sr,Y, Zr, Nb, Cs, Ba, La, Ce, Pr, Nd, Sm, Eu, Gd, Tb, Dy, Ho, Er, Tm, Yb, Lu, Hf, Ta, Pb, Th, U. XRF data was given preference over LA-ICP-MS values where elements were analysed using both systems because the XRF values provided more consistent results.

6.5.3 Geochemical Analysis

Geochemical analysis focused on assessing the geochemical variability encountered within sediment source group classifications. This variability was measured using standard deviation expressed as a percentage (S.D. %) and was calculated for each element within each source group. This approach was adopted primarily to focus on individual tracer variability for each source group independently from one another.

Further geochemical indicators were derived to guide statistical analysis and represent the data. Multi-element diagrams were constructed for Major, Trace and Rare Earth Elements (REE's) to represent geochemical trends for each sediment source expressed as both means as well as minimum and maximum values. Upper Continental Crust (UCC) values, after McLennan (2001) but revised from Taylor and McLennan (1985), were used for normalization of the major and trace element diagrams. REE's were normalized using average CI chondrite values from McDonough and Sun (1995). Post-Archean Australian Shale (PAAS) values after McLennan (2001) were also plotted for reference. Diagrams were constructed using *PetroGraph* from Petrelli *et al.* (2005). Chemical Index of Alteration (CIA), Index of

Compositional Variability (ICV), K_2O/Al_2O_3, Eu/Eu* , Zr/Sc, Th/Sc, and $(La/Yb)_N$ values for this data were also obtained for reference from Vale *et al.* (2016b).

6.5.4 Statistical Discrimination

Analysis of the sediment fingerprinting data involves several statistical approaches following the traditional approach after Collins *et al.* (1998) which employs a two-step approach to select appropriate tracers. The first step typically explores the ability of an individual tracer to discriminate between sediment sources using non-parametric tests such as Kruskal-Wallis. The second stage seeks to select the best suite of variables in order to provide adequate differentiation. This is achieved using multivariate stepwise discriminant function analysis through the minimization of Wilk's Lambda. Because of the relatively high number of source groups coupled with the unique geochemistry of the limestone source group, the Kruskal-Wallis step provides negligible benefit (Vale *et al.*, 2016b), hence it is not used in this instance. Instead, an initial screening, based on the S.D. %, is implemented to directly remove variables which display high variability. This is based on the objective to provide the best discrimination of sources, so that variables with lower S.D. % provide more stable and clear representations of the source group and are less likely to overlap with the mean distributions of other sources.

Two thresholds for the S.D. % were utilized to compare the effects of removing specific tracers with each other, as well as with the results presented in Vale *et al.* (2016b). The two thresholds used for the S.D % were 40 % and 35 %, whereby elements were removed if they displayed S.D. % values in excess of these limits. The levels were partly influenced by the number of variables removed from the solution whereby dropping below a S.D. = 35 % removed too many variables. This produced a < 40 % and a < 35 % solution. Discriminant function analysis was undertaken using SPSS (IBM Corp., 2012) and the stepwise discriminant analysis based on the minimization of Wilks' Lambda function. Default values of 3.84 (probability = 0.5) and 2.71 (probability = 0.1) are used for F to enter and F to remove respectively.

6.5.5 Multivariate Mixing Model

The elements selected from the discriminant function analysis in decreasing order of significance were SrO, SiO_2 MgO, Al_2O_3, P_2O_5, Cs, ZrO_2, Na_2O, Fe_2O_3, MnO, U, Pb, and Lu for the < 40 % solution, and SrO, SiO_2 Sm, MgO, Al_2O_3, Cs, ZrO_2, Na_2O, Fe_2O_3, U, and Pb for the < 35 % solution. These elements were incorporated into the multivariate mixing model following the approach outlined by Collins *et al.* (1997), which employs a Monte Carlo repeat sampling approach to produce calculated values based on the mean and standard deviation of each

source group. The relative proportions of each source group are estimated through minimizing the sum of the residual (objective) equations which relate source proportions and individual variable values to the sediment sink sample.

The mixing model is illustrated in Eq. 21:

$$R_{es} = \sum_{i=1}^{n} \left(\frac{C_i - \sum_{j=1}^{m} X_j \bar{S}_{ij}}{C_i} \right)^2 \quad \text{(Eq. 21)}$$

R_{es} = the sum of squares of the residuals
n = the number elements in the composite fingerprint (e.g. P_2O_5)
C_i = the concentration of element (i) in the sediment sink sample
m = the number of source groups (e.g., mudstone, hill surface etc.)
X_i = the relative proportion from source group (j) to the sediment sink sample
$\bar{S}_{ij}$ = the mean concentration of element (i) from the sample in source group (j)

The model adheres to two constraints that must be satisfied to produce realistic values; the first constrains each source group proportion to being a positive value between 0 and 1, i.e.

$$0 \leq P_i \leq 1 \quad \text{(Eq. 22)}$$

The second constraints the sum of all source group contributions to being equal to 1, i.e.

$$\sum_{i=1}^{n} P_i = 1 \quad \text{(Eq. 23)}$$

The optimization of these models was conducted using the solver extension on Microsoft Excel and expanded on from an initial spreadsheet arrangement after Roddy (2010). The 'Generalized Reduced Gradient (GRG) Nonlinear' method was employed using the multi-start parameter which automatically runs repeated iterations using different random starting values for the decision variables, thereby providing a selection of locally optimal solutions of which the best can be selected as a globally optimal solution.

6.6 Results and Discussion

6.6.1. Geochemical Analysis

6.6.1.1. Sediment Source Group Variability

Identification of geochemical variability is important to understand the nature of the tracers being used to differentiate the sediment sources and understand if the high variability of specific tracers have implications on sediment source estimation. Revisiting and analysing the Vale *et al.* (2016b) dataset revealed that geochemical variability varied both between

sediment source groups, as well as between individual geochemical concentrations. The Mountain Range sediment source displayed the greatest geochemical variability, exhibiting an average S.D. % of 39.4 % which is visually seen as the large range between maximum and minimum values (Fig 51, Fig 52, and Fig 53). This is followed by Gravel Terrace (mean S.D. % = 34.6) and Loess (mean S.D. % = 28.1) displaying large variations. These values are in contrast to Limestone, Channel Bank, and Mudstone sediment sources which display mean S.D. % of 18.1, 18.3 and 19.6 respectively. Sediment source group variability can be caused by inherent variation in the geological origin, combined with subsequent geochemical alteration due to changes in the chemical environment to which sediment is subjected during transport and over time. It is difficult to know the exact cause or combination of causes actually responsible for the observed variability encountered in these sediment source groups without additional information. Thus, it raises challenges for interpreting the observed geochemical signals and the extent weathering has on sediment geochemistry conservation and the ability to accurately classify sediment source groups.

6.6.1.1. Sediment Source Group Interpretation

The Mountain Range sediment originates from the greywacke range within a very active physical weathering environment giving rise to immature soils and a range of sediment at different weathering stages. The largest individual geochemical range occurs for Copper (Cu) concentrations expressed by a S.D. % of 102.5. This high variability can be attributed to areas of the Ruahine and Tararua Ranges which contain high metal concentration deposits. One particular site is located within an area known as Coppermine Creek and was historically prospected for development of a commercial copper mine. Similar trends are observed with other transition elements such as Nickel (Ni) and Chromium (Cr).

Greater geochemical variability encountered in the Gravel Terrace sediment sources and to a lesser extent in the Loess sediment sources can be attributed to several geochemical features. The first feature relates to Zirconium (Zr) and Hafnium (Hf) concentrations which display significant enrichment in these deposited alluvial sources. Zr and Hf are typically associated with the mineral zircon, which possesses relatively high resistance towards weathering which can result in Zr and Hf enrichment. The higher variability of Zr and Hf encountered appears to occur in sediment sources which have been subject to fluvial (e.g. Gravel Terrace) or aeolian (e.g. Loess) forming processes. This indicates that processes may have contributed to sediment recycling between these sediment sources and is sufficient enough to produce unique sediment source groups compared to primary sediment sources.

Table 30: *Comparison of Mean and S.D % (underlain with bar graph representations) for analysed geochemical elements of each sediment source group*

	Mudstone		Hill Subsurface		Hill Surface		Channel Bank		Mountain Range		Gravel Terrace		Loess		Limestone	
	Mean	S.D. %	Mean	S.D. %	Mean	S.D. %	Mean	S.D. %	Mean	S.D. %	Mean	S.D. %	Mean	S.D. %	Mean	S.D. %
SiO_2 (%)	70.6	4.7	71.8	3.5	74.1	3.3	71.8	3.4	63.0	11.2	66.4	7.4	68.9	4.0	34.1	20.3
Al_2O_3(%)	14.9	8.0	15.5	7.7	14.2	6.5	14.9	10.3	19.4	15.2	17.4	21.1	15.9	8.9	5.9	17.7
Fe_2O_3(%)	4.1	23.7	4.2	21.7	3.6	20.0	3.9	18.3	6.3	39.6	6.4	21.1	5.7	43.5	2.9	10.4
MgO (%)	1.4	31.0	1.1	33.1	0.9	25.5	1.2	18.4	2.0	67.7	1.2	24.2	1.2	26.1	1.1	36.6
P_2O_5 (%)	0.1	35.9	0.1	44.4	0.2	42.8	0.1	20.0	0.2	54.2	0.2	18.0	0.2	48.4	0.1	24.4
MnO (%)	0.0	23.7	0.0	26.9	0.1	27.3	0.1	20.5	0.1	87.0	0.1	25.2	0.1	35.5	0.0	60.6
CaO (%)	2.0	38.8	1.1	38.1	1.2	28.6	1.4	31.8	1.2	70.0	1.1	81.3	1.7	46.5	53.1	17.3
Na_2O(%)	3.3	11.1	3.1	10.4	3.1	11.3	3.3	7.4	2.6	12.3	2.8	23.8	3.1	11.1	1.2	17.6
K_2O (%)	2.4	21.0	2.0	21.7	1.7	23.3	2.3	18.9	3.5	29.2	2.4	36.5	2.2	10.4	1.1	33.9
TiO_2 (%)	0.6	11.5	0.6	15.4	0.5	15.9	0.6	15.3	1.0	45.7	0.9	20.0	0.7	8.9	0.3	13.3
V_2O_5 (ppm)	149.3	20.7	158.4	18.4	147.4	18.6	144.5	17.6	228.5	26.8	190.5	20.4	172.4	12.7	71.5	11.0
Cr_2O_3(ppm)	78.6	15.4	81.5	20.1	89.8	84.6	81.7	11.7	104.2	70.6	87.3	18.9	99.0	30.6	28.0	36.1
Rb_2O(ppm)	109.3	24.1	99.3	19.7	87.0	23.3	103.7	22.2	167.3	33.0	110.9	41.2	102.1	15.8	44.3	28.5
Nb_2O_5(ppm)	16.5	10.7	15.6	14.2	13.6	18.6	20.4	21.2	25.6	29.0	23.9	18.6	23.0	23.6	4.4	10.2
SrO (ppm)	345.0	14.0	295.2	13.7	289.8	13.6	318.9	16.0	218.7	25.4	272.7	43.1	337.1	19.8	1707.7	39.0
Y_2O_3 (ppm)	32.8	7.7	25.0	22.2	20.5	20.9	31.5	15.8	42.1	25.8	40.4	24.8	39.7	20.8	18.2	23.8
ZrO_2 (ppm)	478.5	27.8	502.0	29.4	492.0	29.9	768.6	28.8	543.9	29.4	688.1	54.5	776.9	43.8	160.6	14.4
CoO (ppm)	14.7	51.4	12.7	28.8	10.3	25.7	13.2	26.3	26.7	46.6	26.5	49.8	17.8	29.4	12.9	6.6
NiO (ppm)	25.1	37.7	21.7	35.3	30.0	194.4	21.9	27.4	44.6	134.3	27.7	29.5	26.9	31.8	24.3	12.0
BaO (ppm)	539.9	12.6	516.9	13.3	477.6	14.5	570.8	13.0	856.7	47.4	575.4	23.4	537.8	11.1	230.0	25.0
Sc (ppm)	11.9	12.4	9.8	17.9	8.6	12.4	10.6	8.7	14.3	34.3	12.8	20.2	14.4	28.5	6.4	3.2
Cu (ppm)	7.3	42.2	6.5	47.9	7.5	34.1	7.7	33.4	19.5	102.5	9.8	20.4	7.7	39.6	8.7	33.5
Zn (ppm)	49.1	27.8	37.7	24.2	38.8	18.7	43.3	18.1	71.9	28.4	44.8	9.6	56.8	47.3	26.8	21.3
Ga (ppm)	13.9	18.9	12.2	17.8	11.5	11.6	12.5	12.4	18.4	22.8	13.0	9.6	15.6	35.1	6.3	14.9
Cs (ppm)	4.0	38.0	3.2	24.9	2.8	17.9	3.4	26.7	8.9	38.8	3.3	36.2	4.0	60.0	1.5	32.1
La (ppm)	27.3	18.4	17.9	45.6	15.8	27.0	23.6	13.7	26.4	24.2	24.8	29.2	34.8	25.7	21.5	7.3
Ce (ppm)	53.5	11.3	37.6	24.4	31.5	25.3	49.3	14.0	70.8	23.9	133.0	89.2	72.7	28.4	38.2	24.4
Pr (ppm)	6.0	11.1	3.8	27.0	3.3	26.8	5.4	13.1	6.3	27.2	5.7	32.9	8.0	24.8	4.7	15.4
Nd (ppm)	23.8	10.7	14.8	27.4	12.8	27.7	21.1	13.2	25.2	28.7	21.9	35.2	31.3	25.2	19.4	12.3
Sm (ppm)	4.8	12.8	2.9	28.0	2.4	28.5	4.1	14.2	5.0	29.9	4.5	35.0	6.1	23.3	3.6	15.9
Eu (ppm)	1.0	9.7	0.6	27.9	0.5	24.5	0.8	10.6	1.1	37.7	0.9	30.9	1.2	23.7	0.8	4.4
Gd (ppm)	3.9	10.9	2.3	27.2	1.9	27.6	3.4	14.0	4.3	33.6	3.7	32.2	5.0	24.5	3.0	3.3
Tb (ppm)	0.6	10.7	0.4	27.4	0.3	26.2	0.5	13.4	0.7	31.2	0.6	30.1	0.8	26.6	0.5	1.5
Dy (ppm)	3.7	11.0	2.3	25.9	2.0	27.0	3.3	13.2	4.3	30.5	3.6	32.8	4.6	22.6	2.7	1.5
Ho (ppm)	0.7	9.0	0.5	23.5	0.4	24.2	0.7	13.1	0.8	27.4	0.7	35.0	0.9	24.3	0.5	5.5
Er (ppm)	2.1	9.8	1.4	23.1	1.2	20.6	2.0	12.7	2.5	27.7	2.1	34.9	2.7	21.1	1.5	7.2
Tm (ppm)	0.4	65.5	0.1	58.3	0.1	57.5	0.2	76.0	0.3	95.7	0.1	139.0	0.3	66.9	0.2	0.0
Yb (ppm)	2.2	8.0	1.5	19.6	1.4	18.9	2.2	13.7	2.5	23.3	2.2	41.6	2.7	20.1	1.4	4.7
Lu (ppm)	0.3	7.2	0.2	18.8	0.2	17.3	0.3	13.9	0.4	18.3	0.3	41.2	0.4	19.1	0.2	12.1
Hf (ppm)	7.6	24.1	6.8	31.5	6.9	31.9	11.2	30.5	7.9	22.9	9.6	75.2	12.1	40.4	2.8	18.5
Ta (ppm)	0.7	14.2	0.5	17.4	0.4	18.6	0.6	16.7	0.9	36.1	0.6	19.4	0.8	30.2	0.3	24.4
Pb (ppm)	13.5	22.3	10.2	19.9	9.3	11.5	11.4	17.8	21.8	31.1	18.5	36.4	16.3	34.7	10.4	27.2
Th (ppm)	9.6	13.5	7.2	18.5	6.0	16.1	8.6	16.2	11.8	29.0	10.1	22.1	12.0	26.6	5.1	13.6
U (ppm)	2.5	13.3	2.0	13.8	1.9	10.2	2.4	12.0	2.7	26.3	2.5	31.2	3.1	34.2	2.0	35.4
Average		**19.6**		**24.4**		**27.5**		**18.3**		**39.4**		**34.6**		**28.1**		**18.1**

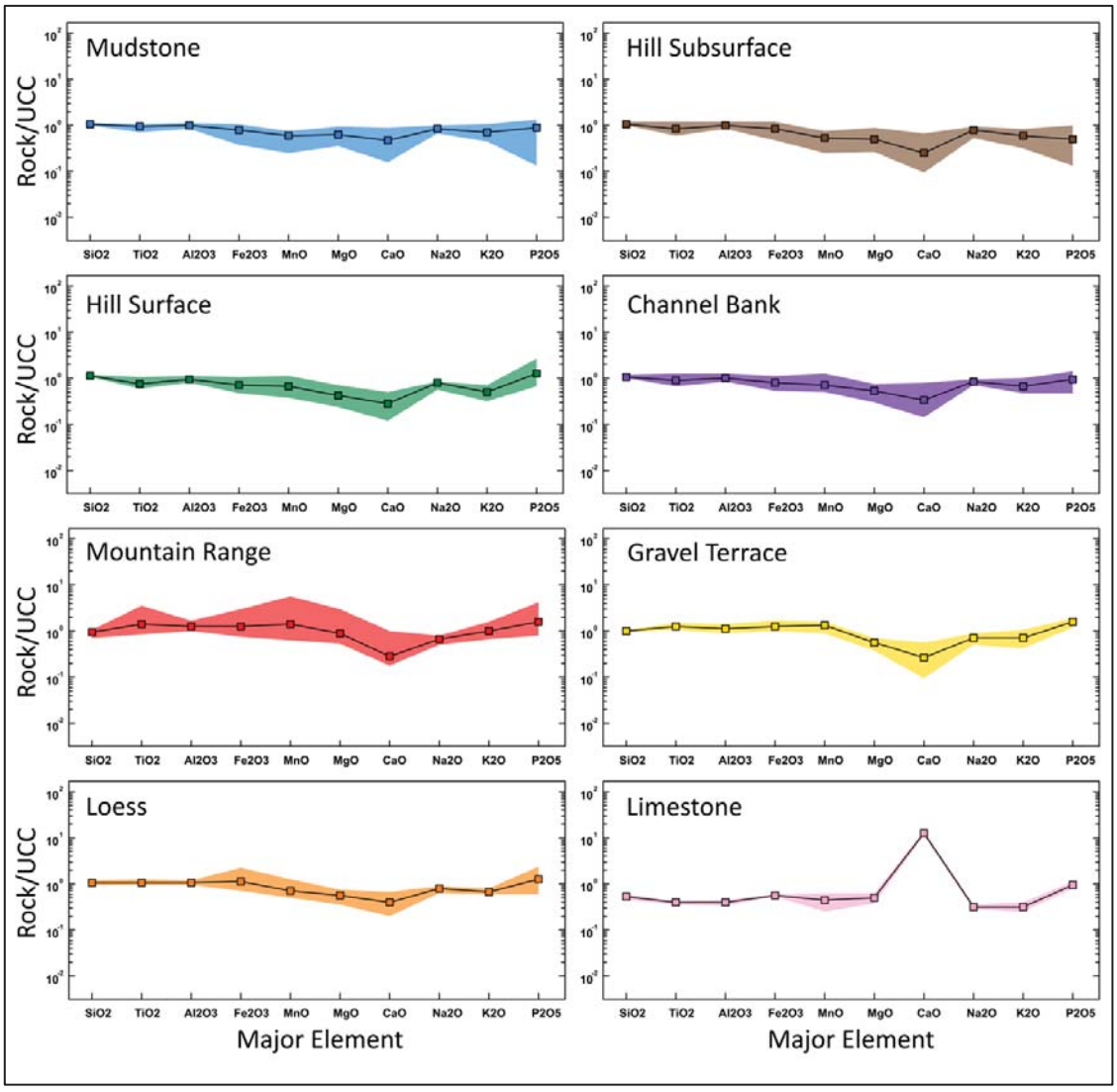

Fig 51: *Mean major geochemistry for each sediment source group with range displayed through shading.*

Limestone, Channel Bank and Mudstone have noticeably lower overall geochemical variability with a mean S.D. % of 18.1, 18.3 and 19.6 respectively. Lower variability in Limestone is due to its unique geochemistry which is dominated by Calcium (Ca) rather than Silicon (Si). This results in lower concentrations of many minor geochemical elements and subsequently lower inherent variability. The exception for Limestone is Ca itself, in addition to similar group elements Mg and Sr, which display higher variability between different Limestone sources.

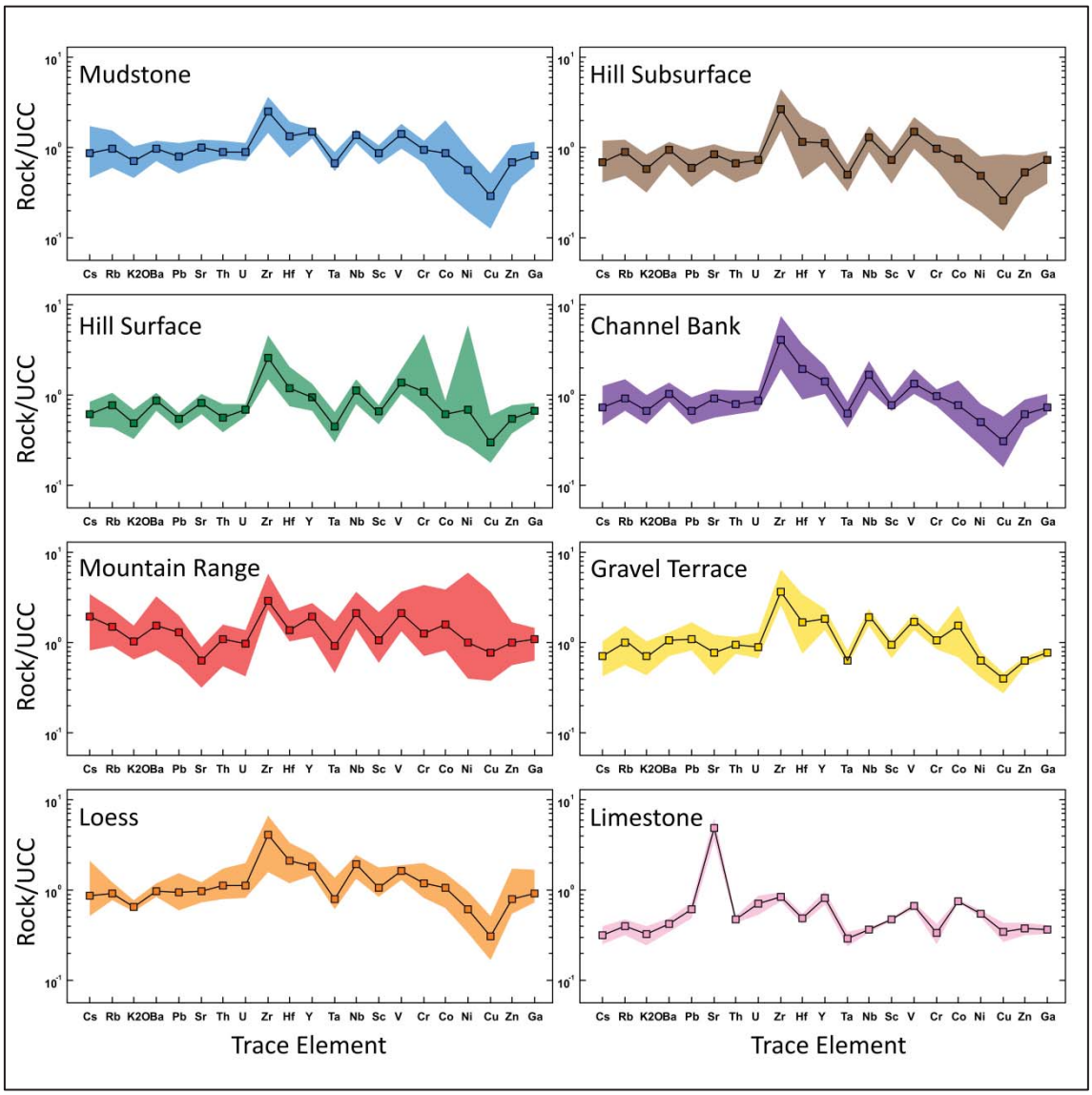

Fig 52: *Mean minor geochemistry for each sediment source group with range displayed through shading*

Channel Bank sediment originates from deposition of fluvial sediment during overbank flow, and although the Gravel Terrace sediment also occurs from fluvial processes, Channel Bank sediment is both composed of younger and finer sediment. Wilkinson *et al.* (2013) identified the tributary sediment from within the channel as being less-variable than catchment soil and sediment sources. This likely arises due to two processes acting on the sediment. The first process is from the sediment being subjected to aquatic geochemical weathering environments whereby the most susceptible elements are leached away upon entering the active channel. The second process likely occurs from homogenisation of geochemical signatures through mixing occurring within the sediment transport process.

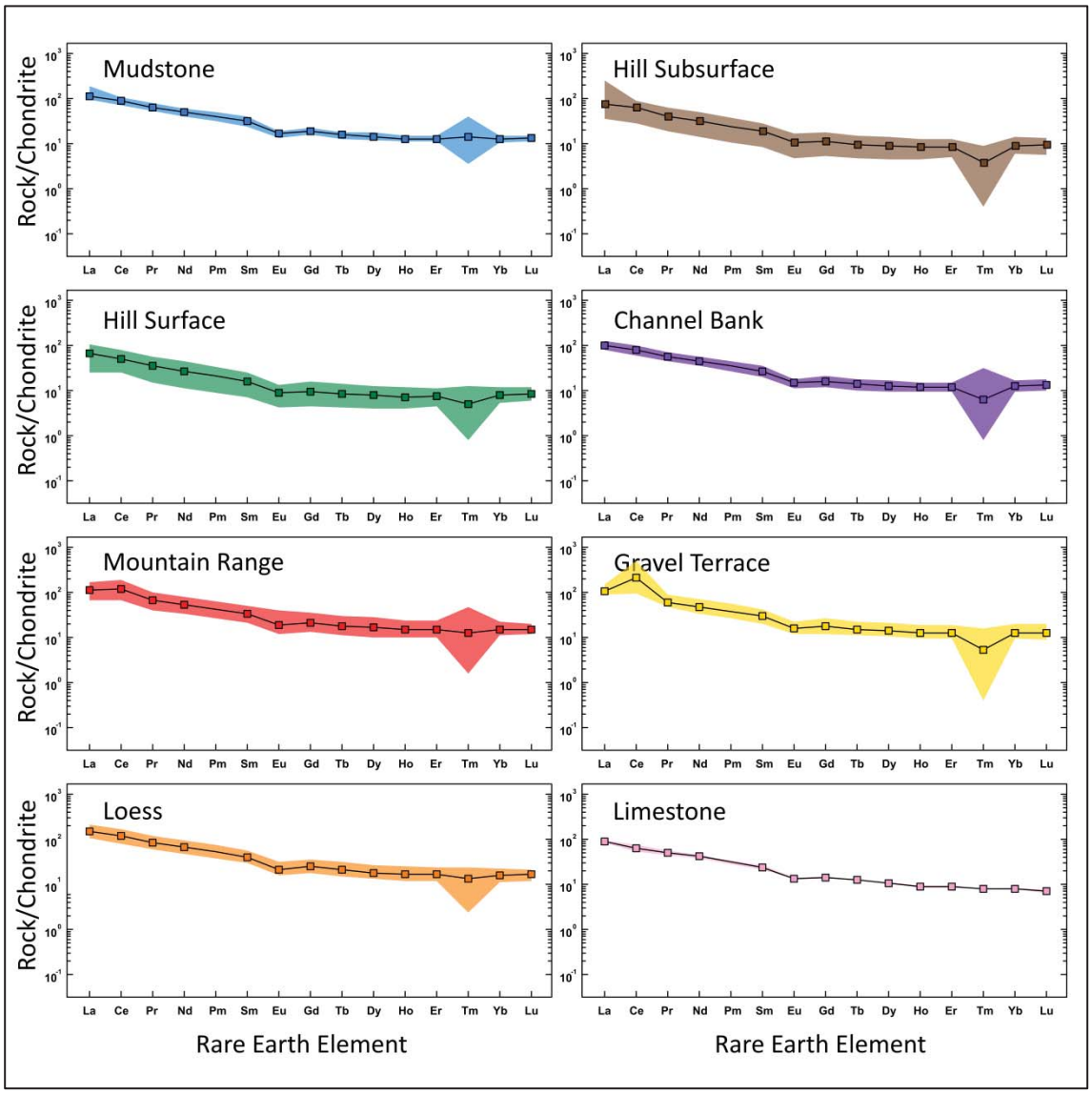

Fig 53: *Mean REE geochemistry for each sediment source group with range displayed through shading*

Mudstone represents a fine grained clay-silt sized sedimentary material and displays a visibly lower geochemical variability. This variability reflects the original sediment production processes, as well as the transport and depositional processes which produced the mudstone deposits. Despite the Mudstone sediment source occurring throughout the entire catchment, it appears to possess comparable geochemistry throughout when compared to the variability within other sediment sources. This is advantageous for characterizing mudstone derived sediment sources from other sediment sources in the catchment, however it is problematic for differentiating between spatially separated mudstone sediment sources located within different sub-catchments.

Rare earth elements typically displayed the lowest variation within each of the source groups (Fig 53; Table 30). This is most noticeable within the mudstone sediment source where S.D. % for REE is ≈ 10 %, whereas the remaining major and minor elements typically feature S.D. % values between ≈ 20 % and ≈ 30 %. This reaffirms the value of REEs as important (and stable) tracers in sediment fingerprinting. The main exception within the REE is Tm, which showed an inconsistent and typically depleted concentration relative to the other REE values and a S.D. % of ≈ 65 %. Values between 57.5 – 139.0 % are experienced for REEs in the remaining sediment sources with the exception of Limestone, which had an S.D. % of zero due to the low sample numbers. Transition elements, such as Ni, Cr, Co and Cu, show significant variations within Mountain Range and Hill Surface source sediments. The most extreme of the transition elements is Ni with S.D. % of 194.4 % for Hill Surface and 134.3 % respectively (Table 30).

6.6.1.2. Geochemical Enrichment and Depletion

Samples from three sediment source groups were submerged within the Manawatu River for 4 months and compared geochemically to the original samples (Fig 54). Mudstone sediment sources showed enrichment for most of the elements analysed, most visibly for Co and Cu concentrations while another transition element, Ni, shows dramatic depletion (Fig 54). It is possible one of the explanations for the enrichment relates to the severity of the shift in geochemical environments which occurs upon the in-situ mudstone entering the river channel. It appears that changes occurring at this interface represent a significant unknown, which requires further research to understand implications for sediment fingerprinting.

Hill Subsurface and Hill surface sediment display variability in-between the mean S.D. % of 24.5 and 27.5 respectively. The Hill Subsurface tended to show higher variability within major element concentrations, particularly noticeable within CaO and P_2O_5 concentrations. This pattern continues for minor and transition elements, with the exception of Cr_2O_3 and NiO concentrations which display considerable range within the Hill Surface sediments. The Hill Subsurface sediments also appeared to be the most geochemically stable during submersion, with most elements showing little to no change in concentration (Fig 54). Tm shows the most depletion, followed by Co and Ca, and La shows high levels of enrichment. The relatively stable character of the sediment is assumed to be due to extensive weathering having already occurred in formation of minerals in the subsurface soil horizon. This would cause the most unstable minerals and elements to have already been removed from the sediment. The Hill Surface sediment sample appears to show stable concentrations for the major elements, but

depletion in the transition and REE elements whereby concentrations is underestimated. However, individual samples which comprise the average for Hill Surface do not show this trend and it may in fact be an artefact and only produced upon averaging the data (Fig 54).

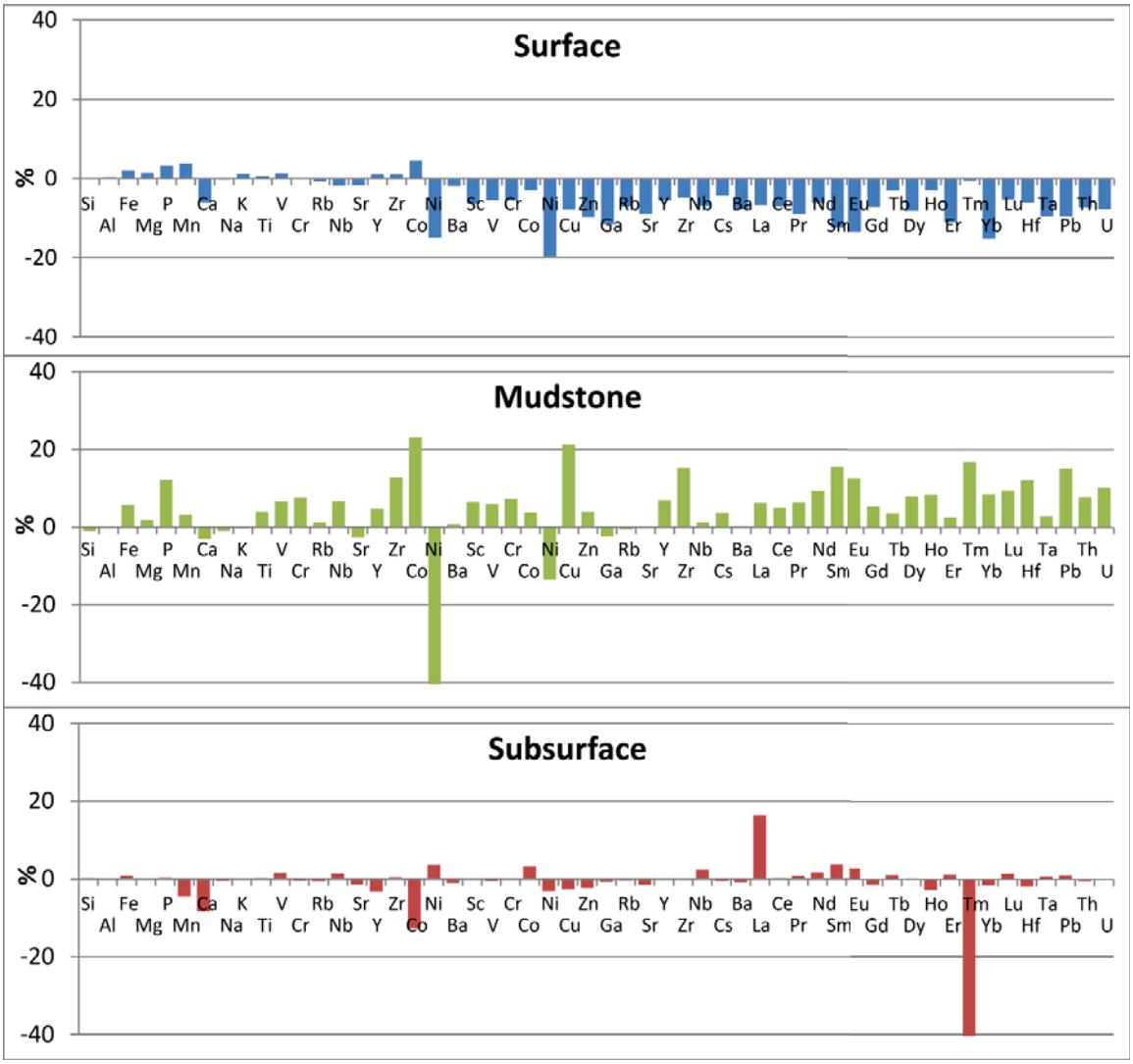

Fig 54: *Percentage change of each element after extended exposure to river environment for Hill Surface, Hill Subsurface and Mudstone sediment sources*

6.6.2. Statistical Differentiation

Two geochemical tracer suites were derived in order to compare with each other as well as against the original data set published by Vale *et al.* (2016b). The S.D. < 40 % (Table 30) resulted in the removal of Tm (S.D. % ≈ 69.9), NiO (S.D. % ≈ 62.8), Cu (S.D. % ≈ 44.0), and CaO (S.D. % ≈ 44.0), while the S.D. < 35 % cut-off additionally removes P_2O_5 (S.D. % ≈ 36.0), MnO (S.D. % ≈ 38.3) and Cr_2O_3 (S.D. % ≈ 35.9) as reliable, conservative geochemical tracers in this catchment.

Discriminant function analysis revealed two slightly different tracer arrays from the two different screening solutions (Table 31). The main difference between the two tracer suites is that solution employing a mean tracer S.D. < 35 % does not utilize Lu, MnO, and P_2O_5 but has the addition of Sm. The removal of P_2O_5 and MnO from the solution is directly due to the lower threshold of 35 %. Sm was removed from the S.D. < 40 % solution despite being the 3rd added variable during the discriminant function analysis. The variance Sm explained as the contribution to that function has likely become redundant and replaced by Lu and Pb. This appears to be a statistical decision There are several variables also removed from the S.D < 40 % solution compared to the original dataset presented in Vale *et al.* (2016b). The variables, Tm, CaO, P_2O_5, MnO have been removed directly, and the final solution has not included Zn, Nb, Y and Hf, although the exclusion of Hf is substituted Zr.

Discriminant function analysis revealed several key functions and their relationship to the individual tracers. Limestone was able to be differentiated within the first function (Table 32, Table 33). This is mainly through Sr concentrations in Function 1 which act as an analogue to CaO having been screened out (Table 31). Sediment from the Mountain Range was differentiated mostly through the REE's (represented by Lu) as well as Pb and Cs concentrations in Function 2.

Table 31: *Variables Entered for Step-wise discriminant Function Analysis*

	Vale *et al.* (2016b)		Mean S.D. % < 40 %			Mean S.D. % < 35 %	
Step	**Entered**	**Removed**	**Entered**	**Removed**	**λ Statistic**	**Entered**	**λ Statistic**
1	CaO	0.02331	SrO		0.16086	SrO	0.16086
2	Lu	0.0085	SiO_2		0.05246	SiO_2	0.05246
3	Cs	0.00406	Sm		0.01852	Sm	0.01852
4	Sr	0.0023	MgO		0.00955	MgO	0.00955
5	Tm	0.0011	Al_2O_3		0.00499	Al_2O_3	0.00500
6	Na_2O	0.00056	P_2O_5		0.00249	Cs	0.00303
7	P_2O_5	0.00033	Cs		0.00147	ZrO_2	0.00207
8	Fe_2O_3	0.00021	ZrO_2		0.00100	Na_2O	0.00153
9	Pb	0.00014	Na_2O		0.00073	Fe_2O_3	0.00103
10	U	0.0001	Fe_2O_3		0.00050	U	0.00080
11	Hf	0.00007	MnO		0.00036	Pb	0.00063
12	MnO	0.00006	U		0.00028		
13	Zn	0.00004	Pb		0.00022		
14	MgO	0.00003	Lu		0.00017		
15	Nb	0.00002		Sm	0.00019		
16	Y	0.00002					

Table 32: *Structure matrix showing function contributions of selected (shaded beige) and unselected variables*

Structure Matrix							
Variable	Function						
	1	2	3	4	5	6	7
SrO	-0.266	-0.124	-0.194	0.104	-0.148	0.188	0.037
Pb	0.01	0.608	-0.047	-0.048	0.279	-0.417	-0.178
Cs	0.025	0.598	0.155	-0.381	0.018	-0.267	0.101
Er	-0.019	0.581	-0.446	0.114	0.023	0.137	0.107
Yb	-0.004	0.58	-0.452	0.131	0.001	0.279	0.171
Lu	0.035	0.568	-0.518	0.163	-0.013	0.403	0.202
Dy	-0.048	0.561	-0.416	0.123	0.034	0.005	0.051
Nd	-0.046	0.545	-0.439	0.124	0.034	-0.042	0.041
Gd	-0.037	0.543	-0.404	0.099	0.038	-0.008	-0.002
Pr	-0.03	0.541	-0.452	0.132	0.029	-0.055	0.056
Ta	0.068	0.536	-0.256	-0.087	0.046	-0.076	-0.004
Ho	-0.01	0.535	-0.442	0.151	0.008	0.067	0.069
Tb	-0.019	0.535	-0.397	0.127	0.039	-0.005	0.015
Sm	-0.03	0.533	-0.444	0.111	0.031	-0.056	0.028
Zn	0.048	0.513	-0.015	-0.147	0.091	-0.332	-0.098
Th	0.019	0.511	-0.338	-0.044	0.145	-0.137	0.072
Y_2O_3	-0.066	0.491	-0.176	0.027	0.186	0.033	0.016
Nb_2O_5	0.104	0.471	-0.149	0.074	0.314	0.431	0.11
Ga	0.043	0.462	-0.135	-0.179	0.159	-0.336	0.061
SiO_2	0.152	-0.455	-0.046	0.175	-0.304	0.188	0.13
Sc	0.049	0.443	-0.271	-0.036	0.109	-0.135	-0.071
Eu	-0.008	0.441	-0.38	0.13	0.006	-0.047	-0.001
Rb_2O	0.025	0.42	0.103	-0.403	0.141	-0.134	-0.176
Al_2O_3	0.086	0.41	0.127	-0.259	0.393	-0.299	-0.098
K_2O	-0.001	0.399	0.051	-0.376	0.104	-0.073	-0.221
La	-0.025	0.391	-0.342	0.191	0.064	-0.093	0.092
TiO_2	0.049	0.388	-0.007	-0.044	0.22	-0.085	-0.079
V_2O_5	0.009	0.341	0.067	-0.111	0.295	-0.31	0.026
BaO	-0.133	0.327	-0.052	-0.302	0.026	-0.079	-0.128
MnO	0.012	0.318	0.159	0.064	0.146	-0.005	-0.208
MgO	0.003	0.267	-0.011	-0.203	0.013	-0.12	-0.205
Cr_2O_3	0.012	0.192	-0.056	0.011	-0.047	0.059	-0.061
U	0.012	0.321	-0.347	0.11	0.073	0.062	0.244
P_2O_5	0.002	0.381	0.185	0.426	-0.126	-0.185	0.169
Fe_2O_3	0.018	0.316	0.001	-0.025	0.41	-0.357	0.138
ZrO_2	0.034	0.078	-0.204	0.267	0.114	0.826	0.221
Hf	0.002	0.142	-0.312	0.291	0.015	0.781	0.228
Na_2O	0.083	-0.215	-0.256	0.114	-0.306	0.428	-0.206
CoO	0.043	0.335	0.102	-0.008	0.285	-0.348	-0.187

Function 3 provided differentiation of the Loess sediment through Lu while Function 4 provided differentiation of Gravel Terrace with positive P_2O_5 values as well positive Fe_2O_3 values within Function 5. The P_2O_5 values from Function 4 also contributed to differentiation of Hill Subsurface and Hill Surface material with positive correlations associated with Hill Surface sediment. Mudstone and Channel Bank sediment show weaker relationships to specific functions, but provide slight differentiation of Mudstone in Function 5 through SiO_2 and Na_2O and Channel Bank with Function 6 through ZrO (Table 32).

The ability to predict the group membership was 87.8 % for the S.D < 40 % solution, and 71.9 % for the S.D < 35 % solution (Table 34). These were both lower than the 92.1 % value reported in Vale *et al.* (2016b), although the S.D. < 40 % solution differs by < 5 % of the correct predictions from Vale *et al.* (2016b) solution, while the S.D < 35 % solution is significantly lower indicating some crucial elements able to provide discrimination were screened out between these two solutions.

Table 33: *Variance explained by each function and centroid values for each source and group function*

Discriminant Function % of Variance explained							
Variable	**Function**						
	1	**2**	**3**	**4**	**5**	**6**	**7**
Eigenvalue	71.42	3.256	1.75	1.149	0.849	0.39	0.138
% of Variance	90.5	4.1	2.2	1.5	1.1	0.5	0.2
Cumulative %	90.5	94.6	96.8	98.3	99.3	99.8	100
Group Centroids Functions							
Group	**Function**						
	1	**2**	**3**	**4**	**5**	**6**	**7**
Mudstone	0.042	0.146	-1.812	-0.251	-1.261	-0.82	-0.485
Hill Subsurface	0.926	-1.727	0.226	-1.129	0.749	-0.161	0.03
Hill Surface	1.381	-1.21	2.006	1.271	-0.971	-0.455	0.266
Channel Bank	1.223	0.038	-0.37	0.304	-0.245	0.877	-0.063
Mountain Range	1.452	4.327	1.319	-1.009	0.093	-0.184	0.069
Gravel Terrace	0.345	1.023	0.734	3.321	3.138	-0.573	-1.123
Loess	0.546	1.136	-2.923	1.259	0.947	-0.531	0.982
Limestone	-67.808	0.122	0.401	-0.013	-0.019	0.146	0.061
Unstandardized canonical discriminant functions evaluated at group means							

Table 34: *Predicted group membership of samples based on discriminant function analysis values*

Group	Predicted Group Membership							
	Mudstone	Hill Subsurface	Hill Surface	Channel Bank	Mountain Range	Gravel Terrace	Loess	Limestone
Mudstone	100	-	-	-	-	-	-	-
Hill Subsurface	-	88.6	2.9	8.6	-	-	-	-
Hill Surface	-	5.6	94.4	-	-	-	-	-
Channel Bank	4.9	4.9	2.4	87.8	-	-	-	-
Mountain Range	6.7	-	-	13.3	80	-	-	-
Gravel Terrace	-	-	-	-	-	75	25	-
Loess	25	-	-	-	-	12.5	62.5	-
Limestone	-	-	-	-	-	-	-	100
87.8 % of selected original grouped cases correctly classified								
Mudstone	75	-	-	25	-	-	-	-
Hill Subsurface	2.9	65.7	22.9	8.6	-	-	-	-
Hill Surface	5.6	16.7	72.2	5.6	-	-	-	-
Channel Bank	17.1	7.3	-	75.6	-	-	-	-
Mountain Range	-	-	-	20	80	-	-	-
Gravel Terrace	-	25	-	-	-	50	25	-
Loess	25	-	-	12.5	-	-	62.5	-
Limestone	-	-	-	-	-	-	-	100
71.9 % of selected original grouped cases correctly classified								

6.6.3. Mixing Model Comparison

Comparison between the sediment source estimates from the two model solutions produced in this analysis along with the solution presented from Vale *et al.* (2016b) shows the influence individual geochemical tracers have on sediment source proportion estimation (Table 35). The S.D. < 35 % and S.D. < 40 % model solutions produce similar values to each other (Table 35; Fig 55; Fig 56) with only minor variations in relative sediment source group contributions. The standard deviations of the model outputs decrease from Vale *et al.* (2016b) from S.D. < 40 % to S.D. < 35 % indicating lower variation in the model outputs as a result of tracers with less variation (standard deviation) being entered into the model. The objective functions produced form the S.D. < 40 % and S.D. < 35 % (Fig. 57) were both significantly lower than the objective functions produced from Vale *et al.* (2016b) indicating that the models were able to produce a solution with less residual difference between the actual sample and the modelled parameters. Again, this is likely due to the lower variation input into the model. Important sediment source group differences are seen in comparison to the Vale *et al.* (2016b) model. The main differences were observed within the Mudstone, Gravel Terrace and Loess sediment

sources. Mudstone and Gravel Terrace sediment sources showed significantly higher sediment proportions for S.D < 40 % and S.D. < 35 % solutions (Mudstone = 59.3 % and 61.8 %; Gravel Terrace = 7.3 % and 6.3 %) compared to 37.8 - 46.6 % and 0.2 – 3.6 % respectively (Table 35). The opposite trend is observed for Loess sediment sources whereby contributions of 2.7 % are observed for the S.D. < 40 % and S.D. < 35 % solution compared to 9.1 – 10.2 % (cf. Vale *et al.*, 2016b). This indicates that one or more of the variables removed (i.e. Tm, NiO, Cu, CaO, P_2O_5, MnO and Cr_2O_3) from the original Vale *et al.* (2016b) solution through discriminant function analysis contribute to model sensitivity for those specific source groups by significantly influencing derived sediment source estimates. Whether this provided a greater certainty in the sediment source estimates is unclear, but it does demonstrate the sensitivity that these models have to single variables despite possessing a larger geochemical suite to reduce single variable effects. The remaining source groups displayed minor variations between the estimated solutions and were less affected by the different geochemical suite used.

Sediment source estimates from the S.D. < 40 % and S.D. < 35 % solutions for Hill Surface (11.5 % and 11.3 %), Hill Subsurface (6.6 % and 6.2 %), and Mountain Range (12.0 % and 11.4 %) source groups (Fig 55, Fig 56) displayed slightly lower values compared with Vale *et al.* (2016b) estimates of Hill Surface = 12.1 – 16.3 %; Hill Subsurface = 9.2 - 10.8 %; and Mountain Range = 15.9 – 17.5 % respectively. The Channel Bank and Limestone source estimates from the S.D < 40 % and S.D < 35 % remained effectively 0 % for both of these sources as with values published by Vale *et al.* (2016b).

Table 35: *Comparison of sediment source estimates with those of Vale et al. (2016b)*

Sediment Source	Comparison of Sediment Source Estimates					
	S.D. < 35 %	S.D.	S.D. < 40 %	S.D.	Vale *et al.* (2016b)	S.D.
Mudstone	61.8 %	8.8	59.3 %	9.8	37.8 – 46.6 %	10.6
Hill Subsurface	6.2 %	6.5	6.6 %	6.8	9.2 – 10.8 %	6.9
Hill Surface	11.3 %	6.7	11.5 %	7.5	12.1 – 16.3 %	6.5
Channelbank	0.3 %	1.6	0.6 %	2.1	0.0 – 4.3 %	2.7
Mountain Range	11.4 %	4.1	12.0 %	4.2	15.6 – 17.5 %	3.9
Gravel Terrace	6.3 %	6.0	7.3 %	6.0	0.2 – 3.6 %	4.3
Loess	2.7 %	4.6	2.7 %	4.6	9.1 – 15.2 %	7.5
Limestone	0.7 %	0.4	0.1 %	0.4	0.0 – 0.0 %	0.0

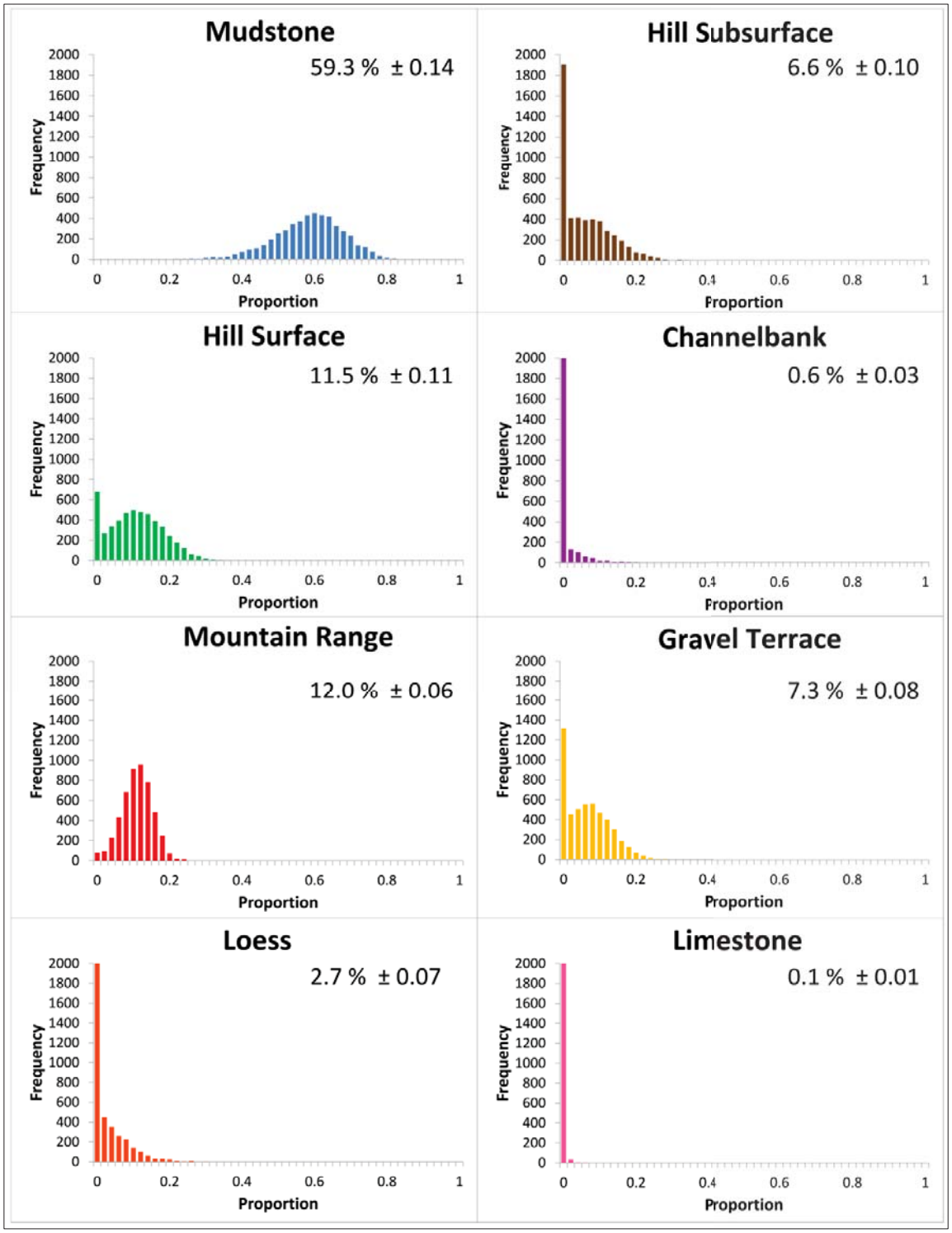

Fig 55: *Frequency distributions for the sediment source estimations based on the S.D. < 40 % solution*

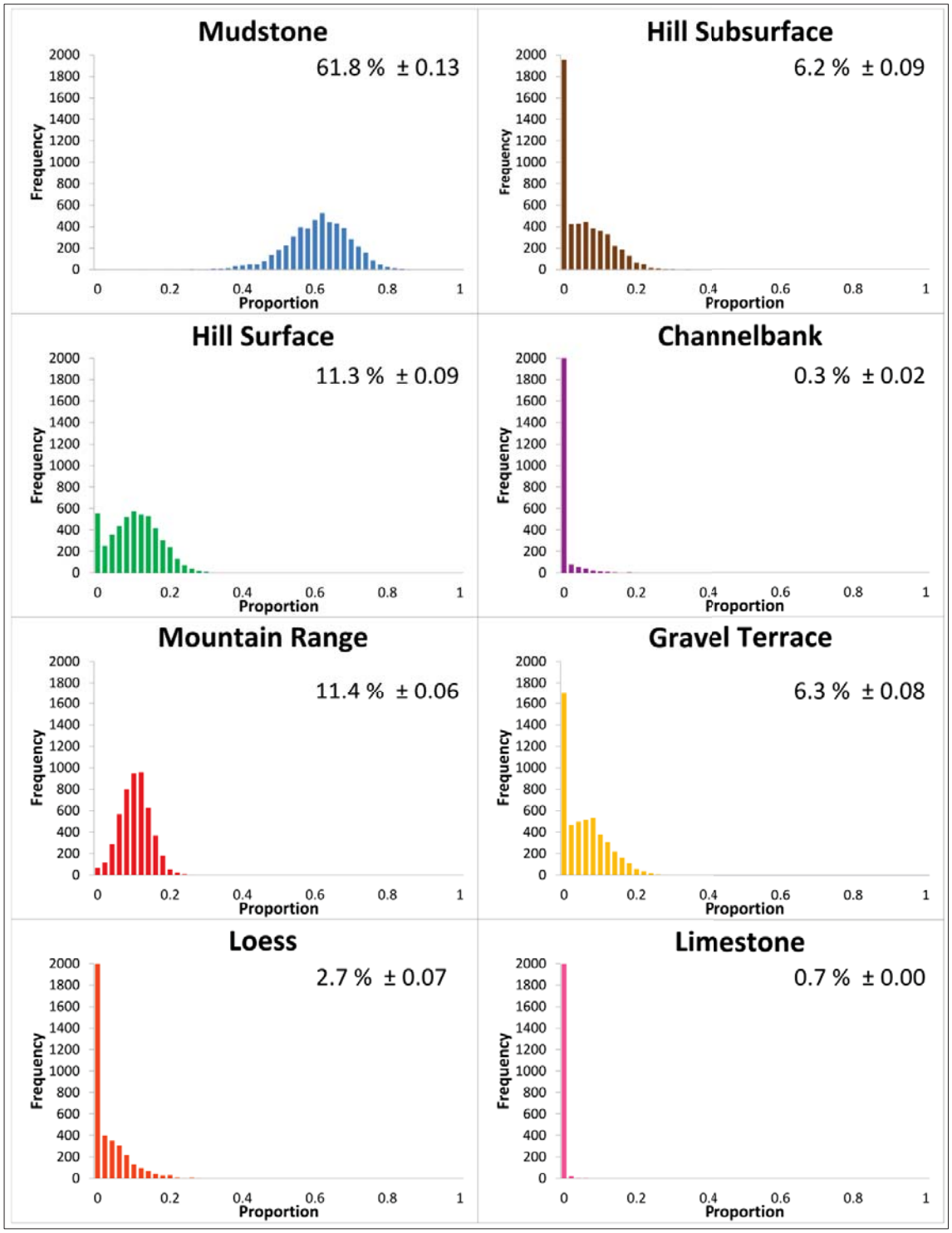

Fig 56: *Frequency distributions sediment source estimations based on the S.D. < 35 % solution*

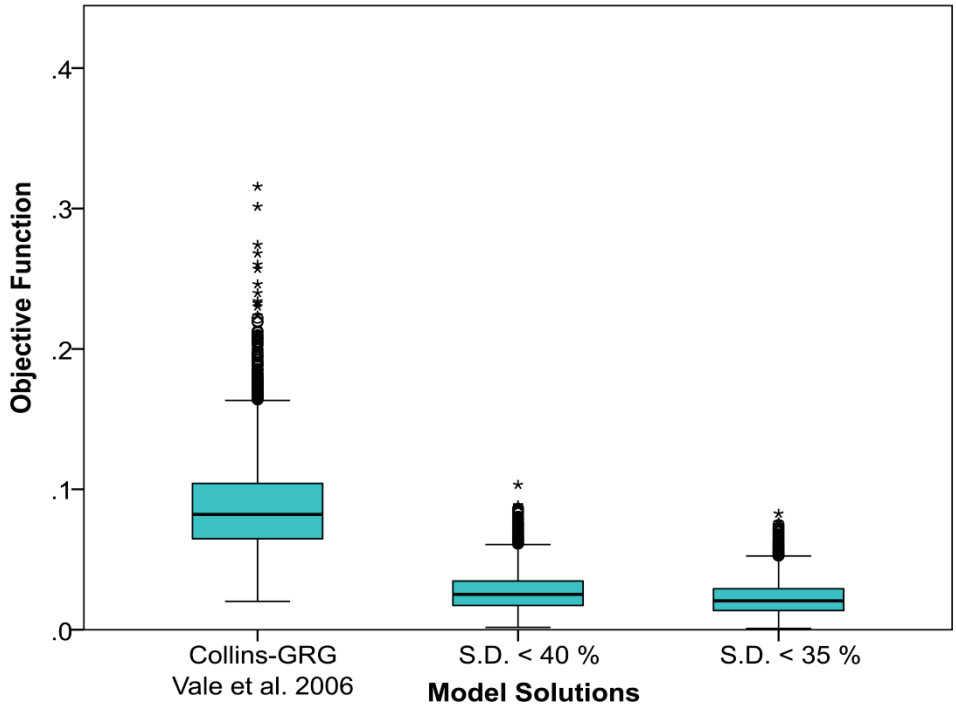

Fig. 57: *Boxplot showing comparison of Objective Function statistics of the model solutions*

6.7 Conclusion

This research showed the significant challenges to account for sediment source estimate uncertainty in sediment fingerprinting research. Notably, geochemical variation between sediment source groups as well as the geochemical variation of individual elements is an important concern pertaining to the uncertainty of sediment source estimates. In this research specific tracers were removed from the sediment mixing model due to their high geochemical variability which increased the proportion of sediment attributed to Mudstone sources by 15 %. Some of the variables which provide good discrimination between sources also have high standard deviation values, which could inhibit valid differentiation of individual sources within the model. Although the general pattern of sediment source estimation from the two mixing models in this paper displayed similar patterns to the research from Vale *et al.* (2016b), there was significant change in the proportions for some of the sediment sources which evidences the sensitivity sediment fingerprinting models can have to individual tracers. A major limitation however was that there was no comparison with artificial mixtures to know how accurately the models are estimating sediment source group contribution. Geochemical change was observed in sediment samples submerged within the river, but appeared to vary

between the different sediment source groups. The full extent of these changes is inconclusive and requires a substantial investigation in order to fully understand the mechanism and extent of geochemical change occurring in the sediment. Measured information could provide greater certainty by quantifying the geochemical change or informing decisions to exclude individual tracers from source estimation.

6.8 Acknowledgements

We would like to acknowledge funding support from Landcare Research by way of the Murray Jessen PhD Scholarship with which this research is made possible

6.9 Summary

This chapter reviewed the geochemical variability encountered in the Manawatu sediment source data set, finding that some of the sediment source groups i.e. Mountain Range, display a high variability compared to Mudstone sediment which has an overall lower geochemical variability. Additionally, some individual tracers provide good discrimination between sources, yet have high variability between samples. Removal of these elements from the geochemical suite used to characterize the sediment source groups can influence the estimated proportions for some sediment source groups. This has implications for how geochemical tracers are selected and highlights the need to critically assess tracers on an individual basis for their suitability and impact on source proportion estimation.

Chapter 7

Synthesis of Discussion

7.1 Introduction

The aim of this thesis was to investigate sediment source differentiation and quantification using sediment fingerprinting techniques within a New Zealand setting, particularly in a large, homogenous catchment such as the Manawatu. In doing this, the research also addresses, key ongoing challenges in sediment fingerprinting research.

The research is underpinned by a comprehensive literature review covering the major components and developments of the technique (Chapter 2), including an indexed table summarizing sediment fingerprinting research (Appendix A). This provided a robust context to implement a confluence-based sediment fingerprinting approach which was targeted towards identifying broad scale geochemical variability of suspended sediment within the Manawatu catchment (Chapter 3). This demonstrated the ability to discriminate between sub-catchments and, a comprehensive sampling scheme followed, focused on understanding the key geomorphic sediment source contribution (Chapter 4). An intra-storm analysis of sediment source change at an hourly resolution was implemented to evaluate sediment sources contributing to a spring flood event in the Manawatu (Chapter 5). Finally an experiment investigating sediment source variability and methodological uncertainty issues

(conservativeness of geochemical tracers) was undertaken to identify constraints and limitations in the sediment fingerprinting approach used in this study (Chapter 6).

This synthesis chapter links together the five main components of this research into one single thread of understanding. This is achieved within two main emphases which relate; firstly, to the understanding gained for the sediment fingerprinting technique itself contextualized within current literature; and secondly to the implications of the estimated sediment source proportions in relation to the geomorphological understanding of the catchment.

The Manawatu River is well suited to understanding some of the ongoing challenges encountered in sediment fingerprinting as it represents the larger end of catchment sizes (≈ 6,000 km^2) where sediment fingerprinting has to date been employed. The geological composition of the catchment is almost entirely sedimentary, with significant deposits of greywacke, mudstone and alluvium, all capable of generating sediment which can be delivered into the active channel throughout the entire catchment. This creates a challenging issue whereby the main tributaries drain similar landscapes, albeit in disparate patterns i.e. east and west sub-catchments drain the axial range and include soft sedimentary hill country, which results in sources that are not spatially limited to specific sub-catchments or exclusive to specific processes. This arrangement emphasizes the specific challenge for sediment fingerprinting in large complex catchments and makes it difficult to ascertain the spatial origin of individual sediment sources or assess the dissimilarities in relative proportions between tributary sub-catchments.

7.2 Geochemical Characterization in Large Catchments

The main challenges encountered in this research relate to the capacity of the sediment fingerprinting approach to account for natural geochemical variability within catchment scale processes. This is both within the sediment sources as well as within river transport systems. Sediment sources can display a large geochemical range within short spatial scales as well as within geological and pedological groups (Chapter 4 & Chapter 6). This inherent intra-source geochemical variability presents a challenge for characterization of sediment sources since geochemically unique sediment sources can in some instances arise from similar processes and conversely, geochemically similar sediment sources can be produced from different erosion and deposition processes. This continues during sediment transport where disparate mixing of suspended sediment at, and downstream of, river confluences (Chapter 3) as well as the high temporal fluctuations of suspended sediment (Chapter 5) adds uncertainty to the retention of

sediment source geochemical character. This is compounded within larger catchments providing a challenge for clear characterization of sources.

One approach to negate this issue is to avoid sampling the sediment sources directly, but instead sample the channel sediment which represents each tributary because sediment from within the channel is less-variable than catchment soil and sediment sources (Wilkinson *et al.*, 2013). In Chapter 3, a confluence approach was employed to target the main sub-catchments flowing into the main stem of the Manawatu River in order to establish whether there was enough geochemical variability to discriminate between sediment exiting the main sub-catchments; Upper Manawatu, Tiraumea, Mangatainoka, Mangahao, Pohangina and Oroua. Quantification of sediment source contributions was not possible due to the low sample replication, but sub-catchment sediment sources evidenced clear discrimination between respective upstream sources. This suggested potential for the technique to simplify larger complex catchment systems into manageable sections and be integrated into a traditional sediment sampling programme for step-wise discrimination. The discriminant function analysis between each of the confluences was able to effectively differentiate each of the upstream sediment source components. Each confluence used a different array of elements to differentiate sources, with only CaO, P_2O_5 and Cu being utilized in each confluence analysis. The C3 and C5 confluence (Fig. 15) had over twice as many significant elements available for discrimination mostly from REEs (Table 9). In the case of C5, this is attributed to sediment recycling occurring in the dune environment supported by the extremely high Zr concentrations which are associated with REE's. In C3, the importance of the REE possibly reflects a 'cleaner' geological signal coming from the greywacke sandstone in the Tararua Range which contrasts to the mudstone dominated sediment from the Upstream Manawatu sediment source. Despite being able to discriminate the upstream sources, there was still a significant amount of geochemical variation displayed within the channel sediment, particularly closer to the confluence point and between point bars. This suggests that homogeneous mixing may not occur as quickly as assumed, with implications for the sample position within a channel. If the channel sediment is sampled, sampling density needs to be significantly higher even through channel sediment is considered less geochemically variable.

Further source sediment sampling was undertaken throughout the catchment (Chapter 4) and involved targeting the sediment sources within the Manawatu Catchment with the intention that this would delineate erosion processes. However, exclusive and clear relationships between geological sources and processes made this impractical highlighting methodological limitations facing sediment fingerprinting in this catchment, which involve a balance between

an appropriate sampling density to cater for the geochemical variability and the total spatial extent, all ultimately limited by resources available. This is compounded when vertical stratification produces multiple geochemical sources contained within a single erosion mechanism (e.g. landslide). Conversely, a unique geochemical signature can occur in multiple erosion process settings throughout the catchment and not reside exclusively within a particular process or spatial location. This is well displayed in the Manawatu catchment through the Mudstone sediment source which is abundant throughout the catchment, and although the Mudstone provides a geochemically unique signature relative to other sediment sources (Chapter 4), introduction of mudstone derived sediment into the active channel can occur through a variety of pathways including cliff collapse, channel incision, gullying, and landslides, and in spatially assorted patterns. Because of this issue, source groups were defined based on geological and geomorphological contexts in order to produce geochemically unique sources. This provided eight potential source groups including; Mudstone, Hill Subsurface, Hill Surface, Channel Bank, Mountain Range, Loess, Gravel Terrace and Limestone.

Limitations for the geochemical characterization within a large catchment are the challenge to adequately sample all appropriate erosion sources and account for the unknown issues occurring throughout transport, which require longer time frames for sediment to move from source to catchment outflow. This relates to issues raised by several authors, notably Koiter *et al.* (2013b) identifying the black-box approach to sediment fingerprinting and the limited knowledge of what happens to the sediment properties between input and output. This particularly relates to the storage component and in the indirect relationship between source and suspended sediment sample and the changes to the sediment properties throughout this time. Geochemical Source Characterization

All the analysed geochemical variables displayed significantly different concentrations between at least two sediment sources attributed to the high number of sediment sources being characterized and the vastly different geochemistry from Limestone. Discriminant Function Analysis (DFA) produced a 16 variable solution consisting of (in order of significance) CaO, Lu, Cs, Sr, Tm, Na_2O, P_2O_5, Fe_2O_3, Pb, U, Hf, MnO, Zn, MgO, Nb, and Y. The most readily differentiated sediment sources were Limestone, Mountain Range, Hill Surface and Loess due to their distinctive geochemistry, while Channel Bank and Hill Subsurface provided the most difficulty for geochemical classification, possessing closer geochemical signatures and similar origins. This is displayed in the DFA plot (Fig. 26) where Channel Bank sediment is plotted relatively centrally to all other source groups reflecting the mixed origin of the floodplain deposits, and raises challenges pertaining to differentiation of primary and secondary sources

due to sediment recycling. Retaining a similar geochemical signature to the primary sediment source is important for understanding historical sediment sources and requires conservative tracers to retain the geochemical signature. However, for contemporary sediment fingerprinting those same sediments need to have chemically altered enough to be able to differentiate between the channel bank sediment as a distinct source. It is possible that some of the channel bank sediment samples retained enough geochemical character from their primary source to limit full distinction from other sources, but alludes to the need to incorporate an understanding of weathering pathways and individual geochemical behaviour into the sediment fingerprinting research in a catchment of this nature.

Individual geochemical concentrations can be explained for some of the source groups, but full geochemical interpretation requires additional information. Limestone characterization is clearly provided by the CaO and Sr concentrations associated with mineral calcite, while Mountain Range sediment, Loess and Gravel Terrace tend to display relatively higher concentrations of trace elements and REEs. In the example of Mountain Range, the geochemical values reflect the rock fragments and muddy matrix of greywacke material as well as the depleted Si, Ca and Na concentrations of the weathering profile on a greywacke range (Anderson *et al.*, 2002). In contrast, Hill Surface and Hill Subsurface display lower trace and REE concentrations than most other sources and display similar geochemical signatures due to the same mineral origins. The most significant differentiation between these two sources is due to higher P_2O_5 concentrations in the Hill Surface source.

7.3 Geomorphological Interpretation

The source sediment fingerprinting identified the dominant fine sediment source to be originating from Mudstone terrain with model estimates ranging between 37.8 – 46.6 % (Chapter 4). Mudstone sources are abundant throughout the entire catchment, particularly in the eastern sub-catchments where the soft erodible hill country are identified as erosion prone land (Ausseil and Clark, 2007). Cliff erosion, channel and gully incision, as well as mass movements are all processes evident in the catchment, and are all capable of delivering fine mudstone sediment into the active channel.

The confluence based fingerprinting (Chapter 3) also supports a mudstone-laden suspended sediment load by attributing the Tiraumea, followed by the Upper Manawatu sub-catchment,

as main sources of this sediment. C1-2 represents the confluence of the Tiraumea, Mangatainoka and the Upper Manawatu, and the Tiraumea sub-catchment provided the dominant geochemical signature at this major confluence. The Tiraumea represents the sub-catchment with the highest areal percentage of Mudstone and fits the conceptual premise that soft sedimentary terrain is a significant sediment source. The highest mean suspended sediment concentrations of 198 g m^{-3} are also experienced in the Tiraumea compared to 126 g m^{-3} from the Pohangina sub-catchment as the next highest concentration (Basher *et al.*, 2012). However, total sediment yield from Upper Manawatu (5,813 t x 10^3) is over twice that of Tiraumea (2673 t x 10^3) due to significantly larger flow originating from the Upper Manawatu sub-catchment (Basher *et al.*, 2012). This indicates major suspended sediment loads originating from the Upper Manawatu should be observed in the discriminant function analysis of C1-2 which is not immediately the case (Chapter 3).

The discrepancy presents several implications for interpreting sediment fingerprinting source estimation. Firstly, it could reveal a failing in the sampling method to capture the inherent spatial variability encountered in this channel, or exposes the influence of prior flow conditions and hysteresis in producing temporal fluxes and sediment deposition which may not reflect the prevailing catchment sediment source. Preferential deposition or transport within the Upper Manawatu due to these prior conditions could mean the geochemical character does not completely denote mudstone sediment to the same degree as it would in the Tiraumea due to the presence of the greywacke sandstone source which feeds into the Upper Manawatu. Remobilization of fine sediment stored in the channel will also influence sediment source discrimination and introduces additional complexity to suspended sediment signals, and as Collins *et al.* (1998) suggests may have an averaging effect on interpretation. A collection of stored sediment in the channel does not necessarily represent a single temporal component, but likely a mixture sediment sources eroded at different times. Koiter *et al.* (2013b) points out the issue of primary and secondary sources and at which point significant change in the properties has occurred that stored sediments should represent a new and unique source. Some researchers have explored this component and indicated the significance of remobilized fine sediment as a major source (e.g. Collins and Walling, 2006, Collins and Walling, 2007).

It is also possible the discrepancy is due to a misalignment between sediment size fractions used for geochemical analysis and those associated with the calculated suspended sediment values. Geochemical analysis required sediment samples to be sieved to a < 63 µm grain size fraction to represent the suspended sediment component. However, suspended sediment

samples taken during a storm event (Chapter 5) resulted in a considerable quantity of discarded sediment following extraction of the < 63 µm grain size fraction indicating a component of the suspended sediment collected during the event was > 63 µm. Furthermore, grain size analysis of the confluence based samples (Chapter 3) showed D_{50} values of the suspended load ranged from 16- 44 µm which situates the samples in the silt range. Flocculation effects from clay particles into silt-sized aggregates are also a possibility that have not been investigated in this research. An estimated 12 - 16 % of fine sediment originates from the Mountain Range (Chapter 4). The Tararua and Ruahine Range represent active mountain ranges where significant erosion occurs throughout the eastern flanks of the Ruahine Range. The relatively low sediment source estimation suggests that the sediment derived from this area is either coarser and contributes more to the bedload than the suspended sediment load, since this sediment originates from the more resistant greywacke sandstone, or there are (dis)connectivities between sediment sources and the active channel.

The Hill Surface and Hill Subsurface sediment components provide similar values to one another. Hill Subsurface accounts for 9 – 11 % while Hill Surface accounts for 12 – 16 % of sediment proportions (Chapter 4). These estimates, as well as the similar geochemical signatures, suggest a relationship between the contributing processes. Shallow translational landslides in the Manawatu transport the soil horizon (Dymond *et al.*, 2006b), which would include both the surface and subsurface components. The subsurface component typically comprises a thicker component of the landslide material which should display greater Hill Subsurface sediment relative to Hill Surface sediment sources. Landslides occurring from the hill country are typically underlain by similar geologies which Crozier (2005) identified as being the leading variable in determining the length of runout but does not indicate the relative proportion of surface and subsurface sediment reaching the channel from a landslide. One study in the Manawatu found that following a large storm event, the majority of the eroded material generated remained in the hillslope system, while an average of 25 % reached the fluvial system (Wright, 2005). This is in agreement with the sediment fingerprinting research, which suggests storage effects are could be influencing the relative proportions of subsurface and surface sediment reaching the active channel. Additionally, higher surface sediment proportions could also reflect the agricultural nature of the catchment, whereby intensification of agricultural practices cause significant disturbance to topsoil more so than subsurface soils, allowing greater erosion of the topsoil material.

The Loess sediment accounted for between 9 – 15 % of the sediment proportion in the catchment. This material tends to sit above the mudstone deposits particularly in the

Pohangina sub-catchment. Channel Bank Sediment was found to account for 0 – 4.3 % of suspended sediment and although the Channel Banks are widespread throughout the catchment, they are primarily found within a depositional floodplain environment and don't provide large enough exposed surfaces relative to Mudstone or Mountain Range sediment sources. Despite channel erosion being a target of widespread management strategies which involve planting streambanks with little demonstration of effectiveness (Marden, 2011). This research suggests that channel bank sediment is of little importance to total suspended sediment yield in this catchment and although erosion of channel banks is visible, the volume of suspended sediment produced is negligible in comparison to other sources. This is in alignment with conclusions drawn by De Rose and Basher (2011a) on research in the Waipaoa catchment which represents similar hillslope terrain to the Manawatu although admittedly displays much higher hillslope erosion rates. De Rose and Basher (2011a) state the sediment derived from cliff retreat (i.e. the mudstone) far outweigh the sediment originating from the alluvial banks. It would also suggest that resources devoted to management of bank erosion should be kept in perspective and successful bank erosion strategies are not going to have a significant influence on sediment loads. Limestone sediment provided little to no contribution to the suspended sediment of the Manawatu River. Sources of Limestone within the catchment are relatively minor and together with highly soluble carbonates within the limestone means that any limestone components delivered to suspended sediment transport would be rapidly dissolved.

7.4 Storm Flow Sediment Analysis

Sediment source apportionment was investigated in relation to a storm event using suspended sediment samples taken at hourly intervals (Chapter 5). The hourly samples displayed considerable variability between adjacent samples whereby average mean Mudstone proportions fluctuated ≈ 20 – 60 % throughout the storm duration; Hill Subsurface and Hill Surface both neared 0 % minimum, but approached maximum values of ≈ 23 % and ≈ 24 % respectively; Channel Bank sediment remained close to 0.0 % ; Mountain Range sediment fluctuated from ≈ 24 – 46 %; Gravel Terrace and Loess both displayed estimates near 0 % but reached as much as ≈ 6.0 % and 0.3 % respectively; and Limestone showed a low average mean range between ≈ 1 – 3 %.

The high variability could originate from uncertainties inherent in sediment fingerprinting techniques which have been noted in Chapter 6 as well as other research (e.g. Pulley *et al.*,

2015, Belmont *et al.*, 2014, Koiter *et al.*, 2013b). The key issues relate to assumptions of unconstrained factors connected to tracer and mode selection and imply limitations on how much information can be interpreted from sampling which may not fully capture the geochemical changes. The high variability could also indicate the 'jerky conveyor belt' and sporadic patterns of sediment movement through a channel (Ferguson, 1981, Benda and Dunne, 1997, Gomi *et al.*, 2002). As sediment moves through a channel in pulses and waves, each wave of sediment could represent quite a diverse combination of geochemical sources. Sediment waves occur at a variety of scales and lengths of times with multiple superimposed pulses occurring in a single event (Nicholas *et al.*, 1995). In addition to temporal complexity, the confluence research (Chapter 3) displayed evidence of non-homogenous mixing downstream of station C4, compared to C1-2, C3 and C5. This was thought to be caused by a disparity in transverse mixing occurring at each confluence. The planform geometry and associated parameters such as channel width and inflowing tributary angle influence the degree of transverse mixing (Best, 1988, Kenworthy and Rhoads, 1995, Rhoads and Sukhodolov, 2008) and appear to have an influence at the C4 site for a considerable distance downstream. This has implications for the sampling locations, and positioning of sediment samplers which use a time-integrated approach to account for temporal variability, but seldom account for cross-sectional variation experienced from incomplete mixing. It is possible some of the variability observed is due to sediment variations in the channel cross-section.

Although there is high variability between hourly samples, a moving average reveals sediment source switching occurring throughout the storm duration. A distinct occurrence was observed between 2:00 and 8:00 am, 28th November whereby Mudstone proportions averaged ≈ 50 % compared to ≈ 40 % for the remainder of the event; Mountain Range exhibited contributions of ≈ 40 % compared to a remaining event average of ≈ 30 %; and Loess sediment near reaches ≈ 0.4 %, compared to ≈ 0.1 % for the remainder of the event. This is inversely reflected for Hill Subsurface and Hill Surface exhibiting ≈ 2.5 % compared to ≈ 13.5 % and ≈ 10 % for the remaining duration respectively; Gravel Terrace contributed ≈ 1.0 % during 2:00 – 8:00 am and ≈ 3.5 % for the remainder of the storm duration; Channel Bank is effectively 0 % throughout, and Limestone sediment source contributions do not appear to display any pattern.

These observations partly reflect a switching of flow from the Pohangina towards more flow from the Upper Manawatu. Although flow increased from the Upper Manawatu, the sediment load is still dominated by the Pohangina-derived sediment which suggests there is a difference in sediment source between the rising and falling limb of the Pohangina storm flow. Hysteresis has been widely observed during high flow events (e.g. Klein, 1984, Walling, 1977, Lenzi and

Marchi, 2000). This has typically looked at total load, but here the observed patterns indicate source switching in the falling limb of the first Pohangina sediment load maxima which coincides with a reduction in Hill Surface and Hill Subsurface sediment contributions. This reduction may indicate the distal location of these sediment sources from the active channel and relate to intermittent sediment movement generated from the transport pathways in a similar suggestion from Krein *et al.* (2003) whereby sources further from the channel are active during the winter season and high flow events.

A limitation to the storm analysis was that this was not replicated for different storm events (due to resource constraints) to more rigorously identify storm trends. In addition, replication within a storm event by collecting samples at multiple locations throughout the catchment would provide information linking the transit of material throughout the catchment.

7.5 Sediment Fingerprinting Uncertainty

A significant amount of variation exists in sediment fingerprinting source proportion estimations which can occur from poor characterization of the sediment sources as well as model inadequacy. In this research, the sediment mixing model estimates were run under four variations (Chapter 4). These included two different models after the 'Collins' and the 'Hughes' mixing models which were each combined with a Generalized Reduced Gradient (GRG) Nonlinear' and an 'Evolutionary' optimization technique within Monte-Carlo simulation. These four model scenarios generally displayed consistent sediment proportion trends which suggests globally optimal solutions were approached for each the models. The Collins model scenarios showed negligible difference between the two optimization techniques with identical mean objective functions (0.087) and standard deviations (0.032). The Hughes-Evo showed a similar mean (0.086) while the Hughes-GRG displays a slightly lower mean value (0.070). However both showed significantly lower standard deviations of 0.002 and 0.019 respectively. The degree to which the objective function approaches zero has direct bearing on some of the sediment proportions. High objective functions (less optimized) from all models except Hughes-GRG displayed lower proportions of mudstone sediment. Within the Collins models this resulted in higher Loess, Hill Surface and Channel Bank proportions. In the Hughes-Evo model differences related more to higher Loess, Gravel Terrace and Channel Bank when objective function was less optimized. Although there were some significant differences between high and low objective functions for each model, the high objective functions are relatively infrequent and have a minor influence on the mean estimates

The variations in estimates are largely due to the re-sampling method used in each model, however these variations are relatively minor and indicate that in this context, the model selection is less important than the selected variables which potentially influence the source estimates considerably when altered (Chapter 6). Transition elements such as Ni, Co and Cu display the very high geochemical variability, reflecting the chemical properties that transition elements display, but may suggest that transition elements are unsuitable for sediment fingerprinting work. The effect of individual tracers on source estimates was evidenced in the proportion of Mudstone sediment changing from 37.78 - 46.60 % in Vale *et al.* (2016b) to 59.3 % and 61.8 % respectively upon removal of multiple tracers from the geochemical suite. This is in contrast to Haddadchi *et al.* (2014) where the source contribution has been found to have a dependence on the mixing model which emphasises the need to understand the mixing model, the data set, as and how the two interact as it may be that sometimes the variable selection have a dominant influence, and other times the model selection does. Despite these variations the general distribution of sediment source proportions estimated in Vale *et al.* (2016b) are retained in revised model estimates from Chapter 6 and while the specific value varies, the geomorphological interpretations remain valid.

The variation between source estimates does nevertheless have implications for the absolute confidence of these estimates and their interpretations. This is particularly notable when implementing more detailed investigations which aim to detect small variations and fluctuations between sediment sources. An example of this is the storm analysis in Chapter 5 where the adjacent hourly samples display high variability; however it remains unclear whether the minor fluctuations between source group proportions are actual sediment changes or simply differences arising from uncertainty. Therefore the level of resolution and detail in sediment fingerprinting studies may be severely limited by issues of uncertainties generated from high geochemical variability and lack of conservativeness in specific tracers. It is suggested in Chapter 4, that in order to quantify these uncertainties, individual tracer geochemistry needs to be properly understood so that mechanisms and processes for the occurrence of specific geochemical signatures and their modification through sediment transport can be qualified. This could be aided with geochemical analysis of the individual minerals to identify which minerals give rise to the specific geochemical concentrations, allowing for less resistant minerals or minerals which are more chemically active to be excluded thereby lessening susceptibility to unstable geochemical tracers.

A limitation faced in mixing model estimations for sediment source was the lack of artificial mixtures to test the accuracy of the estimates. This would have provided greater certainty to

the sediment source quantifications. A way to incorporate changes in the sediment properties over time would also be a useful addition if these changes can be measured (Chapter 6) and incorporated in order to adequately account for geochemical change.

7.6 Catchment Management

The research findings have implications for catchment management in several forms. Firstly, it reinforces focus on soft erodible mudstone hill country as a prime source of fine sediment within the Manawatu catchment. These areas are prone to erosion and thus need to be managed to reduce elevated erosion rates and subsequent loss of topsoil. It is unclear what the baseline sediment delivery is for this terrain, but natural rates are likely derived from locations where the channel incises directly into mudstone. A significant focus is often placed on bank erosion of the channels and this is perhaps inflated beyond its relative importance to other sediment sources. In this research, the input from channel bank has been found to be relatively minor. This is possibly because they are naturally depositional features from previous flood events, combined with a significant amount of catchment management work that has been done throughout the catchment to stabilize channel banks. Channel Bank erosion may not contribute a significant quantity of sediment relative to other sediment sources, but its importance is pronounced because of the immediate implications it has for human activities i.e. direct loss of land for agriculture, infrastructure and human settlement. Sediment derived from the Mountain Range was another significant source in the Manawatu sediment cascade. The mountain ranges are generally under indigenous forest and this sediment produced from these sources would be predominantly of natural origin and thus arguably does not require significant intervention for management.

7.7 Summary

The sediment fingerprinting approach has demonstrated the ability to characterize sediment sources and provide quantitative source estimations in the Manawatu Catchment. Sub-catchment characterization of sediment sources sampled at major confluences was effective, despite draining similar geomorphological terrains. Quantification of the proportion of eight key sediment sources were also attained providing information regarding the geomorphological processes occurring in the catchment. Change in sediment sources throughout a storm event was observed in accordance with hysteresis and changing dominant

sub-catchment flow, despite the highly variable hourly suspended sediment sources proportions. However, investigation into geochemical variability of these data highlights significant uncertainties in the accuracy of source estimates and highlights the need for pressing reviews of individual tracers in order to understand their geochemical reactions and changes which may occur during transport. Nevertheless, while questions may remain regarding the detailed level of accuracy of sediment fingerprinting applied in the Manawatu catchment, the key patterns and processes have been established. What is now needed is further refinement of the approach in this catchment to improve levels of certainty in the application of sediment fingerprinting here. This research has taken an important first step in deployment of fingerprinting in a large, homogenous sedimentary catchment, which shows considerable promise.

Chapter 8

Conclusion

8.1 Introduction

The aim of this thesis was to investigate sediment source differentiation and quantification using sediment fingerprinting techniques within a New Zealand setting, particularly within a large, homogenous catchment such as the Manawatu, as well as understand some of the ongoing challenges in sediment fingerprinting research. The results from this research has identified the main sources of sediment in the Manawatu Catchment and provided the steps towards being able to quantify the contribution each lithology in each tributary provides to sediment supply in the Manawatu River.

The research is underpinned by a comprehensive literature review covering the major components and developments of the technique (Chapter 2) including an indexed table summarizing sediment fingerprinting research (Appendix A). This provided a robust context to implement a confluence-based sediment fingerprinting approach targeted towards identifying broad scale geochemical variability of suspended sediment within the Manawatu catchment (Chapter 3). This demonstrated the ability to discriminate between sub-catchments and, a comprehensive sampling scheme followed, focused on understanding the key geomorphic sources of sediment contribution (Chapter 4). An intra-storm analysis of sediment source change at an hourly resolution was implemented to evaluate sediment sources contributing to a Spring flood event in the Manawatu (Chapter 5). Finally an experiment investigating sediment source variability and methodological issues of trace selection is investigated (Chapter 6).

8.2 Conclusion of objectives

The conclusions of this study pertaining to the objectives of this study were:

a. A comprehensive review draws on a very large body of literature which has seen the sediment fingerprinting technique develop from simple approaches looking at one or two tracers, to significantly more complex processes using a large suite of geochemical tracers and complex sediment mixing models for sediment source quantification. A key challenge to applying sediment fingerprinting is geochemical variability, uncertainty and lack of knowledge pertaining to chemical alteration during transport.
b. Results demonstrated the feasibility of sediment fingerprinting in the Manawatu catchment, despite the occurrence of similar geomorphological terrains underlain by similar geologies throughout the catchment.
c. Deployment of sediment fingerprinting characterized and quantified eight key sediment sources in the Manawatu catchment, finding that:
    i. Mudstone derived sediment was the dominant sediment source sediment sources in the Manawatu catchment contributing between 37.8 - 46.6 % although some estimates gave values as high as 61.8 %. The next largest contribution was from Mountain Range, 15.9 – 17.5 %; followed by Hill Surface, 12.1 – 16.3 %; Hill Subsurface, 9.2 - 10.8%; Loess, 9.1 – 10.2 %; Gravel Terrace, 0.2 – 3.6 %; Channel Bank, 0.0 - 4.3 %; and Limestone, 0.0 %.
    ii. Hourly suspended sediment source quantification during a 53 hr storm event was highly variable although general trends indicated changes in sediment sources were related to flow hysteresis as well as switching of the sub-catchment flow
d. Assessing the reliability (conservativeness) of key geochemical tracers demonstrated that geochemical variability and uncertainty can make sediment source characterization challenging. Furthermore removal of individual tracers on the basis of high variability can significantly influence specific source estimates.

8.3 Future Research

It is clear that sediment fingerprinting can be a useful tool for understanding patterns of sediment source generation within a catchment. However there are some significant uncertainties and limitations which present a challenge for ongoing research.

In order to understand uncertainty issues, the origin of the geochemical signal within a sediment source needs to be more thoroughly investigated and linked to mineral analysis. This is of even greater importance for sedimentary environments where sediment recycling introduces unclear geochemical distinctions.

A significant limiting factor for sediment fingerprinting pertains to availability of resources. To do a full catchment sampling program is expensive and many projects aren't able to do the ideal sample replication. Nevertheless, the potential and value of sediment fingerprinting using an appropriate suite of geochemical tracers has been demonstrated and further application to more fully explore the suspended sediment flux in the Manawatu would be worthwhile, particularly in conjunction with assessment of sediment sources in a range of storm events. Only a single flood was assessed in this study, and it is likely that floods generated by different rainstorms will have distinctive signatures according to rainfall distribution and intensity.

Sediment fingerprinting needs to be incorporated with other research techniques to maximise findings into meaningful information. This research was able to identify the dominant source of fine sediment within the catchment, however this provided little information of the spatial origin of the generating process in itself; it simply showed that mudstone sediment was the major contributor (although a not insignificant finding). Parallel lines of evidence are necessary to elucidate further understanding of erosion and transport processes. Spatial information and geological maps could add further value, but even in conjunction with this sort of information it still is has difficulty since spatial extent is not the only determining factor and 2D maps fail to account for the layered complexity of geological sources. The vertical stratification of soil horizons and geological material adds a level of complexity which is not fully appreciated from spatial analysis. In many locations multiple samples were taken to represent each of the distinct geochemical sources. The ratio of distinct sources that actually contribute and compose sediment for that specific process is difficult to quantify, but may start with using sediment cores from the layered sediment sources to derive relative proportions of each geochemically distinct layer for each process.

Sediment storage needs to also be considered and information provided on how sediment from de-coupled processes, such as landslides in the hill country, reaches the active channel. The duration that sediment from a landslide remains stored on the hillslope has potential for continued geochemical change to occur and may not reflect the landslide origin. Furthermore, aquatic-geochemical analysis needs to be investigated to understand which elements are more susceptible to depletion and enrichment within fluvial transport.

Implications of the sediment source patterns for sediment management in the Manawatu suggest a greater focus on exposed areas of mudstone and erosion from the mountain ranges is important. The research has implications for other New Zealand catchments, many of which share similar catchment characteristics. Steep agricultural hill country underlain by soft sedimentary geology is particularly common for New Zealand's central North Island, as are catchments which have their headwaters in Mountain Ranges which produce comparable hydrological regimes and sediment supply. The findings presented here may be less relevant for high stream power and braided rivers of the South Island.

Incorporating some of these additions into future sediment fingerprinting research will likely improve the ability for sediment fingerprinting research to be utilized to influence environment management strategies globally.

References

Abu-Zeid, M. M., Baghdady, A. R. & El-Etr, H. A. 2001. Textural attributes, mineralogy and provenance of sand dune fields in the greater Al Ain area, United Arab Emirates. *Journal of Arid Environments,* 48**,** 475-499. Available: DOI 10.1006/jare.2000.0776.

Adams, R. & Elliott, S. 2006. Physically based modelling of sediment generation and transport under a large rainfall simulator. *Hydrological Processes,* 20**,** 2253-2270. Available: DOI 10.1002/hyp.6050.

Alt-Epping, U., Stuut, J. B. W., Hebbeln, D. & Schneider, R. 2009. Variations in sediment provenance during the past 3000 years off the Tagus River, Portugal. *Marine Geology,* 261**,** 82-91. Available: DOI 10.1016/j.margeo.2008.11.008.

Anderson, S. P., Dietrich, W. E. & Brimhall, G. H. 2002. Weathering profiles, mass-balance analysis, and rates of solute loss: Linkages between weathering and erosion in a small, steep catchment. *Geological Society of America Bulletin,* 114**,** 1143-1158.

Arribas, J., Critelli, S., Le Pera, E. & Tortosa, A. 2000. Composition of modem stream sand derived from a mixture of sedimentary and metamorphic source rocks (Henares River, Central Spain). *Sedimentary Geology,* 133**,** 27-48. Available: DOI 10.1016/s0037-0738(00)00026-9.

Ausseil, O. & Clark, M. 2007. *River Classification of the Manawatu-Wanganui Region to Support the Definition of the Life-Supporting Capacity Value: Technical Report to Support Policy Development*. Horizons Regional Council.

Basher, L. R., Payne, J. & Watson, B. 2012. *Suspended sediment yields in the Manawatu catchment analysis of data collected by Horizons Regional Council*. Report number: Report prepared by Landcare Research for AgResearch and Horizons Regional Council, April 2012.

Belmont, P., Willenbring, J., Schottler, S., Marquard, J., Kumarasamy, K. & Hemmis, J. 2014. Toward generalizable sediment fingerprinting with tracers that are conservative and nonconservative over sediment routing timescales. *Journal of Soils and Sediments,* 14**,** 1479-1492. Available: DOI 10.1007/s11368-014-0913-5.

Belyaev, V. R., Golosov, V. N., Markelov, M. V., Evrard, O., Ivanova, N. N., Paramonova, T. A. & Shamshurina, E. N. 2013. Using Chernobyl-derived ^{137}Cs to document recent sediment deposition rates on the River Plava floodplain (Central European Russia). *Hydrological Processes,* 27**,** 807-821. Available: DOI 10.1002/hyp.9461.

Benda, L. & Dunne, T. 1997. Stochastic forcing of sediment routing and storage in channel networks. *Water Resources Research,* 33**,** 2865-2880.

Best, J. L. 1988. Sediment transport and bed morphology at river channel confluences. *Sedimentology,* 35**,** 481-498. Available: DOI 10.1111/j.1365-3091.1988.tb00999.x.

Betts, H. D., Trustrum, N. A. & De Rose, R. C. 2003. Geomorphic changes in a complex gully system measured from sequential digital elevation models, and implications for management. *Earth Surface Processes and Landforms,* 28**,** 1043-1058.

Bilotta, G. S. & Brazier, R. E. 2008. Understanding the influence of suspended solids on water quality and aquatic biota. *Water Research,* 42**,** 2849-2861. Available: DOI 10.1016/j.watres.2008.03.018.

Blake, W. H., Ficken, K. J., Taylor, P., Russell, M. A. & Walling, D. E. 2012. Tracing crop-specific sediment sources in agricultural catchments. *Geomorphology,* 139/140**,** 322-329. Available: DOI 10.1016/j.geomorph.2011.10.036.

Blake, W. H., Wallbrink, P. J., Doerr, S. H., Shakesby, R. A. & Humphreys, G. S. 2006. Magnetic enhancement in wildfire-affected soil and its potential for sediment-source ascription. *Earth Surface Processes and Landforms,* 31**,** 249-264. Available: DOI 10.1002/esp.1247.

Bracken, L. J. 2010. Overland Flow and Soil Erosion. *In:* Burt, T. & Allison, R. (eds.) *Sediment Cascades: An Integrated Approach.* Chichester: John Wiley & Sons, Ltd.

Brasington, J. & Richards, K. 2000. Turbidity and suspended sediment dynamics in small catchments in the Nepal Middle Hills. *Hydrological processes,* 14**,** 2559-2574.

Brigham, M. E., Mccullough, C. J. & Wilkinson, P. 2001. Analysis of Suspended-Sediment Concentrations and Radioisotope Levels in the Wild Rice River Basin, Northwestern Minnesota, 1973-98. *Water Resources Investigations Report 01-4192.* U.S. Geological Survey.

Brown, A. G. 1985. The potential use of pollen in the identification of suspended sediment sources. *Earth Surface Processes and Landforms,* 10**,** 27-32. Available: DOI 10.1002/esp.3290100106.

Brunsden, D. 1974. *The degradation of coastal slope, Dorset, England*. Institute of British Geographers, Special Publication No. 7, 79 - 98.

Burrus, D., Thomas, R. L., Dominik, B., Vernet, J. P. & Dominik, J. 1990. Characteristics Of Suspended Sediment In The Upper Rhone River, Switzerland, Including The Particulate Forms Of Phosphorus. *Hydrological Processes,* 4**,** 85-98. Available: DOI 10.1002/hyp.3360040108.

Burt, T. P. & Allison, R. J. 2010. *Sediment Cascades: An Integrated Approach*, Wiley-Blackwell.

Caitcheon, G. G. 1993. Sediment Source Tracing Using Environmental Magnetism - A New Approach With Examples From Australia. *Hydrological Processes,* 7**,** 349-358. Available: DOI 10.1002/hyp.3360070402.

Caitcheon, G. G. 1998. The significance of various sediment magnetic mineral fractions for tracing sediment sources in Killimicat Creek. *CATENA,* 32**,** 131-142. Available: DOI 10.1016/s0341-8162(97)00057-x.

Calmano, W., Hong, J. & Förstner, U. 1993. Binding and mobilization of heavy metals in contaminated sediments affected by pH and redox potential. *Water Science & Technology***,** 223-235.

Carter, J., Owens, P. N., Walling, D. E. & Leeks, G. J. L. 2003. Fingerprinting suspended sediment sources in a large urban river system. *Science of The Total Environment,* 314–316**,** 513-534. Available: DOI 10.1016/s0048-9697(03)00071-8.

Charlesworth, S. M. & Lees, J. A. 2001. The application of some mineral magnetic measurements and heavy metal analysis for characterising fine sediments in an urban catchment, Coventry, UK. *Journal of Applied Geophysics,* 48**,** 113-125. Available: DOI 10.1016/s0926-9851(01)00084-2.

Charlton, R. 2008. *Fundamentals of Fluvial Geomorphology* London, Routledge.

Collins, A. J. & Owens, P. N. 2006. Introduction to Soil Erosion and Sediment Redistribution in River Catchments: Measurement, Modelling and Management in the 21st Century. *In:* Owens, P. N. & Collins, A. J. (eds.) *Soil Erosion and Sediment Redistribution in River Catchments: measurement, modelling and management* United Kingdom Cabi.

Collins, A. L., Naden, P. S., Sear, D. A., Jones, J. I., Foster, I. D. L. & Morrow, K. 2011. Sediment targets for informing river catchment management: international experience and prospects. *Hydrological Processes,* 25**,** 2112-2129. Available: DOI 10.1002/hyp.7965.

Collins, A. L., Pulley, S., Foster, I. D. L., Gellis, A., Porto, P. & Horowitz, A. J. Sediment source fingerprinting as an aid to catchment management: A review of the current state of knowledge and a methodological decision-tree for end-users. *Journal of Environmental Management*. Available: DOI http://dx.doi.org/10.1016/j.jenvman.2016.09.075.

Collins, A. L. & Walling, D. E. 2002. Selecting fingerprint properties for discriminating potential suspended sediment sources in river basins. *Journal of Hydrology,* 261**,** 218-244. Available: DOI 10.1016/s0022-1694(02)00011-2.

Collins, A. L. & Walling, D. E. 2004. Documenting catchment suspended sediment sources: problems, approaches and prospects. *Progress in Physical Geography,* 28**,** 159-196. Available: DOI 10.1191/0309133304pp409ra.

Collins, A. L. & Walling, D. E. 2006. Investigating the remobilization of fine sediment stored on the channel bed of lowland permeable catchments in the UK. *IAHS PUBLICATION,* 306**,** 471.

Collins, A. L. & Walling, D. E. 2007. The storage and provenance of fine sediment on the channel bed of two contrasting lowland permeable catchments, UK. *River Research and Applications,* 23**,** 429-450. Available: DOI 10.1002/rra.992.

Collins, A. L., Walling, D. E. & Leeks, G. J. L. 1997. Source type ascription for fluvial suspended sediment based on a quantitative composite fingerprinting technique. *Catena,* 29**,** 1-27. Available: DOI Doi 10.1016/S0341-8162(96)00064-1.

Collins, A. L., Walling, D. E. & Leeks, G. J. L. 1998. Use of composite fingerprints to determine the provenance of the contemporary suspended sediment load transported by rivers. *Earth Surface Processes and Landforms,* 23**,** 31-52. Available: DOI 10.1002/(sici)1096-9837(199801)23:1<31::aid-esp816>3.0.co;2-z.

Collins, A. L., Walling, D. E., Sichingabula, H. M. & Leeks, G. J. L. 2001. Suspended sediment source fingerprinting in a small tropical catchment and some management implications. *Applied Geography,* 21**,** 387-412. Available: DOI http://dx.doi.org/10.1016/S0143-6228(01)00013-3.

Collins, A. L., Walling, D. E., Webb, L. & King, P. 2010a. Apportioning catchment scale sediment sources using a modified composite fingerprinting technique incorporating property weightings and prior information. *Geoderma,* 155**,** 249-261. Available: DOI 10.1016/j.geoderma.2009.12.008.

Collins, A. L., Zhang, Y., Mcchesney, D., Walling, D. E., Haley, S. M. & Smith, P. 2012. Sediment source tracing in a lowland agricultural catchment in southern England using a modified procedure combining statistical analysis and numerical modelling. *Science of The Total Environment,* 414**,** 301-317. Available: DOI http://dx.doi.org/10.1016/j.scitotenv.2011.10.062.

Collins, A. L., Zhang, Y., Walling, D. E., Grenfell, S. E. & Smith, P. 2010b. Tracing sediment loss from eroding farm tracks using a geochemical fingerprinting procedure combining local and genetic algorithm optimisation. *Science of The Total Environment,* 408**,** 5461-5471. Available: DOI http://dx.doi.org/10.1016/j.scitotenv.2010.07.066.

Collins, A. L., Zhang, Y. S., Duethmann, D., Walling, D. E. & Black, K. S. 2013. Using a novel tracing-tracking framework to source fine-grained sediment loss to watercourses at sub-catchment scale. *Hydrological Processes,* 27**,** 959-974. Available: DOI 10.1002/hyp.9652.

Cooper, R. J., Krueger, T., Hiscock, K. M. & Rawlins, B. G. 2014. Sensitivity of fluvial sediment source apportionment to mixing model assumptions: A Bayesian model comparison. *Water Resources Research,* 50**,** 9031-9047. Available: DOI 10.1002/2014WR016194.

Cotton, J. A., Wharton, G., Bass, J. a. B., Heppell, C. M. & Wotton, R. S. 2006. The effects of seasonal changes to in-stream vegetation cover on patterns of flow and accumulation of sediment. *Geomorphology,* 77**,** 320-334. Available: DOI http://dx.doi.org/10.1016/j.geomorph.2006.01.010.

Cox, R., Lowe, D. R. & Cullers, R. L. 1995. The influence of sediment recycling and basement composition on evolution of mudrock chemistry in the southwestern United States. *Geochimica et Cosmochimica Acta,* 59**,** 2919-2940. Available: DOI http://dx.doi.org/10.1016/0016-7037(95)00185-9.

Crozier, M. 2005. Multiple-occurrence regional landslide events in New Zealand: hazard management issues. *Landslides,* 2**,** 247-256.

D'haen, K., Verstraeten, G. & Degryse, P. 2012. Fingerprinting historical fluvial sediment fluxes. *Progress in Physical Geography*. Available: DOI 10.1177/0309133311432581.

D'haen, K., Verstraeten, G., Dusar, B., Degryse, P., Haex, J. & Waelkens, M. 2013. Unravelling changing sediment sources in a Mediterranean mountain catchment: a Bayesian

fingerprinting approach. *Hydrological Processes,* 27**,** 896-910. Available: DOI 10.1002/hyp.9399.

Davies, T. R. & Korup, O. 2010. Sediment Cascades in Active Landscapes. *In:* Burt, T. & Allison, R. (eds.) *Sediment Cascade: An Integrated Approach.* Wiley-Blackwell.

Davis, C. M. & Fox, J. F. 2009. Sediment Fingerprinting: Review of the Method and Future Improvements for Allocating Nonpoint Source Pollution. *Journal of Environmental Engineering-Asce,* 135**,** 490-504. Available: DOI 10.1061/(asce)0733-9372(2009)135:7(490).

De Boer, D. H. & Crosby, G. 1995. Evaluating the potential of SEM/EDS analysis for fingerprinting suspended sediment derived from two contrasting topsoils. *CATENA,* 24**,** 243-258. Available: DOI http://dx.doi.org/10.1016/0341-8162(95)00029-4.

De Miguel, E., Charlesworth, S., Ordóñez, A. & Seijas, E. 2005. Geochemical fingerprints and controls in the sediments of an urban river: River Manzanares, Madrid (Spain). *Science of The Total Environment,* 340**,** 137-148. Available: DOI http://dx.doi.org/10.1016/j.scitotenv.2004.07.031.

De Rose, R. C. & Basher, L. R. 2011a. Measurement of river bank and cliff erosion from sequential LIDAR and historical aerial photography. *Geomorphology,* 126**,** 132-147.

De Rose, R. C. & Basher, L. R. 2011b. *Strategy for the development of a New Zealand SedNet*. Landcare Research. Report number: Landcare Research Contract Report LC226 for AgResearch and Ministry of Science and Innovation

Devereux, O. H., Prestegaard, K. L., Needelman, B. A. & Gellis, A. C. 2010. Suspended-sediment sources in an urban watershed, Northeast Branch Anacostia River, Maryland. *Hydrological processes,* 24**,** 1391-1403.

Dietrich, W. E. & Wilson, C. J. 1978. Sediment budget for a small catchment in mountainous terrain. *Zeitschrift für geomorphologie supplementband,* 29**,** 191 - 206.

Dill, H. G. 1998. A review of heavy minerals in clastic sediments with case studies from the alluvial-fan through the nearshore-marine environments. *Earth-Science Reviews,* 45**,** 103-132. Available: DOI 10.1016/s0012-8252(98)00030-0.

Douglas, G. B., Gray, C. M., Hart, B. T. & Beckett, R. 1995. A Strontium Isotopic Investigation of the Origin of Suspended Particulate Matter (SPM) in The Murray-Darling River System, Australia. *Geochimica Et Cosmochimica Acta,* 59**,** 3799-3815. Available: DOI 10.1016/0016-7037(95)00266-3.

Dymond, J., Herzig, A. & Ausseil, A.-G. 2014. *Using SedNetNZ to assess the impact of the Sustainable Land Use Initiative in the Manawatu-Wanganui region on river sediment loads*. Horizons Regional Council. Report number: Lancare Research Contract Report prepared for Horizons Regional Council 2014/EXT/1367.

Dymond, J., Shepherd, J. D. & Horizons Regional Council. 2006a. *Highly erodible land in the Manawatu-Wanganui region*. Landcare Research. Report number: Landcare Research Contract Report: 0607/027.

Dymond, J. R., Ausseil, A.-G., Shepherd, J. D. & Buettner, L. 2006b. Validation of a region-wide model of landslide susceptibility in the Manawatu–Wanganui region of New Zealand. *Geomorphology,* 74**,** 70-79. Available: DOI http://dx.doi.org/10.1016/j.geomorph.2005.08.005.

Eberl, D. D. 2004. Quantitative mineralogy of the Yukon River system: Changes with reach and season, and determining sediment provenance. *American Mineralogist,* 89**,** 1784-1794.

Ergin, M., Keskin, S., Dogan, A. U., Kadioglu, Y. K. & Karakas, Z. 2007. Grain size and heavy mineral distribution as related to hinterland and environmental conditions for modern beach sediments from the Gulfs of Antalya and Finike, eastern Mediterranean. *Marine Geology,* 240**,** 185-196. Available: DOI 10.1016/j.margeo.2007.02.006.

Erskine, W. D. 2013. Soil colour as a tracer of sediment dispersion from erosion of forest roads in Chichester State Forest, NSW, Australia. *Hydrological Processes,* 27**,** 933-942. Available: DOI 10.1002/hyp.9412.

Evrard, O., Navratil, O., Ayrault, S., Ahmadi, M., Nemery, J., Legout, C., Lefevre, I., Poirel, A., Bonte, P. & Esteves, M. 2011. Combining suspended sediment monitoring and fingerprinting to determine the spatial origin of fine sediment in a mountainous river catchment. *Earth Surface Processes and Landforms,* 36**,** 1072-1089. Available: DOI 10.1002/esp.2133.

Evrard, O., Nemery, J., Gratiot, N., Duvert, C., Ayrault, S., Lefevre, I., Poulenard, J., Prat, C., Bonte, P. & Esteves, M. 2010. Sediment dynamics during the rainy season in tropical highland catchments of central Mexico using fallout radionuclides. *Geomorphology,* 124**,** 42-54. Available: DOI 10.1016/j.geomorph.2010.08.007.

Evrard, O., Poulenard, J., Némery, J., Ayrault, S., Gratiot, N., Duvert, C., Prat, C., Lefèvre, I., Bonté, P. & Esteves, M. 2013. Tracing sediment sources in a tropical highland catchment of central Mexico by using conventional and alternative fingerprinting methods. *Hydrological Processes,* 27**,** 911-922. Available: DOI 10.1002/hyp.9421.

Ferguson, R. I. 1981. Channel form and channel changes. *In:* Lewin, J. (ed.) *British Rivers.* London: Allen and Unwin.

Foster, I. D. L., Boardman, J. & Keay-Bright, J. 2007. Sediment tracing and environmental history for two small catchments, Karoo Uplands, South Africa. *Geomorphology,* 90**,** 126-143. Available: DOI 10.1016/j.geomorph.2007.01.011.

Foster, I. D. L. & Lees, J. A. 2000. Tracers in Geomorphology: Theory and Applications in Tracing Fine Particulate Sediments. *In:* Foster, I. D. L. (ed.) *Tracers in Geomorphology.* Chichester, UK: John Wiley and Sons.

Foster, I. D. L., Lees, J. A., Owens, P. N. & Walling, D. E. 1998. Mineral magnetic characterization of sediment sources from an analysis of lake and floodplain sediments in the catchments of the Old Mill reservoir and Slapton Ley, South Devon, UK. *Earth Surface Processes and Landforms,* 23**,** 685-703. Available: DOI 10.1002/(sici)1096-9837(199808)23:8<685::aid-esp873>3.0.co;2-8.

Fox, J. F. & Papanicolaou, A. N. 2008a. Application of the spatial distribution of nitrogen stable isotopes for sediment tracing at the watershed scale. *Journal of Hydrology,* 358**,** 46-55. Available: DOI 10.1016/j.jhydrol.2008.05.032.

Fox, J. F. & Papanicolaou, A. N. 2008b. An un-mixing model to study watershed erosion processes. *Advances in Water Resources,* 31**,** 96-108. Available: DOI 10.1016/j.advwatres.2007.06.008.

Frontline Systems Inc. 2010. *Frontline Solver: Premium Solver Platform for Mac User Guide.* [Online]. Available: Retrieved from http://www.solver.com/files/support/PSP-for-MacOS_Manual.pdf Retrieved from http://www.solver.com/files/support/PSP-for-MacOS_Manual.pdf].

Fryirs, K. A., Brierley, G. J., Preston, N. J. & Kasai, M. 2007. Buffers, barriers and blankets: The (dis) connectivity of catchment-scale sediment cascades. *CATENA,* 70**,** 49-67.

Fuller, I. C. 2009. Statement of Evidence In the Matter of the proposed One Plan of the Council. *Manawatu-Whanganui Regional Council Hearings Panel.*

Fuller, I. C. & Heerdegen, R. G. 2005. The February 2004 floods in the Manawatu, New Zealand: Hydrological significance and impact on channel morphology. *Journal of hydrology. New Zealand,* 44**,** 75-90.

Fuller, I. C., Riedler, R. A., Glade, T., Bell, R. & Marden, M. 2016. Landslide-driven erosion and slope-channel coupling in steep, forested terrain, Ruahine Ranges, New Zealand, 1946-2011. *Catena,* 142**,** 252-268.

Gellis, A. C., Hupp, C. R., Pavich, M. J., Landwehr, J. M., Banks, W. S., Hubbard, B. E., Langland, M. J., Ritchie, J. C. & Reuter, J. M. 2009. *Sources, transport, and storage of sediment at selected sites in the Chesapeake Bay Watershed*, US Geological Survey.

Gellis, A. C. & Noe, G. B. 2013. Sediment source analysis in the Linganore Creek watershed, Maryland, USA, using the sediment fingerprinting approach: 2008 to 2010. *Journal of Soils and Sediments***,** 1-19.

Gibbard, R. 2006. *Water quality trends in the manawatu-wanganui region 1989-2004*, Horizons Regional Council.

Gibbs, M. M. 2008. Identifying source soils in contemporary estuarine sediments: A new compound-specific isotope method. *Estuaries and Coasts,* 31**,** 344-359. Available: DOI 10.1007/s12237-007-9012-9.

Gingele, F. X. & De Deckker, P. 2005. Clay mineral, geochemical and Sr-Nd isotopic fingerprinting of sediments in the Murray-Darling fluvial system, southeast Australia. *Australian Journal of Earth Sciences,* 52**,** 965-974. Available: DOI 10.1080/08120090500302301.

Gomez, B., Banbury, K., Marden, M., Trustrum, N. A., Peacock, D. H. & Hoskin, P. J. 2003. Gully erosion and sediment production: Te Weraroa Stream, New Zealand. *Water Resources Research,* 39. Available: DOI 10.1029/2002wr001342.

Gomi, T., Sidle, R. C. & Richardson, J. S. 2002. Understanding Processes and Downstream Linkages of Headwater Systems: Headwaters differ from downstream reaches by their close coupling to hillslope processes, more temporal and spatial variation, and their need for different means of protection from land use. *BioScience,* 52**,** 905-916. Available: DOI 10.1641/0006-3568(2002)052[0905:upadlo]2.0.co;2.

Grigsby, J. D. 1992. Chemical fingerprinting in detrital ilmenite; a viable alternative in provenance research? *Journal of Sedimentary Research,* 62**,** 331-337. Available: DOI 10.1306/d42678f7-2b26-11d7-8648000102c1865d.

Grimshaw, D. L. & Lewin, J. 1980. Source identification for suspended sediments. *Journal of Hydrology,* 47**,** 151-162. Available: DOI 10.1016/0022-1694(80)90053-0.

Gruszowski, K. E., Foster, I. D. L., Lees, J. A. & Charlesworth, S. M. 2003. Sediment sources and transport pathways in a rural catchment, Herefordshire, UK. *Hydrological Processes,* 17**,** 2665-2681. Available: DOI 10.1002/hyp.1296.

Haddadchi, A., Olley, J. & Laceby, P. 2014. Accuracy of mixing models in predicting sediment source contributions. *Science of The Total Environment,* 497–498**,** 139-152. Available: DOI http://dx.doi.org/10.1016/j.scitotenv.2014.07.105.

Haddadchi, A., Ryder, D. S., Evrard, O. & Olley, J. 2013. Sediment fingerprinting in fluvial systems: review of tracers, sediment sources and mixing models. *International Journal of Sediment Research,* 28**,** 560-578. Available: DOI http://dx.doi.org/10.1016/S1001-6279(14)60013-5.

Haigh, M. 1977. The use of erosion pins in the study of slope evolution. *British Geomorphological Research Group Technical Bulletin,* 18**,** 31-49.

Hancock, G. J. & Revill, A. T. 2013. Erosion source discrimination in a rural Australian catchment using compound-specific isotope analysis (CSIA). *Hydrological Processes,* 27**,** 923-932. Available: DOI 10.1002/hyp.9466.

Hardy, F., Bariteau, L., Lorrain, S., Theriault, I., Gagnon, G., Messier, D. & Rougerie, J. F. 2010. Geochemical tracing and spatial evolution of the sediment bed load of the Romaine River, Quebec, Canada. *CATENA,* 81**,** 66-76. Available: DOI 10.1016/j.catena.2010.01.005.

Hatfield, R. G. & Maher, B. A. 2008. Suspended sediment characterization and tracing using a magnetic fingerprinting technique: Bassenthwaite Lake, Cumbria, UK. *Holocene,* 18**,** 105-115. Available: DOI 10.1177/0959683607085600.

Hatfield, R. G. & Maher, B. A. 2009. Fingerprinting upland sediment sources: particle size-specific magnetic linkages between soils, lake sediments and suspended sediments. *Earth Surface Processes and Landforms,* 34**,** 1359-1373. Available: DOI 10.1002/esp.1824.

Haygarth, P. M., Condron, L. M., Heathwaite, A. L., Turner, B. L. & Harris, G. P. 2005. The phosphorus transfer continuum: Linking source to impact with an interdisciplinary and multi-scaled approach. *Science of The Total Environment,* 344**,** 5-14. Available: DOI http://dx.doi.org/10.1016/j.scitotenv.2005.02.001.

He, Q., Walling, D. E. & Owens, P. N. 1996. Interpreting the Cs-137 profiles observed in several small lakes and reservoirs in southern England. *Chemical Geology,* 129**,** 115-131. Available: DOI 10.1016/0009-2541(95)00149-2.

Henderson, R. & Diettrich, J. 2007. *Statistical analysis of river flow data in the Horizons Region*. Christchurch, New Zealand: NIWA. Report number: NIWA Client Report: CHC2006-154.

Hewitt, A. E. 1998. *New Zealand soil classification, 2nd ed. ,* Lincoln, Canterbury, New Zealand, Manaaki Whenua Press.

Hicks, D. M., Gomez, B. & Trustrum, N. A. 2000. Erosion thresholds and suspended sediment yields, Waipaoa River basin, New Zealand. *Water Resources Research,* 36**,** 1129-1142.

Hicks, D. M., Gomez, B. & Trustrum, N. A. 2004. Event suspended sediment characteristics and the generation of hyperpycnal plumes at river mouths: East Coast continental margin, North Island, New Zealand. *The Journal of Geology,* 112**,** 471-485.

Hicks, D. M. & Griffiths, G. A. 1992. Sediment load. *Waters of New Zealand***,** 229-248.

Hicks, D. M., Hill, J. & Shankar, U. 1996. Variation of suspended sediment yields around New Zealand: The relative importance of rainfall and geology. *In:* Walling, D. E. & Webb, B. W. (eds.) *Erosion and Sediment Yield: Global and Regional Perspectives.* Wallingford: Int Assoc Hydrological Sciences.

Hicks, M. & Hoyle, J. 2012. *Analysis of suspended sediment yields from the rivers in the Horizons sediment monitoring program*. Report number: NIWA Client Report No. CHC2012-107.

Hicks, M., Shankar, U. & Mckerchar, A. 2003. Sediment yield estimates: a GIS tool. *science,* 11**,** 24-25.

Hillier, S. 2001. Particulate composition and origin of suspended sediment in the R. Don, Aberdeenshire, UK. *Science of The Total Environment,* 265**,** 281-293. Available: DOI 10.1016/s0048-9697(00)00664-1.

Horizons Regional Council 2011. Ours. The Manawatu River Leaders' Accord Action Plan. Horizons Regional Council.

Horowitz, A. J. & Elrick, K. A. 1987. The relation of stream sediment surface area, grain size and composition to trace element chemistry. *Applied Geochemistry,* 2**,** 437-451.

Hounslow, M. W. & Morton, A. C. 2004. Evaluation of sediment provenance using magnetic mineral inclusions in clastic silicates: comparison with heavy mineral analysis. *Sedimentary Geology,* 171**,** 13-36. Available: DOI 10.1016/j.sedgeo.2004.05.008.

Hughes, A. O., Olley, J. M., Croke, J. C. & Mckergow, L. A. 2009. Sediment source changes over the last 250 years in a dry-tropical catchment, central Queensland, Australia. *Geomorphology,* 104**,** 262-275. Available: DOI http://dx.doi.org/10.1016/j.geomorph.2008.09.003.

Ibm Corp. 2012. IBM SPSS Statistics for Windows. 21.0 ed. Armonk, New York: IBM Corp.

Jenkins, P. A., Duck, R. W., Rowan, J. S. & Walden, J. 2002. Fingerprinting of bed sediment in the Tay Estuary, Scotland: an environmental magnetism approach. *Hydrology and Earth System Sciences,* 6**,** 1007-1016.

Jin, Z. D., Li, F. C., Cao, J. J., Wang, S. M. & Yu, J. M. 2006. Geochemistry of Daihai Lake sediments, Inner Mongolia, north China: Implications for provenance, sedimentary sorting, and catchment weathering. *Geomorphology,* 80**,** 147-163. Available: DOI 10.1016/j.geomorph.2006.02.006.

Kasai, M., Brierley, G. J., Page, M. J., Marutani, T. & Trustrum, N. A. 2005. Impacts of land use change on patterns of sediment flux in Weraamaia catchment, New Zealand. *CATENA,* 64**,** 27-60. Available: DOI http://dx.doi.org/10.1016/j.catena.2005.06.014.

Kasanzu, C., Maboko, M. a. H. & Manya, S. 2008. Geochemistry of fine-grained clastic sedimentary rocks of the Neoproterozoic Ikorongo Group, NE Tanzania: Implications for provenance and source rock weathering. *Precambrian Research,* 164**,** 201-213. Available: DOI 10.1016/j.precamres.2008.04.007.

Kemp, P., Sear, D., Collins, A., Naden, P. & Jones, I. 2011. The impacts of fine sediment on riverine fish. *Hydrological Processes,* 25**,** 1800-1821. Available: DOI 10.1002/hyp.7940.

Kenworthy, S. T. & Rhoads, B. L. 1995. Hydrologic control of spatial patterns of suspended sediment concentration at a stream confluence. *Journal of Hydrology,* 168**,** 251-263.

Klages, M. G. & Hsieh, Y. P. 1975. Suspended Solids Carried by the Gallatin River of Southwestern Montana: II. Using Mineralogy for Inferring Sources. *J. Environ. Qual.,* 4**,** 68-73. Available: DOI 10.2134/jeq1975.00472425000400010016x.

Klein, M. 1984. Anti clockwise hysteresis in suspended sediment concentration during individual storms: Holbeck catchment; Yorkshire, England. *CATENA,* 11**,** 251-257. Available: DOI http://dx.doi.org/10.1016/0341-8162(84)90014-6.

Koiter, A. J., Lobb, D. A., Owens, P. N., Petticrew, E. L., Tiessen, K. H. & Li, S. 2013a. Investigating the role of connectivity and scale in assessing the sources of sediment in an agricultural watershed in the Canadian prairies using sediment source fingerprinting. *Journal of Soils and Sediments,* 13**,** 1676-1691.

Koiter, A. J., Owens, P. N., Petticrew, E. L. & Lobb, D. A. 2013b. The behavioural characteristics of sediment properties and their implications for sediment fingerprinting as an approach for identifying sediment sources in river basins. *Earth-Science Reviews,* 125**,** 24-42. Available: DOI http://dx.doi.org/10.1016/j.earscirev.2013.05.009.

Krause, A. K., Franks, S. W., Kalma, J. D., Loughran, R. J. & Rowan, J. S. 2003. Multi-parameter fingerprinting of sediment deposition in a small gullied catchment in SE Australia. *CATENA,* 53**,** 327-348. Available: DOI 10.1016/s0341-8162(03)00085-7.

Krein, A., Petticrew, E. & Udelhoven, T. 2003. The use of fine sediment fractal dimensions and colour to determine sediment sources in a small watershed. *CATENA,* 53**,** 165-179. Available: DOI 10.1016/s0341-8162(03)00021-3.

Krishnappan, B. G., Chambers, P. A., Benoy, G. & Culp, J. 2009. Sediment source identification: a review and a case study in some Canadian streams. *Canadian Journal of Civil Engineering,* 36**,** 1622-1633. Available: DOI 10.1139/l09-110.

Laceby, J. P. & Olley, J. 2015. An examination of geochemical modelling approaches to tracing sediment sources incorporating distribution mixing and elemental correlations. *Hydrological Processes,* 29**,** 1669-1685. Available: DOI 10.1002/hyp.10287.

Lamba, J., Karthikeyan, K. G. & Thompson, A. M. 2015. Apportionment of suspended sediment sources in an agricultural watershed using sediment fingerprinting. *Geoderma,* 239–240**,** 25-33. Available: DOI http://dx.doi.org/10.1016/j.geoderma.2014.09.024.

Landcare Research NZ Ltd 2012. LCDB v3.0 - Land Cover Database version 3. https://lris.scinfo.org.nz/layer/304-lcdb-v30-deprecated/.

Lawler, D. 1986. River bank erosion and the influence of frost: a statistical examination. *Transactions of the Institute of British Geographers***,** 227-242.

Lawler, D. M., Thorne, C. R. & Hooke, J. M. 1997. Bank Erosion and Instability *In:* Thorne, C. R., Hey, R. D. & Newson, M. D. (eds.) *Applied Fluvial Geomorphology for River Engineering and Management.* England: Jon Wiley & Sons.

Lee, S. G., Kim, J. K., Yang, D. Y. & Kim, J. Y. 2008. Rare earth element geochemistry and Nd isotope composition of stream sediments, south Han River drainage basin, Korea. *Quaternary International,* 176**,** 121-134. Available: DOI 10.1016/j.quaint.2007.05.012.

Lenzi, M. A. & Marchi, L. 2000. Suspended sediment load during floods in a small stream of the Dolomites (northeastern Italy). *CATENA,* 39**,** 267-282. Available: DOI http://dx.doi.org/10.1016/S0341-8162(00)00079-5.

Lewis, J. 1996. Turbidity-controlled suspended sediment sampling for runoff-event load estimation. *Water resources research,* 32**,** 2299-2310.

Mabit, L., Benmansour, M. & Walling, D. E. 2008. Comparative advantages and limitations of the fallout radionuclides ^{137}Cs, $^{210}Pb_{ex}$ and ^{7}Be for assessing soil erosion and sedimentation. *Journal of Environmental Radioactivity,* 99**,** 1799-1807. Available: DOI 10.1016/j.jenvrad.2008.08.009.

Maher, B. A., Watkins, S. J., Brunskill, G., Alexander, J. & Fielding, C. R. 2009. Sediment provenance in a tropical fluvial and marine context by magnetic 'fingerprinting' of transportable sand fractions. *Sedimentology,* 56**,** 841-861. Available: DOI 10.1111/j.1365-3091.2008.00999.x.

Marden, M. 1984. Geology and its relationship to erosion in the Southern Ruahine Range. *North Island, New Zealand Unpublished PhD thesis, lodged in the library, Massey University, Palmerston North*.

Marden, M. 2011. *Sedimentation History of Waipaoa Catchment. Envirolink project 1015-GS DC95*. Landcare Research. Report number: Landcare Research Contract Report: LC790. Available: http://www.envirolink.govt.nz/PageFiles/735/1015-GSDC95%20Sedimentation%20history%20of%20Waipaoa%20catchment.pdf.

Marden, M., Arnold, G., Gomez, B. & Rowan, D. 2005. Pre-and post-reforestation gully development in Mangatu Forest, East Coast, North Island, New Zealand. *River Research and Applications,* 21**,** 757-771.

Martínez-Carreras, N., Krein, A., Gallart, F., Iffly, J. F., Pfister, L., Hoffmann, L. & Owens, P. N. 2010a. Assessment of different colour parameters for discriminating potential suspended sediment sources and provenance: A multi-scale study in Luxembourg. *Geomorphology,* 118**,** 118-129. Available: DOI 10.1016/j.geomorph.2009.12.013.

Martínez-Carreras, N., Krein, A., Udelhoven, T., Gallart, F., Iffly, J. F., Hoffmann, L., Pfister, L. & Walling, D. E. 2010b. A rapid spectral-reflectance-based fingerprinting approach for documenting suspended sediment sources during storm runoff events. *Journal of Soils and Sediments,* 10**,** 400-413. Available: DOI 10.1007/s11368-009-0162-1.

Marzolff, I. & Poesen, J. 2009. The potential of 3D gully monitoring with GIS using high-resolution aerial photography and a digital photogrammetry system. *Geomorphology,* 111**,** 48-60. Available: DOI http://dx.doi.org/10.1016/j.geomorph.2008.05.047.

Matisoff, G., Bonniwell, E. C. & Whiting, P. J. 2002. Soil Erosion and Sediment Sources in an Ohio Watershed using Beryllium-7, Cesium-137, and Lead-210. *J. Environ. Qual.,* 31**,** 54-61. Available: DOI 10.2134/jeq2002.5400.

Mcconnachie, J. L. & Petticrew, E. L. 2006. Tracing organic matter sources in riverine suspended sediment: Implications for fine sediment transfers. *Geomorphology,* 79**,** 13-26. Available: DOI 10.1016/j.geomorph.2005.09.011.

Mcdonough, W. F. & Sun, S. S. 1995. The composition of the Earth. *Chemical Geology,* 120**,** 223-253. Available: DOI http://dx.doi.org/10.1016/0009-2541(94)00140-4.

Mckinley, R., Radcliffe, D. & Mukundan, R. 2013. A streamlined approach for sediment source fingerprinting in a Southern Piedmont watershed, USA. *Journal of Soils and Sediments***,** 1-16.

Mclennan, S. M. 1993. Weathering and global denudation. *The Journal of Geology,* 101**,** 295-303.

Mclennan, S. M. 2001. Relationships between the trace element composition of sedimentary rocks and upper continental crust. *Geochemistry, Geophysics, Geosystems,* 2. Available: DOI 10.1029/2000GC000109.

Merritt, W. S., Letcher, R. A. & Jakeman, A. J. 2003. A review of erosion and sediment transport models. *Environmental Modelling & Software,* 18**,** 761-799. Available: DOI 10.1016/s1364-8152(03)00078-1.

Milliman, J. D. & Farnsworth, K. L. 2011. *River Discharge to the Coastal Ocean: A Global Synthesis,* New York, Cambridge University Press.

Minella, J. P. G., Walling, D. E. & Merten, G. H. 2008. Combining sediment source tracing techniques with traditional monitoring to assess the impact of improved land management on catchment sediment yields. *Journal of Hydrology,* 348**,** 546-563. Available: DOI 10.1016/j.jhydrol.2007.10.026.

Ministry for the Environment & Statistics New Zealand. 2015. *New Zealand's Environmental Reporting Series: Environment Aotearoa 2015*. Available from www.mfe.govt.nz and www.stats.govt.nz.

Montgomery, D. R. 2007. Is agriculture eroding civilization's foundation? *GSA TODAY,* 17**,** 4.

Moore, J. E. 1961. Petrography of north-eastern Lake Michigan bottom sediments. . *Journal of Sedimentary Petrology,* 31**,** 402 - 436.

Morton, A. C. & Hallsworth, C. R. 1999. Processes controlling the composition of heavy mineral assemblages in sandstones. *Sedimentary Geology,* 124**,** 3-29. Available: DOI 10.1016/s0037-0738(98)00118-3.

Mosley, M. P. 1978. Erosion on the south-eastern Ruahine range: its implications for downstream river control. *New Zealand Journal of Forestry,* 23**,** 20-48.

Motha, J. A., Wallbrink, P. J., Hairsine, P. B. & Grayson, R. B. 2002. Tracer properties of eroded sediment and source material. *Hydrological Processes,* 16**,** 1983-2000. Available: DOI 10.1002/hyp.397.

Motha, J. A., Wallbrink, P. J., Hairsine, P. B. & Grayson, R. B. 2003. Determining the sources of suspended sediment in a forested catchment in southeastern Australia. *Water Resources Research,* 39**,** 1056. Available: DOI 10.1029/2001WR000794.

Motha, J. A., Wallbrink, P. J., Hairsine, P. B. & Grayson, R. B. 2004. Unsealed roads as suspended sediment sources in an agricultural catchment in south-eastern Australia. *Journal of Hydrology,* 286**,** 1-18. Available: DOI http://dx.doi.org/10.1016/j.jhydrol.2003.07.006.

Naden, P. 2010. The Fine-Sediment Cascade. *In:* Burt, T. & Allison, R. (eds.) *Sediment Cascade: An Integrated Approach.* Wiley-Blackwell.

Nagle, G. N. & Ritchie, J. C. 2004. Wheat field erosion rates and channel bottom sediment sources in an intensively cropped northeastern oregon drainage basin. *Land Degradation & Development,* 15**,** 15-26. Available: DOI 10.1002/ldr.587.

Nesbitt, H. & Young, G. 1982. Early Proterozoic climates and plate motions inferred from major element chemistry of lutites. *Nature,* 299**,** 715-717.

Nesbitt, H. W., Young, G. M., Mclennan, S. M. & Keays, R. R. 1996. Effects of chemical weathering and sorting on the petrogenesis of siliciclastic sediments, with implications for provenance studies. *Journal of Geology,* 104**,** 525-542.

Nicholas, A. P., Ashworth, P. J., Kirkby, M. J., Macklin, M. G. & Murray, T. 1995. Sediment slugs: Large-scale fluctuations in fluvial sediment transport rates and storage volumes. *Progress in Physical Geography,* 19**,** 500-519. Available: DOI 10.1177/030913339501900404.

Nichols, K. K., Bierman, P. R., Hooke, R. L., Clapp, E. M. & Caffee, M. 2002. Quantifying sediment transport on desert piedmonts using Be-10 and Al-26. *Geomorphology,* 45**,** 105-125. Available: DOI 10.1016/s0169-555x(01)00192-1.

Nosrati, K., Govers, G., Semmens, B. X. & Ward, E. J. 2014. A mixing model to incorporate uncertainty in sediment fingerprinting. *Geoderma,* 217–218**,** 173-180. Available: DOI http://dx.doi.org/10.1016/j.geoderma.2013.12.002.

Oldfield, F. 2007. Sources of fine-grained magnetic minerals in sediments: a problem revisited. *Holocene,* 17**,** 1265-1271. Available: DOI 10.1177/0959683607085135.

Oldfield, F. & Crowther, J. 2007. Establishing fire incidence in temperate soils using magnetic measurements. *Palaeogeography Palaeoclimatology Palaeoecology,* 249**,** 362-369. Available: DOI 10.1016/j.palaeo.2007.02.007.

Oldfield, F., Rummery, T. A., Thompson, R. & Walling, D. E. 1978. Identifying Sources of Suspended Sediments in Streams by Means of Magnetic Measurements. *Geophysical Journal of the Royal Astronomical Society,* 53**,** 146-146.

Oldfield, F., Rummery, T. A., Thompson, R. & Walling, D. E. 1979. Identification of Suspended Sediment Sources by Means of Magnetic Measurements - Some Preliminary-Results. *Water Resources Research,* 15**,** 211-218. Available: DOI 10.1029/WR015i002p00211.

Olley, J., Burton, J., Smolders, K., Pantus, F. & Pietsch, T. 2013. The application of fallout radionuclides to determine the dominant erosion process in water supply catchments of subtropical South-east Queensland, Australia. *Hydrological Processes,* 27**,** 885-895. Available: DOI 10.1002/hyp.9422.

Olley, J. & Caitcheon, G. 2000. Major element chemistry of sediments from the Darling-Barwon River and its tributaries: implications for sediment and phosphorus sources. *Hydrological Processes,* 14**,** 1159-1175. Available: DOI 10.1002/(sici)1099-1085(200005)14:7<1159::aid-hyp6>3.0.co;2-p.

Owens, P. N., Batalla, R. J., Collins, A. J., Gomez, B., Hicks, D. M., Horowitz, A. J., Kondolf, G. M., Marden, M., Page, M. J., Peacock, D. H., Petticrew, E. L., Salomons, W. & Trustrum, N. A. 2005. Fine-grained sediment in river systems: Environmental significance and management issues. *River Research and Applications,* 21**,** 693-717. Available: DOI 10.1002/rra.878.

Owens, P. N. & Walling, D. E. 2002. The phosphorus content of fluvial sediment in rural and industrialized river basins. *Water Research,* 36**,** 685-701. Available: DOI 10.1016/s0043-1354(01)00247-0.

Owens, P. N., Walling, D. E., Carton, J., Meharg, A. A., Wright, J. & Leeks, G. J. L. 2001. Downstream changes in the transport and storage of sediment-associated contaminants (P, Cr and PCBs) in agricultural and industrialized drainage basins. *Science of The Total Environment,* 266**,** 177-186. Available: DOI 10.1016/s0048-9697(00)00729-4.

Owens, P. N., Walling, D. E. & Leeks, G. J. L. 1999. Use of floodplain sediment cores to investigate recent historical changes in overbank sedimentation rates and sediment sources in the catchment of the River Ouse, Yorkshire, UK. *CATENA,* 36**,** 21-47. Available: DOI 10.1016/s0341-8162(99)00010-7.

Page, M., Trustrum, N. & Gomez, B. 2000. Implications of a Century of Anthropogenic Erosion for Future Land Use in the Gisborne-East Coast Region of New Zealand. *New Zealand Geographer,* 56**,** 13-24. Available: DOI 10.1111/j.1745-7939.2000.tb01571.x.

Parkner, T., Page, M. J., Marutani, T. & Trustrum, N. A. 2006. Development and controlling factors of gullies and gully complexes, East Coast, New Zealand. *Earth Surface Processes and Landforms,* 31**,** 187-199.

Peart, M. R. 1993. Using sediment properties as natural tracers for sediment source: two case studies from Hong Kong. *In:* Peters, N. E., Hoehn, E., Liebundgut, C., Tase, N. & Walling, D. E. (eds.) *Tracers in Hydrology.* Wallingford: IAHS Press.

Peart, M. R. & Walling, D. E. 1986. Fingerprinting sediment source: the example of a drainage basin in Devon, UK. *Drainage Basin Sediment Delivery,* IAHS Publication 159**,** 41 - 55.

Petrelli, M., Poli, G., Perugini, D. & Peccerillo, A. 2005. PetroGraph: A new software to visualize, model, and present geochemical data in igneous petrology. *Geochemistry, Geophysics, Geosystems,* 6. Available: DOI 10.1029/2005GC000932.

Phillips, J. M., Russell, M. A. & Walling, D. E. 2000. Time-integrated sampling of fluvial suspended sediment: a simple methodology for small catchments. *Hydrological Processes,* 14**,** 2589-2602. Available: DOI 10.1002/1099-1085(20001015)14:14<2589::aid-hyp94>3.0.co;2-d.

Porto, P., Walling, D. E. & Callegari, G. 2005. Investigating sediment sources within a small catchment in sourthern Italy. *In:* Walling, D. E. & Horowitz, A. J. (eds.) *Sediment Budgets 1: Proceedings of symposium S1 held during the Seventh IAHS Scientific Assembly at Foz do Iguaçu, Brazil.* Wallingford, U.K.: IAHS Pub.

Porto, P., Walling, D. E. & Callegari, G. 2013. Using ^{137}Cs and $^{210}Pb_{ex}$ measurements to investigate the sediment budget of a small forested catchment in southern Italy. *Hydrological Processes,* 27**,** 795-806. Available: DOI 10.1002/hyp.9471.

Prosser, I., Rustomji, P., Young, B., Moran, C. & Hughes, A. 2001. *Constructing river basin sediment budgets for the National Land and Water Resources Audit*, CSIRO Land and Water Canberra.

Pulley, S., Foster, I. & Antunes, P. 2015. The uncertainties associated with sediment fingerprinting suspended and recently deposited fluvial sediment in the Nene river basin. *Geomorphology,* 228**,** 303-319. Available: DOI http://dx.doi.org/10.1016/j.geomorph.2014.09.016.

Rattenbury, M. & Isaac, M. 2012. The QMAP 1: 250 000 geological map of New Zealand project. *New Zealand Journal of Geology and Geophysics,* 55**,** 393-405.

Reid, L. M. & Page, M. J. 2003. Magnitude and frequency of landsliding in a large New Zealand catchment. *Geomorphology,* 49**,** 71-88. Available: DOI 10.1016/s0169-555x(02)00164-2.

Rhoads, B. L. & Sukhodolov, A. N. 2008. Lateral momentum flux and the spatial evolution of flow within a confluence mixing interface. *Water Resources Research,* 44**,** W08440. Available: DOI 10.1029/2007WR006634.

Rhoton, F. E., Emmerich, W. E., Dicarlo, D. A., Mcchesney, D. S., Nearing, M. A. & Ritchie, J. C. 2008. Identification of suspended sediment sources using soil characteristics in a semiarid watershed. *Soil Science Society of America Journal,* 72**,** 1102-1112. Available: DOI 10.2136/sssaj2007.0066.

Robinson, D. A. & Moses, C. A. 2011. Rock Surface and Weathering: Process and Form. *In:* Gregory, K. J. & Goudie, A. S. (eds.) *The SAGE Handbook of Geomorphology.* London: SAGE Publications.

Roddy, B. 2010. *The use of the sediment fingerprinting technique to quantifiy the different sediment sources entering the Whangapoua Estuary, North Island, in New Zealand.* Doctor of Philosophy in Earth and Ocean Sciences, University of Waikato.

Rosser, B. R., Mildner, T. & Dymond, J. 2008. *Sediment mass balance and adjustment of channel morphology, Pohangina River 1950–2000, Manawatu, New Zealand*. Landcare Research (Contract Report LC0910/011). Report number: Contract Report LC0910/011.

Roygard, J. K. F., Mcarthur, K. J. & Clark, M. E. 2012. Diffuse contributions dominate over point sources of soluble nutrients in two sub-catchments of the Manawatu River, New Zealand. *New Zealand Journal of Marine and Freshwater Research,* 46**,** 219-241. Available: DOI 10.1080/00288330.2011.632425.

Russell, M. A., Walling, D. E. & Hodgkinson, R. A. 2001. Suspended sediment sources in two small lowland agricultural catchments in the UK. *Journal of Hydrology,* 252**,** 1-24. Available: DOI 10.1016/s0022-1694(01)00388-2.

Rustomji, P., Caitcheon, G. & Hairsine, P. 2008. Combining a spatial model with geochemical tracers and river station data to construct a catchment sediment budget. *Water Resources Research,* 44. Available: DOI 10.1029/2007wr006112.

Sabeen, H. M., Ramanujam, N. & Morton, A. C. 2002. The provenance of garnet: constraints provided by studies of coastal sediments from southern India. *Sedimentary Geology,* 152**,** 279-287. Available: DOI 10.1016/s0037-0738(02)00083-0.

Salminen, R., Plant, J. & Reeder, S. 2005. *Geochemical atlas of Europe. Part 1, Background information, methodology and maps*, Geological survey of Finland Espoo.

Samani, A. N., Wasson, R. J. & Malekian, A. 2011. Application of multiple sediment fingerprinting techniques to determine the sediment source contribution of gully erosion: Review and case study from Boushehr province, southwestern Iran. *Progress in Physical Geography,* 35**,** 375-391. Available: DOI 10.1177/0309133311401643.

Sassa, K., Tsuchiya, S., Ugai, K., Wakai, A. & Uchimura, T. 2009. Landslides: a review of achievements in the first 5 years (2004–2009). *Landslides,* 6**,** 275-286. Available: DOI 10.1007/s10346-009-0172-5.

Singh, P. 2009. Major, trace and REE geochemistry of the Ganga River sediments: Influence of provenance and sedimentary processes. *Chemical Geology,* 266**,** 242-255. Available: DOI 10.1016/j.chemgeo.2009.06.013.

Singh, S. K. & France-Lanord, C. 2002. Tracing the distribution of erosion in the Brahmaputra watershed from isotopic compositions of stream sediments. *Earth and Planetary Science Letters,* 202**,** 645-662. Available: DOI 10.1016/s0012-821x(02)00822-1.

Slattery, M. C., Burt, T. P. & Walden, J. 1995. The application of mineral magnetic measurements to quantify within-storm variations in suspended sediment sources. *Tracer technologies for hydrological systems.* Wallingford, U.K.: IAHS Publ.

Small, I. F., Rowan, J. S. & Franks, S. W. 2002. Quantitative sediment fingerprinting using a Bayesian uncertainty estimation framework. *In:* Dyer, F. J., Thoms, M. C. & Olley, J. M. (eds.) *Structure, Function and Management Implications of Fluvial Sedimentary Systems.* Wallingford: Int Assoc Hydrological Sciences.

Smith, H. G. & Blake, W. H. 2014. Sediment fingerprinting in agricultural catchments: A critical re-examination of source discrimination and data corrections. *Geomorphology,* 204**,** 177-191. Available: DOI http://dx.doi.org/10.1016/j.geomorph.2013.08.003.

Smith, H. G. & Dragovich, D. 2008. Improving precision in sediment source and erosion process distinction in an upland catchment, south-eastern Australia. *CATENA,* 72**,** 191-203. Available: DOI 10.1016/j.catena.2007.05.013.

Smith, H. G. & Dragovich, D. 2009. Interpreting sediment delivery processes using suspended sediment-discharge hysteresis patterns from nested upland catchments, south-eastern Australia. *Hydrological processes,* 23**,** 2415.

Stark, J. D. 2008. *Trends in river health of the Manawatu-Wanganui region 2008 with comments on the SoE biomonitoring programme*. Prepared for Horizons Regional Council. Stark Environmental Report No.2008-07.

Syvitski, J. P. M. & Milliman, J. D. 2007. Geology, Geography, and Humans Battle for Dominance over the Delivery of Fluvial Sediment to the Coastal Ocean. *The Journal of Geology,* 115**,** 1-19. Available: DOI 10.1086/509246.

Syvitski, J. P. M., Vörösmarty, C. J., Kettner, A. J. & Green, P. 2005. Impact of Humans on the Flux of Terrestrial Sediment to the Global Coastal Ocean. *Science,* 308**,** 376-380. Available: DOI 10.1126/science.1109454.

Taylor, S. R. & Mclennan, S. M. 1985. The continental crust: its composition and evolution. *The Journal of Geology,* 94.

Trimble, S. W. 1981. Changes in sediment storage in the Coon Creek basin, Driftles Area, Wisconsin 1853 to 1975. *Science,* 285**,** 1244 - 1246.

Trimble, S. W. 2010. Streams, Valleys, Floodplains in the Sediment Cascade. *In:* Burt, T. & Allison, R. (eds.) *Sediment Cascade: An Integrated Approach.* Wiley-Blackwell.

Udelhoven, T. & Symader, W. 1995. Particle characteristics and their significance in the identification of suspended sediment sources. *In:* Leibundgut, C. (ed.) *Tracer Technologies for Hydrological Systems.* Wallingford: IAHS Press.

Vale, S. 2011. *GIS coupled water budget for spatial and temporal analysis of water resources: Horowhenua, New Zealand: a thesis presented in partial fulfilment of the requirements for the degree of Masters of Science, Geography, School of People, Environment and Planning, Massey University, Palmerston North, New Zealand.*

Vale, S. S., Fuller, I. C., Procter, J. N., Basher, L. R. & Smith, I. E. 2016a. Application of a confluence-based sediment-fingerprinting approach to a dynamic sedimentary catchment, New Zealand. *Hydrological Processes,* 30**,** 812–829. Available: DOI 10.1002/hyp.10611.

Vale, S. S., Fuller, I. C., Procter, J. N., Basher, L. R. & Smith, I. E. 2016b. Characterization and quantification of suspended sediment sources to the Manawatu River, New Zealand. *Science of the Total Environment,* 543**,** 171-186. Available: DOI 10.1016/j.scitotenv.2015.11.003.

Varnes, D. J. 1978. Slope movement types and processes. *In:* Schuster, R. L. & Krizck, R. J. (eds.) *Landslides; Analysis and Control, Special Report.* Washington, DC: Transportation Research Board, National Academy of Sciences.

Von Eynatten, H. & Gaupp, R. 1999. Provenance of Cretaceous synorogenic sandstones in the Eastern Alps: constraints from framework petrography, heavy mineral analysis and mineral chemistry. *Sedimentary Geology,* 124**,** 81-111. Available: DOI 10.1016/s0037-0738(98)00122-5.

Walden, J., Slattery, M. C. & Burt, T. P. 1997. Use of mineral magnetic measurements to fingerprint suspended sediment sources: approaches and techniques for data analysis. *Journal of Hydrology,* 202**,** 353-372. Available: DOI 10.1016/s0022-1694(97)00078-4.

Wall, G. J. & Wilding, L. P. 1976. Mineralogy and related parameters of fluvial suspended sediments in Northwestern Ontario. . *Journal of Environmental Quality,* 5**,** 168 - 173.

Wallbrink, P. J. & Murray, A. S. 1993. Use of fallout radionuclides as indicators of erosion processes. *Hydrological Processes,* 7**,** 297-304. Available: DOI 10.1002/hyp.3360070307.

Wallbrink, P. J., Murray, A. S., Olley, J. M. & Olive, L. J. 1998. Determining sources and transit times of suspended sediment in the Murrumbidgee River, New South Wales, Australia, using fallout Cs-137 and Pb-210. *Water Resources Research,* 34**,** 879-887. Available: DOI 10.1029/97wr03471.

Walling, D. 2008. The changing sediment loads of the world's rivers. *Annals of Warsaw University of Life Sciences-SGGW. Land Reclamation,* 39**,** 3-20.

Walling, D., Woodward, J. & Nicholas, A. 1993. A multi-parameter approach to fingerprinting suspended-sediment sources. *IAHS publication***,** 329-338.

Walling, D. E. 1977. Assessing the accuracy of suspended sediment rating curves for a small basin. *Water Resources Research,* 13**,** 531-538. Available: DOI 10.1029/WR013i003p00531.

Walling, D. E. 2005. Tracing suspended sediment sources in catchments and river systems. *Science of The Total Environment,* 344**,** 159-184. Available: DOI 10.1016/j.scitotenv.2005.02.011.

Walling, D. E. 2006a. Human impact on land–ocean sediment transfer by the world's rivers. *Geomorphology,* 79**,** 192-216. Available: DOI http://dx.doi.org/10.1016/j.geomorph.2006.06.019.

Walling, D. E. 2006b. Tracing versus montoring: new challenges and opportunities in erosion and sediment delivery research *In:* Owens, P. N. & Collins, A. J. (eds.) *Soil erosion and sediment redistribution in river catchments: measurement, modelling and management.* United Kingdom: Cabi.

Walling, D. E. 2013. Beryllium-7: The Cinderella of fallout radionuclide sediment tracers? *Hydrological Processes,* 27**,** 830-844. Available: DOI 10.1002/hyp.9546.

Walling, D. E. & Amos, C. M. 1999. Source, storage and mobilisation of fine sediment in a chalk stream system. *Hydrological Processes,* 13**,** 323-340. Available: DOI 10.1002/(sici)1099-1085(19990228)13:3<323::aid-hyp741>3.0.co;2-k.

Walling, D. E., Collins, A. L. & Stroud, R. W. 2008. Tracing suspended sediment and particulate phosphorus sources in catchments. *Journal of Hydrology,* 350**,** 274-289. Available: DOI 10.1016/j.jhydrol.2007.10.047.

Walling, D. E. & Fang, D. 2003. Recent trends in the suspended sediment loads of the world's rivers. *Global and Planetary Change,* 39**,** 111-126. Available: DOI 10.1016/s091-8181(03)00020-1.

Walling, D. E., Golosov, V. & Olley, J. 2013. Introduction to the special issue 'Tracer Applications in Sediment Research'. *Hydrological Processes,* 27**,** 775-780.

Walling, D. E. & Moorehead, P. W. 1989. The particle size characteristics of fluvial suspended sediment: an overview. *Sediment/Water Interactions.* Springer.

Walling, D. E., Owens, P. N., Carter, J., Leeks, G. J. L., Lewis, S., Meharg, A. A. & Wright, J. 2003. Storage of sediment-associated nutrients and contaminants in river channel and floodplain systems. *Applied Geochemistry,* 18**,** 195-220. Available: DOI 10.1016/s0883-2927(02)00121-x.

Walling, D. E., Owens, P. N. & Leeks, G. J. L. 1997. The characteristics of overbank deposits associated with a major flood event in the catchment of the River Ouse, Yorkshire, UK. *CATENA,* 31**,** 53-75. Available: DOI 10.1016/s0341-8162(97)00034-9.

Walling, D. E., Owens, P. N. & Leeks, G. J. L. 1999. Fingerprinting suspended sediment sources in the catchment of the River Ouse, Yorkshire, UK. *Hydrological Processes,* 13**,** 955-975. Available: DOI 10.1002/(sici)1099-1085(199905)13:7<955::aid-hyp784>3.0.co;2-g.

Walling, D. E., Peart, M. R., Oldfield, F. & Thompson, R. 1979. Suspended Sediment Sources Identified by Magnetic Measurements. *Nature,* 281**,** 110-113. Available: DOI 10.1038/281110a0.

Wang, H., Yang, Z., Saito, Y., Liu, J. P., Sun, X. & Wang, Y. 2007. Stepwise decreases of the Huanghe (Yellow River) sediment load (1950–2005): Impacts of climate change and human activities. *Global and Planetary Change,* 57**,** 331-354.

Warburton, J. 2011. Sediment Transport and Deposition. *In:* Gregory, K. J. & Goudie, A. S. (eds.) *The SAGE Handbook of Geomorphology.* London: SAGE Publications.

Weltje, G. J. & Von Eynatten, H. 2004. Quantitative provenance analysis of sediments: review and outlook. *Sedimentary Geology,* 171**,** 1-11. Available: DOI 10.1016/j.sedgeo.2004.05.007.

Wilkinson, S. N., Hancock, G. J., Bartley, R., Hawdon, A. A. & Keen, R. J. 2013. Using sediment tracing to assess processes and spatial patterns of erosion in grazed rangelands, Burdekin River basin, Australia. *Agriculture, Ecosystems & Environment,* 180**,** 90-102. Available: DOI http://dx.doi.org/10.1016/j.agee.2012.02.002.

Wilkinson, S. N., Olley, J. M., Furuichi, T., Burton, J. & Kinsey-Henderson, A. E. 2015. Sediment source tracing with stratified sampling and weightings based on spatial gradients in soil erosion. *Journal of Soils and Sediments,* 15**,** 2038-2051. Available: DOI 10.1007/s11368-015-1134-2.

Withers, P. J. A. & Jarvie, H. P. 2008. Delivery and cycling of phosphorus in rivers: A review. *Science of The Total Environment,* 400**,** 379-395. Available: DOI http://dx.doi.org/10.1016/j.scitotenv.2008.08.002.

Wood, P. J. & Armitage, P. D. 1997. Biological Effects of Fine Sediment in the Lotic Environment. *Environmental Management,* 21**,** 203-217. Available: DOI 10.1007/s002679900019.

Wright, K. C. 2005. The February 2004 Landslide Event in Geomorphic Perspective.

Zhang, W. G., Xing, Y., Yu, L. Z., Feng, H. & Lu, M. 2008. Distinguishing sediments from the Yangtze and Yellow Rivers, China: a mineral magnetic approach. *Holocene,* 18**,** 1139-1145. Available: DOI 10.1177/0959683608095582.

Zhang, Y. S., Collins, A. L. & Horowitz, A. J. 2012. A preliminary assessment of the spatial sources of contemporary suspended sediment in the Ohio River basin, United States, using water quality data from the NASQAN programme in a source tracing procedure. *Hydrological Processes,* 26**,** 326-334. Available: DOI 10.1002/hyp.8128.

Appendix A – Comprehensive summary of sediment fingerprinting literature

Study	Description of sediment Sources	Tracer type Technique Analysis	Outcomes
Arribas *et al.* (2000)	Composition of stream sediment from sedimentary and metamorphic source rocks in the Henares River, Spain. Sources based on a varied geology, transported from three tributaries: Cañamares, Bornova, and Sorbe rivers.	**Tracers:** Mineralogy **Size fraction:** 0.25 – 0.50 mm and 0.25 – 0.063 mm **Analysis:** Ternary diagrams and percentages	Proportions of bedrock lithologies in the drainage sub-basins are the main control on detrital modes of the tributaries. The high content of metamorphic lithic grains in the lithic grain population over-represents this lithology (slate plus schist) at the source terrain.
Belmont *et al.* (2014)	Channel–floodplain processes investigated for alluvial bank/floodplain sources and non-conservative challenges in the Maple River watershed, southern Minnesota, USA.	**Tracers**: measurements of ^{10}Be, $^{210}Pb_{ex}$, ^{137}Cs **Size fraction**: **Analysis:**	Measurements of ^{10}Be, $^{210}Pb_{ex}$, and ^{137}Cs were able to distinguish agricultural uplands, bluffs and banks sediment sources as well as estimate channel–floodplain exchange. Sediment sources systematically vary by location and changed over the length of a single storm hydrograph and were consistent with geomorphic understanding.
Blake *et al.* (2006)	Magnetic enhancement of wildfire-affected soil for sediment source ascription in the Nattai River catchment, Australia. Three sediment sources based on forest fire severity: severely burnt, moderately burnt, and unburnt soils. Small sub-catchment; bedrock comprises mainly relatively Fe-rich Hawkesbury Sandstone.	**Tracers**: Magnetic susceptibility χ_{lf}, χ_{hf}; Frequency dependent susceptibility χ_{fd}, $\chi_{fd\%}$, ARM, IRM, SIRM **Size fraction**: <10 µm **Analysis**: Bivariate plot, students t-test	Burnt soil became magnetically enhanced compared to unburnt soil and varied on the severity of the burning. Magnetic signatures in the < 10 µm are probably not a result of the burnt soils alone. Magnetic grain size indicators contribute to the signal but are not linearly additive which prevents their use in numerical mixing models.

Appendix A – Comprehensive summary of sediment fingerprinting literature

Blake *et al.* (2012)	Tracing crop specific sediment sources in Furze Brook catchment (145 ha), UK. Sources use crop specific sediment sources; soil under (i) maize, (ii) winter, wheat, (iii) grass, and (iv) trees and shrubs; and land-use based sediment sources: (i) cultivated soil, (ii) uncultivated soil, (iii) a specific area of woodland via a geological control, and (iv) channel bank material, composed of 62 samples of soil and 7 samples of channel bank sediment were collected	**Tracers**: Compound Specific Stable Isotope (CSSI) compared to Inorganic Pd, Cd, Sn, Sb, Cs, Bi, Al, As,Ba, Ca, Cr, Cu, Fe, K, La, Mg, Mn, Ni, Pb, Sr, Ti, V, Y and Zn and magnetic susceptibility, χ_{lf} **Size fraction**: < 10 µm **Analysis:** Isosource mixing model, Kruskal–Wallis H-test, Discriminant Function Analysis (DFA), Monte Carlo	δ13C signatures of particle-associated fatty acids were able to be linked to soil enabled sediment in streams to be linked back to fields under specific crop cover. The CSSI method should be applied in conjunction with conventional geochemical fingerprinting approaches and together may allow full discrimination. Understanding of the biogeochemical processes is needed.
Brown (1985)	Suspended sediment sources in the Highland Water catchment U.K. (11.4 km^2), using nine sources based on different pollen/spore producing plants.	**Tracers**: Organic Plant Pollen **Analysis:** Concentrations	Higher pollen counts in the suspended sediment from one source are qualitatively related to higher sediment production from the same region.
Brigham *et al.* (2001)	Suspended sediment concentration and radioisotope levels in Wild Rice River Basin (4038 km^2), North-western Minnesota from 1973 to 1978 using two sources: agricultural surface soils and streambanks.	**Tracers:** ^{210}Pb, ^{137}Cs, ^{7}Be **Size fraction**: Suspended sediment concentrations **Analysis**: Multiple linear regression analysis	Sediment concentrations measured from 1973 to 1998 exhibit strong dependence on streamflow; limited seasonal dependence, with flow-adjusted concentrations slightly higher in the spring than summer-autumn; and no significant temporal trend. ^{210}Pb and ^{7}Be data indicated that suspended sediments originate primarily from upland soil erosion, whereas ^{137}Cs data indicated a mixed source, with streambank sediments slightly more important
Burrus *et al.* (1990)	Suspended sediment characterization and sediment-associated forms of phosphorus in the Upper Rhone River, Switzerland (5220 km^2). Two sediment designations based on timing of sediment collection; sediment recovered during the winter low flow, low turbidity period has been designated SED 1 whereas sediment from the high flow, high turbidity summer condition of the river has	**Tracers:** SiO_2, Al_2O_3, K_2O, MgO, Na_2O, CaO, and Fe_2O_3; Zn, Cu, Ni, Mn, and Cr; Organic C and Kjeldahl N; and the forms of phosphorus bound as Organic P (OP), Apatite P (AP), and Non Apatite Inorganic P (NAIP). **Size fraction**: < 63 µm **Analysis**: mean element	No spatial or temporal change in the major geochemical tracers indicating a well-mixed sedimentary system. AP remained consistent in concentration throughout the year. Org C, OP, and NAIP show a dramatic decrease in concentration from SED 1 to SED 2 due to dilution of point source sewage. This results in variable partitioning of the OP/NAIP and Org C under the different turbidity condition in the river between winter and summer.

	been designated SED 2.	composition and regression	
Caitcheon (1998)	Measuring of the relative contributions of the magnetic mineral components in bulk sediment measurements using two sources: Killimicat Creek (22 km^2) containing rocks of mainly volcanic origin, and a smaller tributary (7 km^2) that is deeply incised and extensive gully erosion	**Tracer**: Mineral magnetic - mass specific susceptibility (x), IRM **Size fraction:** < 63 µm, 63–125 µm, 125–250 µm, 250–500 mm, 500 µm – 1.4 mm, 1.4 – 2 mm **Analysis**: Regression	Heavy mineral components from each tributary where distinctly different. Differences must be substantially influenced by the geochemical properties of the parent rock and extends to the soils The magnetic component in most situations is likely to be representative of the bulk of the transported sediment Stream junctions receiving sediment from distinguishable sources may be useful locations for determining relative sediment contributions.
Carter *et al.* (2003)	Characterizing fine sediments in an urban catchment, Coventry, UK, with four land-use sources (forest, uncultivated agriculture, cultivated agriculture, and streambanks) and four geologic sources (Carboniferous limestone, Carboniferous millstone grit, Carboniferous coal, Permian magnesium limestone) overlain to develop 16 sources. Two additional sources used included urban road dust and wastewater solids effluent.	**Tracer**: Organic: Total organic P, Inorganic: K, Cu, As, Mn, Na, Mg, Fe, Zn, Ca, Cr, TC , TN, TP, ^{210}Pb, ^{137}Cs **Size fraction**: < 2 mm and < 63 µm **Analysis**: Mann–Whitney test, Kruskal–Wallis *H*-test, stepwise selection algorithm based on the minimisation of Wilks' lambda	The suspended sediment in the upper reaches originates largely from channel bank sources (43–84%) and from uncultivated topsoil (16–57%). In the lower reaches local sources of cultivated topsoil contribute 20–45% with urban sources such as road dust (19–22%) and solids from sewage treatment works (14–18%) Geological contribution in the upper reaches largely corresponds to the areal coverage.
Charlesworth and Lees (2001)	Urban sediment sources taken from, storm sewers and gully pots, polluted dusts, slough streams, marsh cores and soils as well as cores from two urban lakes as the sediment sinks.	**Tracer**: Mineral magnetic χ_{lf} and SIRM **Size fraction**: <63 µm and 63 µm – 2 mm **Analysis**: Regression	The complexity of the system, the wide range sediment sources, transport pathways, and biogeochemical processes make any differentiation using this method unsuitable.
Collins and Walling (2002)	Comparison of the tracer selection process between 4 catchments; Upper Kaleya catchment (63 km^2), Zambia; Barle catchment (128 km^2), Devon, UK; Plynlimon (8.7 km^2) and Vyrnwy catchment (778 km^2), Powys, UK.	**Tracer**: $Al_{dithionite}$, $Mn_{dithionite}$, $Fe_{dithionite}$, $Fe_{oxalate}$ $Al_{pyrophosphate-dithionite}$, Al, As, Cd, Co, Cr, Cu, Fe, Mn, Ni, Pb, Sb, Sn, Sr, Zn, Ca, K, Mg, Na, C, N, TP, ^{137}Cs, unsupported ^{210}Pb, ^{226}Ra	Composite fingerprints incorporating constituents selected from several groups of properties using a stepwise statistical selection procedure consistently provide the most robust discrimination of potential sediment sources. A universally applicable composite fingerprint cannot be identified, but a group of properties can be identified.

		Size fraction: <63 µm **Analysis**: Discriminant function analysis using Kruskal–Wallis H-test	A combination of acid and pyrophosphate-dithionite extractable metals, base cations, organic constituents and radiometric properties should be effective.
Collins and Walling (2007)	Storage and provenance of fine sediment of the channel bed using two study sites: Tern catchment: Sandstone and mudstone, intensive cropping (42.6 %), dairy (39.7 %) and woodland (8.9 %); and Pang/Lambourn: chalk: Pang – intensive arable crops (47.9%), pasture (26.4 %), woodland (20.1 %): Lambourn – cultivated land (63.6 %), pasture (21.4 %) and woodland (7.9 %).	**Tracer**: Al, As, Ba, Bi, Ca, Cd, Ce, Co, Cr, Cs, Cu, Dy, Er, Eu, Fe, Ga, Gd, Ge, Hf, Ho, La, Li, Mg, Mn, Mo, Na, Nd, Ni, Pb, Pd, Pr, Rb, Sb, Sc, Sm, Sn, Sr, Tb, Ti, Tl, V, Y, Yb, Zn and Zr, ^{137}Cs, unsupported ^{210}Pb, ^{226}Ra: C, N, Inorganic, organic, and total P **Size fraction**: <63 µm **Analysis**: Multivariate mixing model using Monte Carlo routine, Kruskal–Wallis H-test; Discriminant function analysis	Mean fine sediment storage was 37% (upper Tern), 38% (Pang) and 21% (Lambourn) of the annual suspended sediment loads measured at the catchment outlets. Tern: 35 ±5% (pasture), 51 ±5% (cultivated) and 14 ±3% (channel banks and subsurface sources). Pang: 49 ±8%, (pasture), 33 ±5% (cultivated) and 18 ±5% (channel banks and subsurface sources). Lambourn: 19 ±6%, (pasture), 64 ±5% (cultivated) and 17 ±5% (channel banks and subsurface sources)
Collins *et al.* (1998)	Composite fingerprints for determining suspended sediment load provenance for the Exe Basin (601 km^2): Geological diverse. 10 samples of surface soil from woodland, pasture, cultivated areas and channel bank material for each rock series in the 3 geological systems. Severn Basin (4325 km^2): Geological diverse. 4 samples of surface soil from woodland, pasture, cultivated areas and channel bank material for each rock series in the 3 geological systems.	**Tracers**: Fe, Mn, Al, Cu, Zn, Pb, Cr, Co, Ni, Na, Mg, Ca, K, C, N, total P **Size fraction**: < 63 µm **Analysis**: Multivariate sediment mixing model using non-parametric Kruskal–Wallis H-test	The mixing model estimates are consistent with existing information regarding the suspended sediment yields and erosion processes. Uncertainty exists around the variability associated with source material fingerprint property concentrations is not explicitly incorporated into the mixing model calculations, and are not weighted according to the magnitude of the suspended sediment load transported at the time of sample collection.
Collins *et al.* (1997)	Quantitative composite fingerprinting technique for sediment sources in terms of potential seasonal, inter-, and intra-storm	**Tracers**: Fe, Mn, Al, Cu, Zn, Pb, Cr, Ni, Co, Na, Mg, Ca, K, C, N, total P, ^{137}Cs ^{210}Pb and absolute particle	Surface erosion of pasture soils is dominant, reflecting areal coverage. Seasonal variability is seen in cultivated soils which increase during autumn and spring due to sowing. Bank

	variations in sediment contributions in the Dart Catchment of four sources: forest, pasture agriculture, cultivated agriculture, and eroding streambanks; and the Plynlimon Catchment three sources: coniferous forest, pasture agriculture, and eroding streambanks.	size **Size fraction**: <63 µm **Analysis**: Multivariate mixing model and verification using Mann-Whitney U-test	contributions are highest in winter and spring. Inter-storm variations in sediment source type reflect antecedent conditions, variable contributing areas and timing of sediment sample collection, and highlight the individuality of catchment response for the sampled flood events. Intra-storm variations in source type contributions emphasize the necessity for detailed sampling programmes for suspended sediment in storm periods.
Collins *et al.* (2013)	A novel tracing-tracking framework combining conventional sediment tracing with sediment tracking on the River Glaven (115 km^2) for grassland, arable surface soils, damaged road verges and channel banks/subsurfaces soils sources within 3 sub-catchments.	**Tracers**: Al, As, Ba, Bi, Cd, Ce, Co, Cr, Cs, Cu, Dy, Er, Eu, Fe, Ga, Gd, Ge, Hf, Ho, K, La, Li,Mg,Mn,Mo, Na, Nd, Ni, Pb, Pd, Pr, Rb, Sb, Sc, Sm, Sn, Sr, Tb, Ti, Tl, U, V, Y, Yb, Zn and Zr**,** C and N. **Size fraction**: <63 µm **Analysis**: Kruskal–Wallis H-test, Multivariate mixing model and Discriminant Function Analysis. Particle tracking using fluorescent-magnetic grains	Sediment sources; grassland (1 ± 1% – 12 ± 1%) or arable (25 ± 1% – 46 ± 1%) surface soils, damaged road verges (2 ± 1% – 50 ± 1%) and channel banks/subsurface sources (20 ± 1% – 50 ± 1%) Tracking sediment through high-strength magnets in watercourses allowed links between sediment loss and river channels, greatly improving the information for specific reaches.
Cooper *et al.* (2014)	Investigation of different model setups using Bayesian framework via a one-factor-at-a-time (OFAT) sensitivity analysis for three sources including arable topsoil, road verges and subsurface material from the River Blackwater, Norfolk, U.K.	**Tracers:** Suite of eight elements - Al, Ca, Ce, Fe, K, Mg, Na, and Ti **Size fraction:** < 45 µm **Analysis:** Bayesian framework via a one-factor-at-a-time (OFAT) sensitivity analysis.	All 13 models estimated subsurface sources to be the largest contributor of SPM (median ~ 76%), Model comparisons evidenced varying degrees of sensitivity to changing priors, inclusion of covariance terms, incorporation of time-variant distributions, and methods of proportion characterization. Differences were observed between full and empirical Bayesian setup, and between a Bayesian and frequentist optimization approach. Mixing model structural choices and error assumptions can

			significantly impact sediment source apportionment results with as demonstrated with estimated median variations of 21 % between models.
D'Haen *et al.* (2013)	Bayesian fingerprinting approach to tracing floodplain deposits in Büğdüz, Turkey. Geological sources included Conglomerate, Ophiolitic debris, Limestone, Marl, Mudstone and Ophiolitic mélange.	**Tracers**: Al, Ba, Ca, Co, Cr, Cu, Fe, K, Mg, Mn, Na, Ni, P, Pb, Sr, Ti, V, and Zn **Size fraction**: <63 µm **Analysis**: Kruskal–Wallis, Discriminant Function Analysis, principal component analysis, Bayesian mixing model using Markov chain Monte Carlo	A Bayesian mixing model approach enhances the ability to deal with uncertainties by integrating the instrumental precision and within-source variability of the tracers through probability distributions Discrimination of tracers yielded Co, Sr, Al, Ca, Mg, K, Cr, Ba, Fe, V, Ni, Mn, and Zn, associated with typical concentrations of sources. Natural spatial variability is taken into account through re-estimation of each locality. An indication of variation of sediment dynamics is illustrated through space and time for the Büğdüz catchment.
de Boer and Crosby (1995)	Evaluation of SEM/EDS analysis for two sources; agricultural soil (black chernozemic soil used for cereal grain production) and forest soil (a grey podzolic soil) within Stony Creek basin (116 km^2), Canada.	**Tracers**: SEM mineralogy, size distribution and morphology, EDS for Si, Al, Ca, Fe, Mg, Na, K, Ti, S **Size fraction**: < 63 µm **Analysis**: Hierarchical cluster analysis using SPSS-X	The two simulated suspended sediment samples were similar in particle size distribution, mineralogy, and total chemistry, so that these characteristics did not provide a distinctive fingerprint for the two topsoils. The morphology of the clay class particles, consisting of water-stable clay aggregates provides differentiation of sources; the grey forest soil was irregular whereas those derived from the black farmland soil was rounded. The difference is attributed to land-use.
de Miguel *et al.* (2005)	The use of urban metals as fingerprints from seven sources in the River Manzanares, Spain: rural headwaters, downstream of a WWT plant before urban influence, upstream and downstream of 4 WWT plant with an urban area, and downstream of the urban influence	**Tracers**: Ag, Al, As, Ba, Be, Ca, Ce, Co, Cr, Cu, Fe, Hg, K, La, Mg, Mn, Na, Ni, P, Pb, Ti, V, Y, Zn, mineralogy **Size fraction**: < 50 µm **Analysis**: Hierarchical cluster analysis, direct partition, factor analysis	Madrid influences the geochemistry of Manzanares' sediments, through a marked increase in the concentration of urban elements, Ag, Cr, Cu, Pb and Zn, downstream. This is attributed to illegal/accidental dumping and uncontrolled urban runoff. Ce, La and Y remain fairly constant although changing lithology causes variations in Ca-Mg and Al-Na contents. Carbonate materials seem to exert a strong control on Zn (and to a lesser extent Cu) concentration in immobilized sediments, suggesting reincorporation in the aqueous phase.
Douglas *et al.*	Origin of suspended particulate matter in the	**Tracers**: $^{87}Sr/^{86}Sr$ and $^{87}Rb/^{86}Sr$,	The isotopic variation indicates simple two component mixing of

Appendix A – Comprehensive summary of sediment fingerprinting literature

(1995)	Murray-Darling River system based on strontium ratios in particulate (> 1 µm), colloidal (< 1 µm) and dissolved (< 0.003µm) phases.	LOI, La, Ce, Pr, Nd, Pm, Sm, Eu, Gd, Tb, Dy, Ho, Er, Tm, Yb, Lu, SiO_2, TiO_2, Al_2O_3, Fe_2O_3, MnO, MgO, CaO, Na_2O, K_2O, Cu, Zn, P **Size fraction**: > 1 µm, < 1 µm < 0.003µm phases **Analysis**: Quasi-isochron diagrams, concentrations	silicate grains (aggregates) and natural organic matter present as surface coatings. Organic matter contains higher mounts of unradiogenic Strontium, whereas the particulate (> 1 μm) fractions are dominated by silicate component with more radiogenic Sr. The variation in the strontium isotopes is due to weathering; plagioclase produces an unradiogenic Sr pool, dominant in the colloidal and dissolved fraction; K-feldspar and mica weathering produce the coarser radiogenic silicate particles.
Eberl (2004)	Quantitative X-ray diffraction of Yukon River basin sediment as it changes downstream.	**Tracers**: Clay Mineralogy, Mineralogy **Size fraction**: suspended sediment **Analysis**: Concentration	Mineralogy changes downstream are a related to sediment dilution and concentration effects from tributary sediment; evidenced in carbonate, quartz, feldspar and organic content changes due to tributary confluences. The mineralogies of the suspended sediments change with the season and results from this method indicate that at least three sediment sources can be identified quantitatively with good accuracy
Erskine (2013)	Investigation of sediment sources from forest road erosion in Chichester State Forest, Australia.	**Tracers**: Munsell Soil Colour **Size fraction**: N/A **Analysis**: Direction comparison	Soil colour showed a successful discrimination of sediment sources with sand and mud largely originating from cut and fill batters of roads. Road 107-2 was a dominant source associated with a debris slide-flow associated with a storm. Fine sediment was only deposited in slackwater areas due to high energy channel environments.
Evrard *et al.* (2013)	Sediment source tracing focusing on sediment sources from gullies, cropland and woodland in 3 sub-catchments, Huertitas, La Cortina and Potrerillos, within the Cointzio catchment (630 km^2), Mexico.	**Tracers**: Ce, Eu, La, Lu, Sm, Tb,Yb, Fe, K, Na, As, Ba, Co, Cr, Cs, Hf, Sc, Ta, Th, Zn, ^{241}Am. ^{7}Be, ^{137}Cs, ^{210}Pb, ^{40}K, ^{226}Ra, ^{228}Ra, ^{228}Th, ^{234Th}, bulk C, bulk N, $\delta^{13}C$, Fourier transform infrared analysis **Size fraction**: <250 µm **Analysis**: Kruskal–Wallis H-test, Monte Carlo mixing model	Combining fingerprinting results with sediment export data provides a way of prioritizing the implementation of erosion control measures. Both fingerprinting methods provided very similar results; dominated by Acrisols supplied by gullies in Huertitas sub-catchment. La Cortina sub-catchment was dominated by Andisols supplied by cropland. Potrerillos sub-catchment was characterized by a mix of Andisols and Acrisols and gullies and cropland. In this latter sub-catchment, results provided by both fingerprinting

			methods were very variable. Results outline the need to consider organic carbon content of soils and the difficulty to use geochemical properties to in very altered volcanic catchments.
Evrard *et al.* (2011)	Combination of suspended sediment monitoring with fingerprinting to categorize spatial origin of fine sediment from seven main sediment sources based on geology; black marl (Bathonian), other black marls, grey marls, marly limestones, quaternary deposits, conglomerates, gypsum .	**Tracers**: Ce, Eu, La, Lu, Sm, Tb,Yb, Fe, K, Na, As, Ba, Co, Cr, Cs, Hf, Sc, Ta, Th, Zn, Al, Ca, Mg, Ti, Ag, Ba, Cd, Cu, Mn, Ni, Pb, Sb, Se, Tl, V, ^{241}Am. ^{7}Be, ^{137}Cs, ^{210}Pb, ^{40}K, ^{226}Ra, ^{228}Ra, ^{228}Th, ^{234}Th **Size fraction**: <2 mm **Analysis**: Non-parametric Wilcoxon tests, the Kruskal–Wallis H-test, stepwise discriminant function analysis (SDFA), Monte Carlo mixing model	Strong diversity in erosion processes that fluctuated due to local storms. Quaternary, limestones and conglomerates contributions much higher than the highly erosive black marls.
Evrard *et al.* (2010)	Sediment dynamics (residence times) during the rainy season in three highland sub-catchments (3–12 km^2) in Mexico: Huertitas; Acrisols covered by cropland and rangeland, hilly; La Cortina dominated by pine-oak forests and cropland in undulating hillslopes underlain by Andisols; Potrerillos is underlain by Acrisols and Andisols covered by pine-oak, eucalyptus plantations, cropland and rangeland in rolling hills.	**Tracers**: ^{7}Be, ^{210}Pb, ^{137}Cs **Size fraction**: suspended sediment **Analysis**: modelling via mass balance	Particle residence times in rivers ranged from 50 ± 30 to 200 ± 70 days, and 5000 ± 1500 to 23,300 ± 7000 years in soils. Shortest residence times were in hilly catchment dominated by cropland and rangeland; longest in an undulating catchment dominated by forests and cropland. Heavy storms exported the bulk of the material. Land cover and flood type seem to exert more control on sediment export compared to slope steepness and rainfall erosivity.
Foster *et al.* (1998)	Characterization of sediment sources of lake and floodplain sediments in the catchments. The sources were from two catchments:	**Tracers**: χ_{lf}, χ_{hf}, χ_{fd}, $\chi_{fd\%}$, $ARM_{40\mu T}$, $IRM_{0.025\text{-}0.8T}$, $IRM_{\text{-}0.1T}$, SRatio, HIRM, $HIRM\chi_{fd}$	Mineral magnetic signatures of floodplain deposits are more likely to reflect the particle size composition of the transported material. Mineral magnetic record in the Slapton Ley sediment is most

	Slapton catchment (1232 ha) and Old Mill Reservoir (159.53 ha); both underlain by slates, shales, siltstones and mudstones. Sources focuses on surface and subsurface sampling.	**Size fraction**: < 63 µm **Analysis**: principal component analysis	strongly influenced by dissolution of magnetic minerals. Variability and scatter in the mineral magnetic signatures is high preventing adequate differentiation. The thinner soils, which show more of a sub-soil signature, may be due to mixing from ploughing.
Foster *et al.* (2007)	Sediment tracing and environmental history of two small catchments (633.09 ha and 149.76 ha) where reservoirs were constructed. Sampling designed to account for discrimination based on lithology, land-use and land management as well as topsoils, subsoils, and gully sidewalls.	**Tracers**: ^{210}Pb, ^{234}Th, ^{235}U, ^{214}Pb, ^{7}Be, ^{137}Cs, ^{228}Ac, ^{40}K, K, χ_{lf}, χ_{hf}, χ_{fd}, $\chi_{fd\%}$, ARM, $IRM_{0.88T}$, $IRM_{loss,}$ $IRM_{-0.1T}$, χ_{arm}, SRatio, HIRM, Pb, Cu, ZN, Ni, Mn, F, Al, Ca, Mg, Na, K, Ba, Sr, V, P, LOI **Size fraction**: < 250 µm **Analysis**: Principal component analysis and discriminant function analysis	Lithology and land-use provided successful discrimination in each catchment. Changes in cereal cultivation and livestock grazing density relate to temporal changes in sedimentation rates. Temporal changes in magnitude and frequency of extreme events do not correlate to reconstructed sediment accumulation patterns Gully systems provide connectivity from dominant hillslope sources but have not contributed significantly to the sediment deposited No evidence to suggest sources of sediment has change significantly in ca 70 years
Fox and Papanicolaou (2008a)	Incorporation of a spatial distribution of sediment sources from four land-use sources in the Upper Palouse (600 km^2): winter wheat agriculture, hay agriculture, floodplains experiencing riparian regrowth in hay agriculture, and conifer forest.	**Tracers**: δ^{13}N, C/N **Size fraction**: < 53µm, 53µm – 250 µm **Analysis**: ANOVA tests and spatial model of δ^{13}N	The nitrogen stable isotope is reflective of agricultural land-management practices, accounting for 63.5% of the isotopic variability, especially in winter wheat/barley, hay production and conservation sites. The tracer statistically shows differences between floodplain and upland soils due to recent riparian re-growth and to distinguish soil depths due to litter and root decomposition. Little variation is statistically detected for land management and geomorphologic landform in the forest.
Gellis and Noe (2013)	Investigated suspended sediment sources from stream banks, agriculture and forested areas in the Linganore Creek (147-km$_2$), Maryland	**Tracers**: B, Cu, Pb, Al, V, Cd, Li, Fe, Mn, Mo, Ca, P, Co, Sb, Mg, Ti, Ni, As, K, δ^{13}C, TOC, N, δ^{15}N **Size fraction**: <63 µm **Analysis:** Shapiro–Wilk test, Stepwise discriminant function analysis, frequentist	Stream banks contributed 53% of the annual fine-grained suspended sediment load, agriculture contributed 44%, and forests contributed 3%. The highest peak flows occurred during winter correlating to stream bank erosion, and negatively correlating with agricultural lands which had the greatest contribution in non-winter months. Connectivity disparities between upland sediment and channel

Appendix A – Comprehensive summary of sediment fingerprinting literature

		unmixing model, Monte Carlo simulation,	bank sediment and their interpretation from sediment fingerprinting results for individual storms present temporal challenges due to stored and remobilized sediment.
Gibbs (2008)	Identification of source soils in an estuarine sediments. Three main land-use sources: pasture, native forest and pine forest.	**Tracers**: Compound specific isotopes analysis (CSIA): $\delta^{13}C$ of fatty acids: Decanoic, Lauric, Myristic, Pentadecanoic, Palmitic, Stearic, Oleic, Linolenic, Arachidic, Behenic, Lignocerie; Resin Acid; Abietic acid **Analysis**: Isotopic mixing model, IsoSource.	The source soil contributions varied markedly across the delta, raising concerns about the validity of taking single cores to characterize the sediments of an estuary. Mean percent contribution of pine forest soil in the river delta sediments was almost three times greater than the percent land-use area of pine forest in the catchment. Most of the pine forest soil comes from the much smaller areas exposed to erosion by clear cut harvesting and that the soil contribution from recently harvested areas of pine forest could be as much as 20 times greater than that land-use area in this catchment.
Gingele and De Deckker (2005)	The Murray–Darling Basin covers 1,073,000km^2 to which two sources are focused: The Darling River tributaries which originate from Mesozoic clastic sediments and Tertiary mafic volcanics, Mesozoic granites and Late Palaeozoic volcanics, metasediments and granites. The Murray River drains the Lachlan Fold Belt and Southern Highlands consisting of Early Palaeozoic granites, volcanics, and metasediments.	**Tracer**: Na, Mg, Al, Si, P, S,K, Ca, Ti, Mn, Fe, Sc, V, Y, Cr, Mn, Co, Ni, Cu, Zn, Ga, Rb, Sr, Zr, Nb, Mo, Cd, Sn, Cs, Ba, La, Ce, Pr, Nd, Sm, Gd, Dy, Er, Yb, Lu, Hf, ^{207}Pb, Th, and U, $^{87}Sr/^{86}Sr$, $^{143}Nd/^{144}Nd$ **Size fraction**: < 2µm **Analysis**: Percentages	Clay fraction is imprinted with clay mineral and isotopic signature of geological provinces. Radiogenic isotopic ratios $^{87}Sr/^{86}Sr$, $^{143}Nd/^{144}Nd$ are catchment-sensitive and distinguish sources. Sediment contribution can be estimated from isotope ratios and element concentrations. Nd and Sr both gave 36/64 figure of Darling versus Murray river contribution.
Grimshaw and Lewin (1980)	Sediment source identification in the River Ystwyth catchment (170 km^2) Two sources: channel sediment (grey) and surface (brown)	**Tracers**: Colour of yielded sediments and the sediment-discharge relationships over time **Size fraction**: < 22 mm **Analysis**: Regression	The channel sediments appear to attribute 40.5 % and 53.3 % of yields of 43 4389 and 12 233 t in 2 successive years attributed to the available sediment supply.
Gruszowski *et*	Identification of primary and secondary	**Tracers**: χ_{lf}, χ_{hf}, χ_{fd}, $\chi_{fd\%}$, ARM,	Contributions from primary sources of *c*. 43% and *c*. 27% were

al. (2003)	sediment sources and transport pathways in a small (15 km^2) rural catchment Four sources: surface topsoil (0-5 cm), subsoil (5–35 cm), eroding channel banks, and sediment particles derived from roads used with multivariate tracers	IRM, SRatio, HIRM. χ_{arm}, P, Fe, Al, Na, K, Mg, Ca, Cd, Cu, Ni, Mn, Zn, ^{137}Cs **Size fraction**: < 63 µm **Analysis**: Mann Whitney U-test, principal component and discriminant function analyses, linear unmixing model	estimated from a combined (subsoil and channel bank) subsurface source, and a combined (arable and grassland) topsoil source, respectively. Roads appear to be important as a secondary source and conveyor of topsoils to the channel contributing *c*. 30%
Haddadchi *et al*. (2014)	A comparison of sediment mixing models using artificial mixtures of three well-distinguished geologic sources from Emu Creek catchment, South East Queensland, Australia.	**Tracers**: Geochemical concentrations of SiO_2, TiO_2, Al_2O_3, ,Fe_2O_3, MgO, CaO, Na_2O, K_2O, P_2O_5, MnO, As, Ba, Co, Cr, Cu, Ni, Rb, Sr, Th, U, V, Zn, Zr, Ce, La, Nd, Y, CIA, Rb/Sr, LOI **Size fraction**: **Analysis:** Kruskal–Wallis H test, Modified Hughes, Modified Collins, Landwehr and Distribution models, Mean Absolute Error (MAE)	The distribution model provided the closest estimates to the known sediment source (Mean Absolute Error (MAE) = 10.8%), followed by the Modified Hughes (MAE = 13.5%, SE = 1.1%), Landwehr (MAE = 19%, SE = 1.7) and Collins models (MAE = 29%, SE = 2.1%), respectively. The Modified Hughes model was the most robust predictor with 5.4% error, followed by the Distribution model (MAE = 6.1%), Landwehr model (MAE = 7.8%), and Collins model (MAE = 28.3%) was a significantly weaker source contribution predictor than the three other models. Source attribution is dependent on model selection and should be tested prior to field application
Hancock and Revill (2013)	Erosion source discrimination using key land-use sources, forest, permanent pasture, cultivated soils as well as subsurface soils from channel bank and gullies in Logan and Albert River Catchment (3860 km^2), Australia.	**Tracers**: Compound-specific isotope analysis (CSIA) – fatty acids and $\delta^{13}C$ **Size fraction**: < 63 µm **Analysis**: Isosource mixing model	CSIA provides good discrimination of surface soil sources from forest, pasture and cultivated land, as well as sub-surface soil sources (bank erosion, and gullies). It suggests to also being applicable for distinguishing single crops that have been grown at a decadal time frame. Bank erosion was the main contributor, consistent with other geochemical and radionuclide research, with surface soils being a minor contributor. 40 % of sediment comes from forest land-use in

			the Albert River catchment, possibly mostly subsurface sources.
Hardy *et al.* (2010)	The study aimed to document the compositional continuum of the lower 300 km portion of the river (areal extent of ca 12 000 km^2); sources were graduated distances along the river with the addition of 11 tributary delta measurements.	**Tracers**: Ag, Al, As, Au, Ba, Be, Bi, Ca, Cd, Ce, Co, Cr, Cs, Cu, Dy, Er, Eu, Fe, Ga, Gd, Hf, Ho, K, La, Li, Lu, Mg, Mn, Mo, Na, Nb, Nd, Ni, P, Pb, Pr, Rb, S, Sb, Sc, Sm, Sn, Sr, Ta, Tb, Th, Ti, Tm, U, V, W, Y, Yb, Zn, Zr **Size fraction**: 63 µm – 2 mm **Analysis**: Principal component analysis and multivariate Euclidean distance coefficients	The compositional evolution of the bedload indicate that most of the sediment in the lower course flows out but a significant amount of deposition occurs in the upper course. Compositional breaks correspond to either a significant deposition of the bed load or a significant input.
Hatfield and Maher (2008)	Suspended sediment sources from the 3 main tributaries (Glenderamacklin/Greta/Derwent, Newlands Beck and Chapel Beck) entering Lake Bassenthwaite, collected on a monthly basis.	**Tracers**: χ_{lf}, χ_{arm}, IRM, ARM **Size fraction:** > 63 µm, 31–63, 8–31, 2–8 and <2 µm **Analysis**: t-tests, fuzzy cluster analysis	The 8–31 µm and 31–63 µm clastic grain fractions display the greatest magnetic contrasts of ferromagnetic grain size and magnetic 'hardness'. Postdepositional formation of bacterial magnetosomes is evident in the 2–8 µm and < 2 µm fractions of the lake sediments, so source discrimination is restricted to the 8–31 µm and 31–63 µm fractions. Newlands Beck provides only ~ 10% of the lake's hydraulic load but appears to be the main contributor, opposed to the River Derwent sub-catchment, which contributes ~ 80% of the hydraulic load.
Hatfield and Maher (2009)	Fingerprinting upland sediment sources and linkages with particle size, lake sediments and suspended sediments from two sub-catchments feeding the Bassenthwaite Lake. Sources are based on variations on soil type, geology and physical characteristics such as slope and drainage.	**Tracers**: $\chi_{fd\%}$ χ_{lf}, χ_{arm}, IRM, ARM, **Size fractions:** >63 µm, 31–63, 8–31, 2–8 and <2 µm **Analysis**: Non-parametric Spearman's Rank correlation coefficient, Fuzzy analysis	Soil magnetic properties studied on a particle size-specific basis enable rapid characterization and matching of sources and sinks, especially in areas that are considered too homogeneous Low mineral magnetic concentrations indicate properties mainly reflect geological differences, as opposed to in situ pedogenic formation of magnetite. Magnetic parameters sensitive to the degree of magnetic hardness prove most discriminatory in this context.

			The recent lake sediments show strong affinity with the Newlands suspended sediments and upper and middle Newlands Valley topsoils and a Keskadale subsoil.
He *et al.* (1996)	An empirical approach was employed to demonstrate the influence of the catchment-derived ^{137}Cs input and the post-depositional redistribution into 5 lakes and reservoirs in southern England. The sources were catchment derived and direct atmospheric derived tracers.	**Tracers**: ^{137}Cs **Size fraction**: < 2mm **Analysis**: Concentrations, empirical assessment	A clear linkage between lake sediment ^{137}Cs concentration and the catchment source soils exists for the study sites. The importance of catchment sources was emphasized by dominating the lake cores, ranging from 57% and 97% of the total ^{137}Cs inventories.
Hillier (2001)	Suspended sediment sources were collected throughout the R. Don catchment, Scotland to look at storm flow-related changes in composition and source associations.	**Tracers**: Mineralogy using XRD and vertically attenuated infrared spectroscopy (VATIR), C/N ratios **Size fraction:** <45 μm **Analysis**: Regression	The clay mineralogy of base flow samples was more or less identical to high flow samples but the non-clay components were reduced and, additionally, talc and calcite were present. Organic matter contents ranged from 24% to 13% during base and storm flow respectively. The C/N ratio decreased downstream irrespective of flow conditions. More protein and wax components relative to silicates occurred in base flow samples, whereas the humate/fulvate component was most clearly identified storm samples Mineralogy and organic matter suggest topsoils are the primary source
Jenkins *et al.* (2002)	The sediment origin in the Tay Estuary, Scotland from fluvial and marine sources. The fluvial sources were bed sediment from Rivers Tay and Earn, and marine sources from Angus and Fife coasts.	**Tracers**: χ, χ_{fd}, χ_{arm}, SIRM, IRM_{soft}, IRM_{hard}, SIRM/χ_{lf}, SIRM/χ_{arm}, χ_{arm}/χ_{lf} **Size fraction**: 1 mm **Analysis**: Multivariate discriminant analysis, descriptive statistics and inter-parameter correlations	Multi-domain magnetite signatures, characteristic of unweathered bedrock, dominate the magnetic measurement. Overall contributions of 3% from the River Earn, 17% from the River Tay, 29% from the Angus coast and 51% from the Fife coast source end-members, demonstrated the present-day regime of marine sediment derivation in the Tay Estuary. However, this conceals considerable spatial variability both along-estuary and in terms of sub-environments, with small-scale variations in sediment provenance reflecting local morphology, particularly areas of channel convergence
Jin *et al.* (2006)	Investigation into sediment distribution,	**Tracers**: Si, Al, Ti, Fe, Mn, Mg, Ca,	Enrichment and behaviour of many of the elements suggest low

	catchment weathering, hydraulic sorting, and sediment provenance from Daihai lake sediments, Inner Mongolia, north China. Sources were represented by four rock samples as well as water samples for the Sr isotope measurements.	Nz, K, P, Ba, Be, Co, Cr, Cs, Cu, Ga, Hf, Li, Mo, Nb, Ni, Pb, Rb, Sc, Sn, Sr, Ta, Th, U, V, W, Y, Zn, Zr, Organic C and N, $^{87}Sr/^{86}Sr$ in silicate fraction **Size fraction**: < 32 µm **Analysis**: Variation diagrams	chemical weathering intensity under semiarid conditions in the Daihai catchment. Similar chondrite-normalized REE patterns of lake sediment samples may suggest similar sedimentary source rocks, original sediment provenance can be recognized on the basis of their distinctive $^{87}Sr/^{86}Sr$ (AI) ratios and immobile trace element signature, separating from weathering and sedimentary processes as well as from grain size effect.
Klages and Hsieh (1975)	Examination of silt and clay carried by the Gallatin River, South-western Montana. The sources consisted of four geological types (sedimentary, volcanic, metamorphic, and alluvial and Aeolian materials) spanned over 15 sub-catchments.	**Tracers**: Clay and silt mineralogy: Smectite, Kaolinte, Vermiculite, Quartz, Mica and Feldspar **Size fraction**: **Analysis:**	The mineralogy of the sediment was related to geology of the drainage area but differed between streams from similar geologic materials. The Taylor Fork tributary was the chief source of suspended solids resembling 8 of 10 sampling dates. Similar mineralogy between downstream alluvial materials and current suspended sediment show sources have remained the same.
Koiter *et al.* (2013a)	The source of sediment was determined between topsoil, streambanks and shale bedrock derived sediment in South Tobacco Creek (74.41 km2), Canada	**Tracers**: Ti,^{137} Cs, As, U, Ba, Ga, Mn, Na, Sb, Se, Rb, Si, W, Lu, Sr, La, Li, Gd, Eu, Pr, Nd, K, Hf, Sm, Tm, Dy, Ca, Yb, Er, Mg, Zr, Fe, Ho, Al, Bi, Hg, Ce, Sn, Ni, Th, Ag, Cu, B, Cs, Pb, Co, Tl, Ge, Be, Nb, Mo, Cd, Te, P, Zn, Cr, V **Size fraction**: <2 mm **Analysis:** Kruskal–Wallis H test, Stable Isotope Analysis in R model	Topsoil sources (64%–85%) dominated suspended sediment in the upper reaches while streambank (32%–51%) and shale bedrock (29%–40%) displayed a higher proportion in the lower reaches. The downstream transition was attributed to changes in sediment storage and connectivity, shifting of dominant erosion processes and stream incision into the shale bedrock.
Krause *et al.*	The determination of sediment sources in a	**Tracers**: Cu, Pb, Zn, Fe, Mn, K	Gully walls were identified as the dominant sediment source

(2003)	gullied catchment SE New South Wales (1.2 km^2) in successive downstream pools. Three sources were used: pasture agriculture (sheep and cattle grazing), eroding gully walls, and sediment particles derived from roads.	and ^{137}Cs **Size fraction**: **Analysis**: FR2000 mixing model, Monte Carlo	responsible for 90 % and 98 % of the pool sediment. An unsealed road crossing provided a dominant signal for samples directly downstream.
Krein *et al.* (2003)	This study focused on the changes in characteristics of fine sediment in gravel-bed rivers over time within a 25-km^2 drainage basin in Olewiger Bach, Germany.	**Tracers**: Particle characteristics: loss on ignition, colour, fractal dimensions and manganese, iron and magnesium **Size fraction**: < 63 µm **Analysis**: regression	High spatial and temporal variability during changing flows with sources further from the channel being more active during winter or flood events and in channel sources dominating during summer. Increased regularity of particle morphology from gravel to surface to suspended sediment. Exchange of particles in the gravel bed takes place during and shortly after flood events when the armoured layer is broken up. Deposition onto the sediment surface occurred during the falling limb.
Krishnappan *et al*. (2009)	Identification of agricultural inputs using four streams within a Canadian catchment and comparing sediment in stream, bank sediment and soil cores.	**Tracer**: ^{137}Cs **Size fraction**: < 63 µm **Analysis**: Empirical values	The ^{137}Cs presence in the stream indicated that overland flow contributes to the stream sediment. One of the streams did not contain ^{137}Cs in the streams which was either that there was no input, or that the sediment was transported through without being incorporated into the bed. Some bank samples also contained ^{137}Cs, possibly a result of slumping of surface sediment and incorporation into the bank sediment.
Laceby and Olley (2015)	A modelling approach that re-incorporates correlations between elemental concentrations and models distributions for three South East Queensland catchments, Australia.	**Tracers**: Al_2O_3, Ba, CaO, Ce, Co, Cr, Fe_2O_3 , K_2O, La, MgO, MnO, Na_2O, Nd, P_2O_5 , Rb, SiO_2,Sr, Th, TiO_2, V, Y, Zn, Zr. **Size fraction**: <10 µm **Analysis:** Kruskal–Wallis H test, a step-wise linear discriminant analysis (LDA), minimizing mixing model difference (MMD), GOF	The most accurate model was found to incorporate correlations between elements, use the absolute mixing model difference and did not use any weighting. This model was identified that Quaternary Alluvium is the most dominant source of sediment in these catchments (µ 44%, σ 12%). This study demonstrates that it is important to understand how different weightings may impact modelling results.

Appendix A – Comprehensive summary of sediment fingerprinting literature

Lamba *et al.* (2015)	Identification of suspended sediment sources from agriculture, woodlands, and streambanks during cropping season and snowmelt periods in Pleasant Valley watershed (50 km^2), South Central Wisconsin, USA.	**Tracers**: Inorganic geochemical elements Li, Be, Na, Al, P, S, K, Ca, Sc, Ti, V, Cr, Mn, Fe, Co, Ni, Cu, Zn, Ga, As, Rb, Sr, Y, Nb, Mo, Cd, Sn, Sb, Cs, Ba, La, Ce, Ti, Pb, Bi, Th, and U **Size fraction**: <63 µm **Analysis:** Kruskal–Wallis H test, stepwise discriminant function analysis (DFA), frequentist unmixing model, RULSE 2, GOF	Stream banks and agriculture were identified as important suspended sediment sources ranging from 45 to 97% and from 3 to 47%, respectively. During high sediment loads, agriculture was the main source at most watershed sites except during snowmelt runoff periods where stream banks became dominant. Erosion rates in the crop and pasture lands were highly variable ranging from 0 to 0.00509 t $m^{-2} yr^{-1}$. Temporal and spatial variability of suspended sediment should be considered to develop the optimal management strategies.
Lee *et al.* (2008)	Determination of the retention of river sediment geochemical signature from the parent rock and soil within the south Han River basin (12 154 km^2), Korea. The sources are mainly biotite granite and biotite gneiss. The sediments collected were classed as coarse or fine.	**Tracers**: Mineralogy, Si, Al, Fe, Ca, Mg, K, Nz, Ti, Mn, P, Rb, Sr, Th, U, Ta, Zr, Nb, Ba, Sc, Y, La, Ce, Pr, Nd, Sm, Eu, Gd, Tb, Dy, Ho, Er, Tm, Yb, Lu, Nd isotope ratios **Size fraction**: > 0.1 mm, < 0.1 mm **Analysis**: Variation diagrams	Major elemental composition is not identical to the weathering trend of granite. Molar proportions of Al_20_3, CaO +Na_2O, K_2O indicate granite origin. The total Fe2O3, CaO, MgO, Na2O, MnO and REE concentrations are higher in fine sediments than coarse sediment. There is no change in REE distribution pattern from the fresh rock to the soil but coarse and fine sediment have flattened REE patterns for biotite granite sediment. All coarse sediments have positive Eu anomalies, with negative values in the fine. Nd Isotopic composition of the sediments matches the biotite granite.
Martínez-Carreras *et al.* (2010a)	Estimation of suspended sediment sources in 7 small scale catchments (0.7 – 247 km^2) of the Attert River, Luxembourg based on land-use types and channel banks.	**Tracers**: Sediment colour using diffuse reflectance spectrometry in the visible wavelength range using 24 colour parameters from several colour space models; CIE xyY, CIE XYZ, RGB, Munsel HVCV, Helmholtz chromaticity, CIELUV and CIELAB	Time integrated sediment samples had statistically different colour values which represented mixtures of the sediment sources. The sources all showed inter-source colour contrasts. The greater the size of the catchment the more difficult it is to use colour as a source differentiation tool due to heterogeneous geology, intra source variability and source overlap. In medium sized catchments, colour could differentiate between topsoil and subsoil and up to three source types.

		Size fraction: < 63 µm **Analysis**: Kruskal–Wallis H-test, stepwise discriminant function analysis (SDFA), Monte Carlo mixing model	No colour model was universally capable across catchments, but instead a unique combination for each catchment. Colour lacked the ability to integrate spatial provenance and source type.
Matisoff *et al.* (2002)	Focused on determining sediment input from till vs. no-till management of land following a thunderstorm within Woman Creek, Ohio.	**Tracers**: ^{7}Be, ^{137}Cs, ^{210}Pb **Size fraction**: suspended sediments **Analysis**: Concentrations, regression	The tilled agricultural fields were disproportionately responsible for the majority of the suspended sediment load. About 6–10 times more sediment derived from sub-basins that are predominately tilled. ^{210}Pb and ^{137}Cs activities were homogeneous in tilled area soil profiles. Surface soil was the main source of suspended sediment.
McConnachie and Petticrew (2006)	Evaluation of the organic matter sources in fine sediment within a salmon-bearing stream in Canada.	**Tracers**: Suspended particulate, inorganic and organic matter concentrations (SPM, SIM, SOM), effective particle size distributions (EPSD) were analysed via C:N ratios and stable isotopic signals **Size fraction**: < 0.7 µm **Analysis**: Kruskal–Wallis non-parametric assessment of variance	Indication of the ability of stable isotopes to detect the changing relative contributions of salmon and terrestrial organics in suspended sediment. Seasonal changes of dominant organic matter are important for freshwater flocculation. The presence of salmon in streams is associated with increased particle size within the water column.
Mckinley *et al.* (2013)	Tested a streamlined fingerprinting approach from streambank, construction site, forest, pasture, unpaved and row crop sources, for the North Fork Broad River (NFBR), Georgia, USA.	**Tracers**: stable isotopes of nitrogen (N) and carbon (C) (^{15}N and ^{13}C), total N (TN), and total C (TC) was tested. **Size fraction**: **Analysis:** Multivariate discriminant analysis	Multivariate discriminant analysis showed that three of the four tracers (δ^{15}N, δ^{13}C TC) from the initial pool were capable of accurate classification of the source samples. Streambank material was the main sediment source for this watershed Despite variations in land-use and stream order, the legacy sediments comprising the banks and floodplains were the main factor in impairment for suspended sediment. A statistically significant difference was found between δ15N and

			$\delta^{13}C$ concentrations collected using automated samplers vs. the mobile centrifuge. A cost-effective tracer suite was identified as well as an attempt to make a streamlined approach to the technique.
Minella *et al.* (2008)	Combination of sediment source tracing with traditional monitoring techniques within a small (1.19 km^2) catchment in Brazil focusing on 50 storm events. Five sediment sources based on land-use: cultivated agriculture (mainly tobacco), fallow cultivated agriculture, pasture agriculture, eroding channel banks, and sediment particles derived from unpaved roads.	**Tracers**: P, Ca, K, Mn, Cu, Na, Zn, Fe, Mg, $C_{organic}$, $Fe_{dithionite}$, $Fe_{oxalate}$, $Mn_{dithionite}$, $Mn_{oxalate}$, **Size fraction**: < 150 µm **Analysis**: Multivariate using Kruskal-Wallis discrimination of properties	Introduction of improved land management reduced volumes of storm runoff and sediment loads (80 % reduction for low magnitude, and 40 % for intermediate events) but suspended sediment concentrations were similar throughout. The improved land management also saw sediment contribution from field surfaces and unpaved roads decrease from 63% and 36% to 54% and 24%, respectively, whereas stream channel contributions increased from ca 2% to 22%.
Motha *et al.* (2004)	Sources of sediment from five sediment sources based on land-use: gravel-surfaced-roads, ungravelled roads, pasturelands, cultivated lands, and undisturbed forests during six high frequency rainfall events in S.E. Australia.	**Tracers**: TOC, Fe_2O_3, Al_2O_3, SiO_2, K_2O, CaO, IRM, χ, ^{210}Pb, ^{137}Cs, **Size fraction**: 2, 2–20, 20–40, and 40–63 µm recombined to < 63 µm **Analysis**: Mixing model, ANOVA, Discriminant Function Analysis (DFA), Monte Carlo	Relative contributions from gravel-surfaced roads, grouped lands, cultivated lands on granite-derived soils, and forest to sediments in the falling limbs of event hydrographs were 0.41 ± 0.17, 0.18 ± 0.13, 0.13 ± 0.11 and 0.14 ± 0.07, respectively and during peak discharge were 0.52 ± 0.12, 0.30 ± 0.17, 0.15 ± 0.11 and 0.17 ± 0.08, respectively. Relative contributions per unit area from the gravel-surfaced roads, grouped lands, and cultivated lands on granite soils were as high as 500-, 100- and 10-times, respectively, the areal contributions from the forest indicating unsealed road sources as a significant source.
Motha *et al.* (2002)	Conservativeness of tracers analysed through sediment source properties using simulated rainfall and five sediment sources based on land-use: gravel-surfaced roads within an agricultural land-use, gravel-surfaced roads within a forest land-use, ungravelled roads	**Tracers**: Fe_2O_3, Al_2O_3, CaO, Na_2O, K_2O, IRM_{850} and χ, ^{210}Pb, ^{137}Cs **Size fraction**: 2, 2–20, 20–40, and 40–63 µm recombined to < 63 µm **Analysis**: Concentrations and t-	Results indicate that the concentration of Fe_2O_3 was not conservative for any of the process sources investigated, Al_2O_3 was not conservative for three of the four process sources, and the sum of molecular proportions of CaO**, Na_2O, K_2O and Al_2O_3 was not conservative for two of the four processes Mineral magnetic properties, IRM_{850} and χ were found to be not

	within a forest land-use, pasturelands, freshly cultivated lands.	test	conservative but may be due to particle size effects The radionuclide tracers, ^{137}Cs and $^{210}Pb_{ex}$, were found to be conservative through the sediment generation process.
Nagle and Ritchie (2004)	Quantification of erosion from cultivated fields and sources of channel bottom sediment in the Wildhorse Creek, Oregon. Sources were compared between active floodplain and stream bottom sediment to sediment from cultivated fields and channel banks.	**Tracers**: C, N, ^{137}Cs **Size fraction**: < 63 µm **Analysis**: Mixing model	Bottom sediment was mostly made up of subsurface material (banks and gullies) with < 26 % coming from cultivated sources. Annual estimates of erosion were 3 to 7.5 t ha^{-1} yr^{-1} since 1963.
Nosrati *et al.* (2014)	Geochemical fingerprint analysis using Bayesian-mixing model to estimate sediment sources from rangeland, orchard and stream bank in the Hiv catchment, Iran.	**Tracers**: Total concentrations of Al, B, Ba, Be, Bi, Ca, Cd, Co, Cr, Cu, Fe, Ga, K, Li, Mg, Mn, Mo, Na, Ni, P, Pb, Se, Sr, Te, Tl and Zn **Size fraction**: <63 µm **Analysis**: Kruskal-Wallis, Discriminant Analysis, Bayesian-mixing model (MixSIR) and frequentist model.	Discriminant analysis provided identified four tracers – B, C, Sr and Tl, which afforded more than 97% categorization. The median contribution from rangeland, orchard and stream bank sources was 20.8%, 11.2% and 68%, respectively. Uncertainty analysis was considerable ranging from 2–24% for rangeland, 1– 26% for orchards and 66 – 83% for stream banks respectively. While results provide useful information for sediment management the high uncertainty prevents precise estimates, which needs to be accounted for.
Oldfield *et al.* (1979)	Identification of suspended sediment sources by means of magnetic measurements in the Jackmoor Brook near Exeter, United Kingdom.	**Tracers:** Low-field susceptibility x, saturation isothermal remanent magnetization (IRM_{sat}), and coercivity of IRM **Size fraction:** **Analysis:**	Preliminary results indicate the value of this approach in an area where the contrast in properties is easily characterized, in this case between Permian sandstone bedrock and topsoil. High flows are shown to be associated with suspended sediment, the magnetic properties of which are indistinguishable from those of the cultivated soils of the catchment.
Oldfield and Crowther (2007)	Differentiation of magnetic signatures derived from natural, unburnt topsoils (UK) to samples from known archaeological burn sites (UK and Hungary).	**Tracers**: bulk, low field (χ_{lf}), frequency dependent (χ_{fd}), magnetic susceptibility (χ) and normalized anhysteretic	Ferrimagnetic mineral assemblages produced from fire have significantly finer grain sizes than those produced from soil formation. Burning shows distinctive values on a bilogarithmic plot of

		remanent magnetization (ARM) **Size fraction**: ? **Analysis**: Bilogarithmic plot	χARM/χfd versus χARM/χlf which can be used as indicators of magnetic signatures in soils, archaeological materials and palaeosols that have arisen mainly through burning.
Olley *et al.* (2013)	Application to determine dominant erosion process in water supply catchments of S.E. Queensland (22 600 km^2) for major land-use areas; cropping, grazing and forest, and channel bank sources.	**Tracers**: ^{137}Cs, $^{210}Pb_{ex}$ **Size fraction**: < 10 µm **Analysis**: Discrete mixing model based on proportions.	Composite sampling of 20 subsamples provided sufficient averaging of local variations. Probability distributions are only normally distributed for $^{210}Pb_{ex}$. Probability distributions using ^{137}Cs concentrations show that channel sediment is consistent with channel erosion
Olley and Caitcheon (2000)	Major element chemistry and sediment origin within the Darling-Barwon River, Australia using three source sample areas based on basalt, granite and sedimentary rocks.	**Tracers**: P_2O_5, Na_2O, MgO, Al_2O_3, SiO_2, K_2O, CaO, TiO_2, Mn_2O_2, Fe_2O_3, CIA, Optical stimulated luminescence (OSL) measurements for last sunlight exposure **Size fraction**: <10 µm **Analysis**: Concentrations, chemical index of alteration (CIA)	Major element chemistry indicates the fine sediment is derived from weathered granite not the intensively farmed basalt areas which account for < 5 % Flow conditions during the study probably increased the relatively input from the dominant sub-catchment compared to its long term contributions. The sediment currently in transport is probably derived from the lowland areas that contain more weathered material and not from contemporary upland erosion. Phosphorus concentrations in the sediments are consistent with those in natural soils of the region and have indications are that they have not changed significantly in the last 200 years.
Owens and Walling (2002)	The changes in phosphorus content of fluvial sediment in rural (Swale – 1363 km^2) and industrialized (Aire-Calder – 2862 km^2) river basins comparing suspended, channel bed, and floodplain sources.	**Tracers**: Total P, inorganic P, organic P (OP), organic C and N **Size fraction**: <63 µm **Analysis:** Concentrations	Little evidence of major downstream increase in TP content in the River Swale (500 – 1500 µg g^{-1}). Rivers Aire and Calder exhibit large downstream TP increases (<2000 µg g^{-1} increased to >7000 µg g^{-1}). The downstream TP values exceed quality guidelines and are much higher than similar rivers around the world. Topsoil from upland pasture and cultivated areas, and channel bank material are main sources of particulate P (PP). Channel bed sediment and floodplain sediment are lower in PP concentrations than suspended sediment. Floodplain deposition rates and fine grain sediment storage in the river bed are relatively high. The PP has a large bioavailability which increases the importance of IP increases into the channel.

Appendix A – Comprehensive summary of sediment fingerprinting literature

Owens *et al.* (2001)	Downstream changes of sediment-associated contaminants in the River Swale (1363 km^2) and Aire-Calder (2862 km^2) river basins using floodplain sediment, channel bed sediment and suspended sediment sources.	**Tracers**: Total P, Organic P, Inorganic P, Cr, Organic C and N, PCBs **Size fraction**: < 63 µm **Analysis**: Concentrations	The concentrations of phosphorus, chromium and selected PCBs associated with sediment are significantly higher in the River Aire-Calder than the unindustrialized River Swale catchment. The concentration of the sediment-associated contaminants in the Aire-Calder system increase downstream in association with the urban areas and point source inputs. Higher contaminant concentrations in floodplain and channel bed sediment together with sediment storage measurements indicate that significant sediment-associated contaminants occurs in the Rivers Aire-Calder
Porto *et al.* (2013)	Soil cores of slopes, catchment divides and Valley bottoms analysed to establish a sediment budget for the small (1.39 km2) forested Bonis catchment, located in southern Italy.	**Tracers**: ^{137}Cs and $^{210}Pb_{ex}$ **Size fraction**: <2mm **Analysis:** ^{137}Cs diffusion and migration model, $^{210}Pb_{ex}$ conversion model	Measurements of ^{137}Cs and ^{210}Pb are confirmed to provide a valuable tool for quantifying both erosion and sediment redistribution within a catchment and therefore for establishing It's sediment budget.
Peart (1993)	Investigation of the suitability of sediment properties as natural tracers in two basins in Hong Kong. The sources included litter, surface soil, subsoil, bottom sediment, and suspended sediment for Kwun Yum Shan basin (< 1 km^2), and soil, landslide substrate, cut-and-fill substrate, bottom and suspended sediment for Lam Tsuen River Basin (20 km^2).	**Tracers**: Colour, C, N, C/N, LOI **Size fraction**: <2 mm **Analysis**: Concentrations	Not all the properties were capable of differentiating sources; bed sediments may complicate the issue. Colour was not able to differentiate in either basin, and only LOI was able to be use in the Lam Tsuen River. Traditional information and inventories of potential sources and processes (field surveys, air photographs) aid interpretation Spatial sampling of suspended sediment concentrations proved very useful confirming sources information.
Peart and Walling (1986)	Small 9.3-km^2 basin underlain by sandstones, breccias and conglomerates. Two major soil groups, brown earths in north and south, gleyed brown earths in central area. Land-use is mainly mixed arable farming. Surface soils and channel banks were sampled and stratified into soil type, land-use	**Tracers**: Pyrophosphate Fe, Mn, Magnetic Susceptibility, SIRM, Total P, Organic C, N, Cs^{137} **Size fraction**: < 63 µm **Analysis**: mixing model	Fingerprinting approach provided consistent estimates of relative importance of major sediment sources, potential for wider application. Major advantages over traditional methods involving onsite monitoring as it subsumes the linkages interposed between onsite erosion and downstream sediment yield Several indicators rather than a single indicator are necessary for

	and different components of channel network.		consistency. Indicator properties for surface/subsurface differentiation was made easier due to homogenous geology underneath, heterogeneous geology would complicate the matter. Cs^{137} is particularly useful as it behaves independently in geology. Ratio properties are particularly useful and enrichment issues mean source and suspended material are not directly comparable but particle size fractions may alleviate this issue.
Porto *et al.* (2005)	Focus was on primary sediment sources within a small forested catchment (1.38 ha) in Calabria, Southern Italy. The sources were based on areas; a north facing and a south facing plot and material was the upper 2 cm.	**Tracers**: Total C, Total N, Total P, Inorganic P, Organic P, C/N, ^{137}Cs Total ^{210}Pb, unsupported ^{210}Pb and ^{226}Ra, **Size fraction**: <63 µm **Analysis**: Mann-Whitney test	Most sediment originates from south facing slopes where vegetation is discontinuous. Results are specific to this sub-catchment, other catchments will need more sources i.e. gullies and cultivated areas.
Pulley *et al.* (2015)	Analysed differences sediment estimations between different groups of tracer properties and determined the role of organic matter content, particle size, and within-source variability of channel banks, surface agricultural land, and urban street dusts from the Nene basin, U.K.	**Tracers**: Mineral magnetic measurements; Low frequency susceptibility (X_{lf}), frequency dependent susceptibility (X_{fd}), susceptibility of ARM (X_{arm}), soft isothermal remanent magnetisation (−100 mt) (IRM_{-100}), saturation isothermal remanent magnetisation (1 T) (SIRM), and hard isothermal remanent magnetisation (HIRM) Activities of ^{212}Pb, ^{137}Cs, $^{210}Pb_{un}$, ^{226}Ra, ^{234}Th, ^{235}U, ^{40}K **Size fraction**: <63 µm **Analysis:** Kruskal–Wallis H test, Genetic Algorithm-based Linear	Different tracer groups displayed a mean difference of 24.1% for channel bank sediment sources while urban street dusts sources displayed a mean difference between 8% and 11%. Organic matter content and/or particle size showed little indication that they caused differences between tracer group predictions. Uncertainty was likely caused by within-source variability and small contrasts between source group tracer concentrations.

		Discriminant Analysis (GA-LDA) model, Goodness of Fit (GOF), frequentist unmixing model,	
Rhoton *et al.* (2008)	Identification of primary sources in the Walnut Gulch Experimental Watershed, Arizona, based on major soil unit transects in six watersheds in conjunction with landform.	**Tracers**: Radionuclides, ^{137}Cs, ^{40}K and ^{226}Ra and stable C isotope distributions. Sodium pyrophosphate (p), acid ammonium oxalate (o) and sodium citrate-bicarbonate-dithionite (d) extractable Fe and Mn Quantitative soil colour, Magnetic susceptibility and Mineralogy were also used **Size fraction**: <2 mm **Analysis**: multivariate mixing model	Suspended sediments tended to be enriched with silt, clay, organic C, inorganic C, total N, extractable cations, extractable Fe and Mn, ^{13}C, ^{40}K, and ^{226}Ra. Three suspended sediment samples were enriched with ^{137}Cs. Eleven characterization parameters were used in a multivariate mixing model to identify the SWs contributing the greatest sediment loads in the WGEW. The mixing model results indicated that three sub-catchments that had the highest erodibility were contributing approximately 86% of the sediment These results related to the $\delta^{13}C$ data, which indicated that approximately 65% of the stable C isotopes leaving were derived from C3 plants (shrubs), the dominant vegetation on the three sub-catchments.
Roddy (2010)	Quantification of sediment inputs into an estuary based on native forest, exotic forest, agricultural landscapes as well as subsurface, streambanks and surface sources in Whangapoua catchment, New Zealand.	**Tracers**: Mg, Zn, P, Mn, Fe, Cr, Ca, Al, U, V, S, Cl, Si, Se, Bi, ^{137}Cs **Size fraction**: < 10 μm **Analysis**: Kruskal Wallis H-test, Discriminant functional analysis (DFA), mixing model	Si, P, Se, V, U, In, Bi were used for landscape units showing native forest contributed 62 %, exotic 23 % and agricultural 15 % of sediment into the estuary. Se, Fe, Mn, P, Ca were utilized for the erosion position; most of the sediment was derived from subsurface (79 %), followed by streambanks (13 %) and surface sources (8 %). Radionuclide results support the findings of the relative sediment fingerprinting for of surface vs subsurface, but not the type of subsurface or the landscape units.
Russell *et al.* (2001)	Establishment of suspended sediment sources within two small (<4 km^2) lowland agricultural catchments in the UK. Focus was on surface sources (by land-use, geology, and	**Tracers**: Al, As, Ca, Cu, Fe, K, Mg, Mn, Na, Ni, Pb, Sr, Zn, Fe_p, Mn_p, Al_p, Fe_d, Mn_d, Al_d, Fe_t, Mn_t, Al_t, TP, TN, TC, χ_{fd},, χ_{lf}, ARM, SIRM, IRM,	Field drains accounted for 27–55 % of sediment yield, bank erosion ca. 10 % and surface sources contributing 34–65 %. The estimates conceal significant inter- and intra-storm variability in the source contributions.

	soil type), eroding channel banks and field drains.	^{137}Cs, unsupported ^{210}Pb **Size fraction**: < 63 µm **Analysis**: Kruskal Wallis test, Discriminant functional analysis (DFA), Wilks' lambda minimization , mixing model	
Rustomji *et al.* (2008)	Combining multiple datasets for greater accuracy in Lake Burragorang catchment (9000 km^2), Australia; geochemical tracing, in-stream monitoring and process based modelling. Sediment sources were spatially distributed around stream confluences as well as surface and subsurface sources.	**Tracers**: Si, Al, Mg, Fe, Ca, Na, K, Ti, P, Mn, Ba, Ce, Co, Cr, La, Ni, Pb, Rb, Sr, V, Y, Zn, Zr, ^{137}Cs **Size fraction**: < 10 µm **Analysis**: Bayesian unmixing model	The accuracy of predictions of models such as SedNet can be substantially improved through use of local data. Challenges are met with difference in a 'snapshot' approach from sediment fingerprinting opposed to a long-term representation from modelling as well as differences in definitions of suspended sediment.
Samani *et al.* (2011)	Multiple fingerprint techniques for sediment source contribution of gully erosion of 3 sub-catchments (26.5 ha, 5.1 ha and 175 ha) in Boushehr, Iran. The sources were based on surface soil from rangeland, dry farming and gully wall subsurfaces.	**Tracers**: Organic C, Kjeldahl N, C/N, P, ^{137}Cs **Size fraction**: 63 µm **Analysis**: Multi-parameter mixing model	The optimum combination of tracers is unique for different locations. Organic tracer uncertainty is higher due to the low organic content of the region. Drainage density and catchment area are the most important factors of sediment contribution in gully erosion, but drainage density and hillslope length are also important. Gully erosion becomes the dominant process for sediment production in areas less than 5.6 ha.
Singh (2009)	Comparison of channel, active flood-plain and older flood-plain sediments with catchment source sediments and rocks in the Ganga River, India. Source sampling was acquired over a 800 km distance of the river focused on Surface, flood-plain sediments, and flood deposits on current channel margin.	**Tracers**: Texture, mineralogy, and geochemistry: SiO_2, Al_2O_3, TiO_2, FeO, MgO, MnO, CaO, K_2O, Na_2O,P_2O_5, Ba, Sr, Ni, Zr, Sc, Co, Th, U, La, Ce, Nd, Sm, Eu, Gd, Dy, Yb, **Size fraction**: 0.075 mm **Analysis**: variation diagram, concentration	Catchment sediments supplied to the Ganga River are chemically immature and subjected to mostly physical weathering due to to higher erosion rates. Silica weathering occurs only after entering the plains, likely due to the high residence time and change in environment. This presents issues on using geochemical data for inferring source climate of ancient systems. A combination of erosion, weathering, sorting and Aeolian activity has together played a major role in progressively changing the

			chemistry from source rock to the different catchment sediments Ratios of immobile elements may not be as invariant as once thought indicated with trend line rotation around fine grained end members
Singh and France-Lanord (2002)	Sediment distribution of sediment sources and erosion in the Brahmaputra watershed based on bank sediments and suspended loads.	**Tracers**: Major and trace elements. SiO_2, Al_2O_3, TiO_2, FeO, MgO, MnO, CaO, K_2O, Na_2O,P_2O_5, Rb, Sr, Sm and Nd concentrations and Sr and Nd isotopic compositions **Size fraction**: < 2 μm **Analysis**: Composition	High Sr isotopic ratios and low ε_{Nd} from Himalayan formations and lower Sr isotopic ratios and higher ε_{Nd} from the Transhimalayan plutonic belt make up the main sources. Himalayan sources are dominant representing about 70 % of sediment. Despite dominant Himalayan erosion, the Siang-Tsangpo River which drains the plutonic belt represents the major s source of sediment.
Slattery *et al.* (1995)	Within-storm quantification of suspended sediment sources from three sources based on soil type: cultivated topsoil, channel banks, and a combined topsoil/banks source, in a 6.2-km^2 basin, U.K.	**Tracers**: χ_{lf}, χ_{hf} , IRM, SIRM **Size fraction**: < 2 μm, 2–16 μm, 16–63 μm **Analysis**: Mann-Whitney U-test, mixing model	The magnetic measurements distinguished between three potential source materials showing that cultivated fields provided the major source of suspended sediment, becoming more dominant at times of peak storm runoff. This pattern of variation during storms reflected increased erosion of valley-floor sediment during overbank flooding rather than the delivery of eroded soil to the stream by surface runoff.
Smith and Blake (2014)	Re-examination of critical assumptions relating to (i) the physical and chemical basis for source discrimination and (ii) potential factors that may confound source mixing in agricultural catchments using cultivated and pasture surface soils, and sub-surface material derived from channel banks in the River Tamar (920 km^2) in south-west England that has also been affected by mining.	**Tracers**: Inorganic geochemistry of Mo, Nb, Zr, Sr, Rb, Bi, As, Se, Au, Pb, W, Zn, Cu, Re, Ta, Hf, Ni, Co, Fe, Mn, Cr, V, Ti, Ca, K, Ba, Sb, Sn, Cd, Pd, Ag, Al, P, Si, Cl, S and Mg, Total Organic Carbon (TOC), ^{137}Cs, $^{210}Pb_{ex}$, particle size **Size fraction**: <63 μm **Analysis:** Kruskal–Wallis H test, discriminant function analysis (DFA), frequentist unmixing	Source discrimination was dependent on differences in geochemistry of surface and sub-surface attributed to weathering and pedogenetic effects. Source discrimination was limited by agricultural land-use rotation and similarity of cultivated sources to a mix of pasture and channel bank sources. Metal pollution from historic mines and organic enrichment of sediment from upland peat soils resulted in the non-conservative behaviour of some tracer properties Inconsistent relationships between particle size, organic carbon and tracer property concentrations undermine the use of particle

		model GOF	size and organic matter correction factors, and actually produce large changes in source estimation
Smith and Dragovich (2008)	Improvements on sediment source and erosion process distinction focused on surface and sub-surface source contributions of fine sediment in a small (1.6 km^2) upland catchment in Australia.	**Tracers**: ^{137}Cs and $^{210}Pb_{ex}$, erosion pin data **Size fraction**: < 2 µm **Analysis**: mixing model, Student's t-distribution, Monte Carlo	Employment of channel survey and erosion pin data improved the precision of estimates of sediment-source erosion-process contributions from hillslopes and channel/gully walls. A mean of 81% was found to be amount of sediment exiting the catchment from in-channel deposits and suspended sediment once adjusted for erosion process (up from 74 %). Net erosion of the channel floor was low. Variability in sediment source contributions within the catchment was high, with rapid transition from hillslope to channel source dominance of sediment flux with distance downstream in the study catchment.
Udelhoven and Symader (1995)	Significance of particle characteristics for identification of sources of suspended sediment	**Tracers**: Digitized colour values **Size fraction**: < 60 µm **Analysis**: Kolmogorov Smirnov test, Barlett-Box test, Pillais test, F-test	No general agreement about what characteristics should be considered The determination of particle colour provides a fast and easy approach. Examination of the digital pictures is feasible with standard methods of digital image analysis. This method yields a quantitative description of a sample's colour that can be compared and can be used as an independent input into quantitative models.
Walden *et al.* (1997)	Two major soil series are present within the catchment, the Aberford and the Banbury Series and the vast majority of the catchment consists of cultivated land. Field observation and mineral magnetic data summarised later suggested that three potential sediment source groups can be identified: Aberford series topsoils; Aberford series channel bank material; and either topsoils or channel bank material from the Banbury soil series (which could not be	**Tracers**: magnetic susceptibility (x), frequency dependent susceptibility (xfd), isothermal remanence magnetisation (IRM) **Size fraction**: < 63 µm **Analysis**: R- and Q-mode factor analysis, numerical unmixing modelling	The three source material types possess magnetic behaviours that can be distinguished; the majority of the magnetic behaviours lie within source behaviours. Potential problems with between-group and within-group variation in magnetic properties may cause issues with quantitative sediment source ascription. Identification and quantification of the major source material types is a critical step in any attempt to quantify sediment source contributions. Qualitative and statistical analyses of compositional data for sediment source unmixing perform important tasks in assessing

	distinguished magnetically).		validity for successful modeling. Unmixing errors such as the natural variability within each source type will occur, but provide useful tool to be developed further. Further work, combining magnetic with other forms of compositional analyses is clearly warranted.
Wall and Wilding (1976)	Identification of sources of sediment from rural, urban and geological sources in the Maumee River Basin, Ohio.	**Tracers**: Clay mineralogy **Size fraction**: < 2 µm, 2–50 µm **Processing**:	Little seasonal or downstream variability in clay mineral composition of the clay-sized (< 2 µm) sediments Mineralogy provided differentiation between surficial and geologic (parent material) sources of suspended sediments. Annual suspended sediment load of the Maumee River and tributaries was predominantly surficial in origin.
Wallbrink and Murray (1993)	Erosion processes determined by fallout radionuclides of suspended sediment from generated surface runoff	**Tracers**: ^{137}Cs, ^{210}Pb, ^{7}Be **Size fraction**: suspended sediment **Processing**: concentrations	Suspended sediment derived from sheet flow contained initially high values of ^{137}Cs, ^{7}Be and $^{210}Pb_{ex}$ but decreased over time for the latter two. This is interpreted as indicating a change from sheet dominated erosion to rill dominated erosion. In a eroded gully scenario no detectible ^{137}Cs, ^{7}Be and $^{210}Pb_{ex}$ was found, even when overland flow was allowed to wash down the gully wall side. Correlation between ^{210}Pb and 7Be indicated that ^{210}Pb may be more applicable over longer time scales.
Wallbrink *et al.* (1998)	Determining transit times of four sources: forest, pasture agriculture, cultivated agriculture (wheat and cereal production), and eroding gullies/ streambanks, in the Murrumbidgee River, Australia.	**Tracers**: ^{137}Cs, $^{210}Pb_{ex}$, ^{7}Be **Size fraction**: < 2 µm sediment **Processing**: concentrations	Concentrations of fallout ^{137}Cs and $^{210}Pb_{ex}$ are significantly different between sources and indicate largest contribution of material is derived from subsoil channel/gully sources. $^{210}Pb_{ex}$ decay indicate that residence time of fine grained material is 10 ± 5 years but differences in ^{137}Cs concentrations and the presence of ^{7}Be indicate that some residence times is only a few weeks to months.
Walling *et al.* (2008)	Tracing suspended sediment and particulate phosphorus sources in 7 Hampshire Avon sub-catchments and 5 Middle Herefordshire Wye sub-catchments. The sources focused on surface soils under cultivation, pasture and	**Tracers**: Metals, Al, Cd, Co, Cr, Cu, Fe, Mn, Ni, Pb, Sr, Z, Ca, K, Mg, Na, Inorganic P, Organic P, total P, C, N, ^{137}Cs, $^{210}Pb_{ex}$, ^{226}Ra, LOI500, and LOI850	In the Wye sub-catchments channel/subsurface sources contributed 40–55% of the overall suspended sediment flux and 21–43 % of the PP flux from the catchments. Equivalent values for the Avon were 1–41% and 1–54%, respectively. Combining this information for P flux indicates 15–20 t km^{-2} year^{-1}

	woodland, as well as channel bank/subsurface.	**Size fraction**: < 63µm **Analysis**: Kruskal-Wallis H-test and DFA	from surface sources in some of the Wye sub-catchments, whereas subsurface/channel sources exceeded 0.1 kgP ha^{-1} $year^{-1}$ in the same sub-catchments The results emphasize the need to consider contributions from channel/subsurface sources of PP flux as well as surface sources when applied to modelling.
Walling *et al.* (2003)	Investigation of downstream changes in storage of sediment-associated nutrients in river channel and floodplain systems of Rivers Aire (and tributary, River Calder) and Swale, UK.	**Tracers**: 23 PCB congeners, Inorganic P, Organic P, Total P, Organic C, Cr, Cu, Pb, Zn, **Size fraction**: < 63 µm **Analysis**: coefficient of variation	The contaminant content of the fine sediment generally increases downstream in Rivers Aire and Calder according to main urban centres. The River Swale contaminant levels remain consistent downstream due the low pollution. Pb and Zn decrease downstream due to historic mining. Sediment storage controls the magnitude and spatial variation of contaminant storage, and is therefore reflective of the channel and floodplain surface area and greatest in the middle and lower reaches. Comparisons between annual deposition flux in floodplains and river outlet fluxes indicate importance of floodplain deposition in conveyance loss. The River Aire floodplain deposition flux is between ca. 2% (PCBs) and 36% (Pb) of the outlet flux and equivalent values for the River Swale range between 18% (P) and 95% (Pb).
Walling *et al.* (1999)	Fingerprinting suspended sediment sources based on geological, (Carboniferous, Permian and Triassic, and Jurassic) as well as topsoil, cultivated topsoil and channel bank, in River Ouse, UK.	**Tracers**: Radionuclides; ^{137}Cs, $^{210}Pb_{ex}$, ^{226}Ra, mineral magnetism; χ, SIRM, Geochemical composition; Al, Ca, Cr, Cu, Fe, K, Mg, Mn, Na, Ni, Pb, Sr, Zn, Total P, Organic P, Inorganic P, C, N **Size fraction**: < 63 µm **Analysis**: Kruskal±Wallis H-test, discriminant function analysis, mixing model	Suspended sediment from the River Ouse from topsoil, cultivated topsoil and channel bank sources were estimated to be c. 25, 38 and 37 %, respectively, while for the River Wharfe these sources contributed ca 70, 4 and 23 %, respectively. Channel banks supplied more sediment during higher flows. Source materials were differentiated according to the three main geological source areas (Carboniferous, Permian and Triassic, and Jurassic) estimated to be c. 24, 41 and 35% for the River Ouse and c. 91, 9 and 0% for the River Wharfe, respectively. When suspended sediment samples from tributary streams were used to characterize each geological source area, the equivalent results for

			the River Ouse were c. 30, 46 and 24%. The rivers Swale, Ure and Nidd contribute and estimated 82, 15 and 3 %, to the River Ouse. These are compared with relative magnitude of the suspended sediment loads and differences attributed to the different periods of recording and the timing of sampling relative to storm events.
Walling *et al.* (1997)	Overbank deposit characteristics from flood events in the River Ouse, UK.	**Tracers**: Organic C, C:N ratio, ^{137}Cs **Size fraction**: < 63 µm **Analysis**: Concentration	Sediment deposited nearest to the channel consisted primarily of sand-sized material with evidenced mineral fining at increasing distance from the channel. Sand-sized material was deposited 20-40 m from the channel although were present up to > 100 m from the channel in some sites. Overbank sediment was generally considerably coarser than suspended sediment C:N ratios of the organic fraction of the overbank sediment was approximately constant across the width of the floodplain. The organic C and ^{137}Cs content of the deposited sediment increased with distance from the channel, and both properties were positively related to the magnitude of the < 63 µm fraction. This flood event was more extreme due to the coarser nature of the sediment compared with previous flood events
Walling *et al.* (1979)	Identification of suspended sediment sources in Jackmoor Brook base on land-use and process sources; woodland topsoil, arable soil, streambank erosion scars.	**Tracers**: χ, SIRM, χ/ SIRM ratio, SIRM coercivity **Size fraction**: **Analysis**:	Magnetic properties can provide relative importance of slope and channel sources in a catchment and during storm events. Filter paper residues provide a simple collection method. More work is required on enrichment aspects and relationships with organic matter.
Walling and Amos (1999)	Source, storage and mobilization of sediment sources from ploughed/cultivated agriculture, pasture agriculture, channel margin areas degraded by cattle trampling and farm trackways/roadways, and eroding streambanks, within the Upper River Piddle,	**Tracers**: Particle-size analysis TOC, TON, C/N ratio, ^{137}Cs, ^{210}Pb, **Size fraction**: < 63 µm **Analysis**: discriminant function analysis based on minimization of Wilks' lambda or U-statistic,	Substantial amounts of sediment accumulate in the channel of the upper and middle reaches of the river during the winter months and the 'slug' of sediment slowly moves downstream. The dominant source of suspended sediment was likely to be surface soil from cultivated areas, supported by observations, much of which is stored within the channel system and slowly

	Dorset.	multivariate mixing model	transmitted downstream.
Wilkinson *et al.* (2013)	Surface, subsurface and spatial sources was used to investigate sources within the Burdekin River basin (130,000 km2) in northeast Australia	**Tracers**: Fallout radionuclides and geochemistry; Al, As, Ba, Be, Ca, Ce, Cl, Co, Cr, Cs, Cu, Dy, Er, Eu, Fe, Ga, Gd, Ge, Hf, Ho, K, La, Mn, Mo, Na, Nd, Ni, P, Pb, Pr, 228Ra, Rb, Sc, Se, Si, Sm, S, Sr, Tb, Th, Ti, Tl, Tm, U, V, Y, Yb, Zn, Zr, ^{210}Pbex, ^{137}Cs **Size fraction**: <10 µm **Analysis:** MANOVA, Monte-Carlo numerical mixing model, Mean Relative Error (MRE)	Sediment sources were likely in close proximity to the drainage network, since concentrations were higher on the rising limb than the falling limb of the hydrograph. Between 77% and 89% of fine sediment loss in the study area was derived from subsurface soil sources thought to be dominated by gully erosion. The results contradicted previous sediment budget spatial modelling, which attributed hillslope erosion to be the dominant source area. Sediment contribution estimations had narrow confidence intervals for source areas defined using sediment from geologically distinct river tributaries since tributary sediment has less-variable geochemistry.
Zhang *et al.* (2008)	Distinguishing sediments from two predominant sources based on the Yangtze and Yellow Rivers, separated into size fractions, <2 µm, 2–4 µm, 4–8 µm, 8–16 µm, 16–32 µm, 32–63 µm, and >63 µm.	**Tracers**: Particle-size analysis,χ, SIRM, χ_{ARM}, χ_{fd} and HIRM **Size fraction**: < 2 µm, 2–4 µm, 4–8 µm, 8–16 µm, 16–32 µm, 32–63 µm and > 63 µm **Analysis**: regression relationships	Distinctive contrasts in magnetic properties between sediments from the Yellow and Yangtze River estuaries exist from weathering regimes and lithology in the drainage basins. Sediments from the Yangtze River estuary are characterized by higher SIRM and S_{-100} values, suggesting higher concentrations of ferrimagnetic minerals and increased proportions of ferromagnetic minerals to anti-ferromagnetic minerals. To minimize the problem of biogenic and diagenetic overprint in the marine environment, magnetic discrimination on particle size larger than 4 µm is recommended, as the <4 µm size tends to be influenced by in situ biogenic magnetosomes as well as stronger diagenetic alteration owing to the greater surface area to volume ratio of smaller magnetic grains.
Zhang *et al.* (2012)	Spatial sources of contemporary suspended sediment in Ohio River basin based on key	**Tracers**: Ag, Cu, Pb, Zn, Cd, Cr, Co, Ni, Ba, V, Li, Be, Mo, Sr, As, Sb, Se,	Routine water-quality sampling data for sediment sourcing studies can provide an approach for preliminary screening of sediment

	sub-catchments using routine water-quality monitoring data.	Hg, Fe, Mn, Al, Ti, P, total C, organic C, total S, total N **Size fraction**: **Analysis**: DFA, minimization of Wilks' lambda, Monte Carlo, mixing model	provenance in large drainage basins where conventional erosion assessment techniques in a representative spatially distributed design is impractical and unaffordable.

Appendix B

Statements of Contribution to doctoral thesis containing publications

DRC 16

MASSEY UNIVERSITY
GRADUATE RESEARCH SCHOOL

STATEMENT OF CONTRIBUTION
TO DOCTORAL THESIS CONTAINING PUBLICATIONS

(To appear at the end of each thesis chapter/section/appendix submitted as an article/paper or collected as an appendix at the end of the thesis)

We, the candidate and the candidate's Principal Supervisor, certify that all co-authors have consented to their work being included in the thesis and they have accepted the candidate's contribution as indicated below in the *Statement of Originality*.

Name of Candidate: Simon Vale

Name/Title of Principal Supervisor: Dr. Ian Fuller

Name of Published Research Output and full reference:

Vale SS, Fuller IC, Procter JN, Basher LR, Smith IE. 2016. Application of a confluence-based sediment-fingerprinting approach to a dynamic sedimentary catchment, New Zealand. Hydrological Processes, 30: 812-829. DOI: 10.1002/hyp.10611.

In which Chapter is the Published Work: Chapter 3

Please indicate either:

- The percentage of the Published Work that was contributed by the candidate:

  and / or

- Describe the contribution that the candidate has made to the Published Work:

  Simon Vale carried out all the fieldwork in the Manawatu as well as laboratory work between April 2012 and April 2013 with some assistance from co-authors. Simon Vale was the principal author in the preparation and submission of the manuscript with review and editing provided by co-authors. All data analysis was performed by Simon.

Simon Vale Digitally signed by Simon Vale Date: 2016.04.18 21:26:40 +12'00'
Candidate's Signature

2016/04/18
Date

Ian Fuller Digitally signed by Ian Fuller Date: 2016.04.19 09:14:53 +12'00'
Principal Supervisor's signature

19 April 2016
Date

GRS Version 3– 16 September 2011

DRC 16

MASSEY UNIVERSITY
GRADUATE RESEARCH SCHOOL

STATEMENT OF CONTRIBUTION
TO DOCTORAL THESIS CONTAINING PUBLICATIONS

(To appear at the end of each thesis chapter/section/appendix submitted as an article/paper or collected as an appendix at the end of the thesis)

We, the candidate and the candidate's Principal Supervisor, certify that all co-authors have consented to their work being included in the thesis and they have accepted the candidate's contribution as indicated below in the *Statement of Originality*.

Name of Candidate: Simon Vale

Name/Title of Principal Supervisor: Dr. Ian Fuller

Name of Published Research Output and full reference:

Vale SS, Fuller IC, Procter JN, Basher LR, Smith IE. 2016. Characterization and quantification of suspended sediment sources to the Manawatu River, New Zealand. Science of the Total Environment, 543: 171-186. DOI: 10.1016/j.scitotenv.2015.11.003.

In which Chapter is the Published Work: Chapter 4

Please indicate either:

- The percentage of the Published Work that was contributed by the candidate:

  and / or

- Describe the contribution that the candidate has made to the Published Work:

  Simon Vale carried out all the fieldwork in the Manawatu as well as laboratory work between January 2013 and October 2014 with some assistance from co-authors. Simon Vale was the principal author in the preparation and submission of the manuscript with review and editing provided by co-authors. All analysis was performed by Simon.

Simon Vale Digitally signed by Simon Vale Date: 2016.04.18 21:34:47 +12'00'
Candidate's Signature

18/04/2016
Date

Ian Fuller Digitally signed by Ian Fuller Date: 2016.04.19 09:22:02 +12'00'
Principal Supervisor's signature

19 April 2016
Date

GRS Version 3– 16 September 2011

DRC 16

MASSEY UNIVERSITY
GRADUATE RESEARCH SCHOOL

STATEMENT OF CONTRIBUTION
TO DOCTORAL THESIS CONTAINING PUBLICATIONS

(To appear at the end of each thesis chapter/section/appendix submitted as an article/paper or collected as an appendix at the end of the thesis)

We, the candidate and the candidate's Principal Supervisor, certify that all co-authors have consented to their work being included in the thesis and they have accepted the candidate's contribution as indicated below in the *Statement of Originality*.

Name of Candidate: Simon Vale

Name/Title of Principal Supervisor: Dr. Ian Fuller

Name of Published Research Output and full reference:

Vale SS, Fuller IC, Procter JN, Basher LR, Dymond JR, (In Review). Suspended sediment source characterization during a storm event, Manawatu Catchment, New Zealand. Hydrological Processes

In which Chapter is the Published Work: Chapter 5

Please indicate either:

- The percentage of the Published Work that was contributed by the candidate:

  and / or

- Describe the contribution that the candidate has made to the Published Work:

  Simon Vale carried out all the fieldwork in the Manawatu as well as laboratory work between January 2013 and October 2014. Minor assistance was provided by co-authors. Simon Vale was the principal author in the preparation and submission of the manuscript with review and editing provided by co-authors. All analysis was performed by Simon.

Simon Vale Digitally signed by Simon Vale Date: 2016.04.18 23:18:59 +12'00'
Candidate's Signature

18/04/2016
Date

Ian Fuller Digitally signed by Ian Fuller Date: 2016.04.19 09:20:42 +12'00'
Principal Supervisor's signature

19 April 2016
Date

GRS Version 3– 16 September 2011

DRC 16

MASSEY UNIVERSITY
GRADUATE RESEARCH SCHOOL

STATEMENT OF CONTRIBUTION TO DOCTORAL THESIS CONTAINING PUBLICATIONS

(To appear at the end of each thesis chapter/section/appendix submitted as an article/paper or collected as an appendix at the end of the thesis)

We, the candidate and the candidate's Principal Supervisor, certify that all co-authors have consented to their work being included in the thesis and they have accepted the candidate's contribution as indicated below in the *Statement of Originality*.

Name of Candidate: Simon Vale

Name/Title of Principal Supervisor: Dr. Ian Fuller

Name of Published Research Output and full reference:

Vale SS, Fuller IC, Procter JN, Basher LR, Dymond JR, (Prepared for submission). Sediment source variability and behaviour in the Manawatu River Catchment, New Zealand.

In which Chapter is the Published Work: Chapter 6

Please indicate either:

- The percentage of the Published Work that was contributed by the candidate:

  and / or

- Describe the contribution that the candidate has made to the Published Work:

  Simon Vale carried out all the fieldwork in the Manawatu as well as laboratory work between January 2013 and October 2014 with some minor assistance from co-authors. Simon Vale was the principal author in the preparation and submission of the manuscript with review and editing provided by co-authors. All data analysis was performed by Simon.

Simon Vale Digitally signed by Simon Vale Date: 2016.04.18 23:20:29 +12'00'
Candidate's Signature

18/04/2016
Date

Ian Fuller Digitally signed by Ian Fuller Date: 2016.04.19 09:18:09 +12'00'
Principal Supervisor's signature

19 April 2016
Date

GRS Version 3– 16 September 2011